INL/EXT-21-64549
Revision 0

Light Water Reactor Sustainability Program

Demonstration of the Plant Fuel Reload Process Optimization for an Operating PWR

September 2021

U.S. Department of Energy

Office of Nuclear Energy

INL/EXT-21-64549
Revision 0

Demonstration of the Plant Fuel Reload Process Optimization for an Operating PWR

Yong-Joon Choi[1]
Mohammad Abdo[1]
Diego Mandelli[1]
Aaron Epiney[1]
Jarrett Valeri[2]
Chris Gosdin[2]
Cesare Frepoli[2]
Andrea Alfonsi[3]

[1]Idaho National Laboratory, [2]FPoliSolutions LLC, [3]USNC (Formerly INL)

September 2021

Prepared for the
U.S. Department of Energy
Office of Nuclear Energy
Under DOE Idaho Operations Office
Contract DE-AC07-05ID14517
lwrs.inl.gov

EXECUTIVE SUMMARY

The United States (U.S.) nuclear industry is facing a strong challenge to maintain regulatory-required levels of safety while ensuring economic competitiveness to stay in business. Safety remains a key parameter for all aspects related to the operation of light water reactor (LWR) nuclear power plants (NPPs) and can be achieved more economically by using a risk-informed ecosystem such as that being developed by the Risk-Informed Systems Analysis (RISA) Pathway under the U.S. Department of Energy (DOE) Light Water Reactor Sustainability (LWRS) Program. The LWRS Program is promoting a wide range of research and development (R&D) activities with the goal to maximize both the safety and economically efficient performance of NPPs through improved scientific understanding, especially given that many plants are considering second license renewal.

The RISA Pathway has two main goals: (1) the deployment of methodologies and technologies that enable better representation of safety margins and the factors that contribute to cost and safety; and (2) the development of advanced applications that enable cost-effective plant operation.

This report summarizes the research outcomes in FY-2021, which the project progressed from the planning and methodology development phase to the early demonstration phase. The highlights of these activities are:

- The development of a multi-objective optimization process using Genetic Algorithms (GAs).
- The development and test of an approach for optimization process acceleration using artificial intelligence (AI) that significantly reduces the computational burden.
- The demonstration of the fuel reload optimization framework for a generic pressurized water reactor (PWR).
- The demonstration of limiting design basis accident (DBA) scenarios for evaluation of the transition from deterministic to risk-informed approach for fuel reload optimization.

Page intentionally left blank

CONTENTS

FIGURES

TABLES

ACRONYMS

1D	one-dimensional
2D	two-dimensional
3D	three-dimensional
AC	alternating current
AFW	auxiliary feedwater
AI	artificial intelligence
ANS	American Nuclear Society
ATF	Accident Tolerance Fuel
BA	burnable absorber
BEPU	best estimate plus uncertainty
BOL	beginning of life
BWR	boiling water reactor
CHF	critical heat flux
CSP	core support plate
CV	control variable
CVCS	chemical and volume control system
DBA	design basis accident
DC	direct current
DEG	double-ended guillotine
DNB	departure of nucleate boiling
DNBR	departure from nucleate boiling ratio
DOE	U.S. Department of Energy
DP	pressure drop
DPC	doppler power coefficient
ECC	emergency core cooling
ECCS	Emergency Core Cooling System
EOL	end of life
ESF	engineered safety feature
F	degrees Fahrenheit
FQ	heat flux channel factor
FSAR	Final Safety Analysis Report
FTC	fuel temperature coefficient
FY	fiscal year

FΔH	hot rod enthalpy rise
GA	genetic algorithm
HD	hydraulic diameter
HFP	hot full power
HTC	heat transfer coefficient
HZP	hot zero power
IET	integral effect test
INL	Idaho National Laboratory
LB	large break
LBLOCA	large break loss of coolant accident
LOCA	loss of coolant accident
LOOP	loss of offsite power
LWR	light water reactor
LWRS	Light Water Reactor Sustainability
MDC	moderator density coefficient
MFW	main feedwater
MSIV	main steam isolation valve
MSLB	main steam line break
MSSV	main steam safety valve
NEI	Nuclear Energy Institute
NPP	nuclear power plant
OPA	offsite power available
OTΔT	Overtemperature ΔT
PCT	peak cladding temperature
PF H	pressurizer filling high
PF L	pressurizer filling low
PORV	power-operated relief valve
PPF	power peaking factor
PRZ	pressurizer
PWR	pressurized water reactor
R&D	research and development
RAVEN	Risk Analysis and Virtual Environment
RCCA	rod control cluster assembly
RCP	reactor coolant pump
RCS	reactor cooling system

REA	rod ejection accident
RELAP	Reactor Excursion and Leak Analysis Program
RISA	Risk-Informed Systems Analysis
RTDP	revised thermal design procedure
RWST	refueling water storage tank
SB	small break
SBLOCA	small break loss of coolant accident
SG	steam generator
SGTR	steam generator tube rupture
SI	safety injection
SPH	SuPer-Homogenization
SS	steady state
TAVG	reactor coolant average temperature
TDF	thermal design flow
TMI	Three Mile Island
TR	transient
U.S.	united states
WABA	wet annular burnable absorber

DEMONSTRATION OF THE PLANT FUEL RELOAD PROCESS OPTIMIZATION FOR AN OPERATING PWR

1. INTRODUCTION

1.1 Background

The United States (U.S.) Department of Energy (DOE) Light Water Reactor Sustainability (LWRS) Program Risk-Informed Systems Analysis (RISA) Pathway plant reload optimization project is a response to one of the top-priority requests from the industry, an understandable need given that fuel costs represent approximately 20 percent of the total generation costs per the Nuclear Energy Institute (NEI) *2020 Nuclear Costs in Context* report [1]. The project aims to optimize reactor core thermal limits through the implementation of state-of-the-art computational and modeling techniques. This research is very timely considering that the industry is actively getting ready to transition to Accident Tolerance Fuels (ATFs), and this platform will be capable to perform all necessary ATF evaluations. An additional benefit of this platform is an integrated workflow that incorporates seamlessly all the steps required for the fuel reload analysis, which traditionally is a labor-intensive and time-consuming process.

The optimization of core thermal limits allows a smaller fuel batch size to produce the same amount of electricity, which reduces new fuel costs and saves significant amount of money on the back-end of the fuel cycle by reducing the volume of spent fuel that needs to be processed. The cost of a typical fuel reload for a light water reactor (LWR) is about $50M and this project estimates new fuel volume reduction on the order of 5–10%. This equates to a savings of $2.5–5M per reactor per reload; this is new fuel only cost-savings, which does not account for the back-end cost reduction in spent fuel processing.

1.2 Objectives and Plan

The goal of this research is to develop an integrated, comprehensive platform offering all-in-one solution for the reload evaluations with the special focus on fuel optimization, which allows a reduction in the volume of new fuel [2]. The platform will provide an optimized reactor core configuration based on key safety parameters that must be considered to meet regulatory requirements.

Figure 1-1 shows the technology roadmap and research plan of this project throughout the last several fiscal years (FYs) with four phases of research and development (R&D):

Phase 1 (FY-2019 to FY-2020): Methodology Development

Available tools and methods were investigated and tested. Plant-based design basis accident (DBA) scenarios were simulated via traditional deterministic methods by using the Reactor Excursion and Leak Analysis Program (RELAP5)-3D thermal-hydraulics analysis code developed at Idaho National Laboratory (INL). Simulations used fixed core loading and evaluated recoverable margins.

Phase 2 (FY-2021 to FY-2022): Framework Improvement

The key activities completed in FY-2021 include:

- The demonstration of the plant reload optimization framework for a generic pressurized water reactor (PWR) using ten limiting DBA scenarios.
- The development and deployment of the multi-objective optimization process using genetic algorithms (GAs).
- The development and testing approach for an optimization process acceleration using artificial intelligence (AI), which significantly reduced the computational burden.

- The development of an improved Risk Analysis and Virtual Environment (RAVEN) infrastructure for the performance of neutronics and thermo-hydraulic analyses.
- The identification of limiting DBA scenarios for the evaluation of the transition from a deterministic to a risk-informed approach for fuel analyses.

In FY-2022, the project will continue the progression through the demonstration phase where the framework will be enhanced with additional and extended capabilities to support regulatory-required fuel safety analyses and to allow additional economic benefits from fuel reload optimization. Limiting DBA scenarios will be analyzed for the optimization framework application to identify constraints from the tools and methods. Additionally, the development of a risk-informed approach for fuel assessment will be initiated.

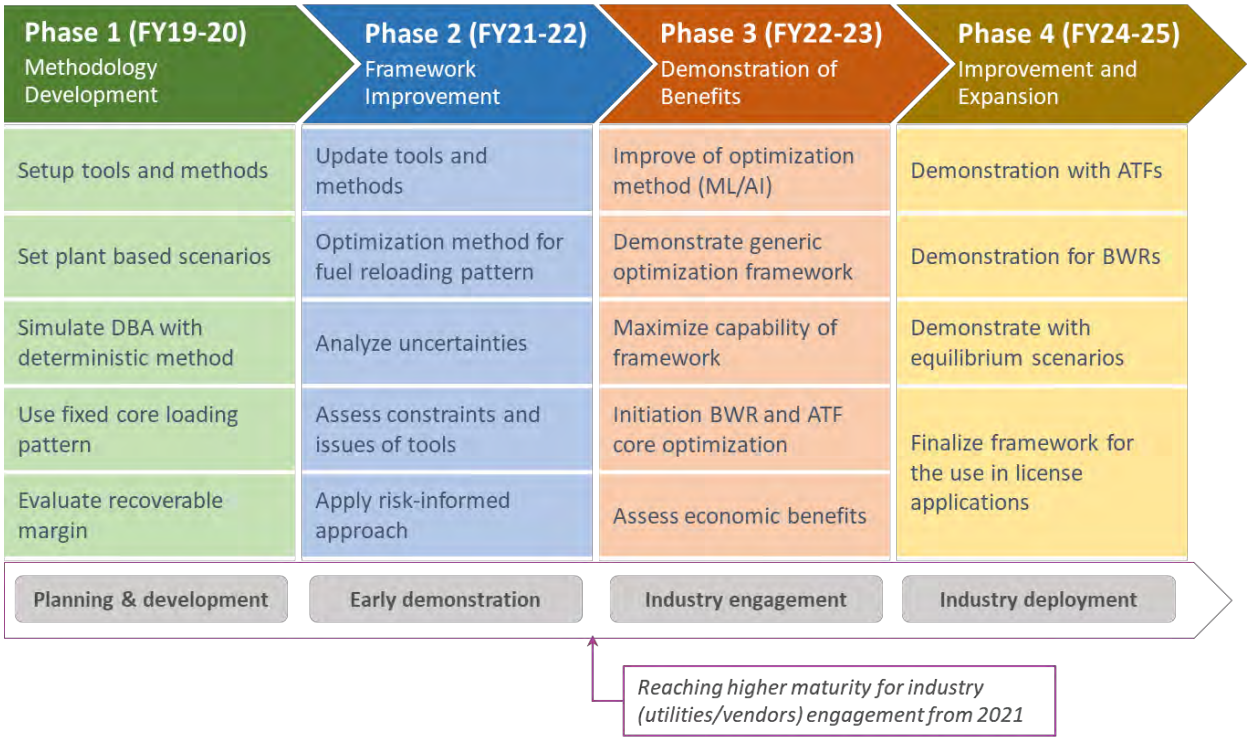

Figure 1-1. Technology roadmap of plant reload optimization project.

Phase 3 (FY-2022 to FY-2023): Demonstration of Benefits

The optimization method will be improved by further integration of machine learning and AI concepts. Tools will be tightly coupled to maximize framework capability. Fuel reload optimization for a boiling water reactor (BWRs) and an ATF will be initiated. Economic benefits will be assessed to promote and expedite framework deployment for industry use.

Phase 4 (FY-2024 to FY-2025): Improvement and Expansion

The framework capabilities will be demonstrated for a BWR and ATF. Equilibrium scenarios will be demonstrated for PWRs, BWRs, and ATFs. Framework development will be finalized, and a pathway will be established to support industry with license applications.

As of FY-2021, the technical maturity of the framework is at the level that supports the engagement of and collaboration with nuclear power plants (NPPs).

Upon finalizing the research, the following benefits will be obtained from the developed plant fuel reload optimization platform:

- This platform will significantly simplify the required process of core reload evaluation performed for each fuel reload because it integrates all the required tasks into one seamless automated process.
- The platform will support flexible plant operations with increased or decreased reactor power levels following the fluctuating demand driven by the integration of renewables.
- The platform will be capable to perform all necessary evaluations of ATF—including the optimization of core design.

2. GENETIC ALGORITHM FOR PLANT RELOAD OPTIMIZATION

2.1 Overview of the Genetic Algorithms

An initial version of the optimization workflow is developed for thermal limits and, consequentially, fuel pattern optimization. The development of such methods has focused on metaheuristic optimization algorithms. In specific, GAs were selected to deal with this problem for the following reasons [3-9]:

- A GA is preferred for non-differentiable, expensive to differentiate, or objective functions with no intrusive access (e.g., black box).
- A GA does not get stuck in local minima; hence, it works with non-convex problems.
- A GA can handle both constrained and unconstrained problems.
- Due to the encoding/decoding step, a GA works with discrete, continuous, or mixed design spaces, with binary, integer, real, or permutation variables.

The GA stems from biological evolution, it contains several evolutionary operations such as parent selection, crossover, mutation, survivor selection, and repair/replacement. Figure 2-1 depicts the flowchart describing the whole process. Each step in the flow chart contains several algorithms that will be outlined in following sections.

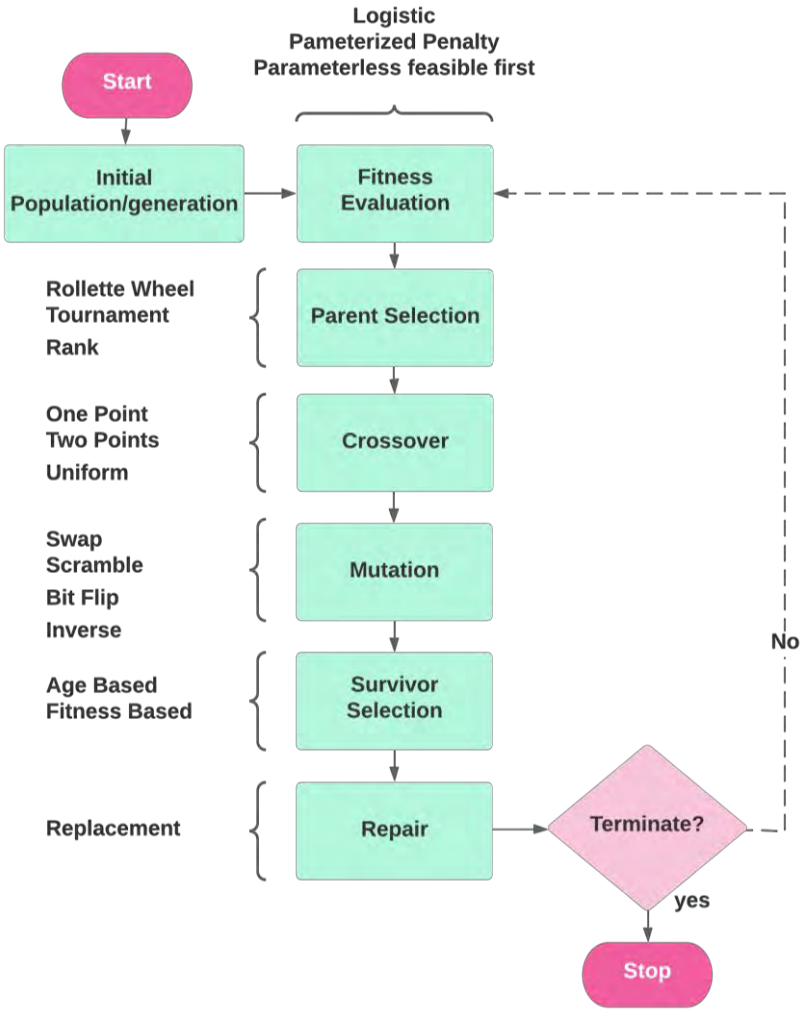

Figure 2-1. GA flow chart.

2.2 Anatomy of the Genetic Algorithms

First, the terminology is introduced, then the notion of fitness is defined, and examples are given followed by the parent selection process to prepare individuals for the mating pool. Next, crossover and mutation processes are explained to show how the new offsprings are formed. The new offsprings/children then undergo another selection process, namely survivor selection, to decide the new population/generation. A quick replacement repair process can take place to fix any offspring that was distorted (and hence is violating constraints/requirements). Finally, this is repeated until the termination criterion is met or the maximum number of generation/populations is exceeded.

2.2.1 Terminology

In GA, most of the terminologies are inspired by evolutionary terms in biology, the single candidate solution for the optimization problem is called chromosome or individual. Figure 2-2 is a schematic diagram of a GA. Each chromosome consists of several genes reflecting the number of design variables in the optimization problem (i.e., the dimension of the search space). The value of each gene is called *Allele*, which depends on the encoding of the problem (i.e., the transformation from the representation in the real-world space, a.k.a., the phenotype representation/space to the representation in the mathematical world, or a genotype representation/space). Allele can be a real number, an integer, binary (0,1), or a permutation of discrete or continuous variables, or even a mix and match between previous types. The modular way of the implementation in RAVEN allows for assigning a different distribution to each gene and hence part of the chromosome can be discrete while the rest can be continuous. Below are a few terminologies used in the GA:

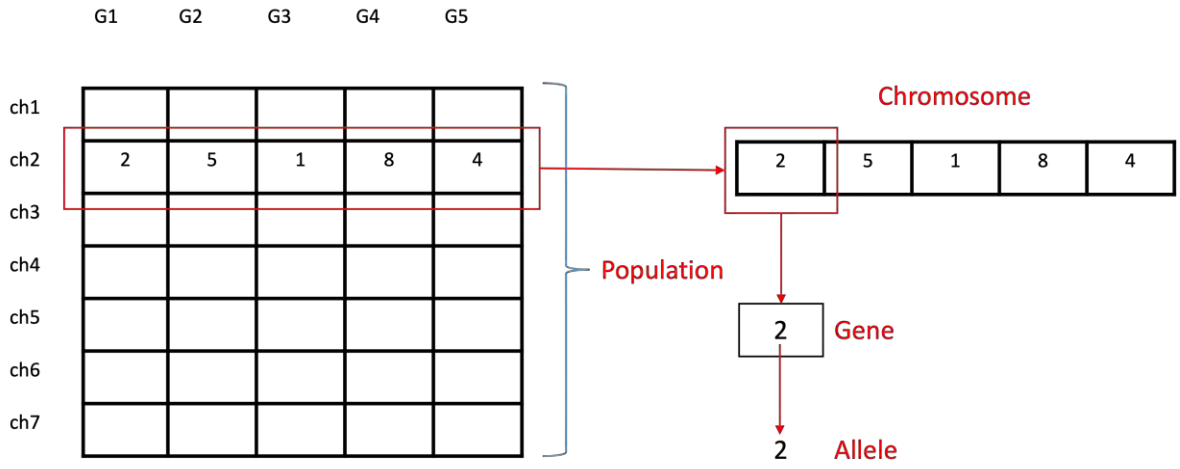

Figure 2-2. GA population, chromosome, and gene concepts [10].

- *Phenotype Space* − The solution space hosting the real problem; solutions in that space are physical and realistic in the row form and not necessarily similar to the mathematical (encoded) solution.
- *Genotype Space* − The mathematical/computational form of the Phenotype Space after the encoding process that transforms the realistic variables to mathematical ones for easier computational treatments.
- *Decoding and Encoding* − The optional processes to convert Phenotype representation (real variables) into Genotype representation (computational representation).
- *Population* − A subset of all solutions in the Genotype Space that are candidates to be the optimal solutions.
- *Chromosomes (Individuals)* − A single candidate solution of the problem.

- *Gene* − A single element in the chromosome representing a unique variable in the mathematical problem.
- *Allele* − The value a gene takes.
- *Mating/Reproduction Pool* – A subset of parents used to reproduce a new generation formed by previous parents and new offsprings.
- *Fitness Function* − The function used to rank the solutions and find the fittest/elitist chromosome in the population. It might or might not be the same as the objective function.
- *Reproduction Operations/Operators* − Operations that change the genes of certain chromosome(s) (e.g., crossover, mutation, repair).

2.2.2 Fitness Evaluation

In GA, the notion of fitness is extremely important since it is used to rank the solutions in a population, and hence, guide the selection processes (e.g., both parent selections to select the fittest parents contributing to the mating process, and survivor selection to decide the next generation). Moreover, it is one of the simplest constraint handling methods as it penalizes the chromosome (solution) violating any of the constraints, rendering it less fit, and hence, less prone to get selected in the next iterations.

There are several ways to design the fitness function and several requirements that should be fulfilled. Below are some of these requirements:

- Fitness functions must be clearly defined and efficiently implemented. It should never be the bottleneck of the algorithm.
- It should be maximum at the optima (for minimization problems, as the objective function decreases, the fitness should increase and vice versa; whereas for maximization problems, as the objective function increases, the fitness also should increase and vice versa).
- The fitness should decrease whenever the constraints are violated.

In RAVEN, the objective function of maximization problems is multiplied by -1, and hence, converted to a minimization problem. So, in all cases, RAVEN tries to find the minima, and the fitness increases as the objective decreases. There are three types of fitness functions that have been implemented thus far. One is only for unconstrained problems—namely 'logistic fitness'—while 'invLin' and 'feasibilityFirst' are used for both constrained and unconstrained problems.

For 'invLin' the fitness is given by:

$$fitness(ch_i) = -a \times objective(ch_i) - b \times \sum_{j=1}^{nConstraints} max(0, -g_j(ch_i)) \quad (1)$$

where ch_i is the i^{th} chromosome/individual; a, b are user-defined constants with 1.0 as the default values; and $g_j(ch_i)$ is the j^{th} constraint function evaluated at the i^{th} chromosome. The constraint function is written as $g_j(ch_i) > 0$, which means that if the solution (chromosome) violates the constraint $g_j(ch_i)$, it will be negative and vice versa. This means that the penalty term (e.g., the second term in the fitness equation) will only exist if $g_j(ch_i)$ is negative, which will cause the fitness to decrease.

For 'FeasibleFirst' the fitness is given by:

$$fitness(ch_i) = \begin{cases} -objective(ch_i), g_j(ch_i) \geq 0;\ \forall j \\ -objective_{worst} - \sum_{j=1}^{nConstraints} max(0, -g_j(ch_i)), o.w \end{cases} \quad (2)$$

In this case, the violating solution not only penalized by the amount of violation but also by the worst fitness in the population.

Finally, for the unconstrained logistic fitness:

$$fitness(ch_i) = \frac{1}{1 + e^{a \times (objective(ch_i) - b)}} \quad (3)$$

where a, and b are user-defined constants with 1.0 as the default values.

2.2.3 Parent Selection

This selection mechanism is used to pick the parents that will enter the mating pool for the next generation. There are several algorithms to perform such a selection—namely 'Roulette Wheel,' 'Rank,' and 'Tournament' selection. All are implemented in RAVEN and the user can pick the method to be used. Figure 2-3 shows the roulette wheel selection mechanism.

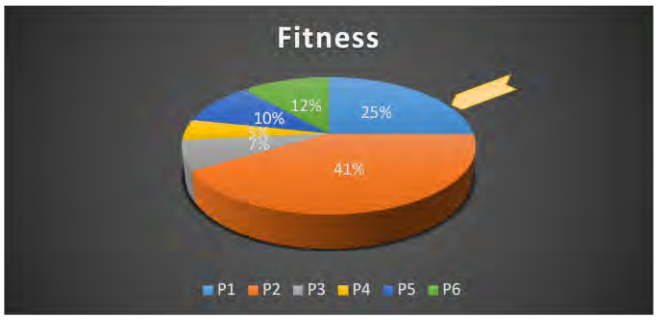

Individual	Fitness
P1	5
P2	8.2
P3	1.4
P4	0.98
P5	2
P6	2.3

Figure 2-3. Roulette wheel parent selection.

The reader should be cognizant of the fact that despite Parent 2 in the previous table having the largest fitness, Parent 1 was selected because randomness is inherent in the roulette wheel; however, Parent 2 has more chances since it occupies the largest portion of the wheel. This randomness is helpful to avoid selecting the same parents in every iteration and stagnating the search for long times, which reflects being stuck in a local opima.

2.2.4 Crossover Operation

The crossover process allows that the new offsprings inherit a part of their genes from each parent. Figure 2-4 shows the *one-point* crossover operation.

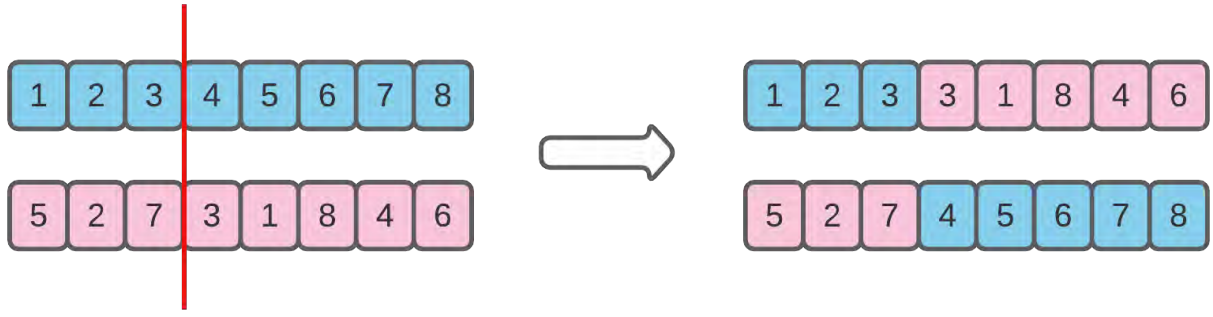

Figure 2-4. One-point crossover.

2.2.5 Mutation Operation

Like the crossover operation, the mutation operation is a way to change the genetic structure of each chromosome, and hence, explore different solutions in the design space. Both mutation and crossover occur if a random number exceeds a user-defined probability, which enforces the change and prevents getting stuck in a local optima. Figure 2-5 paints a picture of the scramble mutation.

Figure 2-5. Scramble mutation.

2.2.6 Survivor Operation

Among a number of chromosomes equal to the 'popSize' (population size), the best parents are selected for the next mating pool. This is done based on two different algorithms: 'fitness-based' and 'age-based.' In fitness-based parent selection, the parents and children/offsprings are aggregated to form a bigger population, and then a user-defined number (i.e., 'nParents') with the highest fitness are selected to continue the process. Figure 2-6 explains the fitness-based survivor selection.

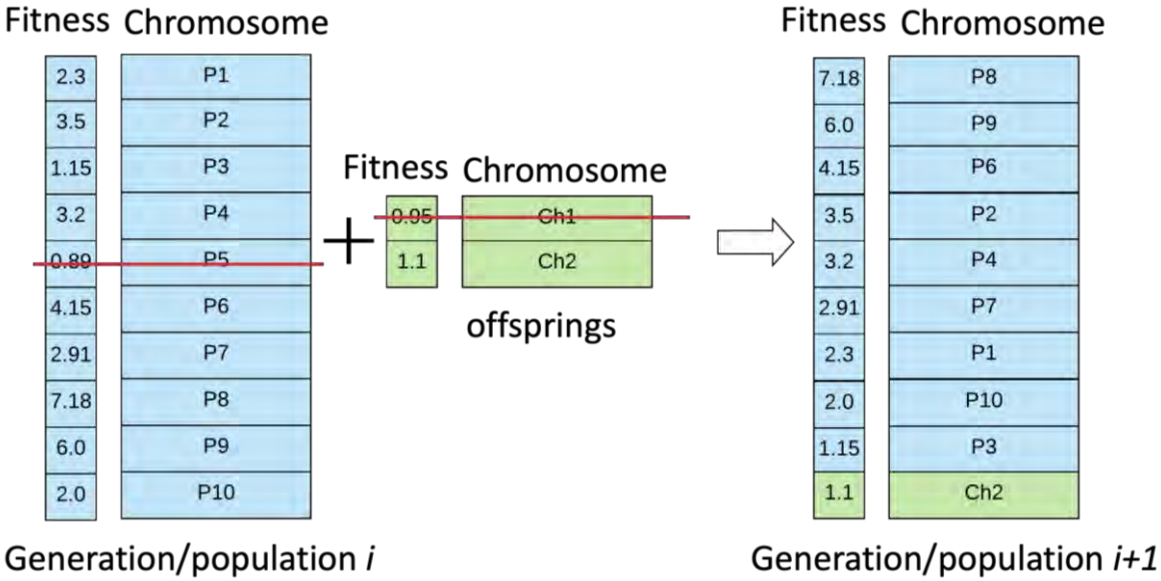

Figure 2-6. Fitness-based survivor selection.

2.2.7 Replacement and Repair

In some cases, the crossover or mutation can cause an offspring to defy one of the constraints or requirements. For instance, the problem encoding dictates that the variables should be withdrawn from an integer space without replacement, but after the crossover or mutation, two genes have the same values. This child should be repaired by replacing the repeated value by a random value withdrawn from the same distribution.

2.2.8 Termination Criterion

Thousands of termination criteria are possible for GA, which is still an open research area. Figure 2-7 shows a quick taxonomy of termination criteria. Currently, the algorithm terminates in one of two cases: (1) if the maximum number of iterations is reached; and (2) if the p-average Hausdroff distance between two consecutive generations reached a user-defined value.

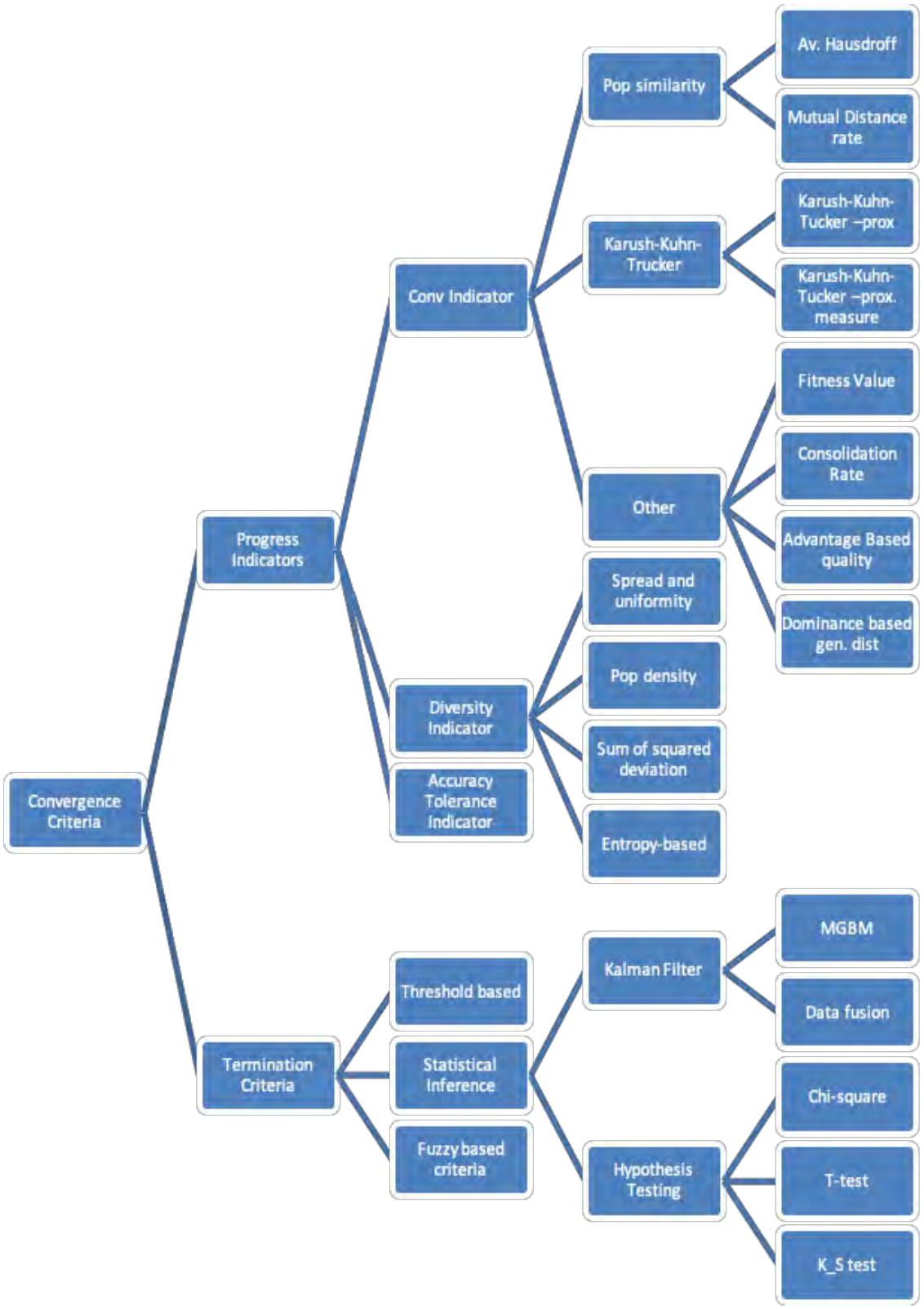

Figure 2-7. GA termination criteria.

Consider to successive generations G1, G2, the following is the derivation of Hausdroff distance [11]:

$$AHDp(G1,G2) = \max\{GD_p\ (G1,G2), IGD_p\ (G1,G2)\}$$

$$GD_p(G1,G2) = \left(\frac{1}{n}\sum_{i=1}^{n} dist(g_i^{(1)},G2)^p\right)^{\frac{1}{p}}$$

$$IGD_p(G1,G2) = \left(\frac{1}{m}\sum_{j=1}^{m} dist(g_j^{(2)},G1)^p\right)^{\frac{1}{p}} \quad (4)$$

$$dist\left(g_i^{(1)},G2\right) = inf_{g_i^{(2)}\in G2}\left\|g_i^{(1)} - g_i^{(2)}\right\|$$

2.3 Optimization Methodology Enhancement

Since the problem at hand is huge—especially if coupled multi-physics phenomena are considered in the optimization space—any vanilla optimization algorithm will be overwhelmed by such a high-dimensional global constrained problem. Consequently, acceleration schemes are indispensable to achieve the optimal solution in a timely manner.

A wide range of literature has been reviewed to assess the possibility of applying the enhanced optimization methodology in the fuel reload optimization. Following methods are selected to enhance and/or accelerate the convergence of GAs:

1. Exploring the active subspace hosting the search directions that increases the fitness, then constrain the mutation to these directions.
2. Coupling with the gradient approximation methods to educate and de-randomize the evolutionary operations to converge faster.
3. Accelerate the GA with Markov chains.
4. Recast the problem as a reinforcement learning problem:
   a. *Objective:* Maximize the cycle length or minimize the number of feeds.
   b. *Constraints:* Enrichment, the amount of gadolinium or burnable poison, the infinite multiplication faction (k_{inf}), the power peaking factor (PPF), the hot rod enthalpy rise (FΔH), etc.
   c. *Action Space:* Discrete fuel inventory.
   d. *State Space:* Fuel enrichment in each location.
   e. *Game Rules:*
      i. Do not violate constraints.
      ii. Do not place specific fuels next to each other (e.g., no gadolinium fuels horizontally or vertically adjacent).
5. Hybridizing and/or benchmarking with other metaheuristic methods, such as ‘Particle Swarm,’ ‘Ant Colony,’ ‘Bee Algorithms,’ etc.

Enhanced optimization methods will be demonstrated in the upcoming years.

3. DEMONSTRATION OF PLANT RELOAD OPTIMIZATION FRAMEWORK

The plant reload optimization framework was demonstrated by using a loss of coolant (LOCA) scenario in a generic PWR model with an equilibrium fuel reload cycle. HELIOS-2 lattice code was used for the cross-section and PHISICS/RELAP5-3D was used for the core performance and accident analysis.

3.1 Core Physics Model Description

The goal of the demonstration is to simulate equilibrium cycle and limiting scenarios by using optimization framework for simplified PWR core design. The outcomes of the limiting scenarios will then be feedback and used to inform further optimization if the core.

Shown in Figure 3-1, the considered simplified core includes only one fresh fuel assembly enrichment for the whole core, no axial lower enriched fuel zones on the assemblies, and the use of wet annular burnable absorber (WABA) rods. Furthermore, to have a modern low leakage loading scheme that allows for reaching high burnups, but still keeping it as simple as possible, all twice burned fuel has been placed at the periphery. For the fuel design, the axial fuel enrichment is constant and a variable number of WABA rods are used to flatten the radial power distribution in the core. The used assembly is a 17 × 17 lattice with 264 fuel rods and 25 non-fuel locations. The non-fuel locations contain the guide tubes, the WABA rods, and the instrumental tubes.

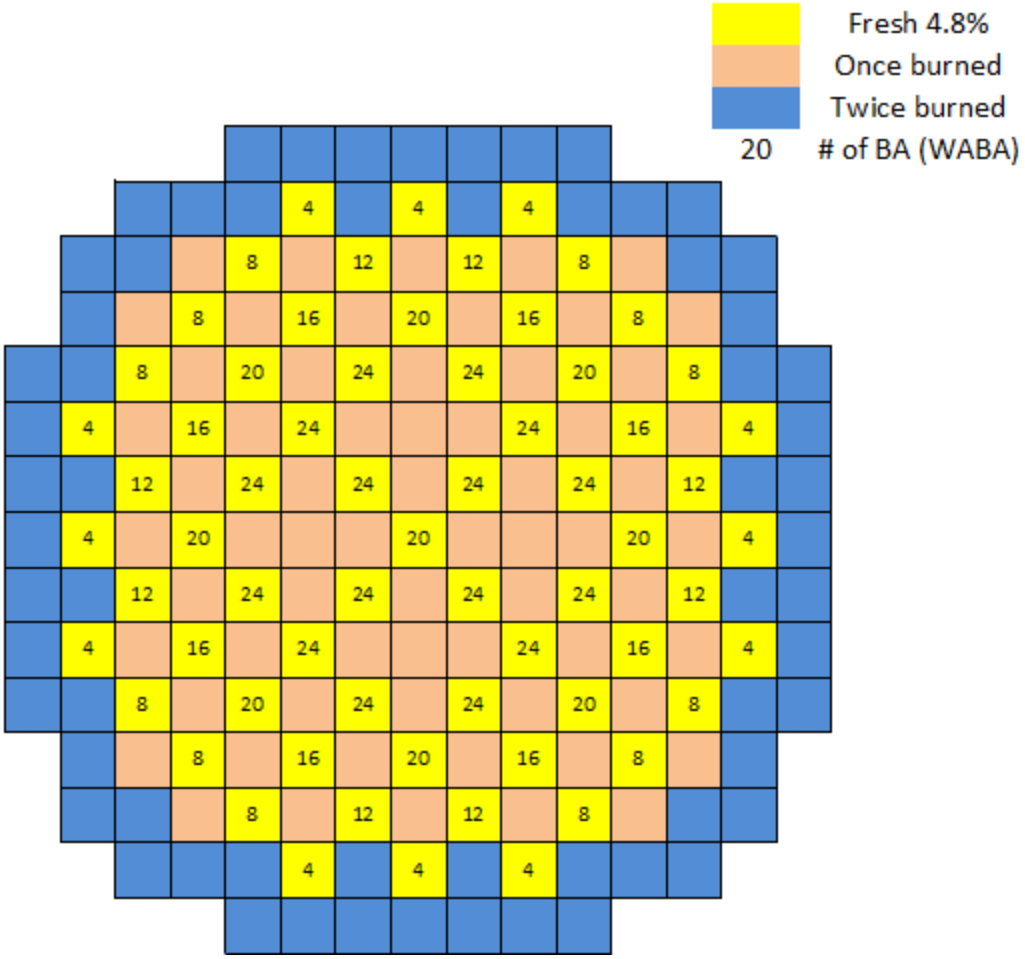

Figure 3-1. Equilibrium cycle reloading pattern, fresh fuel enrichment, and the number of burnable absorber (BA) pins in the fresh fuel assemblies.

The equilibrium cycles for this generic PWR have been analyzed. The calculations to provide the initial data for the LOCA analysis were calculated with PHISICS/RELAP5/HELIOS-2 codes, including cross-section generation [12-14]. Figure 3-2 shows the core design strategy. The cross-sections for an initial guess configuration have been computed. At least eight cycles were computed until the equilibrium cycle was reached. The equilibrium cycle then was analyzed for both options in terms of desired cycle length, maximum assembly burnup, and the radial and axial power distributions. The design subsequently was adjusted to meet the design goals and the equilibrium cycle was recomputed. Once the design goals were reached, the cross-sections were recomputed with HELIOS-2 for the new designs. The equilibrium cycle then was recomputed with the new cross-sections. Since the equilibrium cycle characteristics may have changed due to the updated cross-sections, further optimization and changes in the core design may have become necessary. These "inner" (e.g., change core design and recomputed equilibrium cycle) and "outer" (e.g., the recomputed cross-sections) loops, as shown in Figure 3-2, were repeated until convergence was reached.

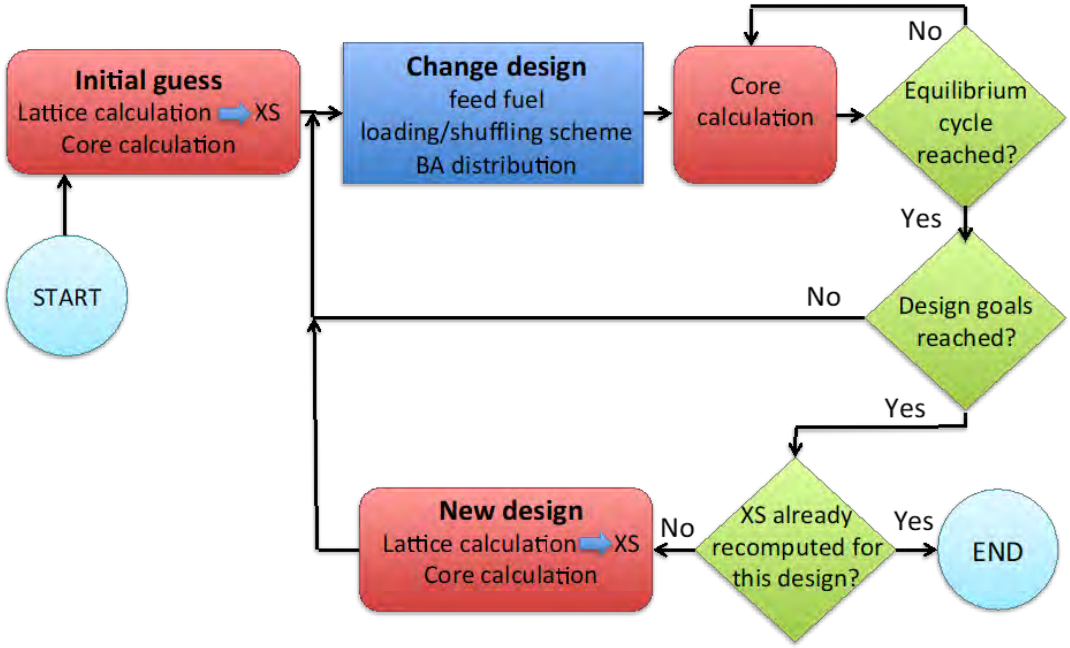

Figure 3-2. Flow chart for core design.

3.2 Cross-Section Library Calculations

As mentioned, for the calculation of the homogenized cross-sections, the lattice code 'HELIOS-2' has been used. In order to identify the number of cross-section sets needed for this calculation, the 'proximity' approach was employed: even if the number of compositions are limited, an assembly is considered different with respect to another when the neighboring ones are different (e.g., different composition, structural material, instrumentation tube locations, etc.). This approach led to the identification of 29 different cross-section sets for the fuel region and one for the radial reflector, composed by the baffle, water between the baffle and the barrel, the barrel, and finally, the thermal shield. A detailed two-dimensional (2D) representation of 1/8 of the core has been modeled with HELIOS-2. Figure 3-3 shows the full HELIOS-2 model (including a zoom on one assembly), while the left image in Figure 3-4 shows the locations of the different cross-section libraries that was produced.

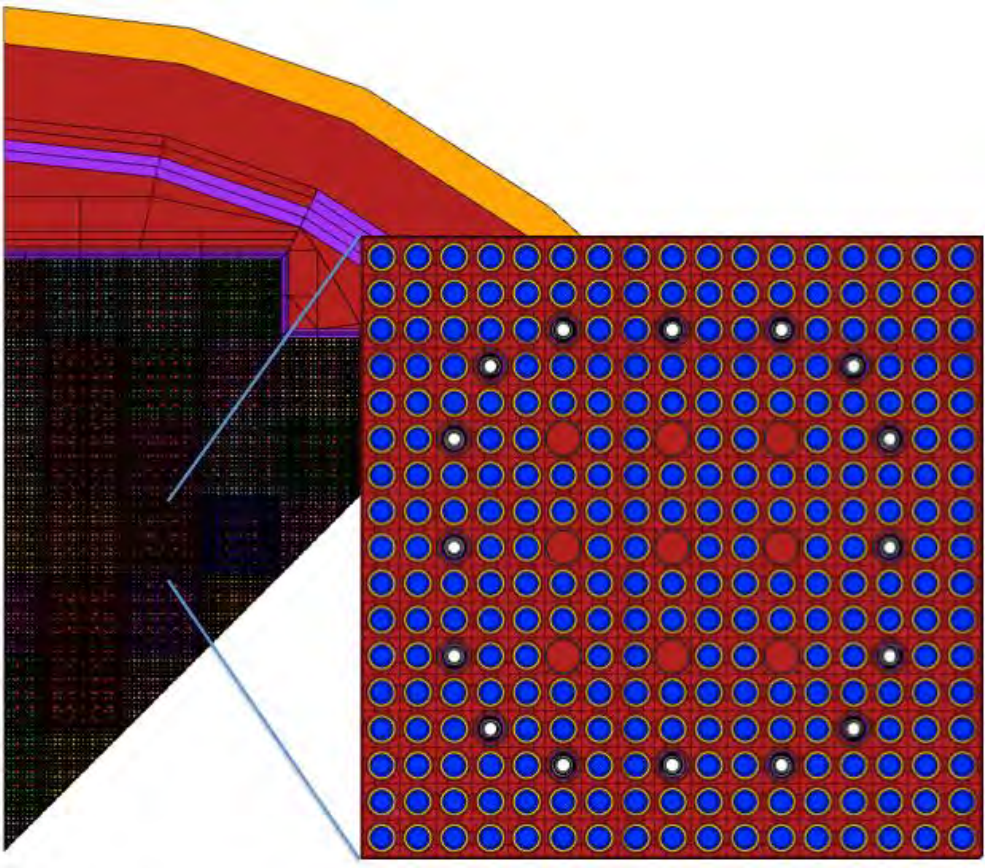

Figure 3-3. HELIOS-2 model for PWR core fuel reload optimization.

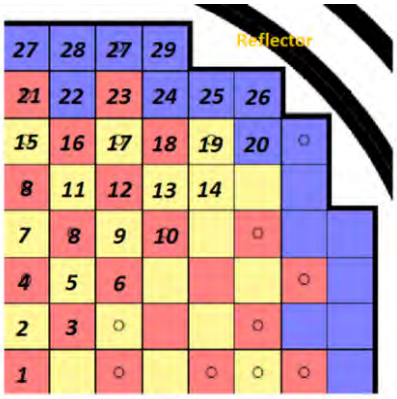

Group	Upper energy bound (eV)
1	2.00E+07
2	2.23E+06
3	8.21E+05
4	9.12E+03
5	1.30E+02
6	3.93E+00
7	6.25E-01
8	1.46E-01

Figure 3-4. Cross-section library locations generated with HELIOS-2 (left); 8-group energy structure generated with HELIOS-2 (right).

The lattice calculations are generally started from pre-collapsed multi-group neutron energy structures. For the computation of the different cross-section sets, the lattice calculations have been performed starting from a 44-energy group structure, and then collapsed into an 8-group structure in the homogenization procedure. The 8-group structure has been used to find the equilibrium cycle. However, the calculation time is still relatively high using the 8-energy groups. For the complete (outermost) optimization loop that includes the feedback from the limiting scenario calculations, the neutron energy groups have been further collapsed into a 2-group structure.

The reactor calculation involves the simulation of the reactor during several operational cycles. In order to exchange feedback between the core design PHISICS tool and the thermal-hydraulic RELAP5-3D code, microscopic cross-section sets for all isotopes except the moderator are tabulated with respect to several field parameters for each library. The cross-sections for the moderator regions have been tabulated as macroscopic cross-sections. This allows to treat boron that is in solution in the moderator, which is a tabulation dimension, and boron in the BAs, which are tabulated microscopic cross-sections, separately. The following parameters and tabulation points have been computed for both core design options:

- Boron concentration in H_2O (ppm): 0.0, 1000, 1900
- Moderator density (kg/m^3): 640.8, 833.0, 945.2, 1000
- Fuel temperature (K): 573.2, 1073.2, 1273.2
- Burnup (GWd/tHM): 0.0, 0.152, 15, 25.

The tabulation dimensions lead to the construction of a complete N-Dimensional (4-Dimensional in this case) grid that is characterized by 108 tabulation points in total. It is noted that the burnup points are for each cycle since the cross-section libraries are computed for fresh, once-burned, and twice-burned assemblies. Finally, the SuPer-Homogenization (SPH) method is applied for all generated cross-section libraries.

3.3 Coupled PHISICS/RELAP5-3D Calculation

As mentioned, to have a "fair comparison" of the behavior for different optimized cores, limiting scenarios need to be initiated from the equilibrium cycle conditions. Hence, the reactor evolution needs to be followed for several operational cycles until reaching the referenced equilibrium cycle. From a loading point of view, the equilibrium cycle can be considered as the cycle from which the fuel reloading pattern is almost constant (i.e., same composition and spatial loading of the fuel batches). The equilibrium cycle might be "reached" after several reloads. In this study, we assume that the equilibrium cycle is reached after the 8th reload.

The PHISICS code is coupled with the thermal-hydraulic RELAP5-3D code. For the search of the equilibrium cycle, the thermal-hydraulic model of the reactor has been set up considering the reactor core only (e.g., without a primary or secondary system). The approach to consider only the core region without the primary system can be taken for base irradiation calculations (e.g., to search for the equilibrium cycle for a given core configuration), since the system does not influence the core during normal operation. For this reason, only the primary system is modeled considering the upper and lower plenum of the core. To make the determination of the initial conditions for the subsequent limiting scenario analysis as accurate as possible, the core is modeled using one core channel per fuel assembly (i.e., 193 in total). The radial reflector is modeled as a bypass channel (i.e., 6% of the mass flow). Figure 3-5 shows the RELAP5-3D nodalization used in the study. It should be noted that this RELAP5-3D model is different than the one used in the subsequent limiting event analysis.

The PHISICS calculation of this coupled simulation is set up as the full core (i.e., all the 193 assemblies are modeled explicitly). The materials are assembly homogenized. One ring of assemblies containing a water/steel mixture has been placed around the active core to represent the reflector. The 3D-PHISICS calculation uses 18 axial layers. The cross-section libraries are associated with the assemblies shown in Figure 3-4 (left).

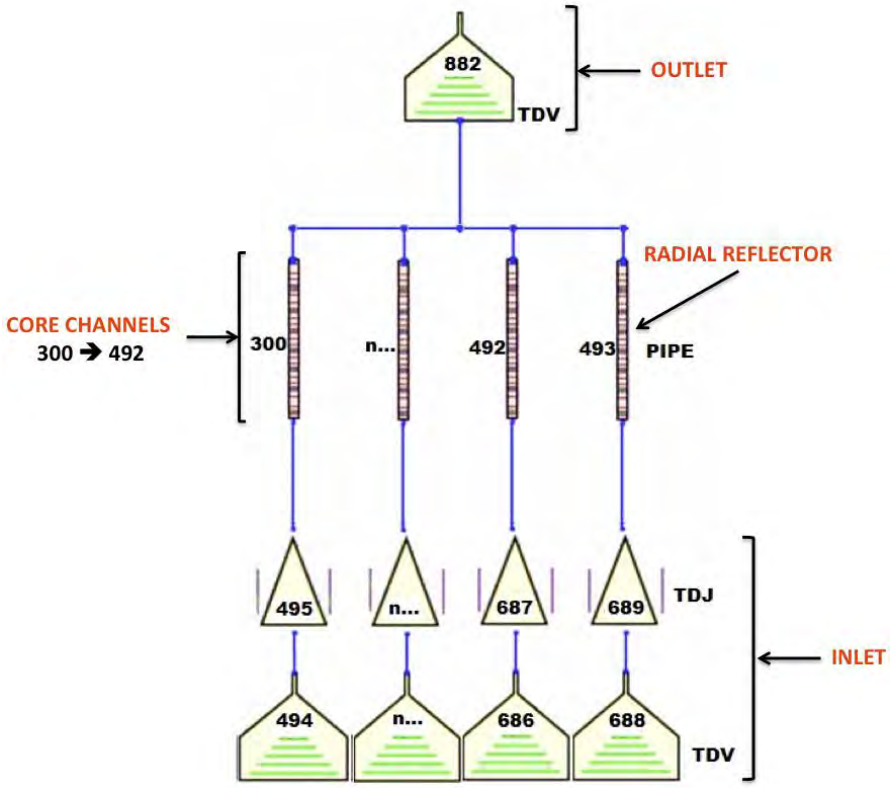

Figure 3-5. RELAP5-3D nodalization for the core simulation.

3.4 Results

The case study considered to test the mechanics of the optimizer is a 1/4 core initial loading problem. There are 56 locations that need to be loaded with five types of fuel assemblies. and hence, the dimensionality of the problem is 56 (i.e., there are 56 genes in each chromosome). The objective function to be maximized is the cycle length and for now it is an unconstrained problem. However, there is a constraint implied by the reactor physics code such that once the soluble boron reaches ≤ 5 ppm, the cycle ends. The inventory of the assemblies includes five different materials:

- Material – 1: Enrichment 2.2% in U-235, no burnable poisons
- Material – 2: Enrichment 2.5% in U-235, no burnable poisons
- Material – 3: Enrichment 2.5% in U-235, burnable poisons (8.0e-6 #/cm·barn)
- Material – 4: Enrichment 3.5% in U-235, no burnable poisons
- Material – 5: Enrichment 3.5% in U-235, burnable poisons (8.0e-6 #/cm·barn).

Figure 3-6 shows the layout and possible materials in 1/4 of the core. For this problem, a population size of 100 is used, 40 parents for the mating pool, the roulette wheel for the parent selection, the 'invLinear' fitness, one-point cross-over with 80% cross-over probability, swap mutation with 90% mutation probability, both locations of cross-over and mutation changes randomly each iteration, a uniform discrete integer encoding with values between 1 to 5, since these are our options for the materials.

Figure 3-7 depicts the results of the optimization problem showing the history of the iterations, as well as the optimal value selected. It is very important to note that the problem is still non-realistic, and that no thermal limits or constraints are considered yet.

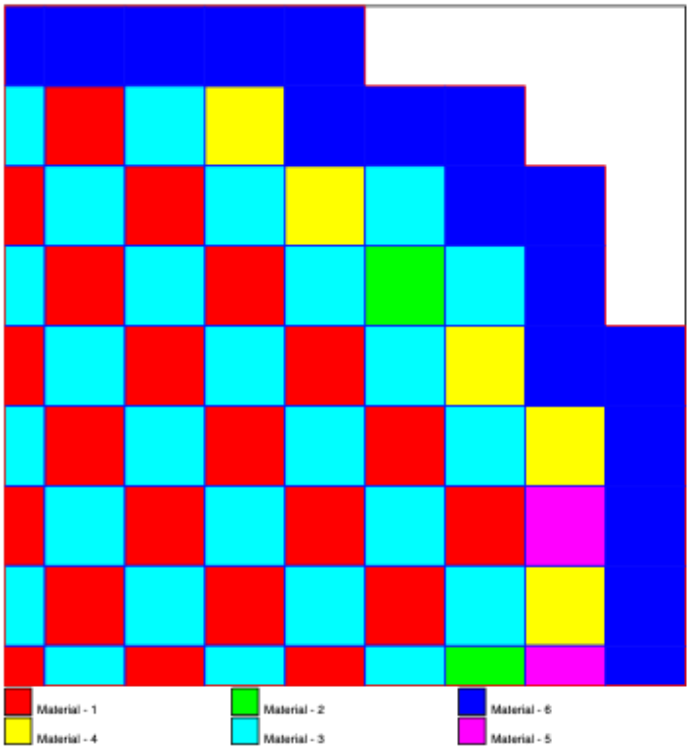

Figure 3-6. Layout of passible materials in 1/4 core.

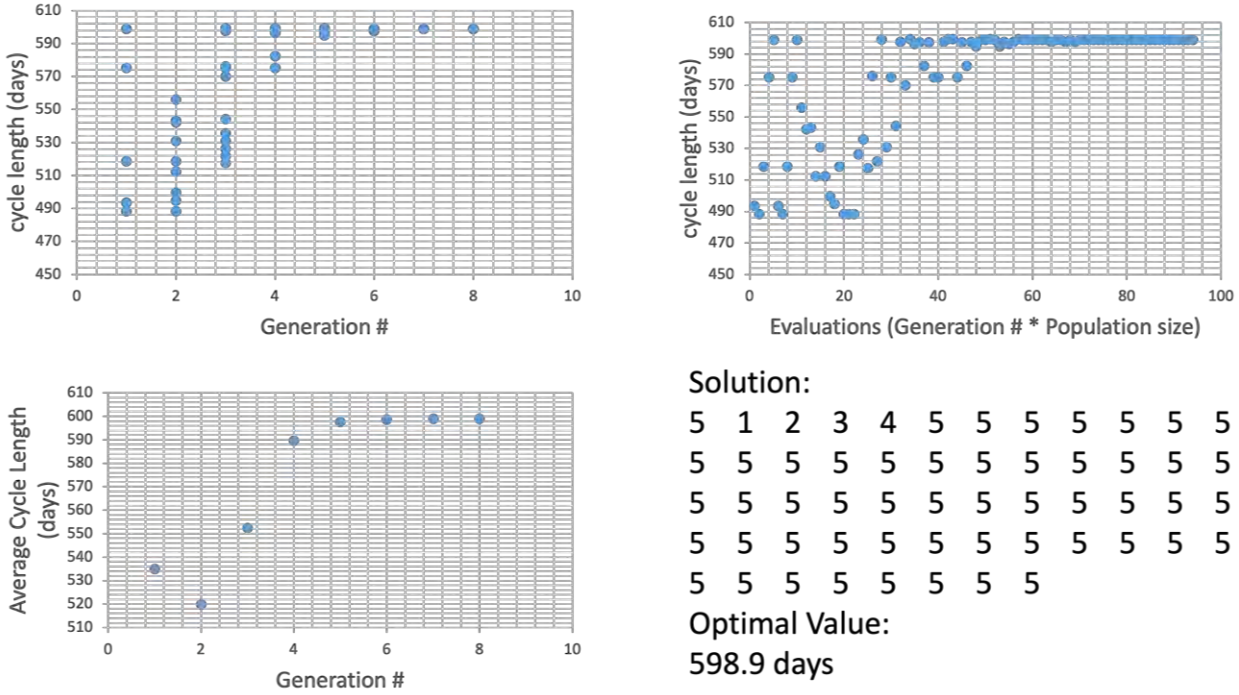

Figure 3-7. Demonstration result of fuel reload optimization framework.

4. ASSESSMENT OF DBA SCENARIOS FOR PLANT RELOAD OPTIMIZATION FRAMEWORK APPLICATION

The RISA plant reload optimization project aims to support the U.S. nuclear industry in the effort of license applications for enhanced fuel reload strategies. To do this, DBA scenarios listed in NUREG-0800 [15] need to be analyzed while applying the plant reload optimization concept. During Phase 1 (FY-2019 and FY-2020) of the project, DBA scenarios in NUREG-800 were reviewed, and ten DBA scenarios shown in Table 4-1 were selected. By using Zion 4-loop Westinghouse PWR model, ten DBA scenarios are assessed in a one-dimensional (1D) deterministic method by using RELAP5-3D and compared with a reference value in order to provide a basis for future risk-informed analyses [2]. This approach will provide the possibility of using NUREG-800, Chapter 19, "Probabilistic Risk Assessment and Severe Accident Evaluation for New Reactors."

Table 4-1. Selective DBA scenarios in Chapter 15.

DBA Scenario	Section in Chapter 15
Steam system piping failure.	15.1.5
Turbine trip.	15.2.3
Loss of nonemergency AC power to the plant auxiliaries.	15.2.6
Reactor coolant pump shaft seizure (locked rotor).	15.3.3
Chemical and volume control system (CVCS) malfunction that results in a decrease in the boron concentration in the reactor coolant.	15.4.6
Spectrum of rod cluster control assembly ejection accidents.	15.4.8
Inadvertent operation of the emergency core cooling system during power operation.	15.5.1
Steam generator tube rupture (SGTR).	15.6.3
Loss of coolant accidents.	15.6.5
Feedwater system malfunctions that result in an increase in feedwater flow.	15.3.2

In FY-2021, the Zion RELAP5-3D model was updated to simulate other U.S. PWRs. Ten selective scenarios were analyzed with multi-dimensional components, as indicated by their MULTID input cards, to simulate the complex phenomena in the reactor vessel area during DBA scenarios. Nodalization in the reactor core was changed to a finer mesh in the axial and radial directions. RAVEN code was used to control RELAP5-3D simulation and uncertainty quantification for a LOCA scenario, as well as to test RAVEN's capabilities to support future risk-informed analyses.

The MULTID component in RELAP5-3D allows the user to model more accurate multi-dimensional hydrodynamic features of reactor applications, primarily in the vessel (i.e., core, downcomer) and steam generator. The multi-dimensional component defines 1D, 2D, or three-dimensional (3D) array of volumes and the internal junctions connecting the volumes. The geometry can be either Cartesian or cylindrical. An orthogonal, 3D grid is defined by mesh interval input data in each of the three coordinate directions. It is also possible to add the full momentum flux terms, as well as the associated input processing and checking.

4.1 RELAP5-3D Model

The following code versions are used for the work herein:

- RELAP5-3D, Version 4.4.2
- RELAP5-3D, best estimate plus uncertainty (BEPU) Version 4.4.2
- RAVEN, Version 2.0
- SNAP, RELAP5 graphic user interface

4.1.1 Component Numbering and Layout

RELAP5-3D nodalization of the reference plant is shown in Figure 4-1.

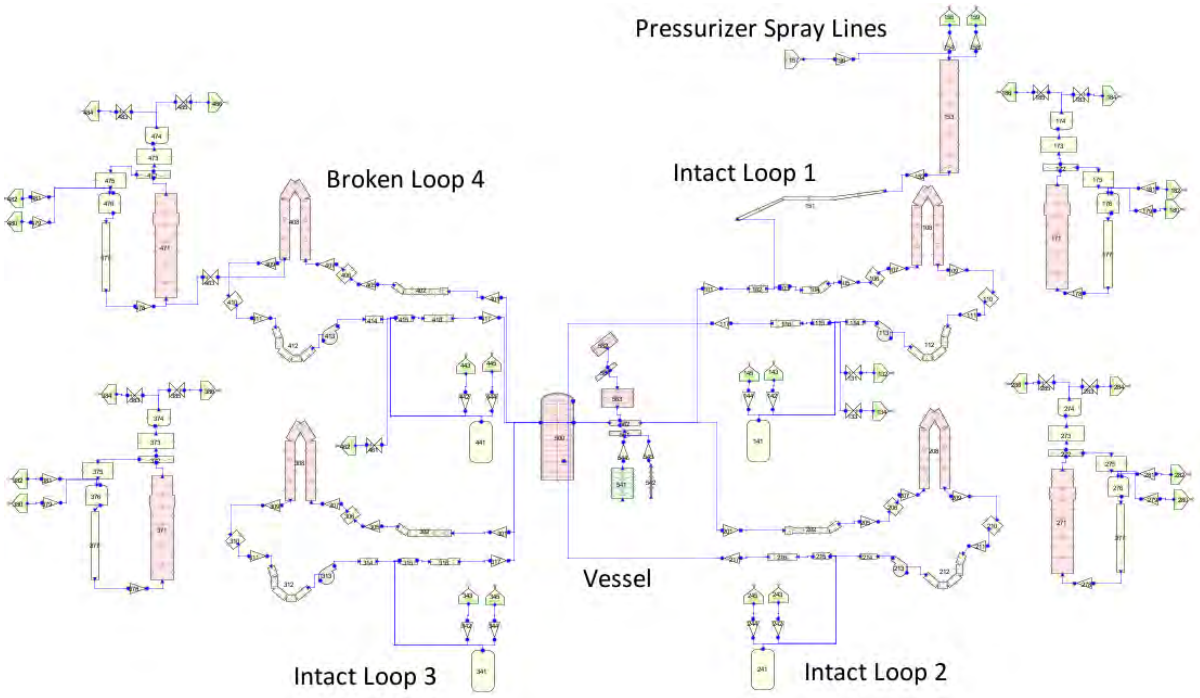

Figure 4-1. RELAP5-3D nodalization of reference plant.

The reference model is intended to have a component naming and numbering scheme that makes the identification of components as easy as possible. The numbering scheme is characterized as follows:

- Loops:
  - The intact loops are assigned numbers 1 through 3, and the “broken” loop is 4, which will generally be used to impose any asymmetric condition affecting loop 1. In the description below, X is the loop number.
  - The pressurizer (PRZ) is connected to loop 1.
  - The primary coolant loop components are numbered X01 through X17. There is room for component numbering up to X30.
  - The steady state (SS) charging, and letdown components are numbered 131 through 134. There is room for component numbering up to X40.
  - The safety injection (SI) components are numbered X41 through X45. There is room for component numbering up to X50.

- The PRZ components are numbered X51 through X59. There is room for component numbering up to X60.
- The break-related components are numbered X61, X62, and X63. There is room for component numbering up to X70.
- The secondary components are numbered X71 through X86. There is room for component numbering up to X89.
- The PRZ spray line components are numbered X90.

- Vessel:
  - The lower plenum and downcomer components from FY-2020 activity [2] were replaced with a multi-dimensional component 500. Multiple junction components 501, 502, and 503 are used to connect the MULTID component to the rest of the vessel. This process is further explained in the next section.
  - The core components are numbered 541 through 545. There is room for component numbering up to 560.
  - The upper plenum components are numbered 561 through 563. There is room for component numbering up to 580.
  - The upper head components are numbered 581 through 582. There is room for component numbering up to 599.
- Heat Structures:
  - The numbering convention is CCCN, where CCC is the lowest component number among the connected fluid channels, and N is 0 for the first connection to a component number and it is increased by 1 for each additional heat structure attached.

The naming convention for the fluid components is that there is an acronym representing the identity of the component. At the end, i1, i2, or i3 are listed for intact loops 1 through 3, while b4 represents broken loop 4. The acronyms should be consistent across all 4 loops; the names are only differentiated by the i1, i2, i3, or b4.

The naming convention for the heat structures is to use a descriptive name to the extent possible. When “vess” is in the name, this indicates that it is part of the vessel wall, and therefore uses an outside “symmetry” condition, while “inthts” in the name indicates an internal heat structure; thus, the inside connection is either a symmetry or a copy of the outside connection for two-sided heat transfer.

4.1.2 Plant-Specific Inputs

To enhance the capabilities of the reference model, the geometry—which was based on the Zion model—was updated for the reference plant design for some key parameters. One of these enhancements was the steam generator (SG) tube geometry, which was revised to reflect the radii and heat transfer surface area of the reference model plant.

Another change was the core modeling. In order to model the Chapter 15 safety analyses, it is necessary to have a model with different power shapes. In order to implement this, the existing core pipe was split into two pipes, and the existing rods heat structure was split into two heat structures. The first pipe is the hot assembly pipe, which means that it models a single assembly connected to the hot assembly heat structure. The second pipe is the average assembly pipe, which means that it models a single assembly connected to the average assembly heat structure. The following information from the reference plant was used to calculate the required information for the model:

- Heat flux channel factor (FQ) – Ratio of the maximum local power to the core average power. This is set to a value of 2.55.
- FΔH – Ratio of the power generated in the hot rod to the power generated in an average rod. This is set to a value of 1.65. Note that this is implemented as the ratio of the power generated in the hot assembly—rather than the rod—to the power generated in an average rod, for simplicity.
- Number of Assemblies – This is set to a value of 193.
- Power Deposition – The fraction of power, which is generated within the fuel rod, as opposed to that which is deposited directly into the moderator, generally by gamma rays. The value of 0.974 is consistent with the typical PWR model input and it is used in most safety analyses.
- Core Length – The fueled length of the reactor core is 12 ft. This is the length of most PWR cores.
- Number of Core Cells – Based on the base model, 6 cells are used to represent the core.

The linear power fraction is shown in Figure 4-2. This shows that a top-skewed cosine type power shape is modeled, as desired.

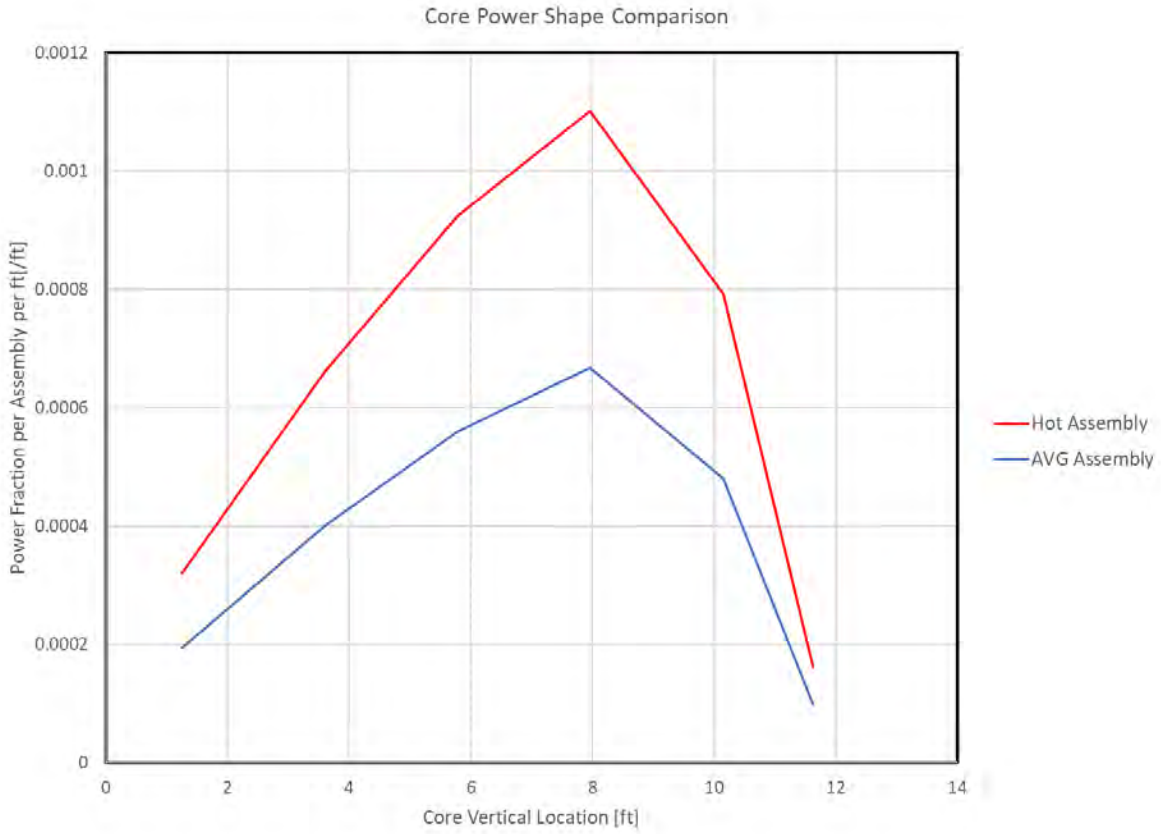

Figure 4-2. Core power shape used.

4.1.3 Update of Model

From the research conducted in FY-2020, one major improvement was the suggestion of remodeling the vessel components—specifically the downcomer and lower plenum portions [2]. The error of the vessel component modeling was found clearly during the examination of the large break LOCA, where the transient (TR) input required a non-physical form loss (500) at the vessel to the broken cold loop junction for the TR to not fail.

Therefore, the overall goal of this 1D to 3D vessel conservation was to add fidelity to the TRs that considered the downcomer and lower plenum nodding important. When no form loss was applied to the broken cold leg, the large break LOCA TR saw zero liquid penetrate the lower plenum. It was assumed that the 1D downcomer was one of the main contributing factors. Therefore, by converting the 1D components to a MULTID component, liquid penetration is more likely to occur. Only some TRs are expected to improve due to this change, but to keep the process streamlined, all TRs will be run with the updated model moving forward. While the vessel update was the main objective, other model updates were investigated and implemented. These changes are documented herein.

4.1.3.1 Model Update Assumptions

The following are the assumptions made for the 1D to 3D model conversion:

- The original geometry is assumed to be correct and kept the same from the conversion of 1D components to the MULTID. There are multiple locations where changes were made to enhance the accuracy of the model, such as the modeling of hot leg obstructions.
- When converting to a MULTID component, specific radii are required to be inputted into the model. The original components only had areas. To figure out the true radii—specifically for the downcomer gap—the Zion facility vessel drawings were used. Using the drawings, a new downcomer area of 26.22 ft^2 was used instead of the original 26.72 ft^2. The calculated value is currently being used.
- The original model specifies the hydraulic diameter (HD) in all downcomer components that were removed. The equivalent values are applied in the MULTID component at their equivalent locations in the Z direction. The HD in the X and Y (or radial and azimuthal) directions are left at zero and calculated by RELAP5-3D. It is assumed that the calculated values are realistic representations of the actual facility. Lower plenum values were kept at zero. It is suggested to re-evaluate this decision later, but it is not needed for the current work.
- The connection between the lower core support plate (CSP) and the core had to be changed as well. In the original 1D model, two junctions connecting the CSP to the core and the hot rod were made. This connecting face is the location where the MULTID component ends. In the 3D model, there are four azimuthal divisions. All four are connected to the hot rod. The connecting areas match the core/hot rod areas:
  - The original form losses applied to the junction connecting the CSP to the average core were divided by four and applied at each junction. This area was set as an abrupt area change in the original model and stayed that for this update. It is suggested that in the future, a smooth area may be more realistic.
  - The connection between the CSP and the hot rod is set to be a smooth area and zero form losses were applied. The area of the hot rod is set to be that of a single rod; however, setting it to be the area of four rods due to core symmetry is suggested in the future.
- The HD of the lower plenum and the CSPs are left at 0 because both regions represent a large open area. The geometry of the actual CSP is unknown. The original 1D model left these values at 0.
- Vertical stratification was turned on in all locations in the 1D vessel model. For this update, it is not turned on in locations within the MULTID since it is not available.
- The top node of component 524 of the original model had a length of 1.5 ft. and an elevation change of 1.1978 ft. The MULTID component does not allow angled cells, so the elevation is set as the cell height instead of the original height. The volume is accounted for and conserved.
- There is an issue with specific cells in the MULTID component. Specifically, cells R3A1Z3 and R3A2Z3 cannot be selected by signal variables or heat structures because the re-nodalization feature was used to reduce the original radial nodes from 6 to 3. As a result, for signal variables, an adjacent

cell is called. For the heat structures, the cylinder height/surface area is set to a very small non-zero (zero is not allowed) in the location that is an issue and all locations that are symmetric to that cell. This is likely to cause small changes, but not the overall results trends. This issue is with the model editor SNAP, and not due to RELAP5-3D.

4.1.3.2 Downcomer and Lower Plenum Modifications

The downcomer was identified with an original 1 azimuthal sector and 1 radial sector. The 3D vessel was created initially to have 16 azimuthal divisions and 6 radial divisions. It was determined that this level of complexity was not required for the purposes of this project and the large number of cells may have had a large increase in runtime. Because of this, the 3D vessel was re-nodalized to have 4 azimuthal divisions and 3 radial divisions. One radial division (e.g., the outer ring, Radial Ring 3) represents the downcomer. Radial Ring 2 represents the DC bypass. The inner ring, Radial Ring 1, represents the core.

The following downcomer components were removed from the model:

- Component 521 – This component represented the lower downcomer region. It is now represented by axial levels 3-10 in Radial Ring 3 of MULTID component 500.
- Component 543 – This component represented the barrel baffle region. It is now represented by axial levels 5-10 in Radial Ring 2 of MULTID component 500.
- Component 522 – This component represented the first level in the upper downcomer. This cell was connected vertically to both the lower downcomer and the barrel baffle region. It is now represented by Axial Level 11 in Ring 3 of MULTID component 500. The connection from this cell to the barrel baffle region was changed from Level 11 to Level 10 and is now connected radially so that it is more in line with the actual facility.
- Component 523 – This component represented the inlet cell of the upper downcomer in the original model. All four cold leg connections were connected at the inlet face of the branch, or at the top of the cell in the vertically downward-facing direction. It is now represented by Axial Level 12 in Radial Ring 3. Each cold leg is connected in the radial direction (e.g., the x axis outlet face) to one of the four azimuthal cells at Level 12 of MULTID component 500.
- Component 524 – This component represented the upper downcomer portion above the inlet level. It was connected to Component 581, but had a noticeably large form loss applied at that location so that it was essentially blocked off. It is now represented by Axial Levels 13-16 in Radial Ring 3 of MULTID component 500. Multiple junction 503 is used to connect the four azimuthal cells at the top of Level 16 to the bottom of Component 581. A large form loss is applied to each junction. It is suggested that this blockage be investigated in the future.

The following lower plenum and CSP components were removed from the model:

- Component 501 – This component represented the bottom level of the lower plenum. It is now represented by Axial Level 1, Radial Rings 1–3, and Azimuthal Sectors 1–4 of MULTID Component 500.
- Component 502 – This component represented the second level of the lower plenum. It is now represented by Axial Level 2, Radial Rings 1–3, and Azimuthal Sectors 1–4 of MULTID Component 500.
- Component 503 – This component represented the lower plenum and lower core plate. It was not connected to the downcomer component. It is now represented by Axial Level 3, Radial Rings 1–3, and Azimuthal Sectors 1–4 of MULTID Component 500.
- Component 504 – This component represented CSP. It was connected to the core baffle component and to both core components. It is now represented by Axial Level 4, Radial Rings 1–3, and Azimuthal Sectors 1–4 of MULTID Component 500. Multiple Junction 501 connects the top face of

all four Ring 1 cells at Level 4 to Component 541. The junction area is 1/4th of Area 541, as is the applied form loss. The top facing area in the MULTID component is set to zero. All cells that have not been specified above have been blocked off completely in the MULTID component. They are inactive and not part of the model. These cells are Ring 1 Axial Levels 5–16 (all azimuthal sectors), and Ring 2 Axial Levels 11–16 (all azimuthal sectors).

Figure 4-3 shows the updated SNAP model from the original 1D model to the model using the MULTID component.

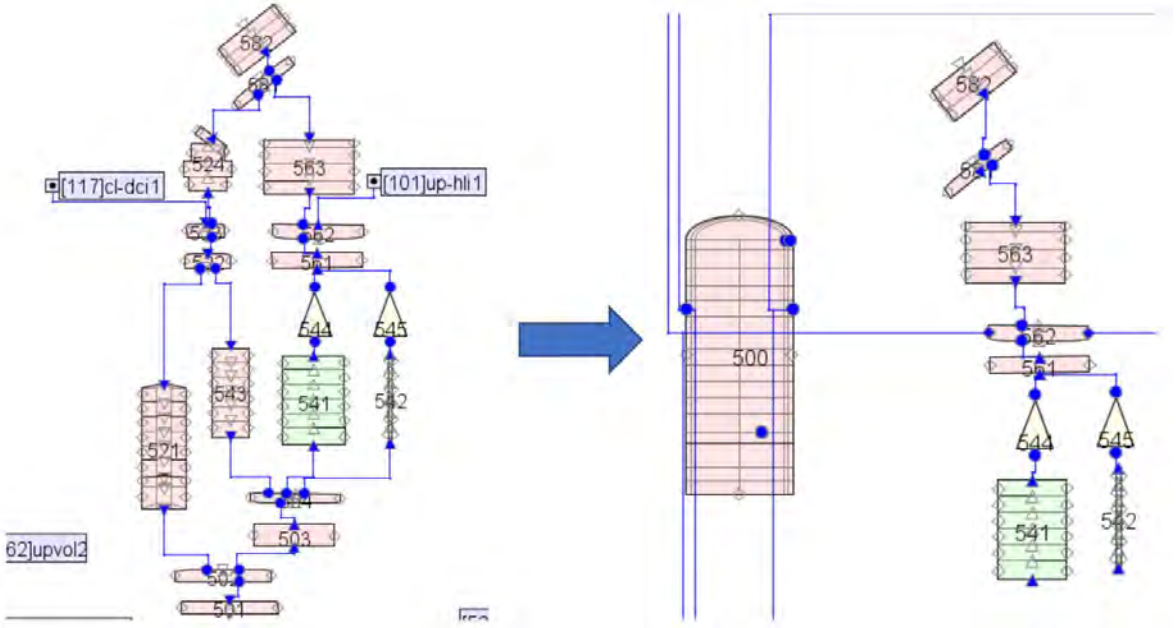

Figure 4-3. 1D vessel (left) and updated MULTID vessel (right)

4.1.3.3 Junction Modifications

All inputs (form losses, hydraulic diameters, area, etc.) present in the removed junctions and components were transposed to the MULTID component unless otherwise noted. Specific locations where the component is now represented by multiple cells connecting to a single cell (such as the CSP connecting to the core), the junction area and form losses were changed to account for this. The updated cold leg connections are shown in Table 4-2. Single junction information was not changed besides the connection inputs.

Table 4-2. Updated cold leg to vessel connections.

Junction	Old Connection In	Old Connection Out	New Connection In	New Connection Out
417	Pipe 416 Cell 2 Outlet	Branch 523 Cell 1 Inlet	Pipe 416 Cell 2 Outlet	MULTID 500 Cell 3,2,12 X Axis Outlet
317	Pipe 316 Cell 2 Outlet	Branch 523 Cell 1 Inlet	Pipe 316 Cell 2 Outlet	MULTID 500 Cell 3,2,12 X Axis Outlet
217	Pipe 216 Cell 2 Outlet	Branch 523 Cell 1 Inlet	Pipe 216 Cell 2 Outlet	MULTID 500 Cell 3,2,12 X Axis Outlet
117	Pipe 116 Cell 2 Outlet	Branch 523 Cell 1 Inlet	Pipe 116 Cell 2 Outlet	MULTID 500 Cell 3,2,12 X Axis Outlet

It is assumed that the reduction in volume from the hot legs is accounted for. With the updated 3D component, the hot legs must be represented in the azimuthal direction as well. Due to the coarse azimuthal mesh, a full blockage is applied at each azimuthal face at the cold leg inlet level. This modeling choice should be evaluated later if the azimuthal mesh is re-nodalized to a finer mesh. By applying zero flow in the azimuthal direction, the emergency core cooling (ECC) liquid is forced to flow in the vertical direction and therefore should increase the downflow greatly. A possible issue maybe that too much liquid goes up instead of down and therefore the azimuthal blockages may not actually be effective. Using calculated form losses for a vessel of similar size would be.302 for a mesh with 16 azimuthal sectors. Therefore, a form loss was applied in the azimuthal direction in all downcomer cells. This value was set as 1.2 (.302 times 4 due to the coarse mesh here) and is applied in both forward and reverse directions. These changes should force the flow path of the incoming liquid to go reach the lower plenum in countercurrent situations like observed during large break loss of coolant accident (LBLOCA) TRs.

4.1.3.4 Heat Structure Modifications

All heat structures connected to vessel related components, were split into 4 heat structures. The only change to the geometry, was dividing the cylinder height by 4 since it is used to calculate the surface area in contact. The updated heat structure component numbering is shown in Table 4-3. The number in the heat structure name indicates the azimuthal sector it is connected to.

Table 4-3. Updated heat structures for vessel components.

Old Heat Structure Name	Old Heat Structure Component Number	New Heat Structures Names	New Heat Structure Component Number
vesslp1	5010	vesslp1	5010
lpinthts	5011	lpinthts1, lpinthts2, lpinthts3, lpinthts4	5011, 5012, 5013, 5014
vesslp2	5020	vesslp3, vesslp4, vesslp5, vesslp6	5020, 5021, 5022, 5023
cbup	5024	cbup1, cbup2, cbup3, cbup4	5024, 5025, 5026, 5027
cblp	5030	cblp1, cblp2, cblp3, cblp4	5030, 5031, 5032, 5033
dcinthts	5210	dcinthts1, dcinthts2, dcinthts3, dcinthts4	5210, 5211, 5212, 5213
vessdccb	5211	vessdccb1, vessdccb2, vessdccb3, vessdccb4	5214, 5215, 5216, 5217
cbcore	5212	cbcore1, cbcore2, cbcore3, cbcore4	5218, 5219, 5220, 5221
vessdcup	5220	vessdcup1, vessdcup2, vessdcup3, vessdcup4	5222, 5223, 5224, 5225
coravgrd	5410	coravgrd	5410

Old Heat Structure Name	Old Heat Structure Component Number	New Heat Structures Names	New Heat Structure Component Number
baffcore	5411	baffcore1, baffcore2, baffcore3, baffcore4	5411, 5412, 5413, 5414
corhotrd	5420	corhotrd	5420
upinthts	5610	upinthts	5610
uhinthts	5810	uhinthts	5810
vessuh1	5820	vessuh1	5820
vessuh2	5821	vessuh2	5821

4.2 Control Logic Input

The general layout of the control variables (CVs) is to produce measured quantities with the first sets of CVs numbers 0 through 399. These measured quantities are then used in the CVs that enact the desired SS control mechanisms (e.g., CVs 400 through 599) or TR control mechanisms (e.g., CV numbers 600 through 899). Note that CVs related to the downcomer and lower plenum was updated appropriately for the new MULTID component.

4.2.1 Quantity Control Variables

4.2.1.1 Mass Calculation (CVs 1 through 33)

These variables are presented in the 'QTY Masses' tab of the SNAP model.

The mass calculation is performed using the total density (e.g., RELAP5-3D variable 'RHO') from a given fluid volume in kg/m^3, because all internal RELAP5-3D control calculations are performed in SI, regardless of unit options, and multiplying by the geometric volume of that fluid volume in ft^3 as a scaling factor for that term. Finally, an overall scaling factor of 0.062428 m^3-lbm/ft^3-kg (e.g., based on 0.028317 m^3/ft^3 and 2.20462 lbm/kg) is used. This produces mass values in lbm.

The sets of CVs are broken out as follows:

- CVs 1 through 5 sum the masses in the core, upper plenum, lower plenum, downcomer, and upper head, respectively. Three additional control blocks were added due to the MULTID component. CV 4 only contains 1/4th of the downcomer. CVs 852, 853, and 856 were added due to the inability of the codes to list more than 50 inputs.
- CV 6 sums CVs 1 through 5 to obtain a total vessel mass.
- CVs 7 through 11 sum the masses in the hot leg, SG primary side, crossover leg, cold leg, and PRZ (plus the surge line), respectively, for Intact Loop 1.
- CVs 12 through 15 sum the masses in the hot leg, SG primary side, crossover leg, and cold leg, respectively, for Intact Loop 2.
- CVs 16 through 19 sum the masses in the hot leg, SG primary side, crossover leg, and cold leg, respectively, for Intact Loop 3.
- CVs 20 through 23 sum the masses in the hot leg, SG primary side, crossover leg, and cold leg, respectively, for Broken Loop 4.
- CVs 25 through 27 produce total primary side masses for Loops 1 through 4, respectively, by summing the appropriate CVs described above.
- CV 28 sums CVs 6 and 24 through 27 to produce a total primary side mass.

- CVs 29 through 32 produce total secondary side masses for Loops 1 through 4, respectively, by summing the appropriate masses.
- CVs 29 through 32 produce total secondary side masses for Loops 1 through 4, respectively, by summing the appropriate masses.
- CV 33 sums CVs 29 through 32 to produce a total secondary side mass.

Room is left in the numbering to allow mass CVs through 49. In the next phase, the new CVs should be renamed into the open spaces between 32 and 49.

4.2.1.2 Level Calculation (CVs 50 through 62)

These variables are presented in the 'QTY Levels' tab of the SNAP model.

The level calculation is performed using the liquid fraction (e.g., RELAP5-3D variable 'VOIDF') from a given fluid volume (unitless) and multiplying by the elevation change in ft. (for vertical components, this is the geometric length of that fluid volume) as a scaling factor for that term. This produces level values in ft.

The sets of CVs are broken out as follows:

- CVs 50 through 55 and 62 calculate the levels in the lower plenum, downcomer, barrel/baffle, average core, upper plenum, upper head, and hot core, respectively.
- CV 56 calculates the level in the PRZ.
- CVs 57 through 60 calculate the levels in the SG secondary side for Loops 1 through 4, respectively.
- CV 61 takes the minimum of the levels in the four SGs (e.g., CVs 57 through 60). This is used for the low SG level reactor trip logic.

Room is left in the numbering to allow level CVs through 69. CVs 854 and 857 were created due to the codes limit of 50 inputs per CV. These each represent half of the downcomer. Each liquid level input is integrated using CVs 858 through 860. This was used for analysis of the TRs. In the next phase, it is suggested that these numbers be renamed so that they take up the free numbers available.

4.2.1.3 Pressure Drop Calculation (CVs 70 through 95)

These variables are presented in the 'QTY DPs' tab of the SNAP model.

The pressure drop calculation is performed using the pressure (e.g., RELAP5-3D variable 'P') from a given fluid volume in Pa, because all internal RELAP5-3D control calculations are performed in SI, regardless of unit options, and subtracting the pressure from the applicable downstream fluid volume. Finally, an overall scaling factor of 0.00014504 psi/Pa is used. This produces pressure drop in psi.

The pressure drops in this section are chosen to create a full accounting of the pressure drop around each loop. This starts at the cell after the pump and ends with the cell before the pump. This is appropriate, as the pump adds head. The breakdown is based on the availability of pressure drops in Chapters 4 and 5 of the Final Safety Analysis Report (FSAR).

The sets of CVs are broken out as follows:

- CV 70 calculates the core pressure drop.
- CVs 71 through 74 calculate the vessel pressure drop—including the hot and cold leg nozzles—for Loops 1 through 4, respectively.
- CVs 75 through 78 calculate the pressure drops across the hot leg for Loops 1 through 4, respectively.
- CVs 79 through 82 calculate the pressure drops across the SG for Loops 1 through 4, respectively.

- CVs 83 through 86 calculate the pressure drops across the crossover leg for Loops 1 through 4, respectively.
- CVs 87 through 90 calculate the pressure drops across the cold leg for Loops 1 through 4, respectively.
- CVs 91 through 95 calculate the average pressure drops of the four loops for the vessel, hot leg, crossover leg, cold leg, and SG, respectively.

Room is left in the numbering to allow pressure drop CVs through 99.

4.2.1.4 Bypass Flow Calculation (CVs 100 through 102)

These variables are presented in the 'QTY Core Byp' tab of the SNAP model.

The bypass flow calculation is performed by dividing the total reactor cooling system (RCS) mass flow (e.g., RELAP5-3D variable 'MFLOWJ'), which is obtained by summing all of the cold leg nozzle flows, by the flow through the upper head spray nozzles and then multiplying by 100. This produces a bypass flow in percentages.

It should be noted that all bypass flow sources described in Chapter 4 of the FSAR are lumped into only the upper head spray nozzle flow in this model. There is not an existing thimble plug bypass component, although that would be expected to produce a significant amount of the bypass flow. The current model uses the form loss coefficient of 250.0 in both directions. This value should be investigated in the future.

The CVs are broken out as follows:

- CV 100 calculates the total RCS mass flow.
- CV 101 calculates the total bypass mass flow.
- CV 102 calculates the bypass flow as a percentage of total mass flow.

Room is left in the numbering to allow bypass flow CVs through 109.

4.2.1.5 Secondary Side Flow Calculations (CVs 110 through 129)

These variables are presented in the 'QTY SG Sec Flow' tab of the SNAP model.

There are two calculated outputs from this section:

- The recirculation ratio calculation is performed by dividing the SG downcomer mass flow (e.g., RELAP5-3D variable 'MFLOWJ') by the SG steam flow for each SG. This produces a recirculation ratio, which is unitless.
- A calculation is also included, which finds the difference between the steam and the feed flow for each SG. This difference is in lbm/s.

For each mass flow rate CV, because all internal RELAP5-3D control calculations are performed in SI, regardless of unit options, an overall scaling factor of 2.20462 lbm/kg is used.

The CVs are broken out as follows:

- CVs 110 through 113 are the downcomer flow for each SG.
- CVs 114 through 117 are the steam flow for each SG.
- CVs 118 through 121 are the main feedwater (MFW) flow for each SG.
- CVs 122 through 125 are the recirculation ratio for each SG.
- CVs 126 through 129 are the steam flow minus the MFW flow for each SG.

Room is left in the numbering to allow secondary side flow CVs through 149.

4.2.1.6 RCS Mass Flow Calculation (CVs 150 through 154)

These variables are presented in the 'QTY RCS Flow' tab of the SNAP model.

These variables point to RELAP5-3D variable 'MFLOWJ,' and because all internal RELAP5-3D control calculations are performed in SI, regardless of unit options, an overall scaling factor of 2.20462 lbm/kg is used. Thus, they are in lbm/s.

The CVs are broken out as follows:

- CVs 150 through 153 are the pump flow for each loop.
- CV 154 takes the minimum of the four loops. This is used for the low RCS flow reactor trip logic.

Room is left in the numbering to allow RCS mass flow CVs through 159.

4.2.1.7 Temperature Calculation (CVs 160 through 175)

These variables are presented in the 'QTY Temps' tab of the SNAP model.

Most of these variables simply point to RELAP5-3D variable 'TEMPF,' and because all internal RELAP5-3D control calculations are performed in SI, regardless of unit options, a term scaling factor of 1.8 F/K is used and an overall additive factor of -459.67 is used. Thus, they are in degrees Fahrenheit (F).

The CVs are broken out as follows:

- CVs 160 through 163 are the hot leg temperature, measured at the first cell after the hot leg nozzle.
- CV 164 through 167 are the cold leg temperature, measured at the last cell before the cold leg nozzle.
- CVs 168 through 171 are the SG secondary side temperature, measured in the downcomer.
- CV 172 is the vessel average temperature, taken as the average of CVs 160 through 167.
- CV 173 is the hot leg average temperature, taken as the average of CVs 160 through 163.
- CV 174 is the cold leg average temperature, taken as the average of CVs 164 through 167.
- CV 175 is the RCS saturation temperature, taken as the saturation temperature at cell 1 of hot leg 1 (component 102). This cell is chosen because a point at hot leg temperature will result in a lower saturation temperature. Loop 1 is chosen arbitrarily, because the variation between loops is negligible.

Room is left in the numbering to allow temperature CVs through 179.

4.2.1.8 Pressure Calculation (CVs 180 through 185)

These variables are presented in the 'QTY Pressures' tab of the SNAP model.

These variables simply point to RELAP5-3D variable 'P,' and because all internal RELAP5-3D control calculations are performed in SI, regardless of unit options, an overall scaling factor of 0.00014504 psi/Pa is used. Thus, they are in psi.

The CVs are broken out as follows:

- CV 180 is the PRZ pressure, measured in the top cell.
- CVs 181 through 184 are the SG secondary side pressures, measured in the steam dome.
- CV 185 is the PRZ pressure, measured in the top cell.

Room is left in the numbering to allow pressure CVs through 199.

4.2.2 Steady State Control Logic

4.2.2.1 Steady State Power Controller (CVs 400 through 407)

This logic is presented in the 'SS Core Power' tab of the SNAP model.

This controller works as follows:

- CV 400 is a constant which is the desired SS rated core power [W]. It uses the numeric '$COREPNUM.'
- CV 401 is the current total core power from 'rktpow' divided by CV 400 and multiplied by 100. This produces the current core power as a percent of rated core power [%].
- General Table 400 is a table of % of rated core power vs. time. For a normal SS, this will be 100 for all times.
- CV 402 is a value taken from General Table 400 at the current time [%].
- CV 403 adds a one second lag to the desired core power on CV 402, so that the comparison used for reactivity change gives the system time to react to the reactivity changes [%].
- CV 404 calculates the deviation between the current core power and the desired core power, and then scales it by 1.0e-2, to avoid huge reactivity changes [delta-k per % RTP].
- CV 405 is a proportional integral of CV 404, and it is used directly as a reactivity insertion.

This control setup essentially allows the user to specify a rated core power value in the numeric $COREPNUM, and then input a table of desired core power (in % of rated thermal power) as a function of time in General Table 400. The logic adjusts a reactivity adder to obtain that power.

CVs 406 and 407 are added to produce the acceptance bands for use in the SS calibration plots for core power. CV 406 is the upper acceptance boundary (+1%) and CV 407 is the lower acceptance boundary (-1%). The +/- 1% acceptance band is chosen arbitrarily.

CV 405 is also present in the TR input file set as a constant. The RAVEN ensemble model functionality is used to set the value to the end of SS value.

Room is left in the numbering to allow SS power CVs through 409.

4.2.2.2 Steady State Pump Speed Controller (CVs 410 through 425)

This logic is presented in the 'SS Core Power' tab of the SNAP model.

This controller works as follows:

- CV 410 is a constant that is the desired SS loop flow rate per loop [gpm]. It uses the numeric '$RCSFLOWNUM.'
- CVs 411 through 414 are the desired mass flow rate [lbm/sec] for each of the loops. This is calculated by taking the RCS flow rate per loop in gpm (CV 410) and multiplying by the density from the pump component (kg/m^3). This is then multiplied by a factor, as follows:
  - $(gal\text{-}kg/min\text{-}m^3)*(1\ m^3 / 264.172\ gal)*(1\ min / 60\ sec)*(2.20462\ lbm/kg)=0.00013909$
  - thus, desired mass flow rate in each loop in lbm/sec is obtained.
- The sensed mass flow rate value (CVs 150 through 153) is then subtracted from the desired mass flow rate (CVs 411 through 414) to obtain the mass flow rate deviation in lbm/sec (CVs 415 through 418).
- The mass flow rate deviation (CVs 415 through 418) is fed into a proportional integral function (CVs 419 through 422); this value is directly used as the pump speed input [rev/min].

- Note that the coefficients in the proportional integral function are arbitrary values that obtain the desired value.

This control setup essentially allows the user to input a desired RCS flow rate in gpm per loop for numeric '$RCSFLOWNUM,' and then adjusts the pump speeds to obtain the correct flow rate in all four pumps.

CVs 423, 424, and 425 are added to produce the acceptance bands for use in the SS calibration plots for loop mass flow rate. Because the desired value used in the controller is in gpm, CV 423 is added to specify a desired value in lbm/sec, which uses the numeric '$RCSFLO2NUM.' CV 424 is the upper acceptance boundary (+1%) and CV 425 is the lower acceptance boundary (-1%). The +/- 1% acceptance band is chosen arbitrarily.

Room is left in the numbering to allow SS Pump Speed CVs through 429.

4.2.2.3 Steady State Steam Flow Controller (CVs 430 through 446)

This logic is presented in the 'SS Steam Flow' tab of the SNAP model.

This controller works as follows:

- CV 430 is a constant, which is the desired SS cold leg temperature [°F]. It uses the numeric '$CLTEMPNUM.'
- The sensed cold leg temperature value (CVs 164 through 167) is then subtracted from the desired cold leg temperature (CV 430) to obtain the cold leg temperature deviation in °F (CVs 431 through 434).
- The cold leg temperature deviation (CVs 431 through 434) is fed into a proportional integral function (CVs 435 through 438), the value is limited between 0 and 1, and this value is directly used as the steam valve open fraction [-].
- Note that the coefficients in the proportional integral function are arbitrary values, which obtain the desired value.

This control setup essentially allows the user to input a desired cold leg temperature (in °F) for the numeric '$CLTEMPNUM,' and then adjusts the steam valve flow area to obtain the correct flow rate in all four SGs.

CVs 439 and 440 are added to produce the acceptance bands for use in the SS calibration plots for the cold leg temperature. CV 439 is the upper acceptance boundary (+1%) and CV 440 is the lower acceptance boundary (-1%). The +/- 1% acceptance band is chosen arbitrarily.

CVs 441, 442, and 443 are added to produce the acceptance bands for use in the SS calibration plots for the hot leg temperature. Since the control logic is actually based on the cold leg temperature, CV 441 is added to specify a desired hot leg temperature (in °F) using the numeric '$HLTEMPNUM.' CV 442 is the upper acceptance boundary (+1%) and CV 443 is the lower acceptance boundary (-1%). The +/- 1% acceptance band is chosen arbitrarily.

CVs 444, 445, and 446 are added to produce the acceptance bands for use in the SS calibration plots for SG pressure. Since this parameter is a consequence of other control logic, rather than a target, CV 444 is added to specify a desired SG pressure (in psia) for the numeric '$STMPRESS2NUM.' CV 445 is the upper acceptance boundary (+3%) and CV 446 is the lower acceptance boundary (-3%). The +/- 3% acceptance band is chosen arbitrarily.

Room is left in the numbering to allow SS steam flow CVs through 449.

4.2.2.4 Steady State Feedwater Flow Controller (CVs 450 through 467)

This logic is presented in the 'SS Feed Flow' tab of the SNAP model.

This controller works as follows:

- CV 450 is a constant, which is the desired SS SG level [ft]. It uses the numeric '$SGLEVELNUM.'
- The sensed SG level value (CVs 57 through 60) is then subtracted from the desired SG level (CV 450) to obtain the SG level deviation in ft. (CVs 451 through 454).
- The SG level deviation (CVs 451 through 454) is fed into a proportional integral function (CVs 455 through 458) to obtain a feedwater mass flow adder [lbm/sec].
- Note that the coefficients in the proportional integral function are arbitrary values that obtain the desired value.
- The feedwater mass flow adder (CVs 455 through 458) is added to the steam valve flow rate (CVs 114 through 117) to produce the flow rate used directly as a time-dependent flow for feedwater (CVs 459 through 462).

This control setup essentially allows the user to input a desired SG level (in ft.) for the numeric '$SGLEVELNUM.' At steady state, the steam flow and feed flow are the same. As such, the steam flow is used as a base value for the feed flow. The logic then uses the deviation from the level to create an adder to the steam flow rate.

CVs 463 and 464 are added to produce the acceptance bands for use in the SS calibration plots for the SG level. CV 463 is the upper acceptance boundary (+10%) and CV 464 is the lower acceptance boundary (-10%). The +/- 10% acceptance band is chosen arbitrarily.

CVs 465, 466, and 467 are added to produce the acceptance bands for use in the SS calibration plots for SG flow (both feed and steam). Since the control logic is actually based on the cold leg temperature and SG level, CV 465 is added to specify a desired flow rate (in lbm/sec) using the numeric '$SGFLOWNUM.' CV 466 is the upper acceptance boundary (+1%) and CV 467 is the lower acceptance boundary (-1%). The +/- 1% acceptance band is chosen arbitrarily.

Room is left in the numbering to allow the SS feedwater flow CVs through 469.

4.2.2.5 Steady State PRZ Level Controller (CVs 470 through 475)

This logic is presented in the 'SS PRZ Level' tab of the SNAP model.

This controller works as follows:

- CV 470 is a constant, which is the desired SS PRZ Level [ft.]. It uses the numeric '$PRZLEVELNUM.'
- The sensed PRZ level value (CV 56) is then subtracted from the desired level (CV 470) to obtain the PRZ level deviation in ft. (CV 471).
- The PRZ level deviation (CV 471) is fed directly into a sum (CV 472), and limited between 0 and 1. This is used directly as the charging valve position [-].
- The PRZ level deviation (CV 471) is multiplied by -1 and fed into a sum (CV 473), and limited between 0 and 1. This is used directly as the letdown valve position [-].

This control setup essentially allows the user to input a desired PRZ level (in ft.) for the numeric '$PRZLEVELNUM.' When the sensed value is below the desired level, CV 472 is positive and CV 473 is negative. This results in charging flow being on with the valve ramped linearly from fully closed to fully open over a level difference of 0 to 1 ft., and the letdown valve being closed. When the sensed value is above the desired level, CV 472 is negative and CV 473 is positive. This results in letdown flow being on with the valve ramped linearly from fully closed to fully open over a level difference of 0 to 1 ft., and the charging valve being closed.

CVs 474 and 475 are added to produce the acceptance bands for use in the SS calibration plots for PRZ level. CV 474 is the upper acceptance boundary (+10%) and CV 475 is the lower acceptance boundary (-10%). The +/- 10% acceptance band is chosen arbitrarily.

Room is left in the numbering to allow SS PRZ Level CVs through 479.

In order to use these CVs, a time-dependent volume and valve was added for both the letdown and charging (valve 131 and time-dependent volume 132 for charging; valve 133 and time-dependent volume 134 for letdown). All the inputs for these components are arbitrary values, as these components are only used to obtain a good SS. These components should be evaluated for applicability before any TR usage.

4.2.2.6 Steady State PRZ Pressure Controller (CVs 480 through 485)

This logic is presented in the 'SS PRZ Pressure' tab of the SNAP model.

This controller works as follows:

- CV 480 is a constant, which is the desired SS PRZ Pressure [psi]. It uses the numeric '$PRZPRESSNUM.'
- The sensed PRZ pressure value (CV 180) is then subtracted from the desired pressure (CV 480) to obtain the PRZ pressure deviation in psi (CV 481).
- The PRZ pressure deviation (CV 481) is fed into a function (CV 482), which uses a General Table (Table 480) to vary the PRZ heaters from off at the desired pressure to 1800 kW at 5 psi below the desired pressure, linearly. This is used directly as the PRZ heater heat [W] distributed evenly in the bottom three cells of the PRZ heater heat structure.

This control setup essentially allows the user to input a desired PRZ pressure in psi for the numeric '$PRZPRESSNUM.' When the sensed value is below the desired level, CV 482 activates the heaters to raise the pressure. When the sensed value is above the desired level, CV 483 activates the spray to lower the pressure.

CVs 484 and 485 are added to produce the acceptance bands for use in the SS calibration plots for the PRZ pressure. CV 484 is the upper acceptance boundary (+1%) and CV 485 is the lower acceptance boundary (-1%). The +/- 1% acceptance band is chosen arbitrarily.

Room is left in the numbering to allow SS PRZ Level CVs through 499.

4.2.2.7 Steady State DP CVs for Optimizer (CVs 500 through 520)

This logic is presented in the 'SS Pressure Drops' tab of the SNAP model.

This set of control logic is primarily used to create the plots showing a pressure drop (DP) convergence. The CVs for this purpose are described as follows:

- CVs 500, 501, and 502 are used to produce the acceptance bands for use in the SS calibration plots for the vessel DP. CV 500 is used to specify a desired DP (in psi) using the numeric '$DPVESSNUM.' CV 501 is the upper acceptance boundary (+1%) and CV 502 is the lower acceptance boundary (-1%). The +/- 1% acceptance band is chosen arbitrarily.
- CVs 503, 504, and 505 are used to produce the acceptance bands for use in the SS calibration plots for the hot leg DP. CV 503 is used to specify a desired DP (in psi) using the numeric '$DPHLNUM.' CV 504 is the upper acceptance boundary (+1%) and CV 505 is the lower acceptance boundary (-1%). The +/- 1% acceptance band is chosen arbitrarily.
- CVs 506, 507, and 508 are used to produce the acceptance bands for use in the SS calibration plots for the crossover leg DP. CV 506 is used to specify a desired DP (in psi) using the numeric '$DPXLNUM.' CV 507 is the upper acceptance boundary (+1%) and CV 508 is the lower acceptance boundary (-1%). The +/- 1% acceptance band is chosen arbitrarily.

- CVs 509, 510, and 511 are used to produce the acceptance bands for use in the SS calibration plots for the vessel DP. CV 509 is used to specify a desired DP (in psi) using the numeric '$DPCLNUM.' CV 510 is the upper acceptance boundary (+1%) and CV 511 is the lower acceptance boundary (-1%). The +/- 1% acceptance band is chosen arbitrarily.
- CVs 512, 513, and 514 are used to produce the acceptance bands for use in the SS calibration plots for the vessel DP. CV 512 is used to specify a desired DP (in psi) using the numeric '$DPSGNUM.' CV 513 is the upper acceptance boundary (+1%) and CV 514 is the lower acceptance boundary (-1%). The +/- 1% acceptance band is chosen arbitrarily.

The remaining CVs in this group are used for the optimizer for the DPs. This consists of the following CVs:

- CVs 515 through 519 obtain the DP deviation from the desired value (calculated as desired minus sensed) for the vessel, hot leg, crossover leg, cold leg, and SG, utilizing CVs 91 through 95 for the sensed values (these CVs are the average of all four loops for each DP segment).
- CV 520 is the sum of all the deviations from CVs 515 through 519.

The description of the use of these CVs in the optimizer was described in Section 4.3. Note that the optimizer is not functional at this time.

Room is left in the numbering to allow SS DP CVs through 529.

4.2.2.8 Steady State Bypass CVs for Optimizer (CVs 530 Through 533)

This logic is presented in the 'SS bypass' tab of the SNAP model.

This set of control logic is primarily used to create the plots, which show bypass flow convergence. The CVs for this purpose are described as follows:

- CVs 530, 531, and 532 are used to produce the acceptance bands for use in the SS calibration plots for core bypass flow. CV 530 is used to specify a desired bypass flow (in %) using the numeric '$COREBYPNUM.' CV 531 is the upper acceptance boundary (+1%) and CV 532 is the lower acceptance boundary (-1%). The +/- 1% acceptance band is chosen arbitrarily.

The remaining CVs in this group are intended for use with an optimizer for the bypass flow. This consists of the following CV:

- CV 533 obtains the bypass flow deviation from the desired value, which is calculated as the desired minus sensed, utilizing CV 102 for the sensed value.

These CVs were intended for use with an optimizer, but early attempts by hand to get the desired bypass flow proved fruitless (e.g., the flow percentage would not change). As such, the bypass flow is abandoned for now. In addition, note that the optimizer is not functional at this time.

Room is left in the numbering to allow SS bypass CVs through 539.

4.2.3 TR Control Logic

4.2.3.1 TR Reactor Trip Control (Variable Trips 410 through 414 and 480, Logical Trips 610 through 614, and General Table 613)

This logic is presented in the 'TR Reactor Trip' tab of the SNAP model.

There are various reactor trips discussed in plant FSARs. The following trips are ignored for now:

- Nuclear Overpower Trips
- Core Thermal Overpower Trips
- Reactor Coolant Pump Undervoltage Trip

- Reactor Coolant Pump Underfrequency Trip
- Reactor Trip on a Turbine Trip (Anticipatory)
- SI Signal Actuation Trip
- Manual Trip
- Solid-State Protection System General Warning Alarm Reactor Trip.

These trips are ignored either due to complexity beyond the scope of the current work because they are related to systems that are outside the scope of this model, or because the inputs needed cannot be located in existing plant documentation.

The following trips are modeled:

- PRZ Low Pressure, which is identified as the numeric '$PRZPLORXTNUM,' Trip 410: This is set to compare CV 180 (i.e., pressure in the PRZ cell adjacent to the power-operated relief valve [PORV]) to this value.
- PRZ High-Pressure, which is identified as the numeric, '$ $PRZPHIRXTNUM," Trip 411: This is set to compare CV 180 (i.e., pressure in the PRZ cell adjacent to the PORV) to this value.
- PRZ High Water Level, which is identified as the numeric, '$PRZLHIRXTNUM,' Trip 412: This is set to compare CV 56 (i.e., PRZ level) to this value.
- Low Reactor Coolant Flow, which is identified as the numeric, '$RCSFLOLORXTNUM,' Trip 413: This is set to compare CV 154 (i.e., the lowest mass flow in any of the four loops) to this value.
- SG Trip (low level), which is identified as the numeric, '$SGLEVLORXTNUM,' Trip 414: This is set to compare CV 61 (i.e., the lowest SG level in any of the four SGs) to this value.

This group of trips can be updated downstream to add other reactor trip conditions needed for the RISA TRs.

The trips are combined as follows:

- Trip 610 combines trips 410 and 411 with an "or" gate.
- Trip 611 combines trips 412 and 413 with an "or" gate.
- Trip 612 combines trips 610 and 611 with an "or" gate.
- Trip 613 combines trips 414 and 612 with an "or" gate.

Overall, this logic functions to trip the reactor if any of the Variable Trips are triggered, and every one of the trips is latched (e.g., once the rods are dropped, they stay there).

Trip 480 is used to take the rod drop delay time into account, using the numeric '$RCCADELNUM.' This trip compares the current time to the RELAP5-3D variable 'TIMEOF' Trip 613 plus the rod drop delay. Because the 'TIMEOF' Trip 613 initializes to -1.0, it can cause this trip to go off before Trip 613. As such, Trip 614 was added, which trips when Trip 480 and Trip 613 trip.

Trip 614 is used as the trip for General Table 613, which is for the reactor trip reactivity insertion (i.e., control rods). When the reactor trip (614) is true, this table inserts negative reactivity as a function of time. The dependent values are entered as 0 to 1, and an overall scaling factor of -5.333 $ is applied, which is a conservatively low value based on the reference plant FSAR for the TRs modeled. The rod position versus time is based on the reference plant FSAR for the TRs modeled.

4.2.3.2 TR PRZ Control (CVs 483, 640, and 641, and General Tables 481, 670, and 690)

This logic is presented in the 'TR PRZ' tab of the SNAP model.

The logic in this section is related to actuation of the PRZ PORV, the PRZ safety valve, and the PRZ spray.

The PORV model is based on generic design information, rather than TR-specific inputs. As such, this logic is generic and without new scenario-specific inputs. The model functions as follows:

- Information from the reference plant FSAR suggests that the PORV should open at 2485 psia and achieve a maximum flow rate of 210,000 lbm/hr of steam. In order to provide stability, it is ramped to that flow rate over an arbitrary pressure range (20 psia).
- The PORV is modeled as time-dependent junction 154 connected to time-dependent volume 155.
- CV 641 and General Table 690 are used to ramp the flow from 0 lbm/sec at 235 psi above the SS pressure to full flow at 255 psi above, using CV 481 (i.e., deviation of the PRZ pressure from desired in psia, calculated as desired minus sensed). This is done so that the setpoint will translate up and down for whatever the SS pressure is set to be. The dependent factor of General Table 690 is used to set the flow rate. For this, the rate of 210,000 lbm/hr is converted to 58.333 lbm/sec.
- Component 154 is set to use the CV 641 mass flows directly.

The PRZ safety valve model is based on generic design information, but has a single TR-specific input. The model functions as follows:

- The PRZ safety valves have a flowrate of 420,000 lbm/hr at 2575 psia and they start to open at 2500 psia, based on the reference plant FSAR. No details are given on the flow development, but a simple linear assumption is used.
- This valve is modeled as time-dependent junction 158 and time-dependent volume 159.
- General Table 670 specifies the safety valve flow rate as a function of the PRZ pressure, linearly ramping flow from 0.0 lbm/sec at a pressure specified by the numeric '$PRZSAFNUM' to 116.67 lbm/s at 2575 psia.
- CV 640 is a function variable that simply uses CV 180 (i.e., the PRZ pressure) as the independent variable in General Table 670, to obtain the PRZ safety valve flow rate in lbm/sec.
- Component 158 is set to use the CV 640 mass flows directly.

The PRZ spray model is based on generic design information, rather than TR-specific inputs. As such, these updates will be generic and without new scenario-specific inputs. There are two different models used for the set of TRs. The model is updated as follows:

- The spray into the PRZ is modeled as Time-Dependent Junction 156 and pulling from Branch 157, which pulls from spray lines 190, 290, 390, and 490:
    - Pipes 190, 290, 390, and 490, as well as accompanying junctions 191, 291, 391, and 491, exist to pull liquid from the cold legs for the spray. The geometry of these components is arbitrary, other than the elevation change.
    - The four elevation change pipes converge at a branch component (Component 157), which has arbitrary geometry.
    - This method is only applied for the loss of offsite power (LOOP) base, charging, and Three Mile Island (TMI) TRs.
- The spray into the PRZ is modeled as Time-Dependent Junction 156, pulling from Time-Dependent Volume 157, which has conditions set to the cold legs.

- Time-Dependent Junction 156 has control logic, which ramps the spray flow from 0 gpm at 10 psia above desired SS pressure to 900 gpm at 60 psia above. In order to better converge the SS, the ramp is from 0 gpm at desired SS pressure during the SS, instead of 10 psi above.
  - General Table 481 specifies velocity as a function of deviation from the desired pressure. For simplicity, the dependent value in the table scales from 0 to 1.0, and a dependent factor is used to apply the correct spray velocity. The dependent factor is set to 2.78037 ft/s (based on 900 gpm and the area of the component).
  - CV 483 uses CV 481 (i.e., deviation of the PRZ pressure from desired in psia, calculated as desired minus sensed) in General Table 481 to obtain the spray velocity.
  - Component 156 is set to use the CV 483 velocities directly.

4.2.3.3 TR Feedwater Control (CVs 600 through 605; Logical Trips 613, 630, and 640; and General Table 640)

This logic is presented in the 'TR Feedwater' tab of the SNAP model.

For the TR feedwater modeling, the following steps are considered:

- After the reactor trip or SI signal, the MFW will start from a SS rate and begin to shut off after logic delays.
- The MFW will have some amount of time to go from full flow to no flow.
- After reactor trip or SI signal, the auxiliary feedwater (AFW) will start from no flow and will begin to ramp up after logic delays.
- The AFW will ramp up over some amount of time, and then continue at a steady rate.

This is implemented as follows:

- General Table 640 is the MFW "status" table. If the reactor trip is false, the time argument is set to -1.0; thus, the value in this table is 1.0. If the trip is true (e.g., the reactor tripped), the factor stays at 1.0 for the duration of the MFW delay time (e.g., the numeric '$MFWDELTIMENUM'), then ramps from 1.0 to 0.0 over the difference between the MFW delay time and the MFW ramp time (e.g., the numeric '$MFWRAMPTIMENUM').
- CV 600 is a function variable using time in General Table 640.
- CVs 601 through 604 multiply CV 600 by the SS MFW flow variables for each loop (CVs 459 through 462). This produces the MFW flow considering reactor trip. Prior to reactor trip, this will just be the SS MFW flow. After reactor trip, it will follow the delay and ramping described above.
- The MFW time-dependent junctions (e.g., Components 179, 279, 379, and 479) are set to have no trip, and to be controlled by CVs 601 through 604 directly.
- The AFW time-dependent junctions (e.g., Components 181, 281, 381, and 481) are set to trip on Trip 640. The flow remains at zero for the duration of the AFW delay time (e.g., the numeric '$AFWDELTIMENUM'), then it ramps from 0 to the full AFW flow rate (e.g., the numeric '$AFWFLONUM') over the difference between the AFW delay time and the AFW ramp time (e.g., the numeric '$AFWRAMPTIMENUM'). The AFW flow rate is specified to continue until 1.0e9 sec.
- Trip 640 is set to be based on the reactor trip (Trip 613) or the SI signal (Trip 630).

  If it is desired to shut off AFW at some point, this logic should be revised.

4.2.3.4 TR Pump Control (CVs 620 through 623; Variable Trips 450 through 457; Logical Trips 650 through 653; and General Tables 680 through 683)

This logic is presented in the 'TR Pump Trip' tab of the SNAP model.

In a pump with velocity controls, there are two separate trips. These are the motor trip, which is word 6 on pump card CCC0301, and the velocity table trip, which is word 1 on pump card CCC6100. If the pump velocity table is being used because the velocity table trip is true, that takes precedence over the motor trip. If the pump velocity table is not being used, then the motor trip is used along with the pump dynamics models.

There are two trips for each of the pumps—one for the velocity table and one for the motor. During the SS, the velocity table trips must be true. During the TR, it will vary with the scenario and the pump. If offsite power is available (OPA), the velocity trip will be left true, and a constant velocity is used for the TR. If there is a LOOP, the velocity trip will be made false, and the pump will continue at a constant speed until the motor trip.

The motor trip is set to become true sometime after reactor trip, based on the numeric '$PMPMOTDELNUM.' Because the motor trip has no effect if the velocity table trip is still being used, the motor trip input can be left this way, even in the case of OPA.

This logic is enacted as follows:

- Variable Trips 450 through 453 (for loops 1 through 4) are set in the SS to be true if time is greater than or equal to 0 (always true). The pumps are set to use these variables for the velocity table trip.
- CVs 620 through 623 (for loops 1 through 4) set to be the RELAP5-3D variable 'TIMEOF' for Trip 613 (reactor trip) plus the numeric $PMPMOTDELNUM.
- Variable Trips 454 through 457 (for loops 1 through 4) are set to be true when time is greater than CVs 620 through 623, respectively.
- Logical Trips 650 through 653 (for loops 1 through 4) are set to trip when Variable Trips 454 through 457 trip, respectively, AND when trip 640 is tripped. This ensures the pumps cannot trip until reactor trip occurs.
- The pump components use trips 650 through 653 for motor trip.

In addition to the TR pump trip controls, this SNAP tab also presents the reactor coolant pump (RCP) heat tables. During hot zero power, the heat to the RCS is provided by some minimal amount of decay heat, and the RCPs. In order to model this, a heat structure is connected to each RCP to supply heat. This setup is only used in TRs with no nuclear power.

The control logic is specified as follows:

- General Tables 680 through 683 are power vs. timetables, which trip off the pump motor trips (e.g., Variable Trips 454 through 457).
- The table data is set to have a value of 1.0 for all negative values, and then ramp to 0 over the first 1 second after trip.
- The actual heat input of the table is set with the dependent factor, which is set in MFW. This factor is set to the numeric '$RCPHEATNUM.'

The heat structures themselves (i.e., heat structures 1131, 2131, 3131, and 4131) use arbitrary geometry and, importantly, deposit all heat directly into the coolant, with the heat coming from General Tables 680 through 683.

4.2.3.5 TR Steam Control (CVs 630 through 633, General Tables 650 and 660)

This logic is presented in the "TR Steam Flow" tab of the SNAP model.

The first function of this logic is to shut off the main steam after reactor trip:

- General Table 650 defines the steam valve position versus time after Trip 640. If the reactor trip is false, the time argument is set to -1.0; thus, the value in this table is the end of SS steam valve position. If the trip is true (i.e., the reactor tripped), the steam valve position ramps to fully closed. This table has five points:
  - At time -1e9 sec, the SS valve position is used.
  - At time 0 sec, the SS valve position is used.
  - At the time set by the numeric '$MSIVDELNUM,' the SS valve position is used.
  - At the time set by the numeric '$MSIVRAMPNUM,' the valve is closed.
  - At time 1e9 sec, the valve is closed.
- In the TR input files, the steam valve position CVs 435 through 438 are re-defined to be functions of General Table 650 (using time after Trip 640).

Thus, in the TR, the steam valve stays at its end of SS position until reactor trip or SI signal, at which point it ramps down to 0 flow after a delay.

The second function of this logic is to implement the main steam safety valves (MSSVs). The MSSV model is based on generic design information, rather than TR-specific inputs. As such, these updates will be generic and without new scenario-specific inputs:

- Based on the reference plant FSAR, the MSSVs have five separate valves at increasing set pressures (e.g., 1199.7 psia, 1214.7 psia, 1224.7 psia, 1234.7 psia, and 1249.7 psia).
- Each valve has the same relieving capacity, and an area of 16 in^2. Thus, they are modeled as a single servo valve per SG, with an area of 80 in^2 (e.g., 0.5556 ft^2).
- The valve area is set to 0 below the minimum set pressure, but 20% area is added at each set pressure (over an interval of 5 psi to help minimize the sudden changes in the code).
- This is accomplished using General Table 660, which sets the area fraction versus pressure. Then CVs 181 through 184 are used with that table to make CVs 630 through 633, which are directly used to control Servo Valves 185, 285, 385, and 485.

4.2.3.6 TR Emergency Core Cooling System (ECCS) Control (Variable Trips 460 through 463, 470, and 471, and Logical Trips 630 and 631)

This logic is presented in the 'TR ECCS' tab of the SNAP model.

The first function of this logic is to set the accumulator actuation pressure:

- Variable Trips 460 through 463 are set to trip when the pressures in the cold legs are less than the pressures in the accumulators.

The second function of this logic is to manage trips for initiating SI:

- Variable Trip 470 is set to trip when the lowest pressure in any SG (CV 185) is less than the SI signal low steam pressure setpoint (e.g., the numeric '$SITRPLSPNUM').
- Logical Trip 630 is set as an OR gate for Trip 470 and Trip 401 (always false). This is set up to facilitate additional SI signal setpoints in the future.

- Trip 480 is used to take the SI signal delay time into account, using the numeric '$SITRPDELNUM.' This trip compares the current time to the RELAP5-3D variable 'TIMEOF' Trip 630 plus the SI signal delay. Because the 'TIMEOF' Trip 630 initializes to -1.0, it can cause this trip to go off before Trip 630. As such, Trip 631 was added, which trips when Trip 471 and Trip 630 trip.
- Trip 631 is used as the trip to actuate Charging Components 144, 244, 344, and 444. When activated, these components inject liquid as a function of pressure in the cold leg.

4.2.3.7 TR Plot Variables (Variable Trip 490 and CVs 800 through 827)

This logic is presented in the 'TR Plot Vars' tab of the SNAP model.

Each set of plot variables is discussed as follows:

- CVs 800 through 802 are used to make core mass flow as a fraction of nominal:
  - CV 800 is set as a constant equal to the initial nominal reactor vessel mass flow in lbm/sec (e.g., the numeric '$RCSVMFLO2NUM').
  - CV 801 is the total core mass flow rate in lbm/sec. This is created by summing the mass flow at the Internal Junction 3 of Components 541 and 542. An overall scaling factor of 2.20462 lbm/kg is used.
  - CV 802 divides CV 801 by CV 800, thus creating the vessel mass flow as a fraction of nominal.
- CVs 803, 153, and 804 are used to make Loop 4 mass flow as a fraction of nominal:
  - CV 803 is set as a constant equal to the initial Nominal Loop 4 mass flow in lbm/s (e.g., the numeric '$RCSMFLO2NUM').
  - CV 153 is the Loop 4 mass flow rate in lbm/sec.
  - CV 804 divides CV 153 by CV 803, creating the Loop 4 mass flow as a fraction of nominal.
- CVs 805 through 807 are used to make average rod heat flux as a fraction of nominal:
  - CV 805 is set as a constant equal to the initial nominal heat flux in the average channel at Node 4 in BTU/sec-ft^2 (e.g., the numeric '$ACHFLUXNUM').
  - CV 806 is the average channel heat flux in BTU/sec-ft^2. This is created by using the RELAP5-3D variable 'HTRNR' from Node 4 of Heat Structure 5410. An overall scaling factor of 8.8055e-5 (BTU/s-ft^2)/(W/m^2) is used.
  - CV 807 divides CV 806 by CV 805, creating the average channel heat flux as a fraction of nominal.
- CVs 808 through 810 are used to make hot rod heat flux as a fraction of nominal:
  - CV 808 is set as a constant equal to the initial nominal heat flux in the hot channel at Node 4 in BTU/sec-ft^2 (e.g., the numeric '$HCHFLUXNUM').
  - CV 809 is the hot channel heat flux in BTU/sec-ft^2. This is created by using the RELAP5-3D variable 'HTRNR' from Node 4 of Heat Structure 5420. An overall scaling factor of 8.8055e-5 (BTU/s-ft^2)/(W/m^2) is used.
  - CV 810 divides CV 809 by CV 808, creating the hot channel heat flux as a fraction of nominal.
- CV 811 is set as the core power as a fraction of nominal. This is done by dividing CV 401 by 100.
- CV 822 is set as the core power as a fraction of nominal for hot zero power (HZP) cases. This is done by dividing RELAP5-3D variable 'RKTPOW' by a static value of 3626 MW.

- CVs 812 and 813 are used to make maximum cladding temperature in °F:
  - CV 812 is set to take the maximum of every radial node in the cladding of the hot rod in K (e.g., Nodes 9 through 17 of Axial Cell 4 of Heat Structure 5420).
  - CV 813 converts CV 812 to °F.
- CV 814 is used to make cladding oxidation as a percentage of cladding thickness. This is done by using the oxide thickness at the hot spot of the hot rod (e.g., a sum of the RELAP5-3D variables 'OXTI' and 'OXTO' for Cell 4 of Heat Structure 5420), divided by the total cladding thickness and multiplied by 100 to obtain a result in percentage. The clad thickness is 0.006 inches, so the total scaling factor is 16666.67.
- CV 815 is used to make the PRZ water volume in ft^3. This is done by multiplying the liquid fraction (e.g., RELAP5-3D variable 'VOIDF') by the volume for each cell of the PRZ (e.g., Component 153).
- CV 816 is used to make the reactivity in pcm. This is done using the RELAP5-3D variable 'RKREAC,' which is in $. This is converted to pcm by multiplying by 0.0075 (e.g., the assumed value for delayed neutron fraction), then dividing by 1e-5. This produces an overall scaling factor of 750 pcm/$.
- CVs 817 and 818 are used to make boron concentration in ppm:
  - CV 817 is set as the liquid fraction (e.g., RELAP5-3D variable 'VOIDF') multiplied by the liquid density (RELAP5-3D variable 'RHOF') in Cell 4 of the hot channel.
  - CV 818 is set as the boron density in Cell 4 of the hot channel (e.g., RELAP5-3D variable 'BORON'), divided by CV 817. This produces the boron concentration in kg/kg. This is multiplied by a scaling factor of 1e6 to obtain the value in ppm.
- CVs 819 through 821 are used to make feedwater mass flow as a fraction of nominal:
  - CV 819 is the initial nominal SG mass flow sum of all 4 SGs in lbm/s (numeric $SGFLOWNUM multiplied by 4).
  - CV 820 is the total FW mass flow rate in lbm/s. This is created by summing the mass flow of Components 181, 183, 281, 283, 381, 383, 481, and 483. An overall scaling factor of 2.20462 lbm/kg is used.
  - CV 821 divides CV 820 by CV 819, thus creating the FW mass flow as a fraction of nominal SG flow.
- CVs 823 and 824 are used to make steam mass flow as a fraction of nominal:
  - CV 823 is the total steam mass flow rate in lbm/sec. This is created by summing CVs 114, 115, 116, and 117.
  - CV 824 divides CV 823 by CV 819, thus creating the steam mass flow as a fraction of nominal SG flow.
- CV 825 is set as the departure of nucleate boiling (DNB) ratio. The DNB ratio is simply calculated by dividing the critical heat flux (CHF) (e.g., RELAP5-3D variable 'HTCHF') by the total heat flux (e.g., RELAP5-3D variable 'HTRNR') for the outside of the maximum power location in the hot rod (e.g., Cell 4 of Heat Structure 5420).
- CV 826 is set as the RCS critical boron concentration, which is a constant value set equal to 1800 ppm.
- Variable Trip 490 and CV 827 are used to make the time of the RCS critical boron concentration:
  - Variable Trip 490 trips when CV 818 is less than or equal to CV 826.

- CV 827 is set equal to RELAP5-3D variable 'TIMEOF' for Trip 490.

- CV 828 is set as the containment pressure in psig. This is set as the pressure in Component 462. A term scaling factor is added to convert from Pa to psia, and then an additive constant of -14.7 psi is included for conversion to gauge pressure.
- CV 829 is set as the core inlet mass flow rate in lbm/sec. This is set as a sum of the mass flow rates from all junctions of Multiple Junctions 501 and 503. An overall scaling factor of 2.20462 lbm/kg is used to convert from kg/sec to lbm/sec.
- CV 830 is set as the core outlet mass flow rate in lbm/sec. This is set as a sum of the mass flow rates from Single Junctions 544 and 545. An overall scaling factor of 2.20462 lbm/kg is used to convert from kg/sec to lbm/sec.
- CV 831 is set as the heat transfer coefficient (HTC) in BTU/hr-ft^2-F. This is set as the HTHTC RELAP5-3D variable at Node 4 of Heat Structure 5420 on the right surface. An overall scaling factor of 0.17611 is used to convert from W/m2-K to BTU/hr-ft^2-F.
- CV 832 is set as the vapor temperature in °F. This is set as the TEMPG RELAP5-3D variable at Node 4 of Pipe 542. A term scaling factor of 1.8 F/K and an additive constant of -459.67 F are used to convert from K to F.
- CV 833 is set as the break mass flow rate in lbm/sec. This is set as the MFLOWJ RELAP5-3D variable at Component 461. An overall scaling factor of 2.20462 lbm/kg is used to convert from kg/sec to lbm/sec.
- CV 834 is set as the break energy flow rate in BTU/sec. This is set as the FLENTH RELAP5-3D variable at Component 461. An overall scaling factor of 0.00094782 BTU/J is used to convert from J/sec to BTU/sec.
- CV 835 is set as the fluid quality (unitless). This is set as the QUALS RELAP5-3D variable at Node 4 of Pipe 542.
- CV 836 is set as the mass flux in lbm/sec-ft^2. This is set as the MFLOWJ RELAP5-3D variable at Junction 3 of Pipe 542 divided by the flow area of the junction. This results in an overall scaling factor of (2.20462 lbm/kg)*(1/0.2767 ft^2) = 7.96755 lbm/kg-ft^2.
- CV 837 is set as the total flow from all three intact loop accumulators. This is set as the sum of the MFLOWJ RELAP5-3D variable for Components 141, 241, and 341. An overall scaling factor of 2.20462 lbm/kg is used.
- CV 838 is set as the total flow from all three intact loop SI junctions. This is set as the sum of the MFLOWJ RELAP5-3D variable for Components 144, 244, and 344. An overall scaling factor of 2.20462 lbm/kg is used.
- CV 839 is set as the total flow from all three intact loop accumulators and SI junctions. This is set as the sum of CVs 837 and 838.
- CV 840 is set as core outlet steam mass flow rate in lbm/sec. This is set as a sum of the steam mass flow rates from Single Junctions 544 and 545. An overall scaling factor of 2.20462 lbm/kg is used to convert from kg/sec to lbm/sec.
- CV 841 is set as the reactor vessel change in temperature in °F. It is set as CV 173 (e.g., the average of all four hot leg temperatures in °F) minus 174 (e.g., the average of all four cold leg temperatures in °F).
- CV 842 is set as the PRZ level in percentage. It is set as CV 56 (e.g., the PRZ level) divided by the PRZ length (48.9611 ft.). This results in an overall scaling factor of (100%)*(1/48.9611 ft) = 2.0424 %/ft.

- CV 843 is set as the intact SG average pressure in psia. It is set as the average of CVs 181, 182, and 183 (e.g., secondary side pressures for Loops 1 through 3).
- CV 844 is set as the intact loop average hot leg temperature in °F. It is set as the average of CVs 160, 161, and 162 (e.g., hot leg temperatures).
- CV 845 is set as the intact loop average cold leg temperature in °F. It is set as the average of CVs 164, 165, and 166 (e.g., cold leg temperatures).
- CV 846 is set as the differential pressure between the RCS and the ruptured SG in psi. It is set as CV 180 (e.g., the PRZ pressure) minus CV 184 (e.g., broken loop secondary side pressure).
- CV 847 is set as the primary to secondary flow in a SG tube rupture in lbm/sec. It is set as the RELAP5-3D variable 'MFLOWJ' for Component 463. An overall scaling factor of 2.20462 lbm/kg is used.
- CV 848 is set as the ruptured SG water volume in ft^3. It is set as the sum of RELAP5-3D variable 'VOIDF' for all loop 4 secondary side cells times the volume for that cell.
- CV 849 is set as the fuel pellet center temperature at the hot spot in °F. It is set as the RELAP5-3D variable 'HTTEMP' at the inner radial node of Axial Node 4 of Heat Structure 5420. A term scaling factor of 1.8°F/K is used and an overall additive factor of -459.67°F is added.
- CV 850 is set as the fuel pellet average temperature at the hot spot in °F. It is set as the average of RELAP5-3D variable 'HTTEMP' at the inner seven radial nodes of Axial Node 4 of Heat Structure 5420. A term scaling factor of 1.8°F/K is used and an overall additive factor of -459.67°F is added.
- CV 851 is set as the cladding outer temperature at the hot spot in °F. It is set as the RELAP5-3D variable 'HTTEMP' at the outer radial node of Axial Node 4 of Heat Structure 5420. A term scaling factor of 1.8°F/K is used and an overall additive factor of -459.67°F is added.
- CV 858 through 860 integrate the collapsed liquid levels of the downcomer, lower plenum, and core.

4.3 RAVEN Input Description

4.3.1 Overall RAVEN Workflow

This section documents the RAVEN inputs files with a focus on the steps enacted and the associated XML nodes.

4.3.2 RAVEN Distributions

This section covers each of the variables sampled from the distributions and their related use as operators in the models.xml file. Note that they will be discussed by their variable name. To get the corresponding distribution name, "dist" is added to the variable name.

- Variable cltemp (e.g., the numerics '$CLTEMPNUM' and '$CLTEMP2NUM') – This is the cold leg temperature in °F. It is used to initialize the target value (CV 430) used to control the steam flow. In addition, it is used to initialize components in the model at the cold leg temperature.
- Variable corep (e.g., the numeric '$COREPNUM') – This is the core power in W. It is used for the kinetics model initial power and to initialize the target value (CV 400) used to control the kinetics model.
- Variable fwtemp (e.g., the numeric '$FWTEMPNUM') – This is the feedwater temperature in °F. It is used to set the temperature of the MFW time-dependent volumes (e.g., Components 180, 280, 380, and 480).

- Variable hltemp (e.g., the numerics '$HLTEMPNUM' and '$HLTEMP2NUM') – This is the hot leg temperature in °F. It is used to initialize the target value (CV 441) for the SS plot. In addition, it is used to initialize components in the model at the hot leg temperature.
- Variable przlevel (e.g., the numeric '$PRZLEVELNUM') – This is the PRZ level in ft. It is used to initialize the target value (CV 470) used to control the SS charging and letdown.
- Variable przpress (e.g., the numeric '$PRZPRESSNUM' and '$PRZPRESSN2NUM') – This is the PRZ pressure in psia. It is used to initialize the target value (CV 480) used to control the SS PRZ heaters and spray.
- Variable rcsflow (e.g., the numeric '$RCSFLOWNUM') – This is the RCS flow rate in gpm per loop. It is used to initialize the target value (CV 410) used to control the SS Pump Speed.
- Variable rcsmflo (e.g., the numerics '$RCSMFLONUM,' '$RCSMFLO2NUM,' '$RCSVMFLONUM,' and '$RCSVMFLO2NUM') – This is used for two separate operators in the RAVEN input:
  - The first uses the value directly as the RCS loop mass flow rate in lbm/sec. It is used to initialize the junction flow rates for the RCS loop components, and it is used to initialize the plot variable CV 803.
  - The second uses the value multiplied by four as the RCS vessel mass flow rate in lbm/sec. It is used to initialize the junction flow rates for the RCS vessel components, and it is used to initialize the plot variable CV 800.
- Variable rcsmflo (e.g., the numeric '$RCSVMFLONUMREVERSE') – This is used for the same thing as the second option as shown in rcsmflo, except in the opposite direction:
  - This uses the value multiplied by four as the RCS vessel mass flow rate in lbm/sec. It is used to initialize the junction flow rates in the MULTID component for the RCS vessel components.
- Variable sglevel (e.g., the numeric '$SGLEVELNUM') – This is the SG level in ft. It is used to initialize the target value (CV 450) used to control the SS feedwater flow.
- Variable stmpress (e.g., the numeric '$STMPRESSNUM' and '$STMPRESS2NUM') – This is the SG steam pressure in psia. It is used to initialize the target value (CV 444) for the SS plot. In addition, it is used to initialize components in the model at the SG steam pressure.
- Variable sgflow (e.g., the numeric '$SGFLOWNUM') – This is the SG flow in lbm/sec. It is used to initialize the target value (CV 465) for the SS plot. In addition, this value multiplied by four is used to initialize the plot variable CV 819.
- Variable dpvess (e.g., the numeric '$DPVESSNUM') – This is the vessel pressure drop in psi. It is used to initialize the target value (CV 500) for the SS plot.
- Variable dphl (e.g., the numeric '$DPHLNUM') – This is the hot leg pressure drop in psi. It is used to initialize the target value (CV 503) for the SS plot.
- Variable dpxl (e.g., the numeric '$DPXLNUM') – This is the crossover leg pressure drop in psi. It is used to initialize the target value (CV 506) for the SS plot.
- Variable dpcl (e.g., the numeric '$DPCLNUM') – This is the cold leg pressure drop in psi. It is used to initialize the target value (CV 509) for the SS plot.
- Variable dpsg (e.g., the numeric '$DPSGNUM') – This is the SG pressure drop in psi. It is used to initialize the target value (CV 512) for the SS plot.
- Variable corbyp (e.g., the numeric '$COREBYPNUM') – This is the core bypass flow in %. It is used to initialize the target value (CV 530) for the SS plot.

- Variable przphirxt (e.g., the numeric '$PRZPHIRXTNUM') – This is the high PRZ pressure reactor trip setpoint in psia. It is used to set the value to which the PRZ pressure (CV 180) is compared for Variable Trip 411.
- Variable przplorxt (e.g., the numeric '$PRZPLORXTNUM') – This is the low PRZ pressure reactor trip setpoint in psia. It is used to set the value to which the PRZ pressure (CV 180) is compared for Variable Trip 410.
- Variable przlhirxt (e.g., the numeric '$PRZLHIRXT') – This is the high PRZ level reactor trip setpoint in ft. It is used to set the value to which the PRZ level (CV 56) is compared for Variable Trip 412.
- Variable rcsflolorxt (e.g., the numeric '$RCSFLOLORXTNUM') – This is the low RCS flow reactor trip setpoint in lbm/sec. It is used to set the value to which minimum loop RCS flow rate (CV 154) is compared for Variable Trip 413.
- Variable sglevlorxt (e.g., the numeric '$SGLEVLORXT') – This is the low SG level reactor trip setpoint in ft. It is used to set the value to which minimum loop SG level (CV 61) is compared for Variable Trip 414.
- Variable mfwdeltime (e.g., the numeric '$MFWDELTIMENUM') – This is the MFW delay time (e.g., time from generation of the signal to shut off until MFW begins to ramp off). It is used to set the third time value for General Table 640.
- Variable mfwramptime (e.g., the numeric '$MFWRAMPTIMENUM') – This is the MFW ramp time (e.g., time from when MFW begins to ramp off to when it is completely off). It is used to set the fourth time value for General Table 640. Note that the inputs for this variable should include the delay time in them (i.e., if a 5 second delay and 5 second ramp time are desired, delay time should be entered as 5 second and ramp time should be entered as 10 second).
- Variable afwdeltime (e.g., the numeric '$AFWDELTIMENUM') – This is the AFW delay time (e.g., time from generation of the signal to start until AFW begins to ramp on). It is used to set the fourth time value for the flow tables for the AFW time-dependent junctions.
- Variable afwramptime (e.g., the numeric '$AFWRAMPTIMENUM') – This is the AFW ramp time (e.g., time from when begins to ramp on until it reaches full flow). It is used to set the fifth time value for the flow tables for the AFW time-dependent junctions. Note that the inputs for this variable should include the delay time in them (i.e., if a 5 second delay and 5 second ramp time are desired, delay time should be entered as 5 second and ramp time should be entered as 10 second).
- Variable afwflo (e.g., the numeric '$AFWFLONUM') – This is the AFW flow rate in lbm/sec. It is used to set the fifth and sixth liquid mass flow rate values for the flow tables for the AFW time-dependent junctions.
- Variable pmpmotdel (e.g., the numeric '$PMPMOTDELNUM') – This is the delay time from the generation of the pump trip signal to the beginning of coast-down in sec. It is used to set the constant adder for the pump delay time CVs 620 through 623.
- Variable achflux (e.g., the numeric '$ACHFLUXNUM') – This is the SS average core channel heat flux at the peak power location in BTU/sec-ft^2. It is used to initialize the plot variable CV 805.
- Variable hchflux (e.g., numeric '$HCHFLUXNUM') – This is the SS hot core channel heat flux at the peak power location in BTU/sec-ft^2. It is used to initialize the plot variable CV 808.
- Variable initreact (e.g., numeric '$INITREACTNUM') – This is the initial reactivity in $. It is used for the kinetics model initial reactivity.

- Variable mdc (e.g., no associated numerics) – This is the moderator density coefficient (MDC) in $\Delta k/g/cm^3$. This variable has two operators associated with it, because it was found that if multiple card/word pairs are listed for one operator, the value calculated using the first card/word value is applied to all card/word pairs. These inputs are used for the reactivity feedback table for density in the kinetics model. Because this input is in $ in the RELAP5-3D model, and the FSAR generally presents values in $pcm/g/cm^3$ or $\Delta k/g/cm^3$, the final inputs are calculated by RAVEN as multiplying the card value by the sampled value and dividing by -0.042 $\Delta k/g/cm^3$, which is the MDC value used to calculate the initial RELAP5-3D inputs.
- Variable accbor (e.g., numeric '$ACCBORNUM') – This is the accumulator boron concentration in mass fraction. It is used to initialize the boron concentration of Accumulator Components 141, 241, 341, and 441.
- Variable chgbor (e.g., numeric '$CHGBORNUM') – This is the charging flow boron concentration in mass fraction. It is used to initialize the boron concentration of Charging Flow Components 145, 245, 345, and 445.
- Variable accvol (e.g., numeric '$ACCVOLNUM') – This is the accumulator liquid volume in ft^3. It is used to initialize the liquid volume of Accumulator Components 141, 241, 341, and 441.
- Variable acctemp (e.g., numeric '$ACCTEMPNUM') – This is the accumulator temperature in °F. It is used to initialize the temperature of Accumulator Components 141, 241, 341, and 441.
- Variable accpress (e.g., numeric '$ACCPRESSNUM') – This is the accumulator pressure in psia. It is used to initialize the pressure of accumulator Components 141, 241, 341, and 441.
- Variable sitrplsp (e.g., numeric '$SITRPLSPNUM') – This is the low steam pressure reactor trip setpoint in psia. It is used to set the value to which the minimum loop SG pressure (CV 185) is compared for Variable Trip 470.
- Variable sitrpdel (e.g., numeric '$SITRPDELNUM') – This is the delay time from the SI signal until the SI flows begin in seconds. It is used as an adder to the RELAP5-3D variable 'TIMEOF' for Logical Trip 630 to create the value to which the current run time is compared for Variable Trip 471.
- Variable msivdel (e.g., numeric '$MSIVDELNUM') – This is the steam valve closure delay time (e.g., time from generation of the signal to shut off until main steam begins to ramp off). It is used to set the third time value for General Table 650.
- Variable msivramp (e.g., numeric '$MSIVRAMPNUM') – This is the steam valve closure ramp time (time from when main steam begins to ramp off to when it is completely off). It is used to set the fifth time value for General Table 650. Note that the inputs for this variable should include the delay time in them (i.e., if a 5 second delay and 5 second ramp time are desired, delay time should be entered as 5 sec and ramp time should be entered as 10 sec).
- Variable rccadel (e.g., numeric '$RCCADELNUM') – This is the delay time from the reactor trip signal until the rods begin to drop in seconds. It is used as an adder to the RELAP5-3D variable 'TIMEOF' for Logical Trip 613 to create the value to which the current run time is compared for Variable Trip 480.
- Variable rcpheat (e.g., numeric '$RCPHEATNUM') – This is the heat generated by the RCPs in MW. It is used as the dependent factor for General Tables 680, 681, 682, and 683.
- Variable przsaf (e.g., numeric '$PRZSAFNUM') – This is the pressure at which the PRZ safety valve begins to open in psia. It is used as the second pressure value in General Table 670.
- Variable rcsbor (e.g., numeric '$RCSBOR') – This is the RCS boron concentration in mass fraction. It is used to initialize RCS components in the model at the correct boron concentration.

- Variable 'ITFD' – This is the interfacial friction multiplier that can be applied globally when using the BEPU RELAP5-3D code.

4.3.3 Steady State Convergence Criteria

As a base for the simulation of TRs, a model must begin with a converged steady state. In this model, a converged steady state can be defined as all boundary conditions, fluid conditions, and internal flow paths in equilibrium.

A converged steady state is a requirement because the process of the model reaching a steady state is a type of TR (e.g., the behavior varies over time until convergence). Thus, if the simulation of a TR accident scenario is done using a model not starting in a steady state, the effects of the TR scenario of interest would be convoluted by the effects of the model trying to reach equilibrium. In addition, the definition of most TR analyses is based on starting in a steady state.

While it is possible to initialize a model to a set of equilibrium conditions, this is very time-consuming in practice, and, crucially, the entire process must be redone to adapt to input changes. Instead, control logic that adjusts boundary conditions is inserted, where possible, with the goal of getting as close as possible to a desired value. The steady state end time is also set to be long enough for equilibrium to be reached. Note that some parameters still require manual calibration, because they cannot be controlled with control logic in RELAP5-3D (e.g., notably the pressure drops).

Model nuances and simplifications generally make it impossible to obtain all the desired SS conditions perfectly. For example, the RCS temperature is controlled in the steady state by the steam valve open area. Specifically, the cold leg temperature is controlled, and thus, the hot leg temperature is a value that is indirectly controlled and depends on the energy balance of the model. As such, it is expected that it will be impossible to get the value exactly right. Therefore, it is also appropriate to quantify an acceptable range of results for the SS criteria. While this would typically be done based on things like the measurement of uncertainty or sensitivity studies, obtaining a justified range for every parameter is considered to be beyond the scope of this work. As such, values which are judged to be reasonable based on industry experience are used. Note that a future improvement for determining better justified convergence bands is listed in Section □.

In order to reach a steady state, the conditions in Table 4-4 below are used. The first column contains a steady state condition, the second column contains the related numerics in the SNAP model, and the third column contains the distribution name in the RAVEN input.

Table 4-4. Steady state conditions for the plant model.

S-S Condition	SNAP Numeric(s)	RAVEN Distribution
Cold Leg Temperature	$CLTEMPNUM, $CLTEMP2NUM	cltempdist
Core Power	$COREPNUM	corepdist
Feedwater Temperature	$FWTEMPNUM	fwtempdist
Hot Leg Temperature	$HLTEMPNUM, $HLTEMP2NUM	hltempdist
PRZ Level	$PRZLEVELNUM	przleveldist
PRZ Pressure	$PRZPRESSNUM, $PRZPRESS2NUM	przpressdist
RCS Flow	$RCSFLOWNUM	rcsflowdist
RCS Mass Flow (also includes Vessel Mass Flow = 4 * Loop Flow)	$RCSMFLONUM, $RCSMFLO2NUM, $RCSVMFLONUM	rcsmflodist
SG Level	$SGLEVELNUM	sgleveldist
SG Steam Pressure	$STMPRESSNUM, $STMPRESS2NUM	stmpressdist
SG Mass Flow	$SGFLOWNUM	sgflowdist

Vessel DP	$DPVESSNUM	dpvessdist
Hot Leg DP	$DPHLNUM	dphldist
Crossover DP	$DPXLNUM	dpxldist
Cold Leg DP	$DPCLNUM	dpcldist
SG Primary DP	$DPSGNUM	dpsgdist
Core Bypass	$COREBYPNUM	corbypdist

At this stage, these conditions define a converged SS. However, additional conditions may be used in the future. Potentially, these could include upper head temperature, SG recirculation ratio, more granular pressure drops across the vessel, or anything else deemed appropriate. In addition, plant-specific SG level and core bypass information should be obtained.

4.4 Limitations and Conditions for Usage of the Plant Model

The following limitations of this model should be acknowledged before use. This model is generally considered acceptable for proof-of-concept or some scoping work, but should not be used for any kind of plant-specific licensing work.

The following limitations apply to the base model used for all cases:

- Zion fluid cell and heat structure input from the base model is left as is (other than the SG tubes); no evaluation for applicability to other plants is performed.
- The material properties from the Zion base model are left as they are (other than gap HTC); no evaluation for validity is performed.
- The kinetics model from the Zion base model is left as is (other than the SS Core Power and moderator feedback); no evaluation for validity is performed.
- The core bypass flow optimizer should be made at some point downstream. It is noted that the current model only has spray nozzle bypass, which is generally only a small or moderate portion of the overall bypass flow. Thimble tube bypass and potentially barrel/baffle region bypass should be added (if the plant is upflow barrel/baffle design).
- All bands to determine an acceptable SS are arbitrary. Justification, such as real uncertainties or sensitivity studies, should be created in the future.
- The included DP values for Vogtle are based on best estimate flow, while the model is run with thermal design flow (TDF). This is adequate for the time being, but this should be updated with the correct DPs at TDF for any real application.
- At this stage, the conditions herein define a converged SS. However, additional conditions may be used in the future. Potentially, these could include upper head temperature, SG recirculation ratio, more granular pressure drops across the vessel, or anything else deemed appropriate. In addition, plant-specific SG level and core bypass information should be obtained.
- The core nodalization should be refined to have more nodes, and to model nodes that only contain active fuel.
- The fuel centerline temperatures in the SS runs herein were significantly higher than seems reasonable, when using the material properties from the base file. This was fixed somewhat when the gap HTC was significantly increased; however, the fuel rod geometry and material properties should be investigated and improved in the future.

- The PRZ spray line geometry is completely arbitrary. This should be updated consistent with plant-specific geometry.
- The full model nodalization should be validated to be appropriate at some point in the future.
- Time step sensitivity studies should be performed to validate or improve on the time step size used herein.

4.5 Reactor Coolant Pump Shaft Seizure (Locked Rotor)

Reactor coolant pump (RCP) shaft seizure is an American Nuclear Society (ANS) Condition IV incident and is commonly referred to as a locked rotor incident.

The RCP rotor has an instantaneous seizure causing rapidly reduced flow through its associated coolant loop. This leads to a reactor trip on low flow signal. The fuel rods continue to transfer heat to the coolant, causing the water to expand. At the same time, heat transfer from the primary loop to the secondary through the SG tubes reduces. This happens for two reasons:

1. The reduced flow results in a decreased tube side film coefficient.
2. The reactor coolant in the tubes cools down while the shell side temperature increases because the turbine steam flow is reduced to zero upon plant trip.

The coolant expansion in the core, combined with the reduced heat transfer in the SG, causes a surge into the PRZ, causing a pressure increase throughout the RCS. Prior to a significant negative reactivity insertion by control rods, the pellet and clad temperatures of the fuel rods increase rapidly because of the degradation of heat transfer from fuel rods to the coolant due to the reduced flow. This pressure increase should activate the automatic PRZ spray system, open the power-operated relief valves, and open the PRZ safety valves. The FSAR states that, “The power-operated relief valves are safety grade and would be expected to function properly during an accident; however, for conservatism, the analysis does not use the pressure-reducing effect of the power-operated relief valves and the pressure-reducing effect of the spray.”

The locked rotor scenario presents two cases in the FSAR:

1. LOOP.
2. OPA.

These cases have identical input, except for pump behavior defined in the TR input files, as discussed in the following section.

4.5.1 Scenario-Specific Inputs in the TR Input File

The TR input file is defined as follows:

- Upfront cards are included that specify this is a restart TR run, which uses the last available printout in the restart file.
- The end time is set to 10 seconds, consistent with the analysis in the reference plant FSAR. The max time step is set to 0.05 seconds, as this is a value that is reasonable for a relatively stable simulation such as this.
- The minor edits are used to specify the variables used in the plots.
- CV 405 (e.g., the reactivity controller) is listed as a constant value of 0.0 $. This is done as a placeholder for RAVEN to substitute in the actual end of SS value of CV 405 using the RAVEN variable “ssreact.” This step is necessary to turn off the reactivity controller, but make the SS reactivity adder persist.

- The pump inputs are specified differently depending on LOOP vs. OPA:
  - For OPA, the pump CVs are used to impose the desired conditions. These CVs are specified in TR input file as constants. CVs 419, 420, and 421 (e.g., Loops 1 through 3) are set as constant values consistent with the end of SS Pump Speed, and these values will be replaced by RAVEN using the variable "sspmpvel." This causes the pumps to simply continue operating like normal SS. CV 422 (e.g., Loop 4) is set as a constant value of 0 rpm. This simulates the locked rotor at the onset of the TR. Variable Trips 450 through 453 must remain true, as this will cause the pumps to continue using CVs 419 through 422. Therefore, these trips need not be specified in the TR input file. In summary, the TR input file only specifies CVs 419 through 422 as constants for the OPA case.
  - For LOOP, CV 422 (loop 4) is set as a constant value of 0 rpm. This simulates the locked rotor at the onset of the TR. Variable trip 453 must remain true, as this will cause the locked pump to continue using CV 422. Therefore, this is not specified in the TR input file. In order to model the motor trip for the remaining three pumps, Variable Trips 450 through 452 are set to false, so the motor trip takes precedence. This is done by setting them to trip at a time greater than or equal to 1E9 seconds in the TR input file. The motor trip specifications from the steady state file already performs the desired motor trip behavior, so nothing needs to be specified in the TR input file. In summary, the TR input file needs to specify CV 422 as a constant zero, and Variable Trips 450 through 452 to always be false for the LOOP case.
- CVs 435 through 438 (e.g., the steam valve position) are changed to be functions of General Table 650. This allows them to be set to the SS valve position prior to the reactor trip or SI signal; then, it will close based on the specified delay and ramp times.
- CVs 459 through 462 (e.g., MFW flow rate) are listed as constant values of 1118.9 lbm/sec. This is done as a placeholder for RAVEN to substitute in the actual end of SS values of CVs 459 through 462 using RAVEN variable "ssmfw..
- CV 472 is listed as a constant value of 0.0. This is used to turn off the SS charging flow.
- CV 473 is listed as a constant value of 0.0. This is used to turn off the SS letdown flow.
- CV 482 is listed as a constant value of 0.0. This is used to turn off the SS PRZ heater.
- CV 483 is listed as a constant value of 0.0. This is used to turn off the SS PRZ spray.
- CV 641 is listed as a constant value of 0.0. This is used to disable the PRZ PORV.
- General Table 640 is listed with values identical to the SS input. This input does not necessarily need to be here, but it is generically listed in the TR input files to allow the analyst to change the trip used for MFW:
  - General Table 650 is listed with values identical to the SS input. This input needs to be here so that the first three valve position entries in the table can be replaced with the end of SS values using RAVEN variable "ssstmvlv." This step is necessary to turn off the steam flow controller, but have the SS steam flow persist.

4.5.2 Scenario-Specific RAVEN Inputs

The RAVEN distribution means are set as shown in Table 4-5. The inputs are consistent with the FSAR, as described below. The remaining inputs are assumptions that are not specifically mentioned in the FSAR:

- The SS conditions are generally set to nominal values, with the exceptions of core power and PRZ pressure, which are skewed high.

- The low RCS flow reactor trip setpoint is set to 87% of the nominal flow rate, consistent with the FSAR analysis. The other reactor trip setpoints are irrelevant, as this setpoint is hit first.
- The MFW is immediately ramped down over 1 second from the reactor trip time; the AFW never comes on by setting 1E+8 second, which is beyond the entire simulation time.
- The pump motors for the non-locked rotor loops trip 2 seconds after the reactor trip.
- The average and hot channel maximum SS heat flux values are set with values consistent with the end of SS.
- The MDC is set based on the appropriate figure in the FSAR.
- The main steam isolation valve (MSIV) is immediately ramped down over 1 second from the reactor trip time.
- The rod control cluster assembly (RCCAs) begin to drop 1 second after the reactor trip.
- The PRZ safety valve is set to open at 2500 psia.
- All inputs related to ECCS flows and timing are irrelevant to this case.

Table 4-5. Summary of RAVEN inputs for reactor coolant pump shaft seizure (locked rotor).

Distribution	Description	Unit	Mean Value
cltempdist	Cold Leg Temperature	°F	556.2
corepdist	Core Power	W	3.657E+09
fwtempdist	Feedwater Temperature	°F	448.7
hltempdist	Hot Leg Temperature	°F	**620.6**
przleveldist	PRZ Level	ft.	29.4
przpressdist	PRZ Pressure	psia	2373
rcsflowdist	RCS Volumetric Flow	gpm	93600
rcsmflodist	RCS Mass Flow	lbm/sec	9684.028
rcsmflorrdist	RCS Mass Flow in Vessel	lbm/sec	-9684.028
sgleveldist	SG Level	ft.	40.1
stmpressdist	SG Steam Pressure	psia	941
sgflowdist	SG Flow Rate	lbm/sec	1132.639
dpvessdist	Vessel Pressure Drop	psi	46.5
dphldist	Hot Leg Pressure Drop	psi	1.2
dpxldist	Crossover Leg Pressure Drop	psi	3.1
dpcldist	Cold Leg Pressure Drop	psi	3.3
dpsgdist	SG Primary Pressure Drop	psi	45.5
corbypdist	Core Bypass Flow	%	5
przphirxtdist	High PRZ Pressure Reactor Trip Setpoint	psia	2514.7
przplorxtdist	Low PRZ Pressure Reactor Trip Setpoint	psia	1714.7
przlhirxtdist	High PRZ Level Reactor Trip Setpoint	ft.	48.9
rcsflolorxtdist	Low RCS Flow Rate Reactor Trip Setpoint	lbm/sec	8425.08
sglevlorxtdist	Low SG Level Reactor Trip Setpoint	ft.	27.1
mfwdeltimedist	MFW Delay Time	sec	0.001

Distribution	Description	Unit	Mean Value
mfwramptimedist	MFW Ramp Time	sec	1
afwdeltimedist	AFW Delay Time	sec	1E+08
afwramptimedist	AFW Ramp Time	sec	1.1E+08
afwflodist	AFW Flow Rate	lbm/sec	105.65
pmpmotdeldist	Pump Motor Trip Delay Time	sec	2
achfluxdist	Average Channel Maximum SS Heat Flux	BTU/sec-ft^2	99.954
hchfluxdist	Hot Channel Maximum SS Heat Flux	BTU/sec-ft^2	164.93
initreactdist	Initial Reactivity	$	0
mdcdist	Moderator Density Coefficient	Δk/g/cm^3	-0.042
accbordist	Accumulator Boron Concentration	Mass Frac	0.0019
chgbordist	Charging Boron Concentration	Mass Frac	0.0024
accvoldist	Accumulator Water Volume	ft^3	900
acctempdist	Accumulator Temperature	°F	120
accpressdist	Accumulator Pressure	psia	600
sitrplspdist	Low Steam Pressure SI Signal	psia	800
sitrpdeldist	SI Signal Delay Time	sec	42
msivdeldist	MSIV Delay Time	sec	0.001
msivrampdist	MSIV Ramp Time	sec	1
rccadeldist	RCCA Delay Time	sec	1
rcpheatdist	RCP Heat Generation	MW	0.00001
przsafdist	PRZ Safety Valve Open Pressure	psia	2500
rcsbordist	RCS Initial Boron Concentration	Mass Frac	0

4.5.3 Steady State Results

The SS plots in Figure 4-4-A through Figure 4-4-O show that the SS is acceptable for both runs. Note that the SS runs are identical for LOOP and OPA, so only one set of plots is shown. The following notes apply to the SS:

- Figure 4-4-B shows the steady state RCS mass flow rate, which converges slightly above the desired value. This deviation is because the “desired value” is based on a mass flow rate from the FSAR, while the model target value is based on volumetric flow rate from the FSAR. Thus, there is a small error likely due to differences in density used to calculate the value, which is acceptable.
- Figure 4-4-C shows the steady state hot leg temperature, which converges slightly above the desired value. It is noted that the hot leg temperature is not controlled in this model, but rather is a consequence of the cold leg temperature, which is controlled using the steam valve, and the energy balance of the rest of the model. This deviation is likely due to small plant-specific differences in geometry or other conditions between Zion and the reference plant, which is acceptable.
- Figure 4-4-I shows the steady state SG pressure, which converges significantly below the desired value. This may be a result of using Zion geometry for the SG model and the rest of the plant conditions from the reference plant. The value is a little more than 3% lower than desired, which is acceptable.

- Figure 4-4-J through Figure 4-4-N show the various RCS pressure drops. They are all near the desired value except for the vessel DP. The addition of the MULTID component greatly increases the DP across the vessel from the desired value of ~46.5 to ~67.0 psia. This has been noticed in other cases where the MULTID component has replaced the 1D components.
- Figure 4-4-O shows the core bypass flow, which is currently unable to reach a SS value due to the lack of a thimble bypass flow. This is acceptable at this stage, but should be updated downstream.

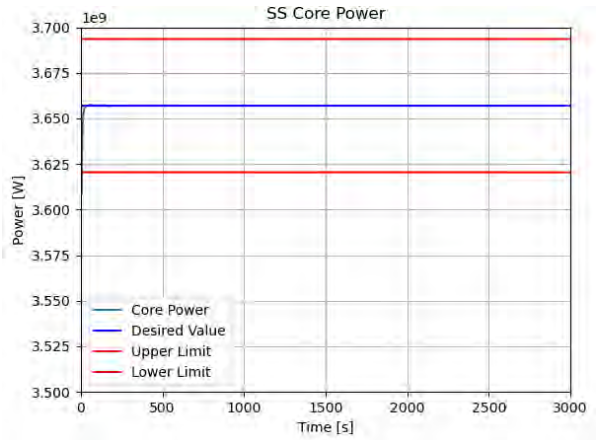

A

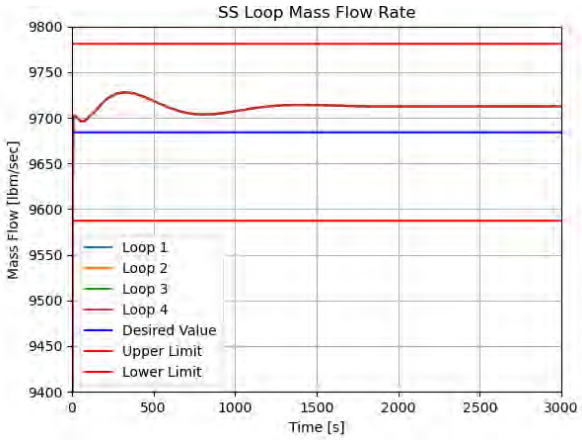

B

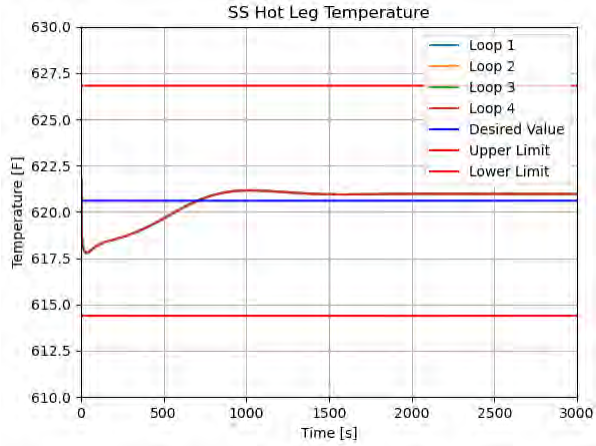

C

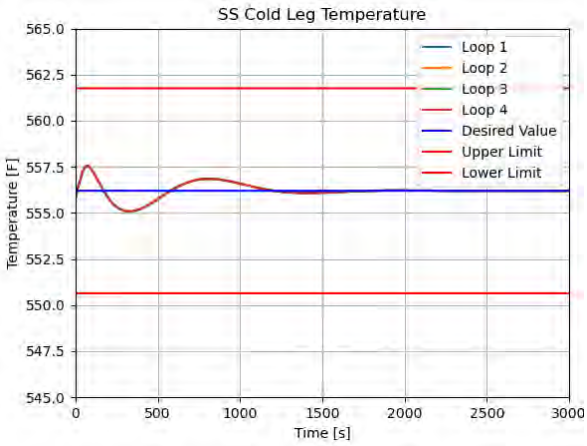

D

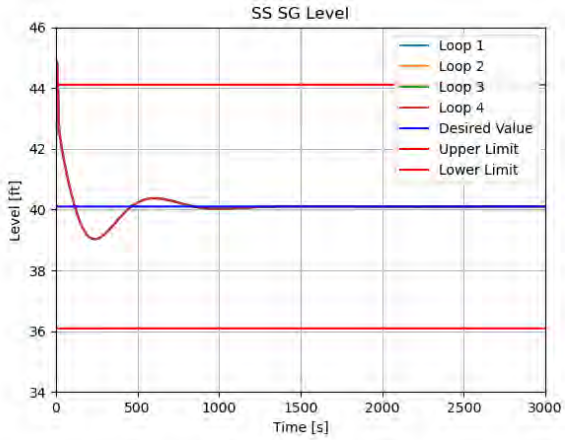
SS SG Level
Loop 1
Loop 2
Loop 3
Loop 4
Desired Value
Upper Limit
Lower Limit
Level [ft]
Time [s]

E

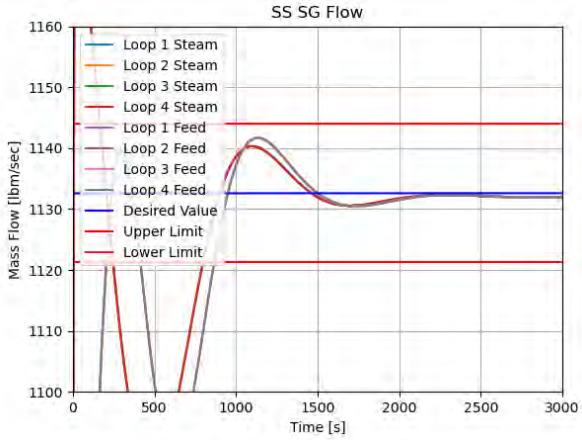
SS SG Flow
Loop 1 Steam
Loop 2 Steam
Loop 3 Steam
Loop 4 Steam
Loop 1 Feed
Loop 2 Feed
Loop 3 Feed
Loop 4 Feed
Desired Value
Upper Limit
Lower Limit
Mass Flow [lbm/sec]
Time [s]

F

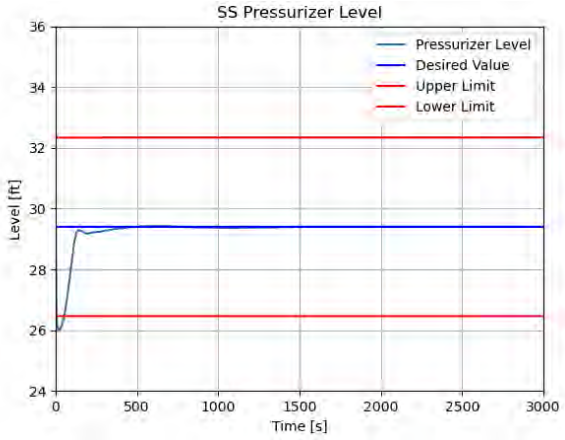
SS Pressurizer Level
Pressurizer Level
Desired Value
Upper Limit
Lower Limit
Level [ft]
Time [s]

G

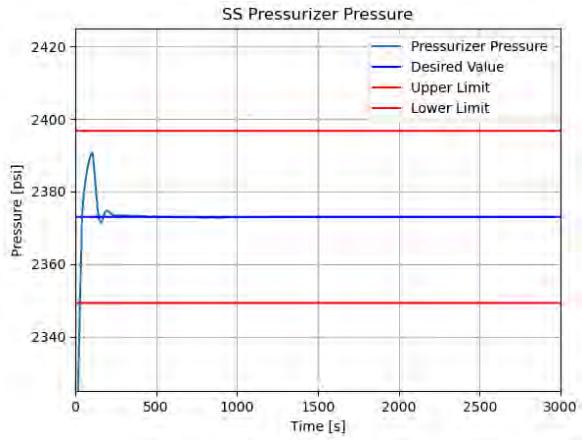
SS Pressurizer Pressure
Pressurizer Pressure
Desired Value
Upper Limit
Lower Limit
Pressure [psi]
Time [s]

H

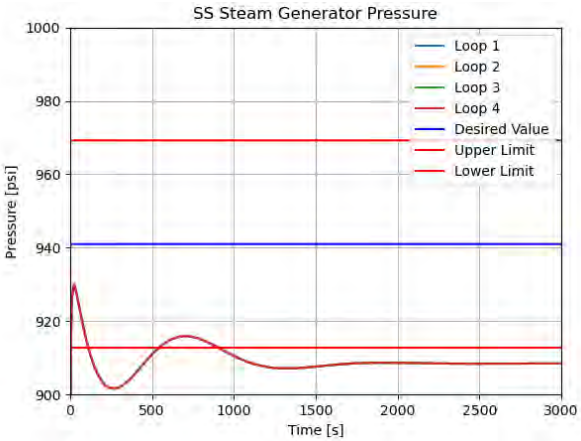
SS Steam Generator Pressure
Loop 1
Loop 2
Loop 3
Loop 4
Desired Value
Upper Limit
Lower Limit
Pressure [psi]
Time [s]

I

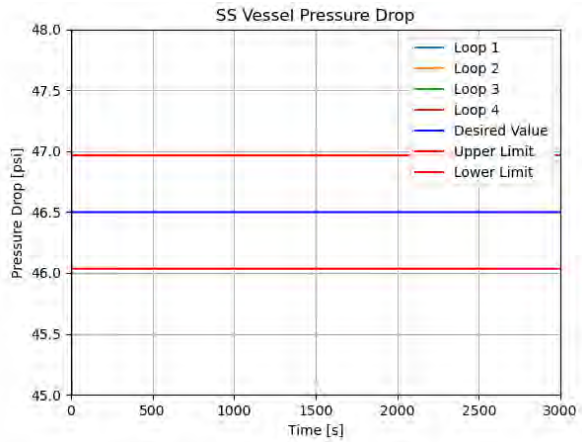
SS Vessel Pressure Drop
Loop 1
Loop 2
Loop 3
Loop 4
Desired Value
Upper Limit
Lower Limit
Pressure Drop [psi]
Time [s]

J

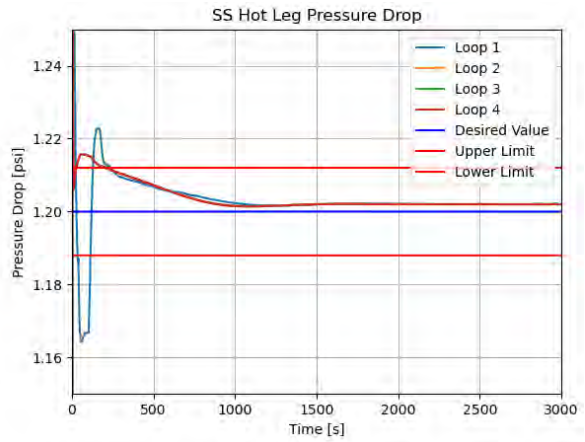

K

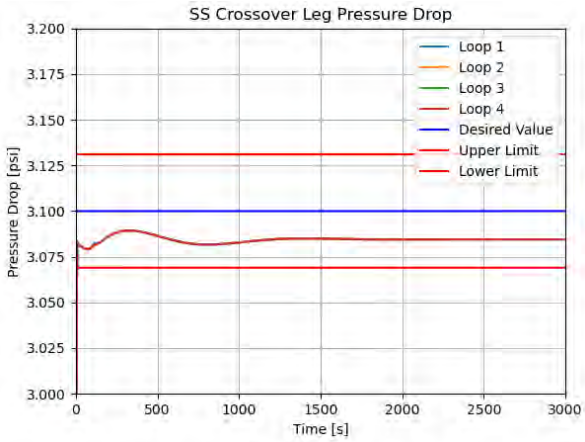

L

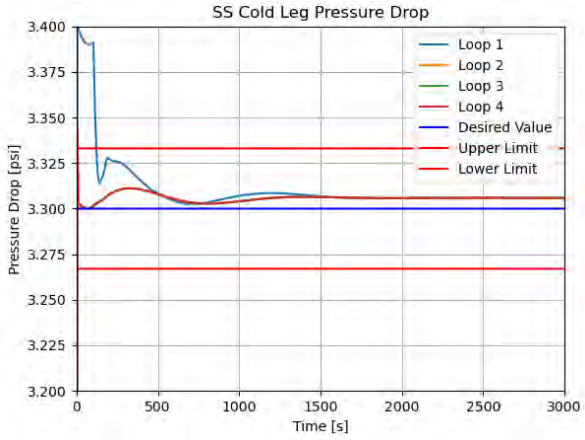

M

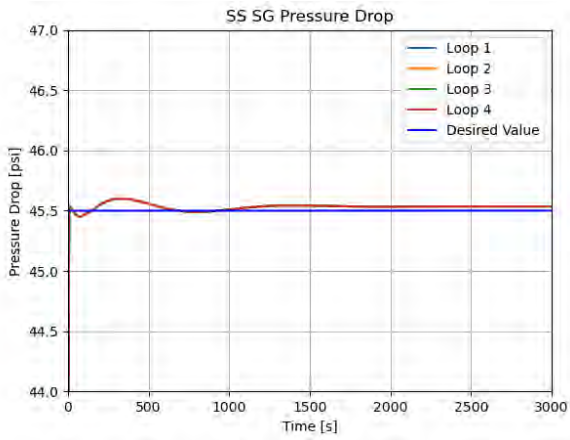

N

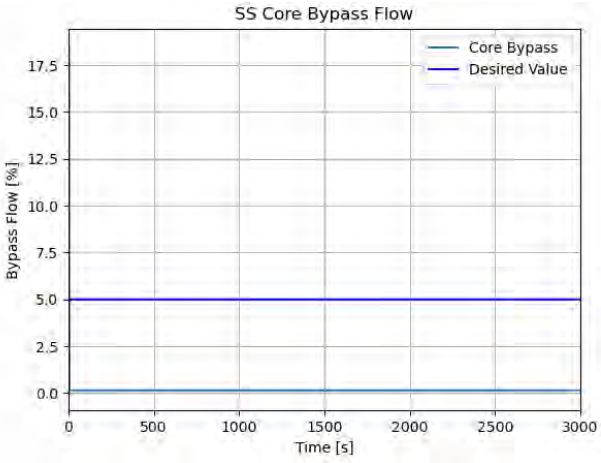

O

Figure 4-4. Steady state acceptance plots for the locked rotor scenario (both LOOP and OPA).

4.5.4 TR Boundary Conditions

The TR boundary conditions are shown in Figure 4-5-A through Figure 4-5-I for LOOP and Figure 4-6-A through Figure 4-6-I for OPA. Based on the following review, the TR boundary conditions are operating as intended for both LOOP and OPA:

- From Figure 4-5-A and Figure 4-6-A:
  - For the LOOP run, Pump 4 immediately drops to 0 rpm and the remaining three pumps coast-down.
  - For the OPA run, Pump 4 immediately drops to 0 rpm and the remaining three pumps remain at the SS velocity.
- From Figure 4-5-B and Figure 4-6-B, the main steam flow ramps from the SS value to no flow over the first 1 second.
- From Figure 4-5-C and Figure 4-6-C, the MFW flow ramps from the SS value to no flow over the first 1 second, and the AFW never comes on.
- From Figure 4-5-D, Figure 4-5-E, Figure 4-6-D, and Figure 4-6-E, SG 4 does not pressurize enough to open the MSSVs, and this is reflected as no flow. The remaining three SGs show MSSV flow increases corresponding to the approximate set pressures.
- From Figure 4-5-F and Figure 4-6-F, the PORV and spray have no flow for the entirety of both TRs. The safety valve flow rate increases beginning at the approximate time that the pressure goes over 2500 psia and stops increasing at the approximate time that the pressure goes over 2575 psia. The timing is similarly consistent during the depressurization.
- From Figure 4-5-G and Figure 4-6-G, the charging and letdown flows are down to zero by 0.1 seconds (e.g., the first plot time step in this run, as the time 0 conditions come from the SS).
- From Figure 4-5-H, Figure 4-5-I, Figure 4-6-H, and Figure 4-6-I, the charging SI and accumulator flows are zero throughout the TRs.

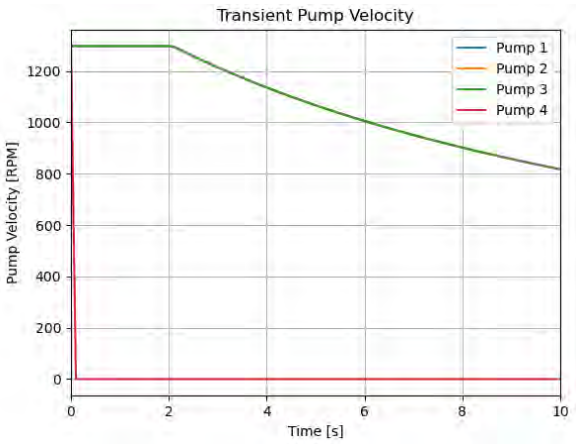

A

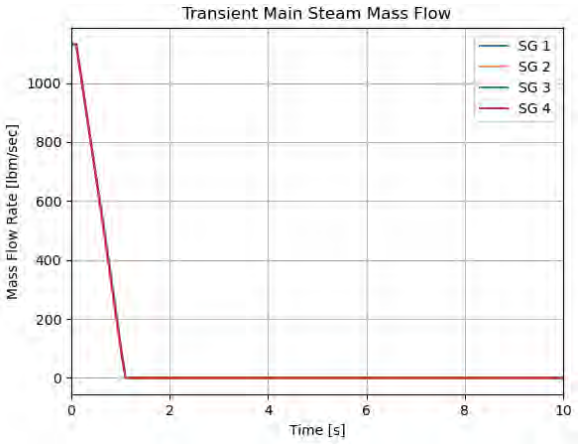

B

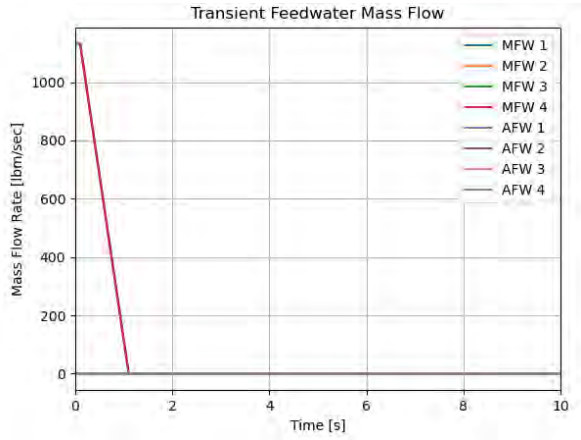
Transient Feedwater Mass Flow
MFW 1
MFW 2
MFW 3
MFW 4
AFW 1
AFW 2
AFW 3
AFW 4
Mass Flow Rate [lbm/sec]
Time [s]

C

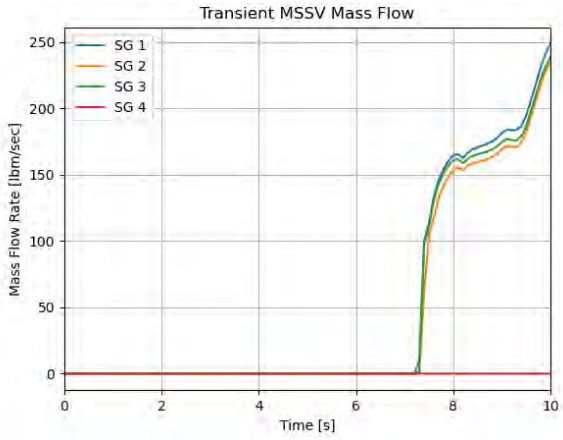
Transient MSSV Mass Flow
SG 1
SG 2
SG 3
SG 4
Mass Flow Rate [lbm/sec]
Time [s]

D

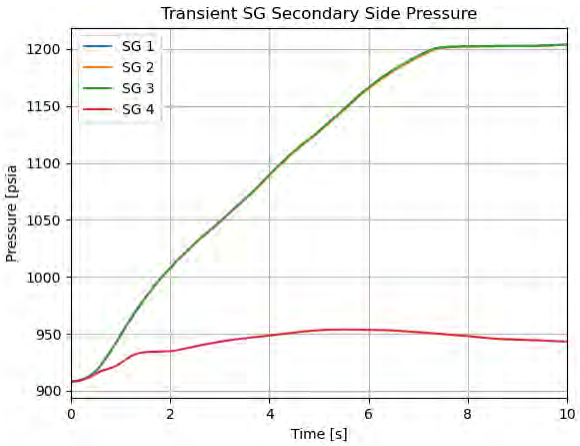
Transient SG Secondary Side Pressure
SG 1
SG 2
SG 3
SG 4
Pressure [psia
Time [s]

E

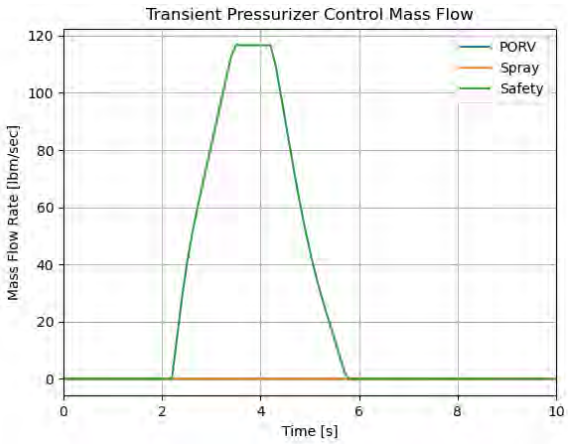
Transient Pressurizer Control Mass Flow
PORV
Spray
Safety
Mass Flow Rate [lbm/sec]
Time [s]

F

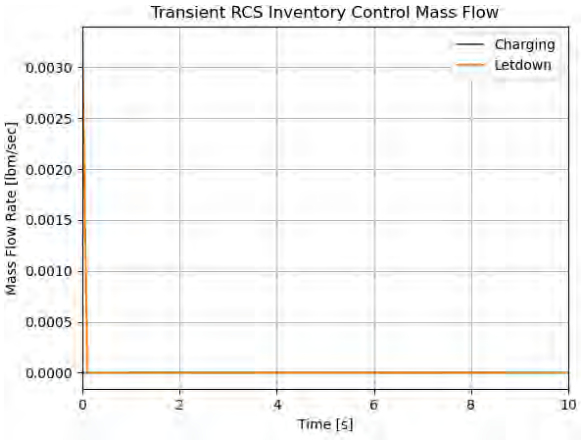
Transient RCS Inventory Control Mass Flow
Charging
Letdown
Mass Flow Rate [lbm/sec]
Time [s]

G

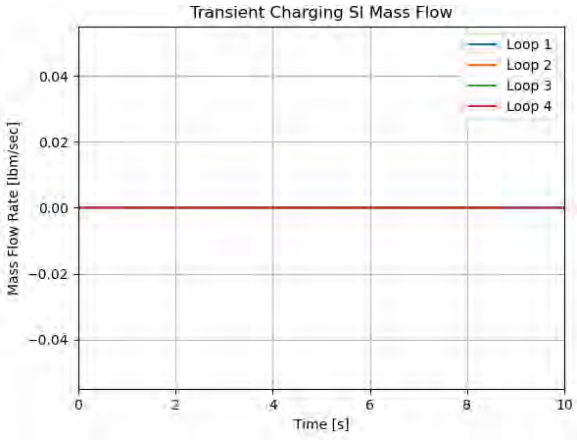
Transient Charging SI Mass Flow
Loop 1
Loop 2
Loop 3
Loop 4
Mass Flow Rate [lbm/sec]
Time [s]

H

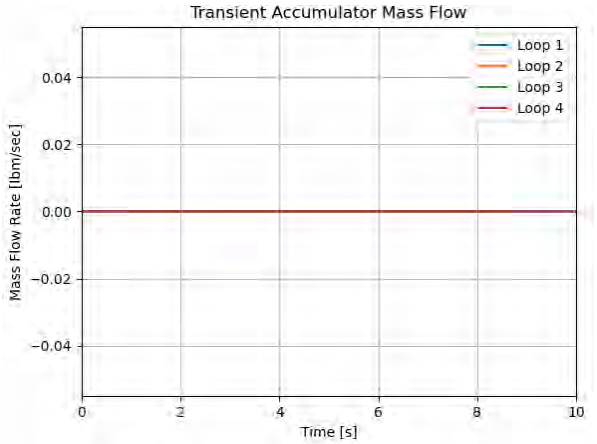

I

Figure 4-5. TR boundary conditions for the locked rotor scenario (LOOP).

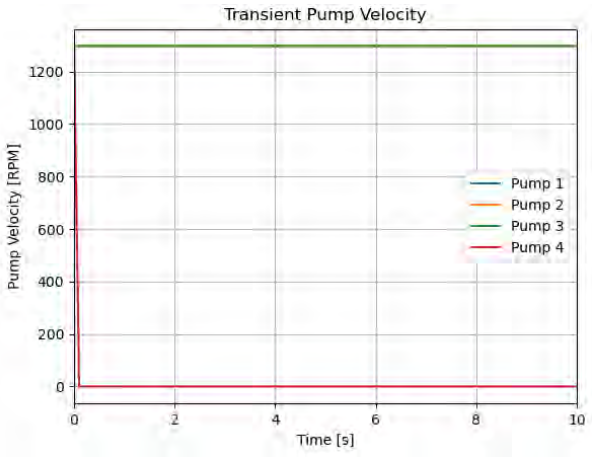

A

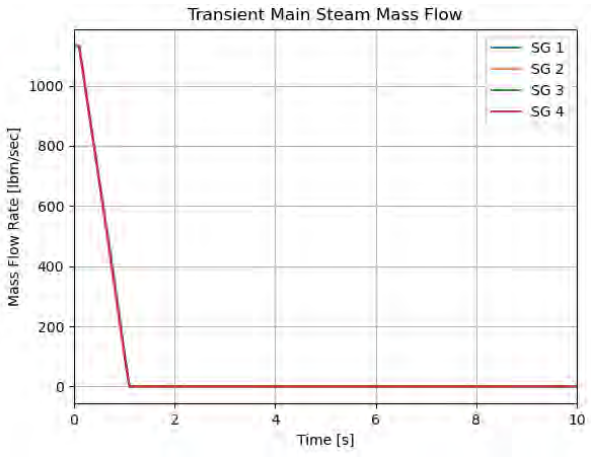

B

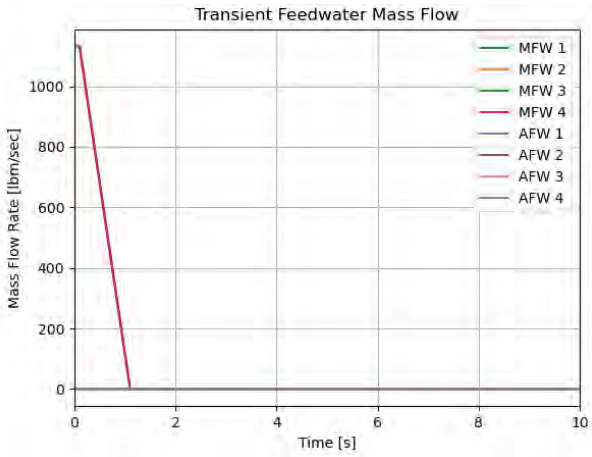

C

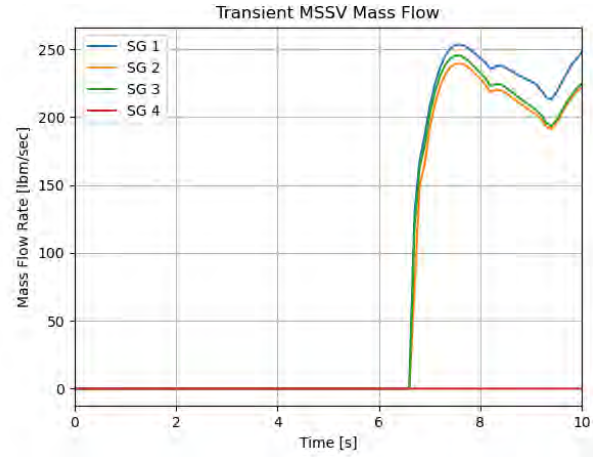

D

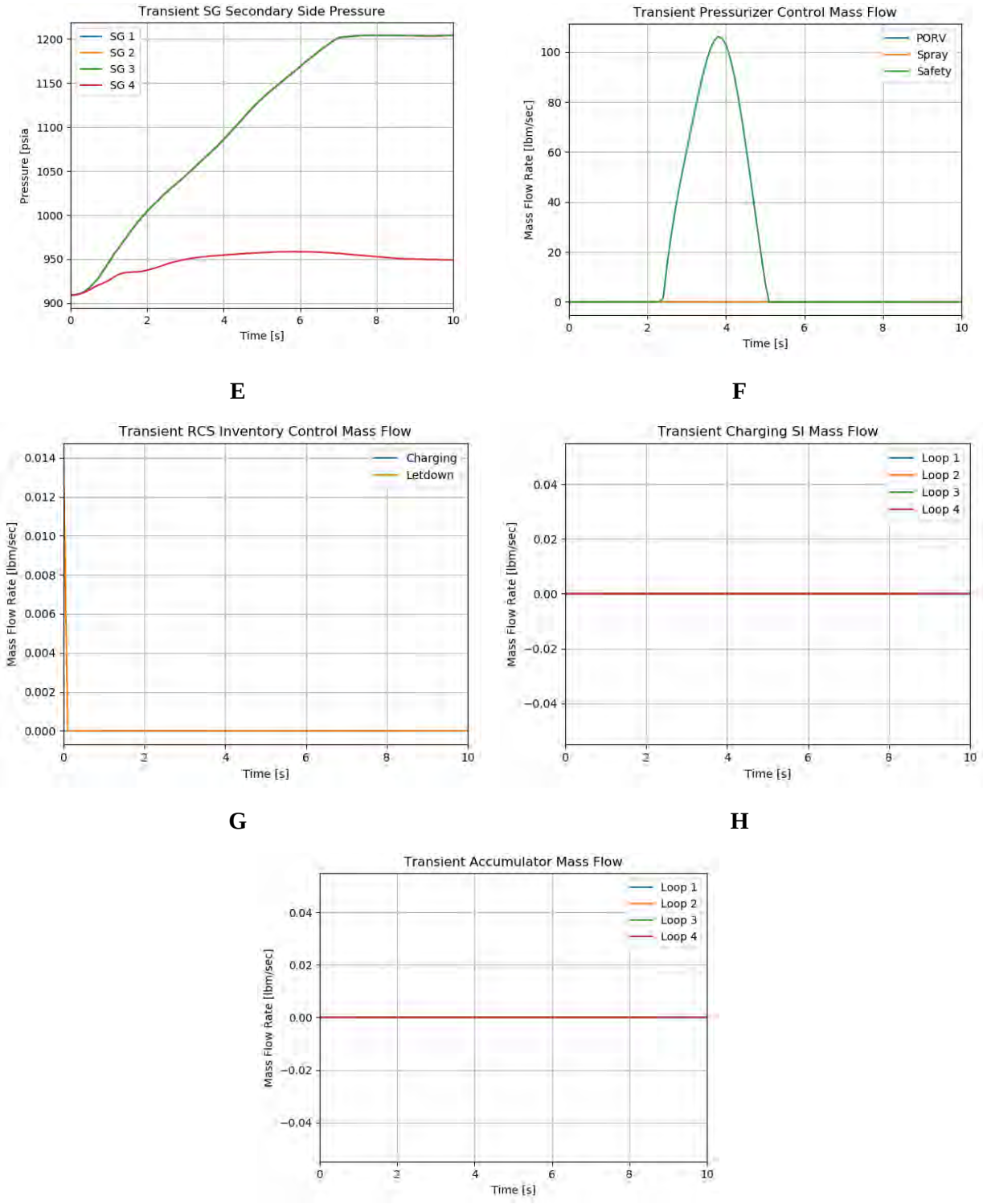

Figure 4-6. TR boundary conditions for the locked rotor scenario (OPA).

4.5.5 TR Results

The RELAP5-3D results are compared to the locked rotor runs from the FSAR in the paragraphs below. Note that the figures labeled with

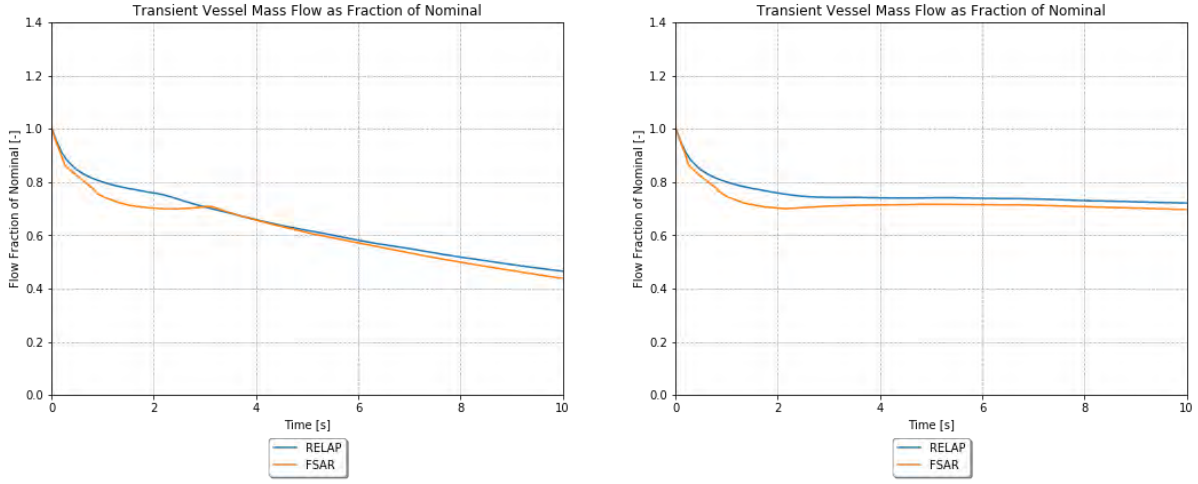

A **B**

Figure 4-7. TR Vessel Mass Flow as a fraction of nominal for the locked rotor scenario (e.g., both the LOOP and the OPA).

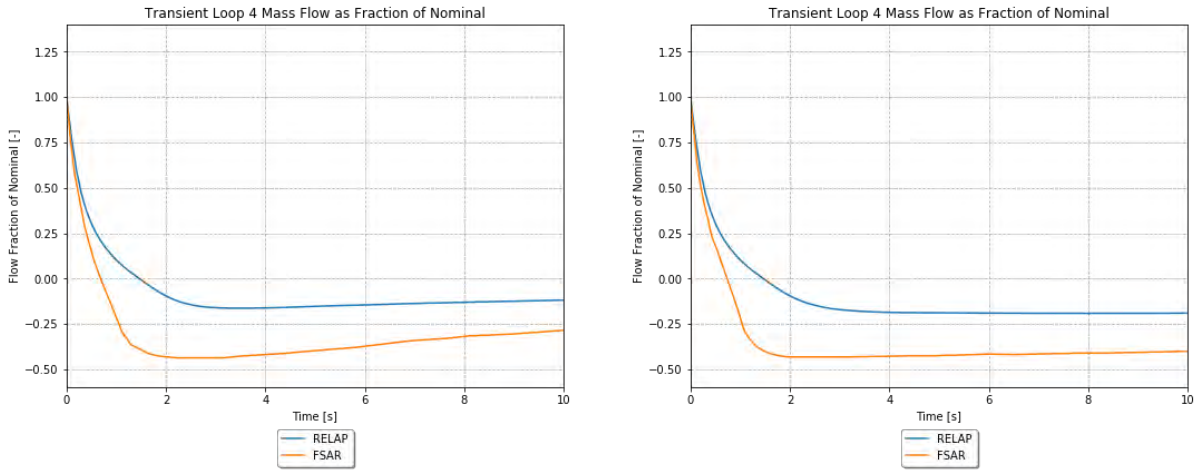

A **B**

Figure 4-8. TR Loop 4 Mass Flow as a fraction of nominal for the locked rotor scenario (e.g., both the LOOP and the OPA).

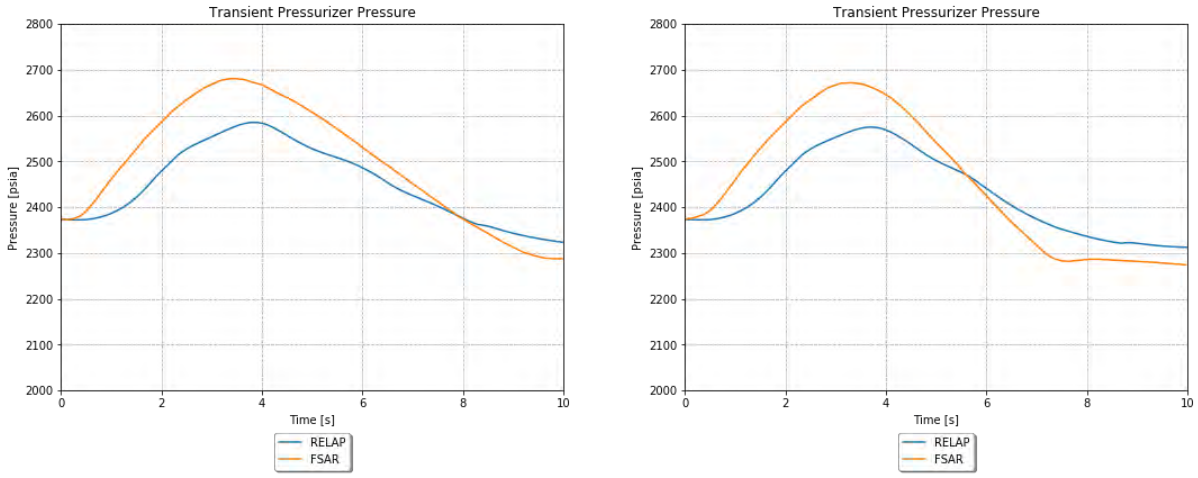

A **B**

Figure 4-9. TR PRZ Pressure for the locked rotor scenario (e.g., both the LOOP and the OPA).

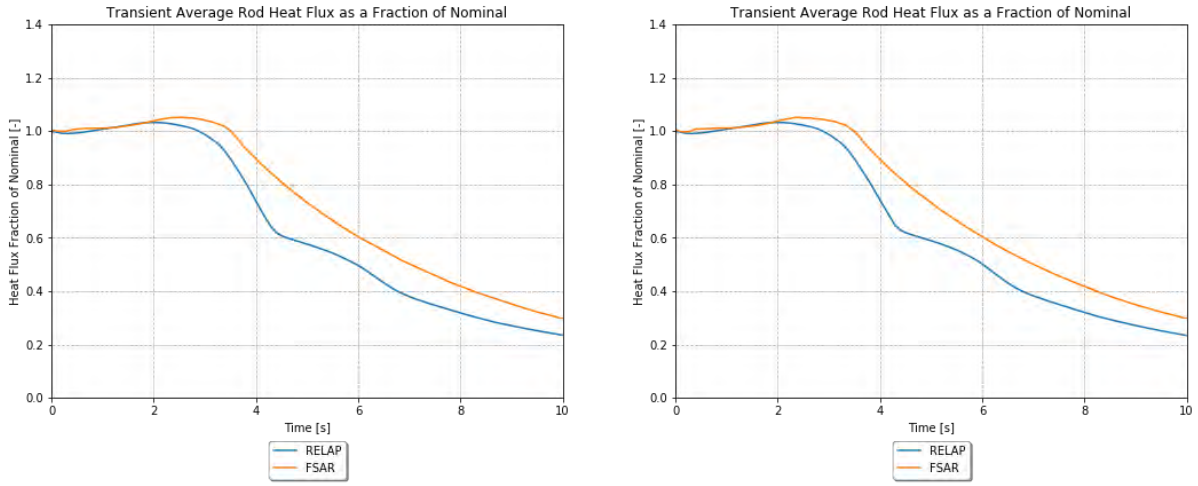

A **B**

Figure 4-10. TR Average Rod Heat Flux as a fraction of nominal for the locked rotor scenario (e.g., both the LOOP and the OPA).

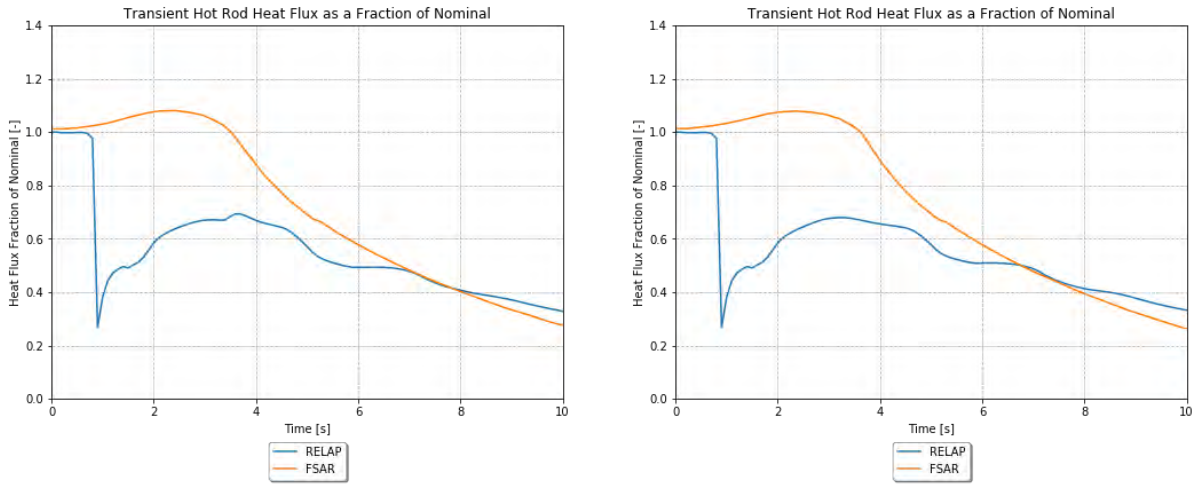

A **B**

Figure 4-11. TR Hot Rod Heat Flux as a fraction of nominal for the locked rotor scenario (e.g., both the LOOP and the OPA).

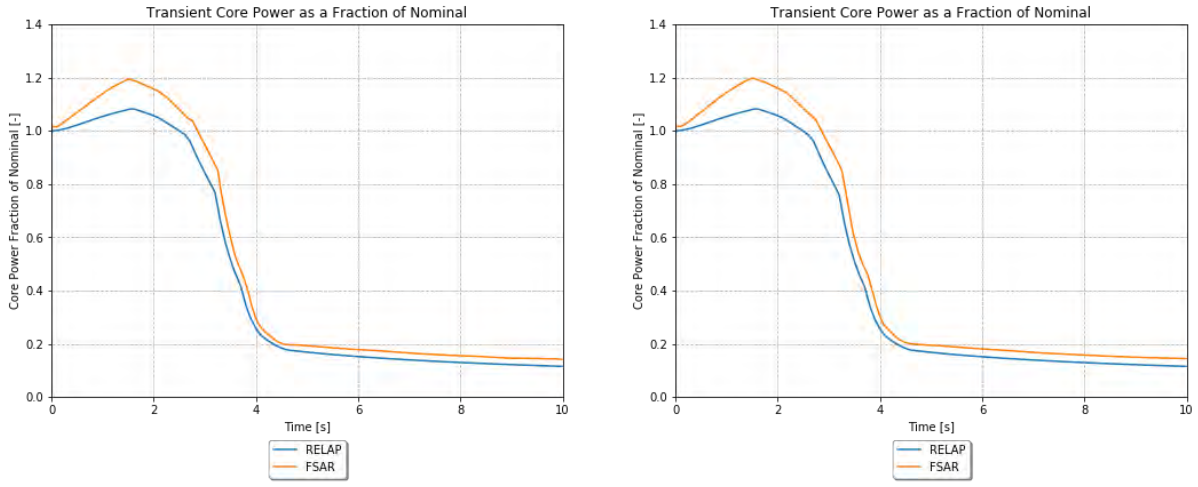

A **B**

Figure 4-12. TR Core Power as a fraction of nominal for the locked rotor scenario (e.g., both the LOOP and the OPA).

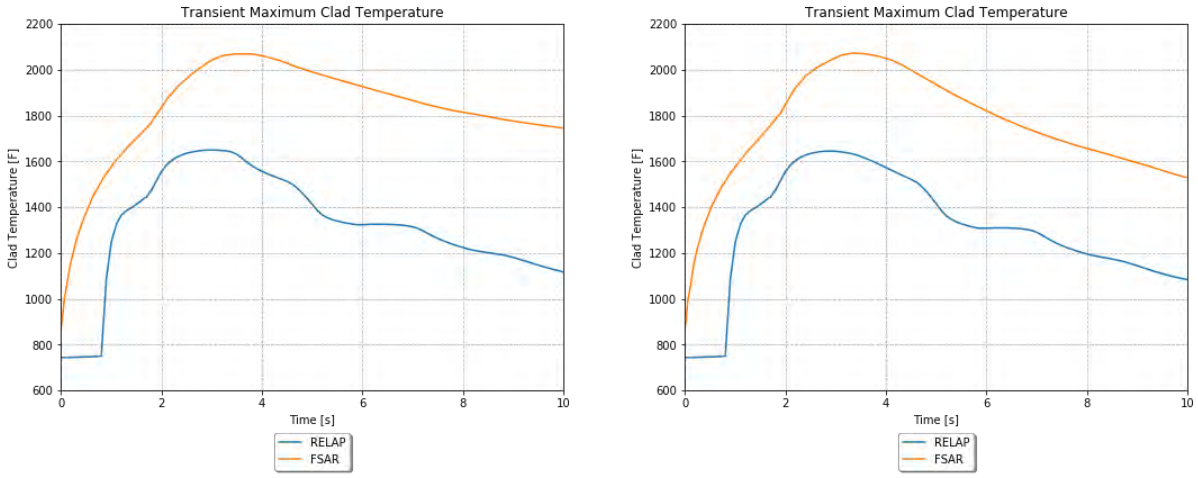

A **B**

Figure 4-13. TR Maximum Clad Temperature for the locked rotor scenario (e.g., both the LOOP and the OPA).

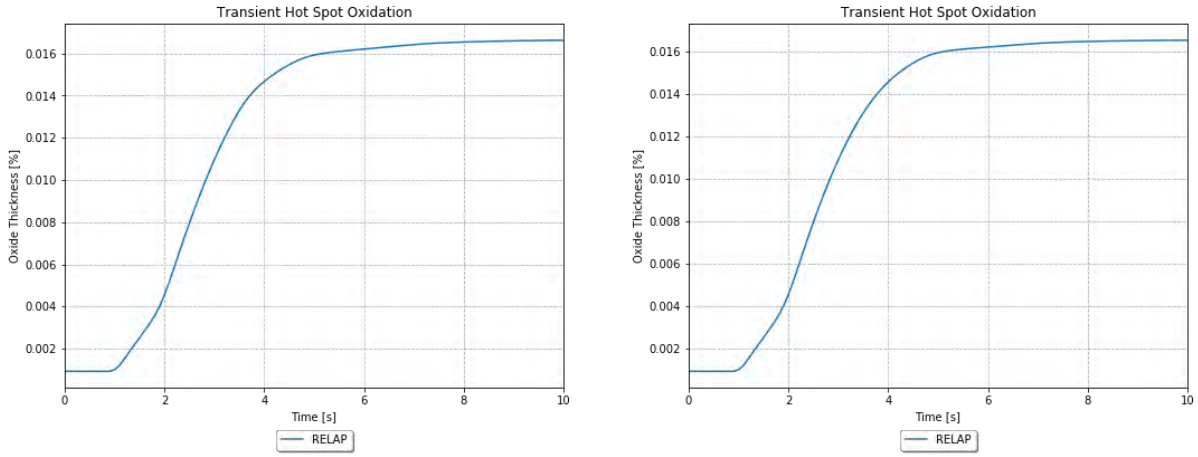

A **B**

Figure 4-14. TR Cladding Oxidation at the peak power location for the locked rotor scenario (e.g., both the LOOP and the OPA).

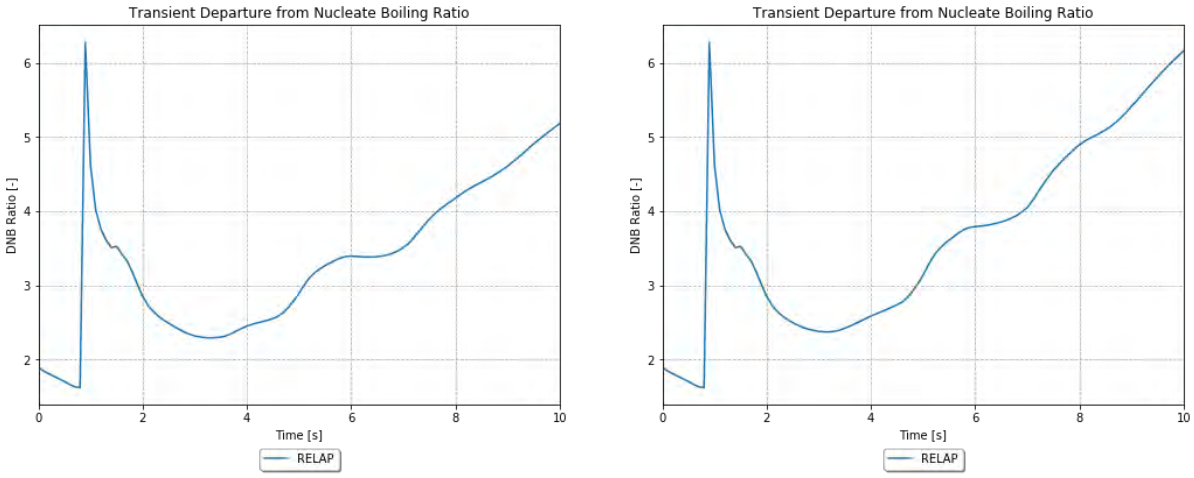

A **B**

Figure 4-15-A are for LOOP and the figures labeled with

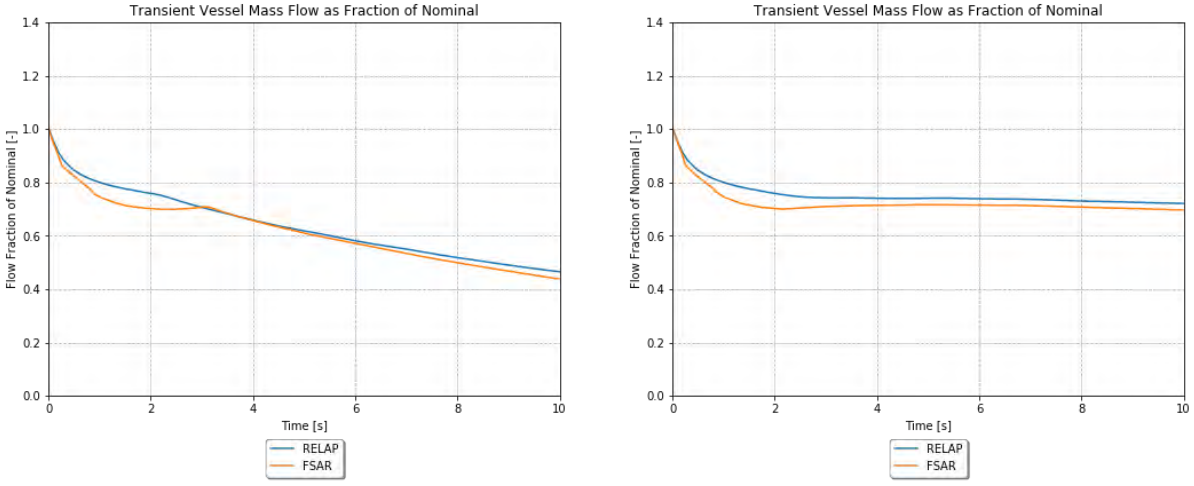

A **B**

Figure 4-7. TR Vessel Mass Flow as a fraction of nominal for the locked rotor scenario (e.g., both the LOOP and the OPA).

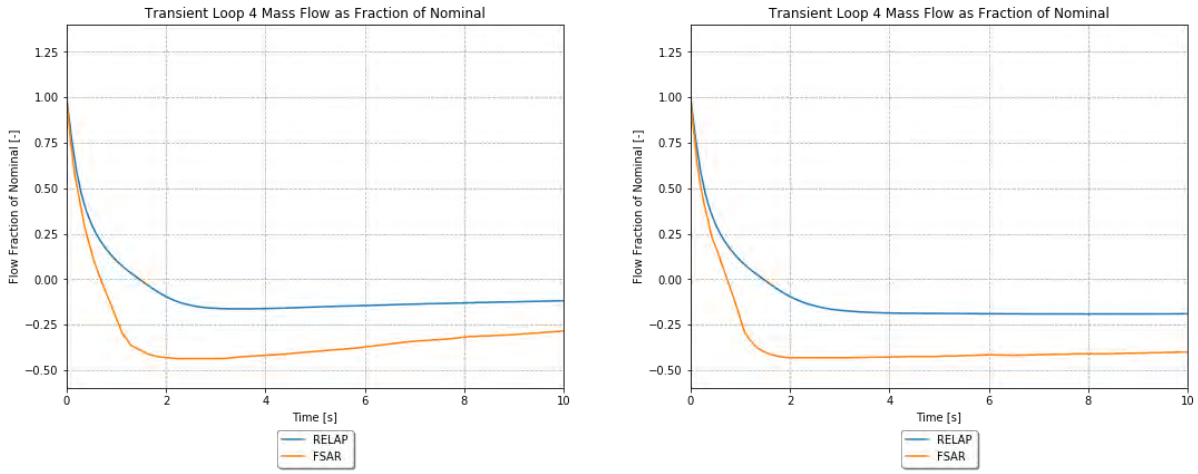

A **B**

Figure 4-8. TR Loop 4 Mass Flow as a fraction of nominal for the locked rotor scenario (e.g., both the LOOP and the OPA).

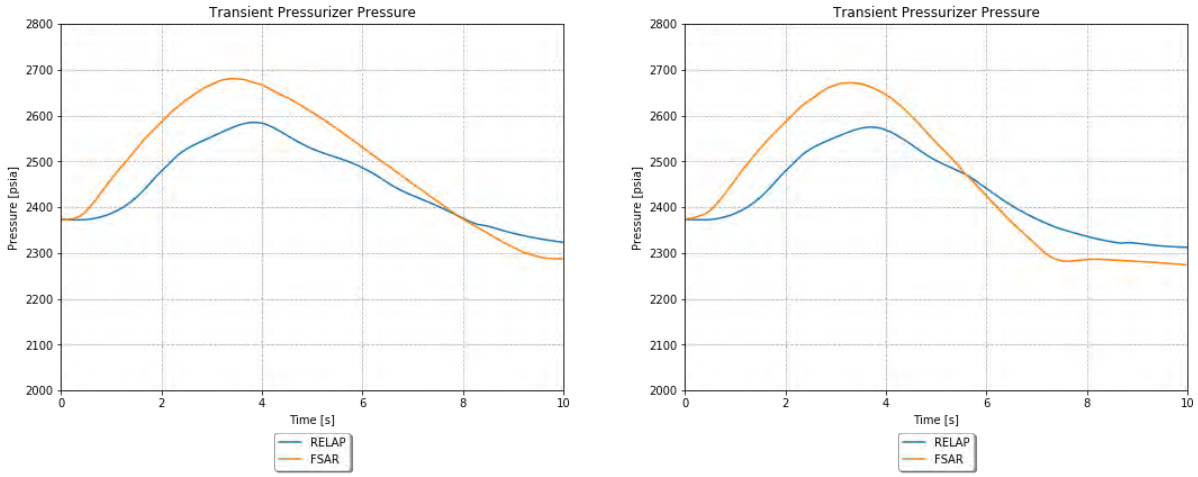

A **B**

Figure 4-9. TR PRZ Pressure for the locked rotor scenario (e.g., both the LOOP and the OPA).

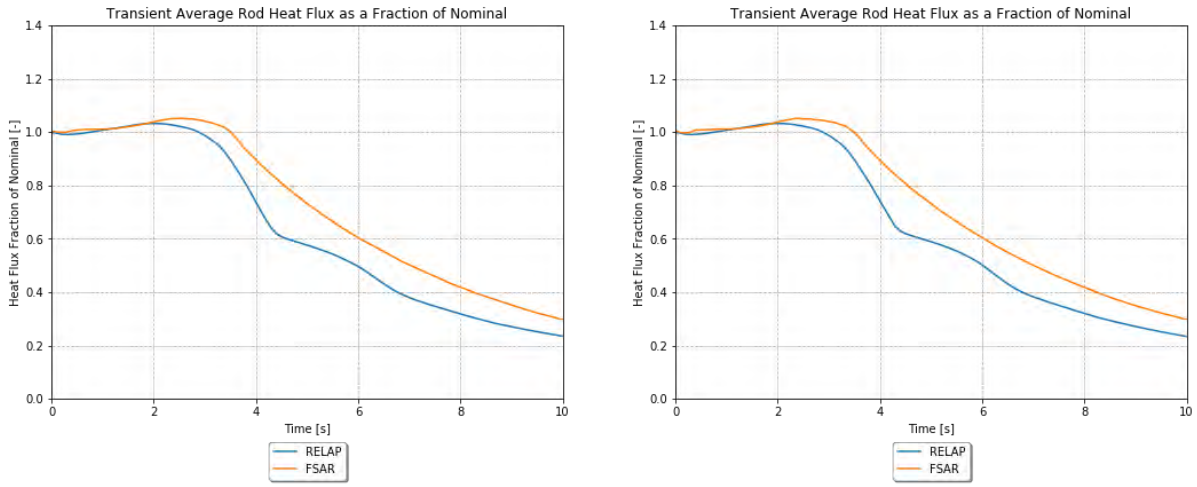

A **B**

Figure 4-10. TR Average Rod Heat Flux as a fraction of nominal for the locked rotor scenario (e.g., both the LOOP and the OPA).

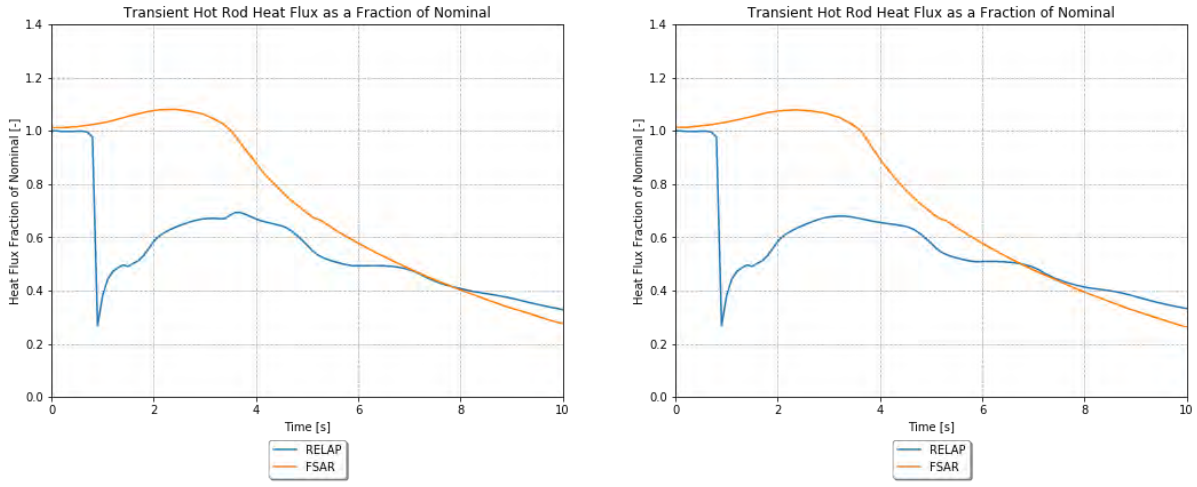

A **B**

Figure 4-11. TR Hot Rod Heat Flux as a fraction of nominal for the locked rotor scenario (e.g., both the LOOP and the OPA).

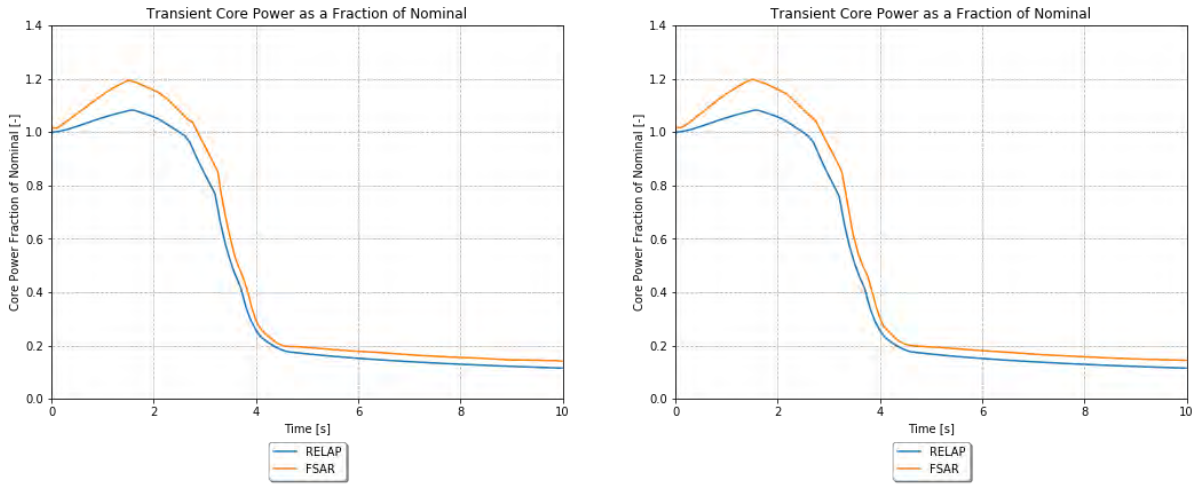

A **B**

Figure 4-12. TR Core Power as a fraction of nominal for the locked rotor scenario (e.g., both the LOOP and the OPA).

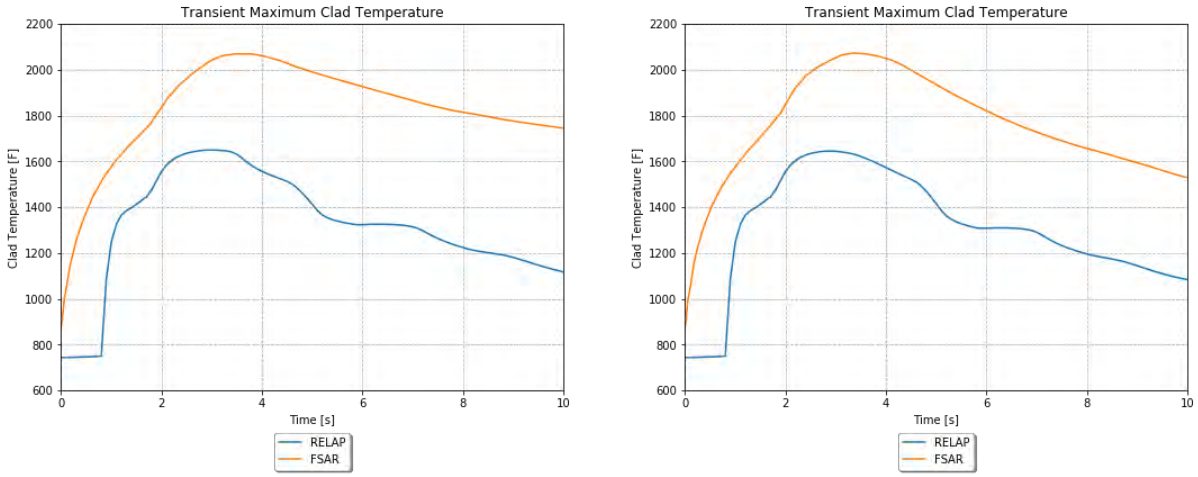

A **B**

Figure 4-13. TR Maximum Clad Temperature for the locked rotor scenario (e.g., both the LOOP and the OPA).

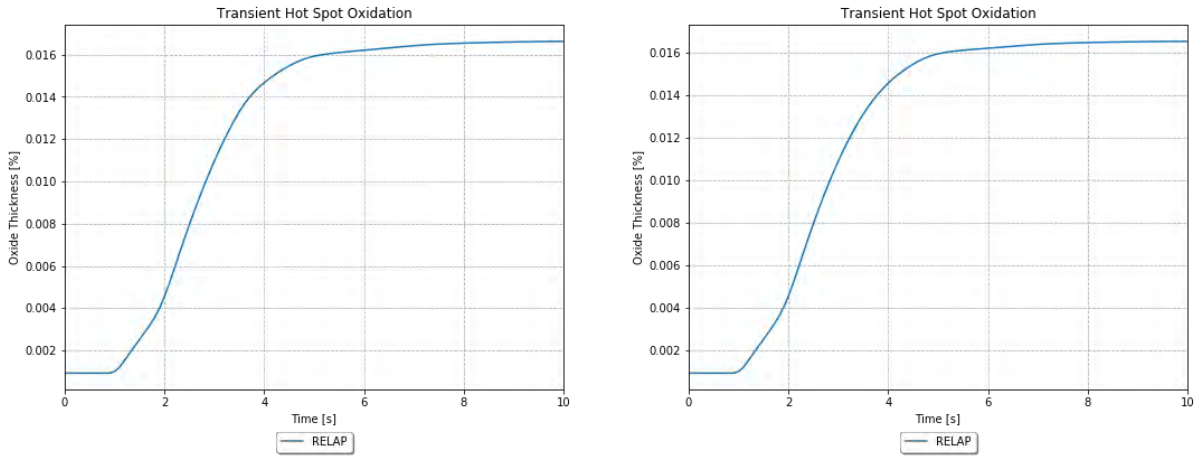

A **B**

Figure 4-14. TR Cladding Oxidation at the peak power location for the locked rotor scenario (e.g., both the LOOP and the OPA).

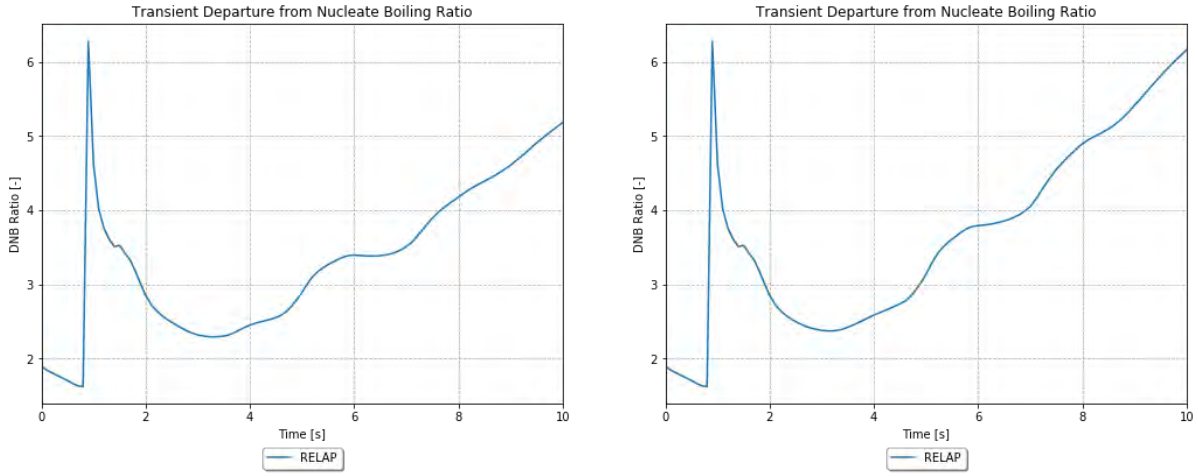

A **B**

Figure 4-15-B are for OPA.

The TR vessel mass flow as a fraction of the nominal flow is shown in

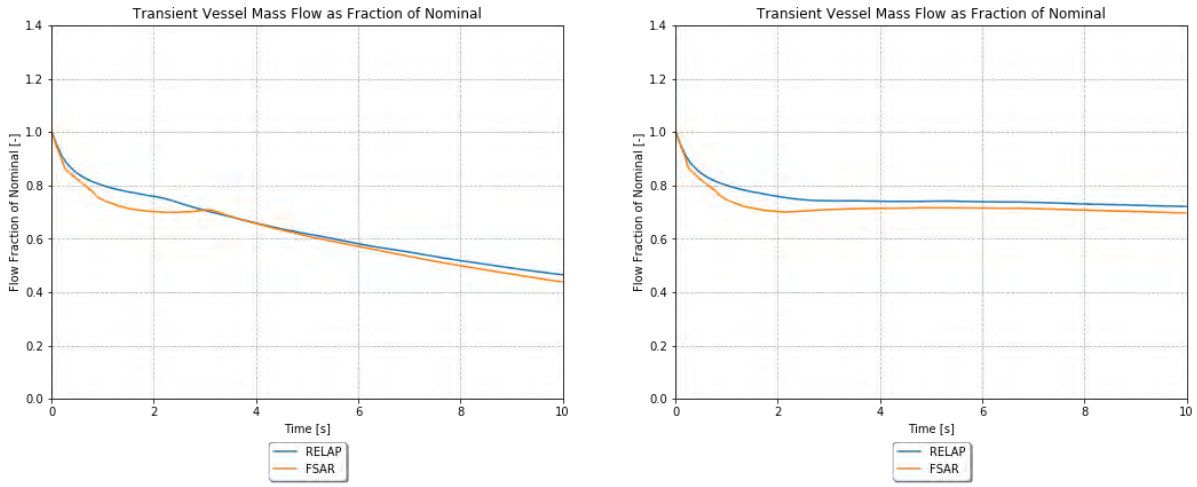

A **B**

Figure 4-7. TR Vessel Mass Flow as a fraction of nominal for the locked rotor scenario (e.g., both the LOOP and the OPA).

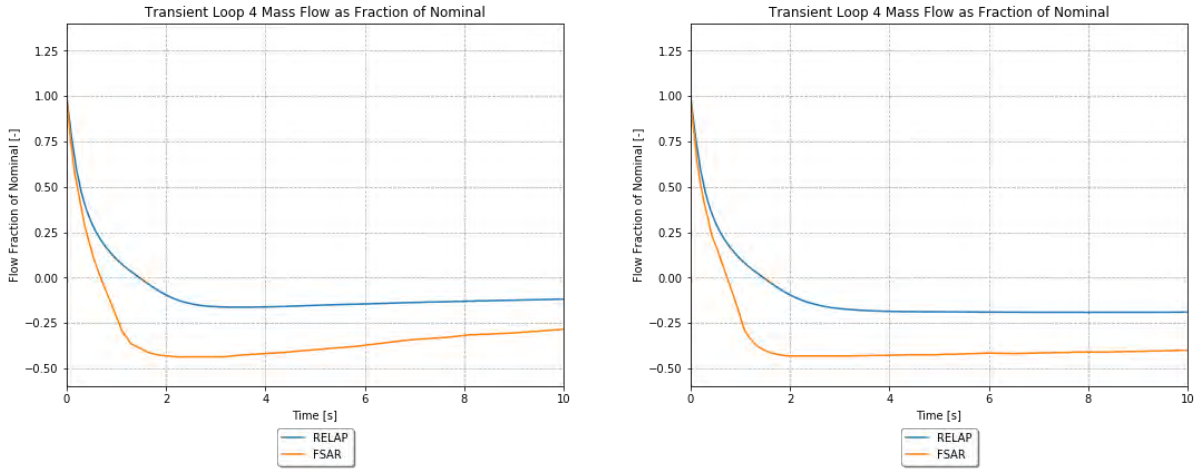

A **B**

Figure 4-8. TR Loop 4 Mass Flow as a fraction of nominal for the locked rotor scenario (e.g., both the LOOP and the OPA).

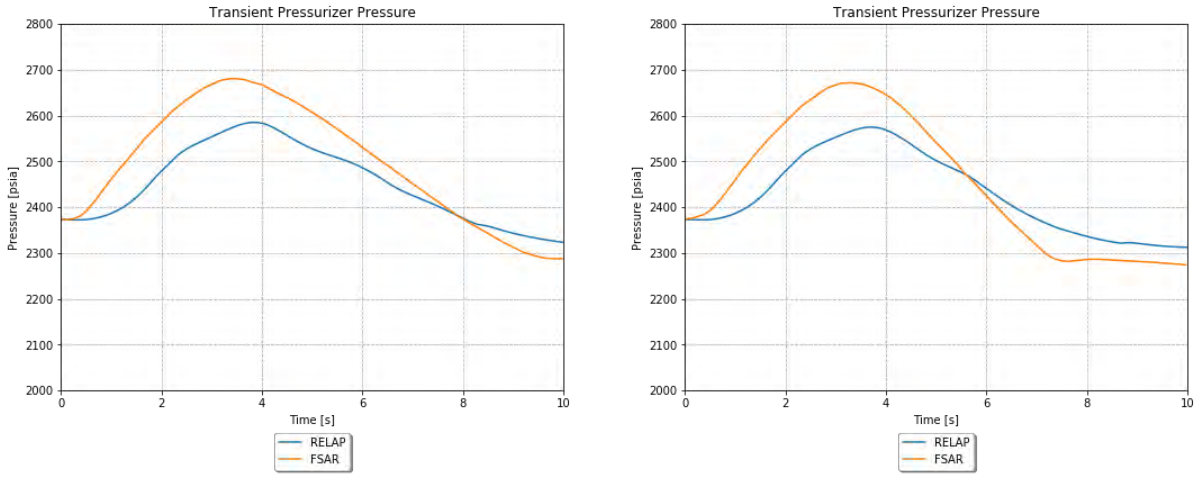

A **B**

Figure 4-9. TR PRZ Pressure for the locked rotor scenario (e.g., both the LOOP and the OPA).

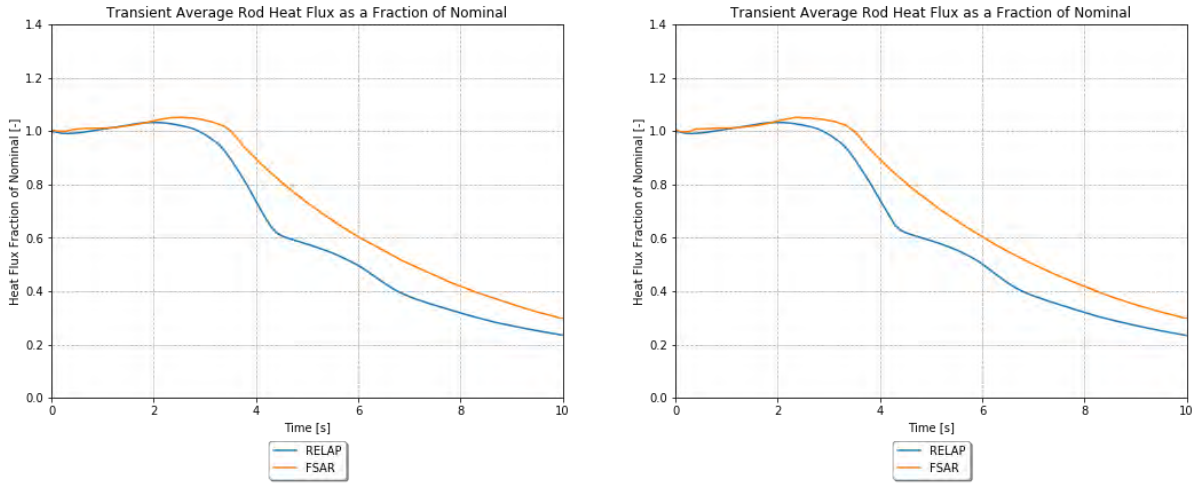

A **B**

Figure 4-10. TR Average Rod Heat Flux as a fraction of nominal for the locked rotor scenario (e.g., both the LOOP and the OPA).

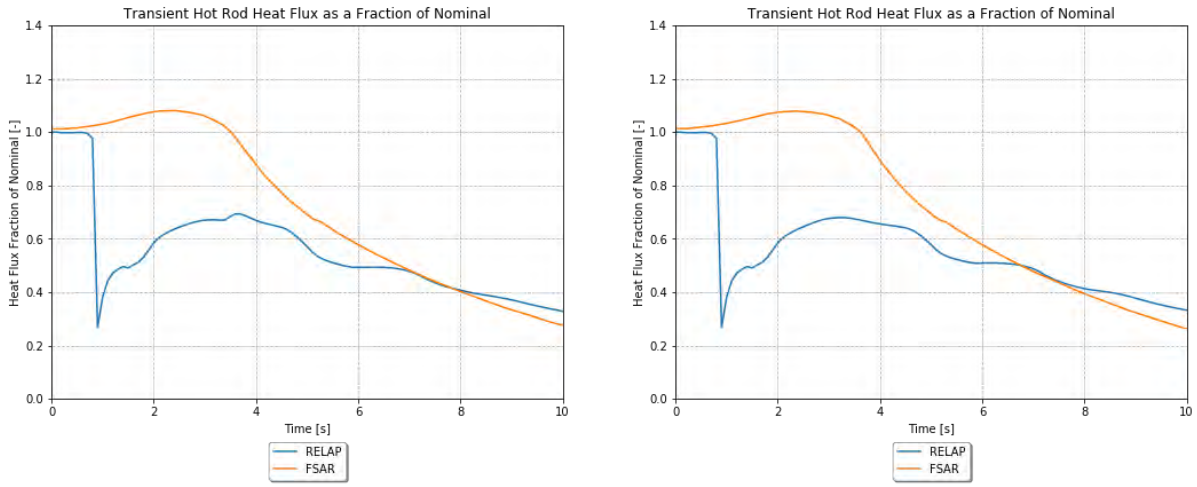

A **B**

Figure 4-11. TR Hot Rod Heat Flux as a fraction of nominal for the locked rotor scenario (e.g., both the LOOP and the OPA).

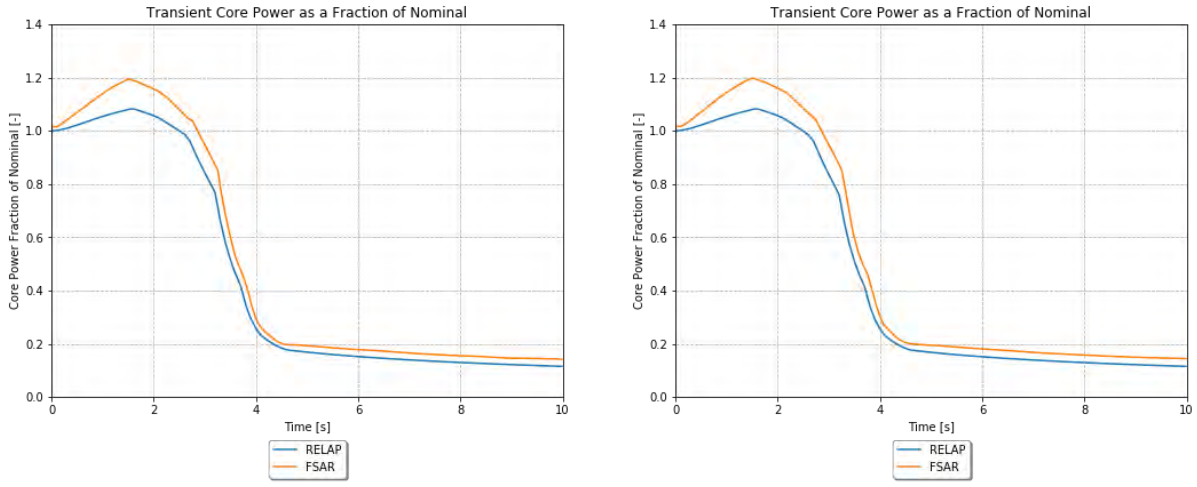

A **B**

Figure 4-12. TR Core Power as a fraction of nominal for the locked rotor scenario (e.g., both the LOOP and the OPA).

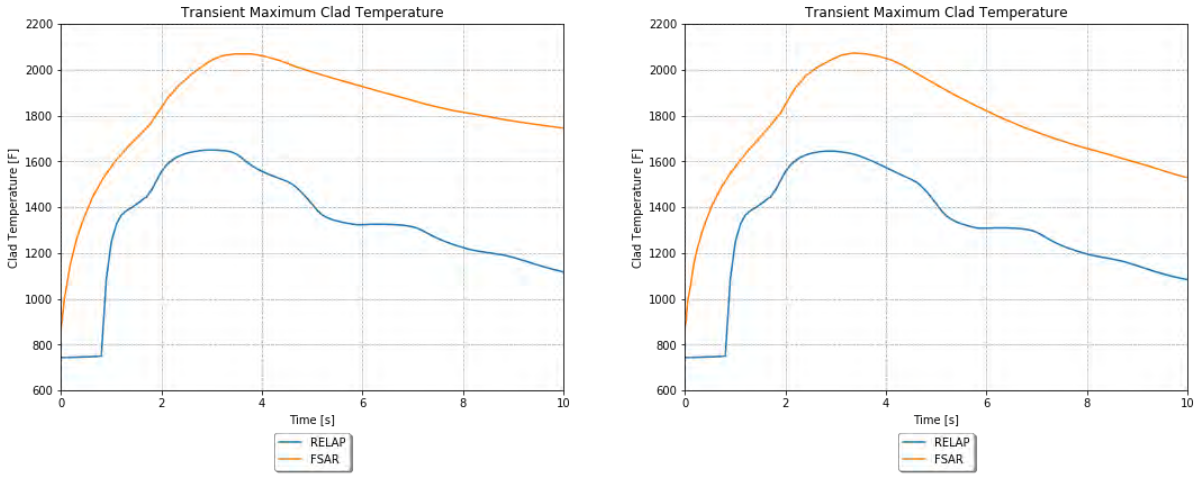

A **B**

Figure 4-13. TR Maximum Clad Temperature for the locked rotor scenario (e.g., both the LOOP and the OPA).

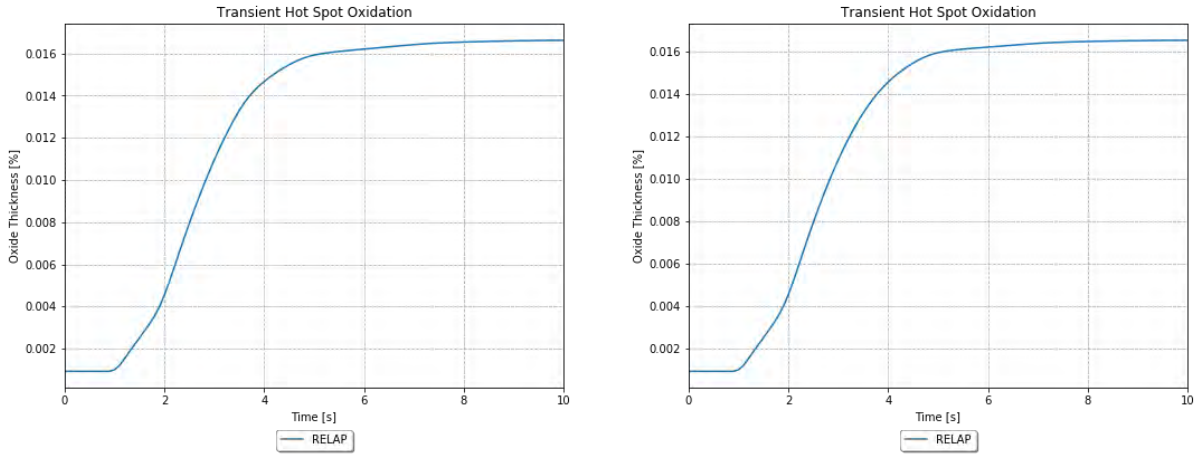

A **B**

Figure 4-14. TR Cladding Oxidation at the peak power location for the locked rotor scenario (e.g., both the LOOP and the OPA).

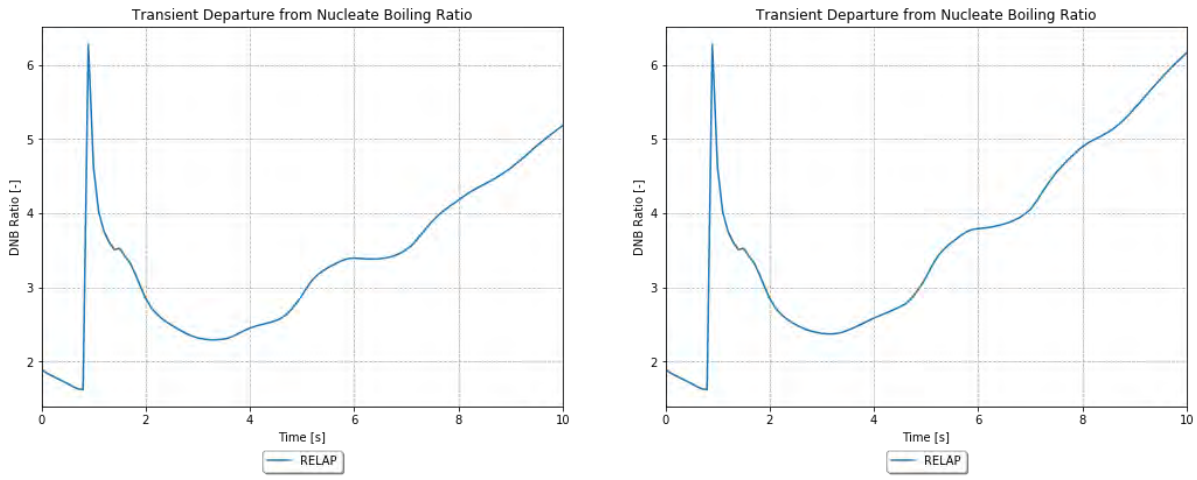

A **B**

Figure 4-15-A and

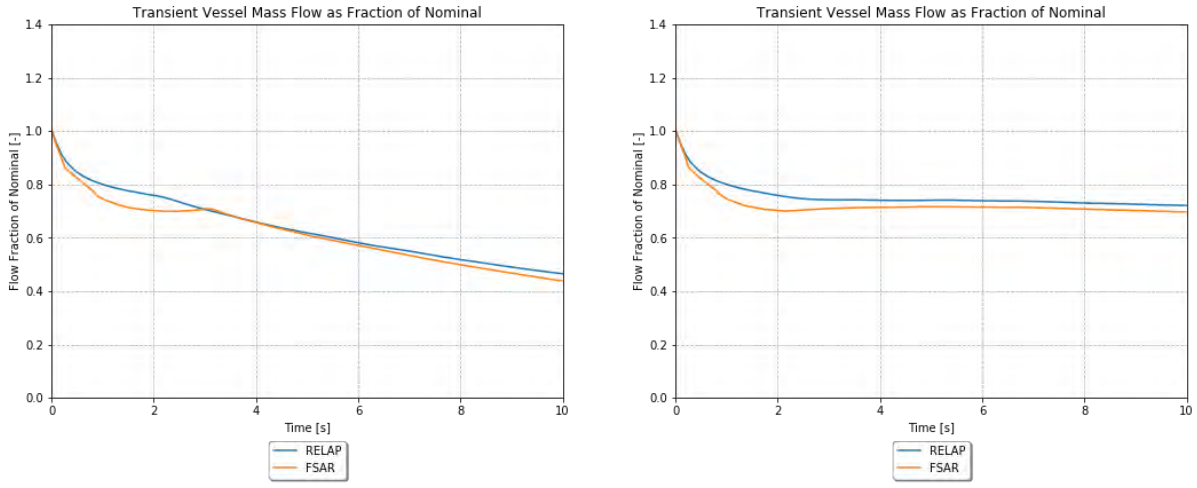

A **B**

Figure 4-7. TR Vessel Mass Flow as a fraction of nominal for the locked rotor scenario (e.g., both the LOOP and the OPA).

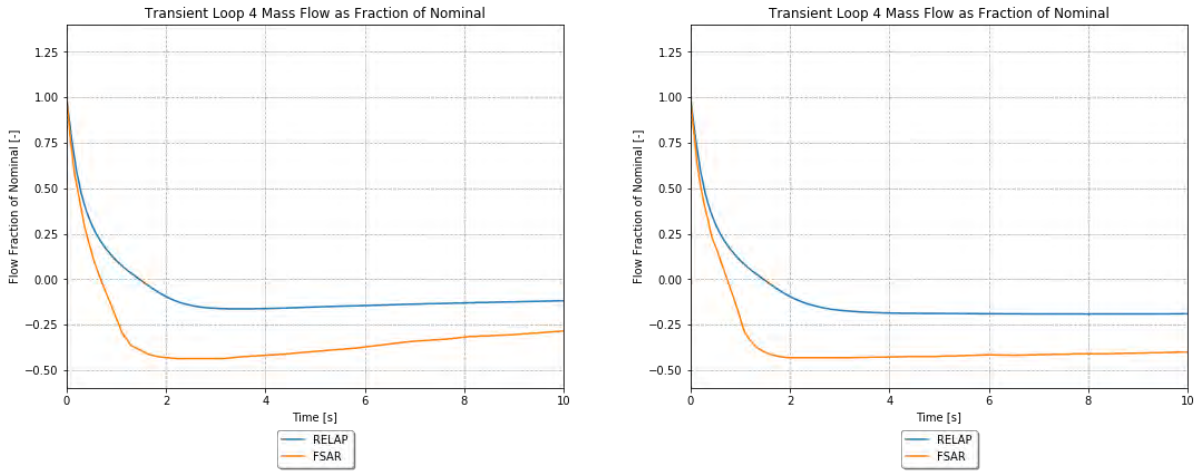

A **B**

Figure 4-8. TR Loop 4 Mass Flow as a fraction of nominal for the locked rotor scenario (e.g., both the LOOP and the OPA).

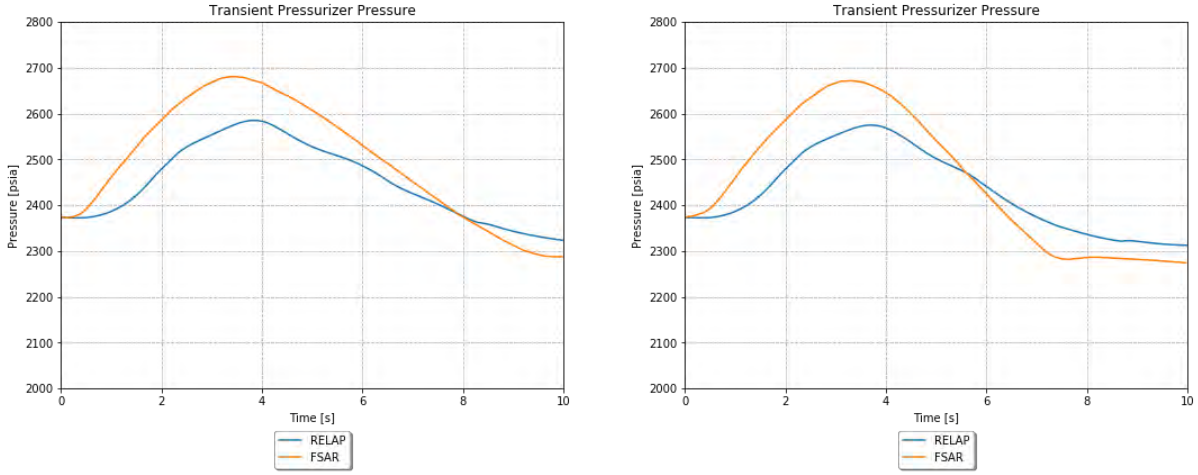

A **B**

Figure 4-9. TR PRZ Pressure for the locked rotor scenario (e.g., both the LOOP and the OPA).

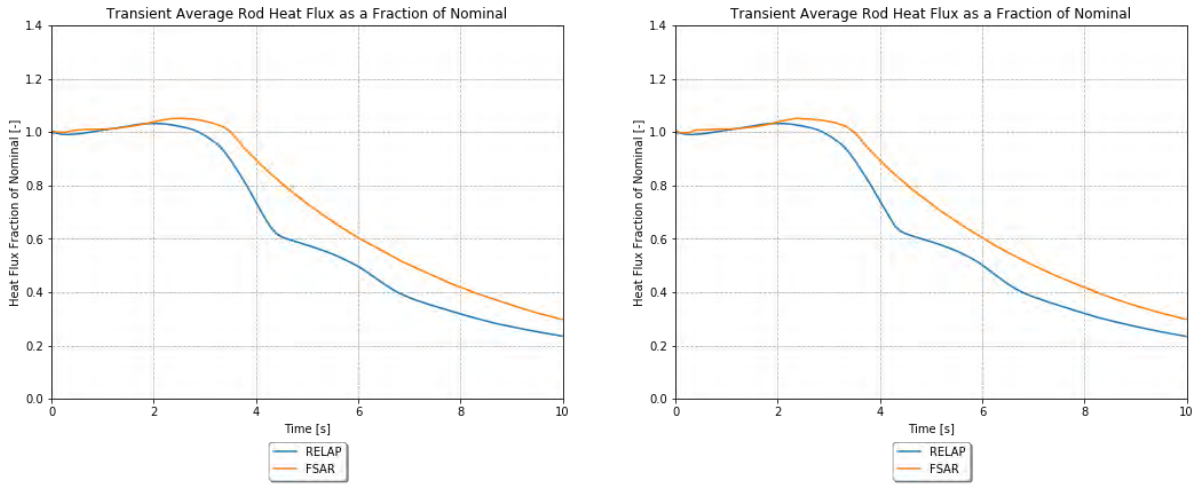

A **B**

Figure 4-10. TR Average Rod Heat Flux as a fraction of nominal for the locked rotor scenario (e.g., both the LOOP and the OPA).

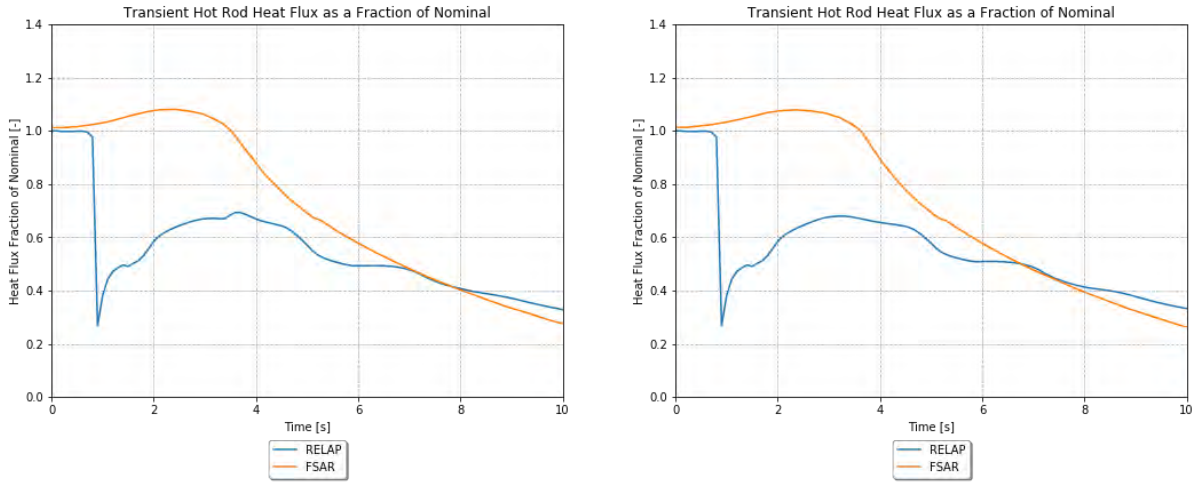

A **B**

Figure 4-11. TR Hot Rod Heat Flux as a fraction of nominal for the locked rotor scenario (e.g., both the LOOP and the OPA).

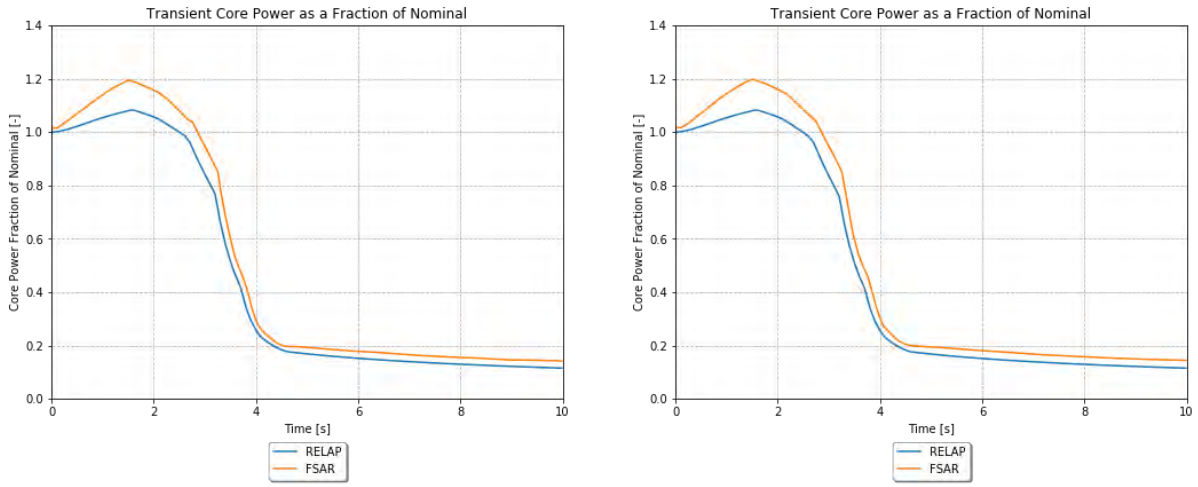

A **B**

Figure 4-12. TR Core Power as a fraction of nominal for the locked rotor scenario (e.g., both the LOOP and the OPA).

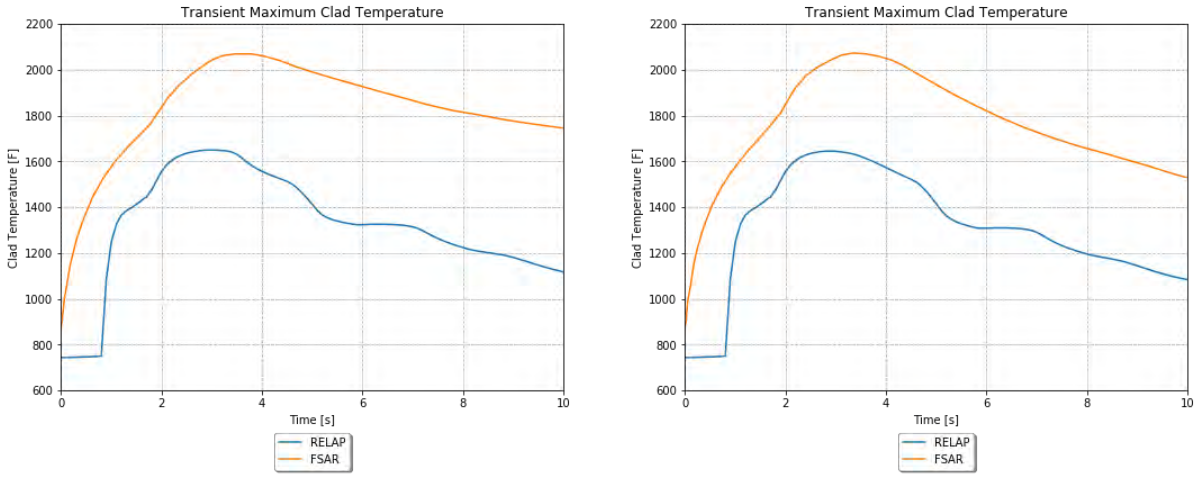

A **B**

Figure 4-13. TR Maximum Clad Temperature for the locked rotor scenario (e.g., both the LOOP and the OPA).

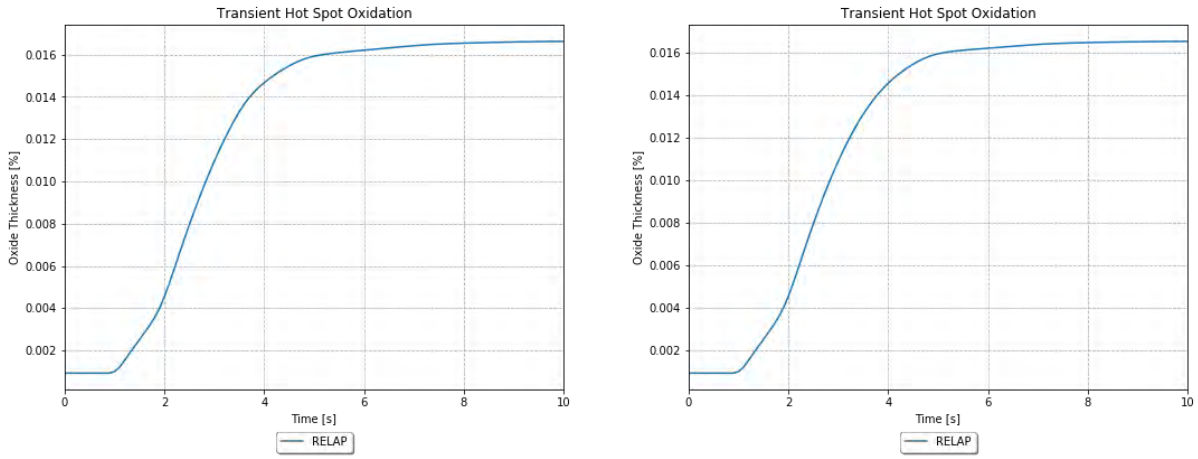

A **B**

Figure 4-14. TR Cladding Oxidation at the peak power location for the locked rotor scenario (e.g., both the LOOP and the OPA).

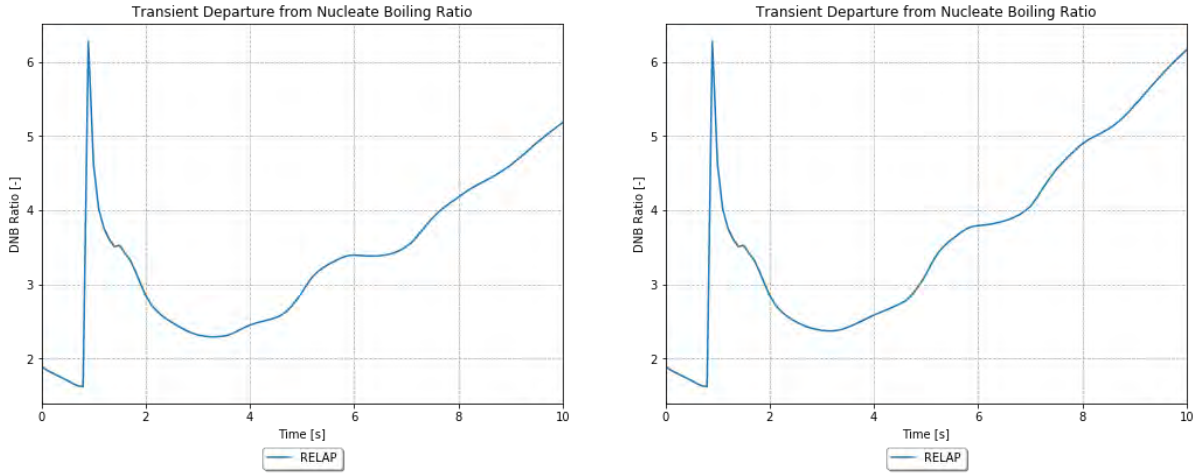

A **B**

Figure 4-15-B. The LOOP RELAP5-3D run initially decreases slightly more slowly than the FSAR run, but the brief plateau encountered by the FSAR run does not happen for the RELAP5-3D LOOP run. As such, the RELAP5-3D LOOP run drops significantly below the FSAR run starting at about two seconds, and they slowly converge by the end of the TR. From

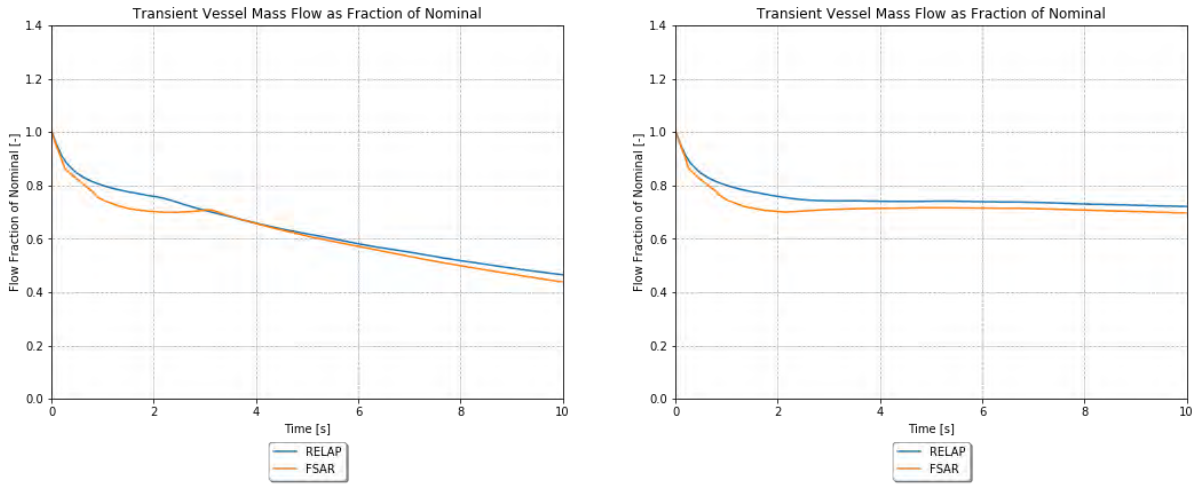

A **B**

Figure 4-7. TR Vessel Mass Flow as a fraction of nominal for the locked rotor scenario (e.g., both the LOOP and the OPA).

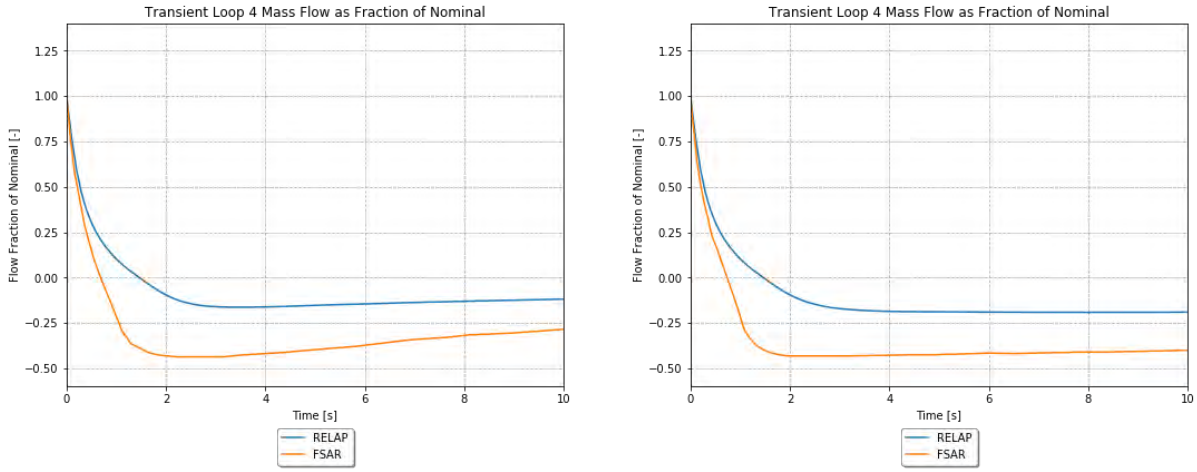

A **B**

Figure 4-8. TR Loop 4 Mass Flow as a fraction of nominal for the locked rotor scenario (e.g., both the LOOP and the OPA).

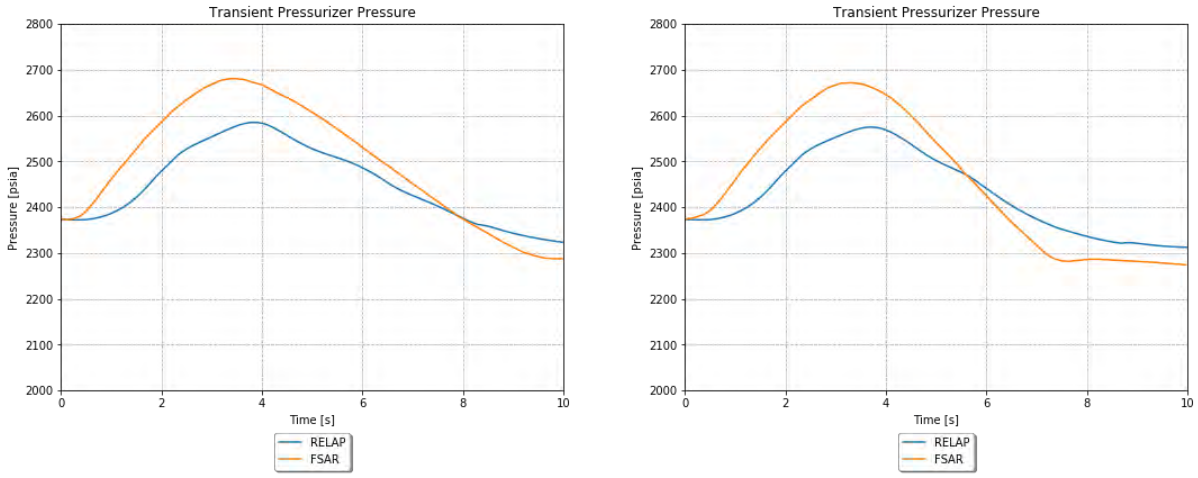

A **B**

Figure 4-9. TR PRZ Pressure for the locked rotor scenario (e.g., both the LOOP and the OPA).

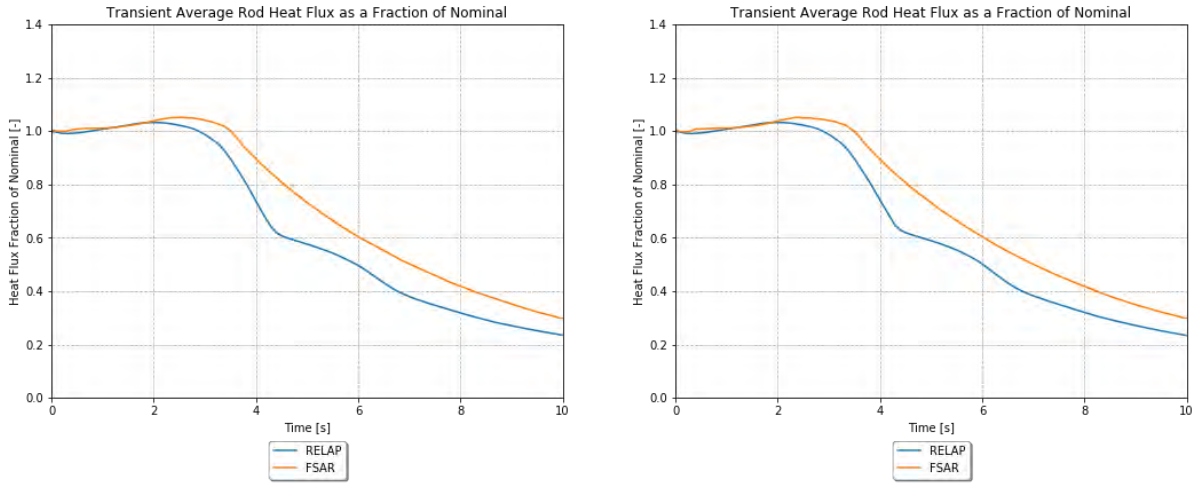

A **B**

Figure 4-10. TR Average Rod Heat Flux as a fraction of nominal for the locked rotor scenario (e.g., both the LOOP and the OPA).

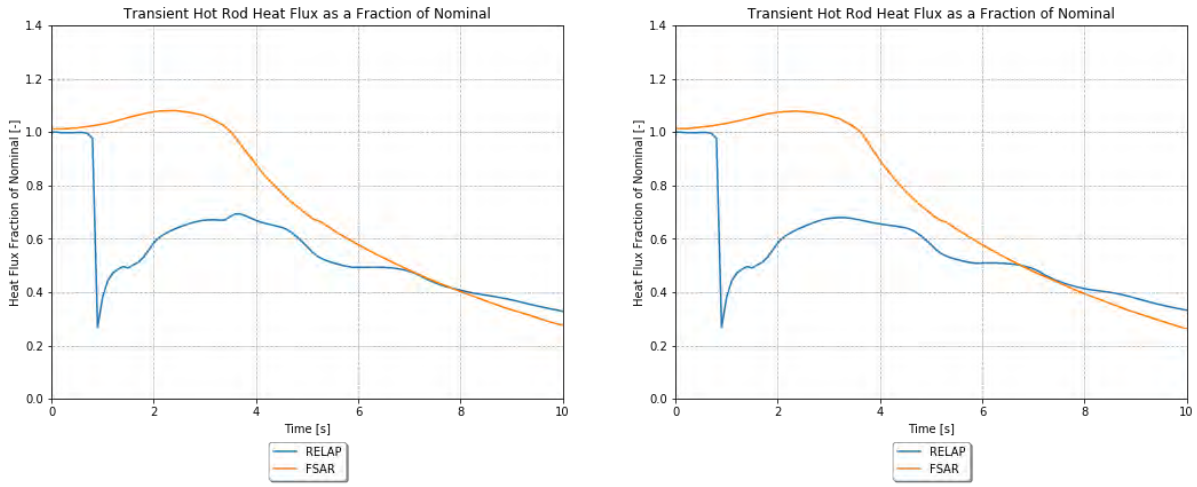

A **B**

Figure 4-11. TR Hot Rod Heat Flux as a fraction of nominal for the locked rotor scenario (e.g., both the LOOP and the OPA).

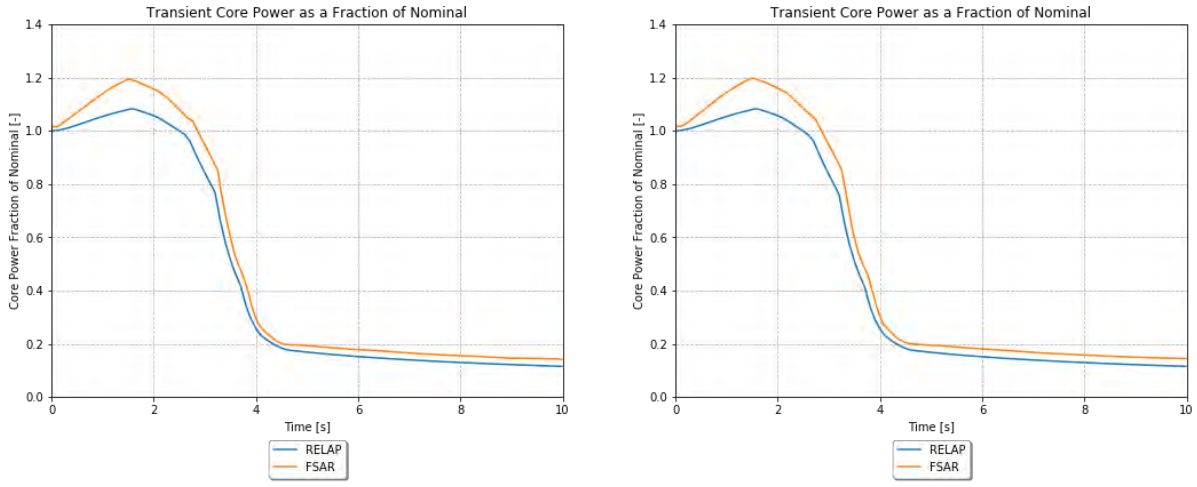

A **B**

Figure 4-12. TR Core Power as a fraction of nominal for the locked rotor scenario (e.g., both the LOOP and the OPA).

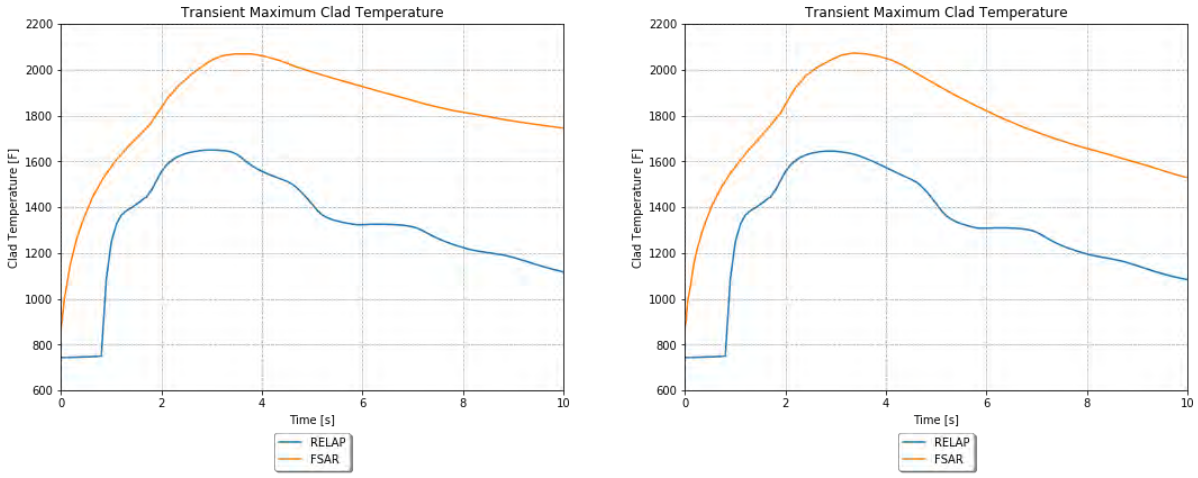

A **B**

Figure 4-13. TR Maximum Clad Temperature for the locked rotor scenario (e.g., both the LOOP and the OPA).

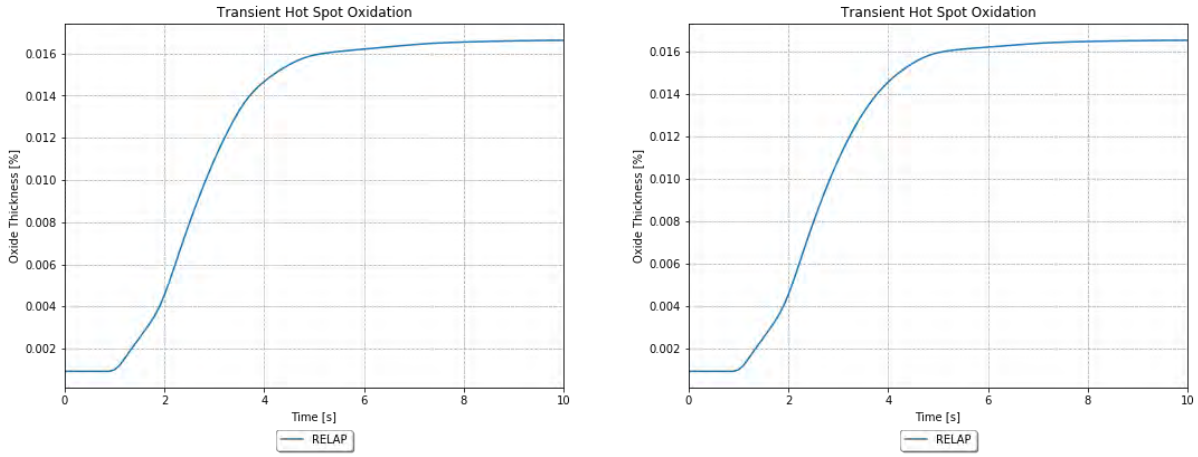

A **B**

Figure 4-14. TR Cladding Oxidation at the peak power location for the locked rotor scenario (e.g., both the LOOP and the OPA).

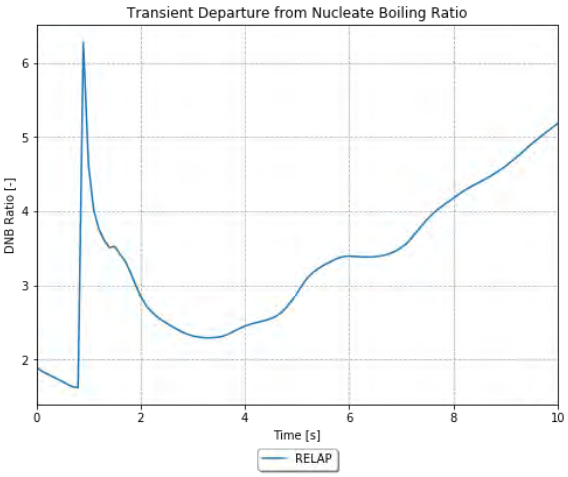

A

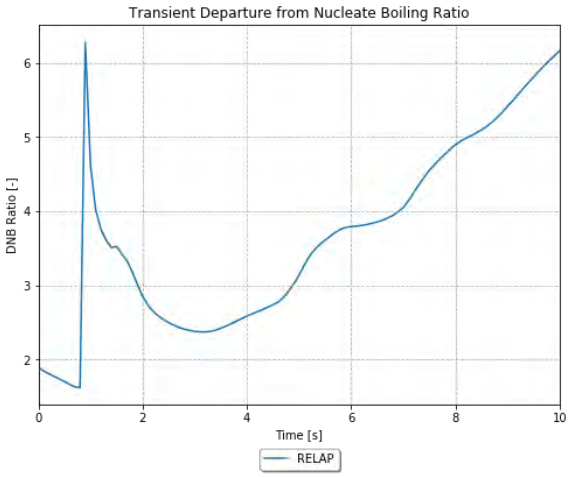

B

Figure 4-15-A and

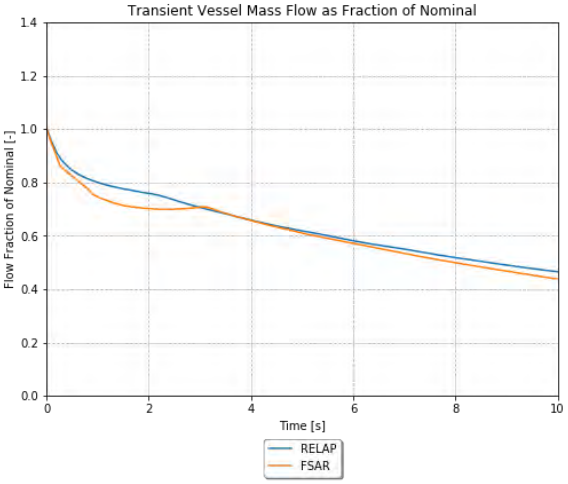

A

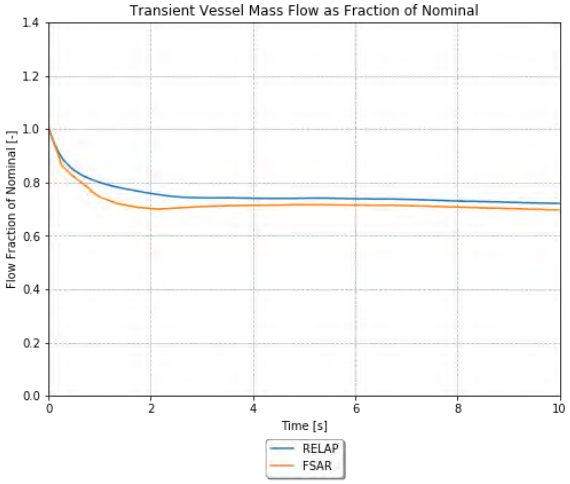

B

Figure 4-7. TR Vessel Mass Flow as a fraction of nominal for the locked rotor scenario (e.g., both the LOOP and the OPA).

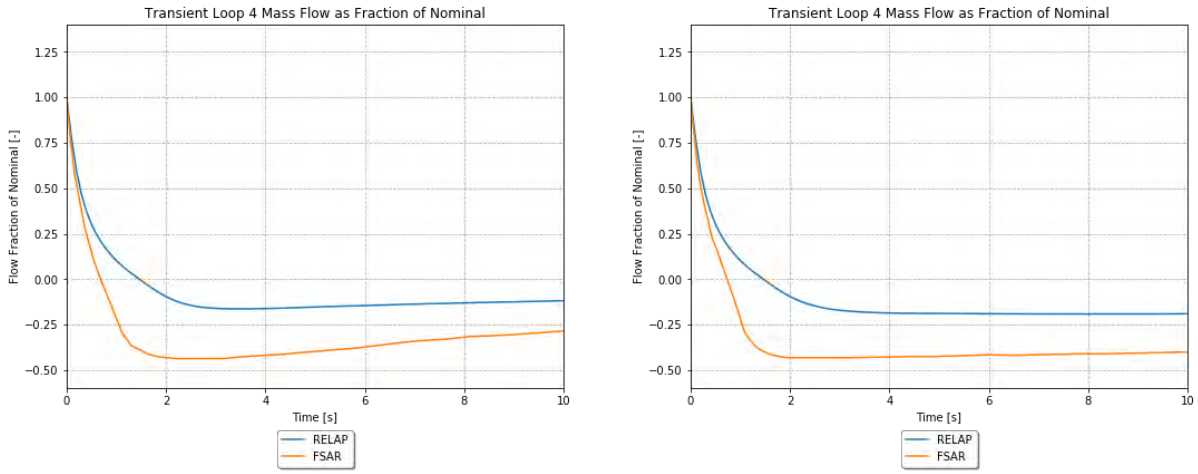

A **B**

Figure 4-8. TR Loop 4 Mass Flow as a fraction of nominal for the locked rotor scenario (e.g., both the LOOP and the OPA).

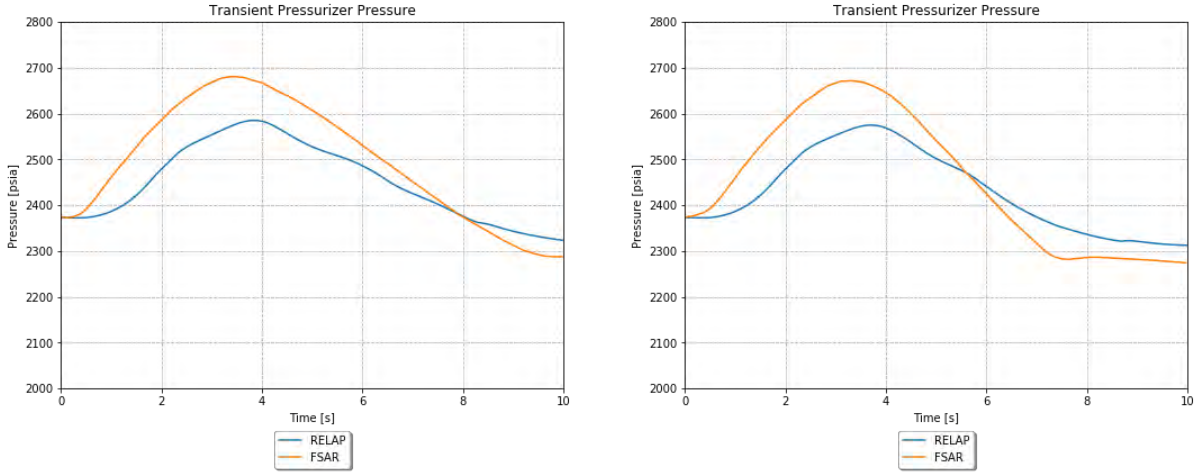

A **B**

Figure 4-9. TR PRZ Pressure for the locked rotor scenario (e.g., both the LOOP and the OPA).

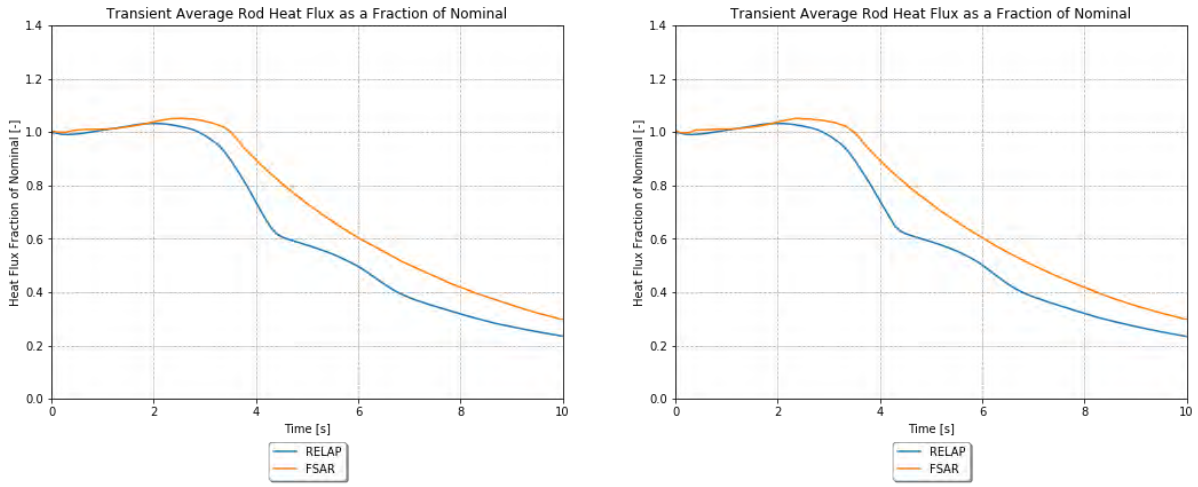

A **B**

Figure 4-10. TR Average Rod Heat Flux as a fraction of nominal for the locked rotor scenario (e.g., both the LOOP and the OPA).

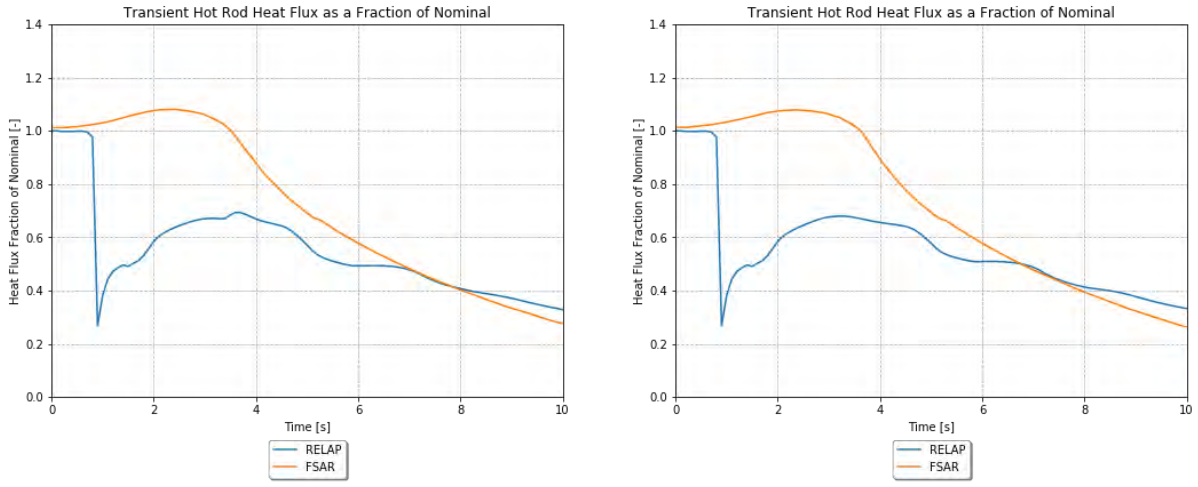

A **B**

Figure 4-11. TR Hot Rod Heat Flux as a fraction of nominal for the locked rotor scenario (e.g., both the LOOP and the OPA).

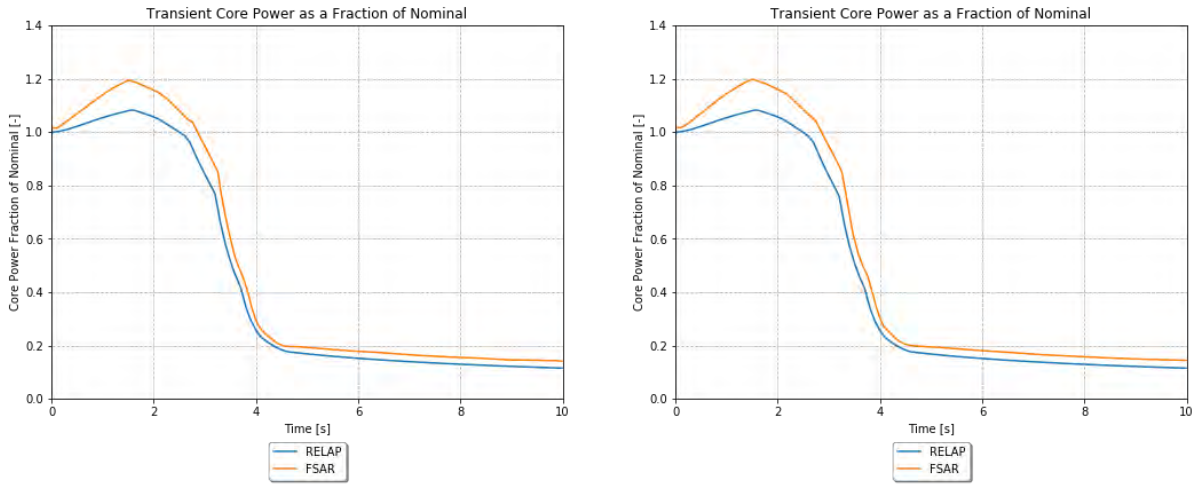

A **B**

Figure 4-12. TR Core Power as a fraction of nominal for the locked rotor scenario (e.g., both the LOOP and the OPA).

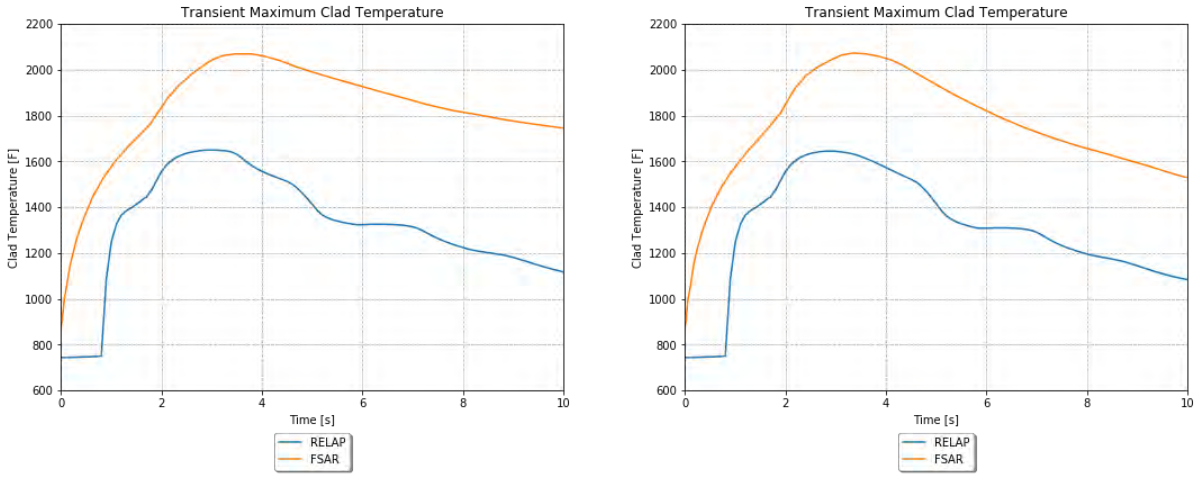

A **B**

Figure 4-13. TR Maximum Clad Temperature for the locked rotor scenario (e.g., both the LOOP and the OPA).

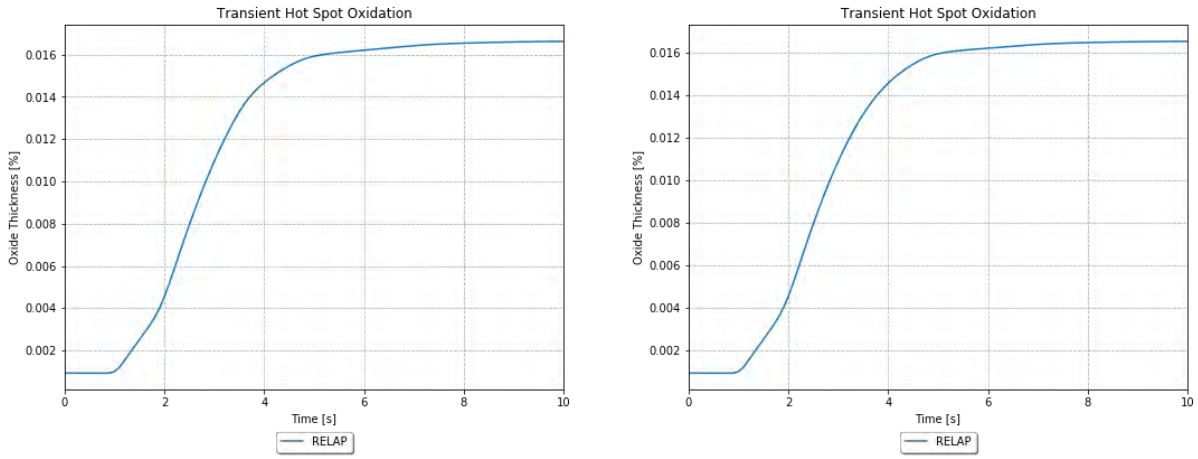

A **B**

Figure 4-14. TR Cladding Oxidation at the peak power location for the locked rotor scenario (e.g., both the LOOP and the OPA).

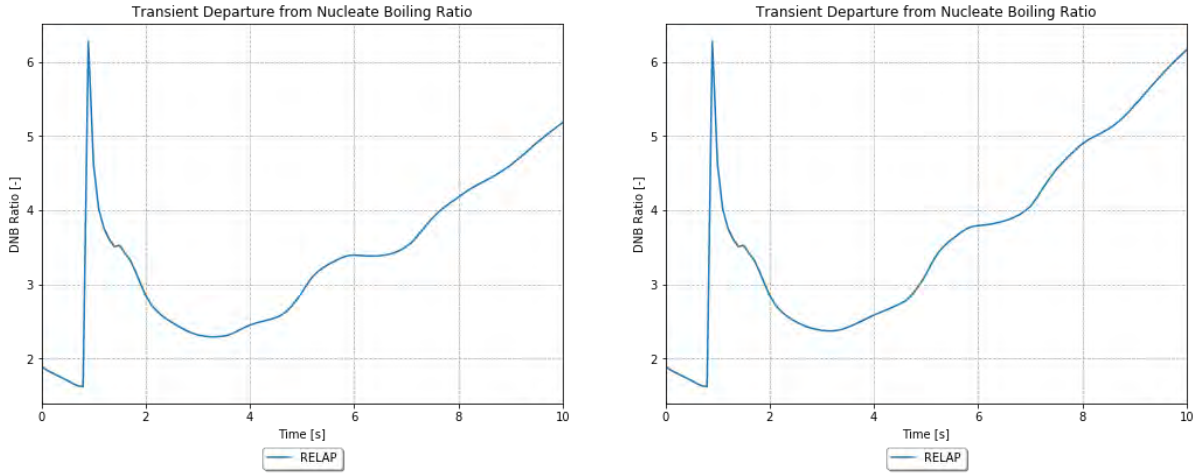

A **B**

Figure 4-15-B, the OPA RELAP5-3D run initially decreases a bit more slowly, but the curves mostly converge by about four seconds. These figures also illustrate the difference between the LOOP and the OPA most clearly. The vessel flow in the LOOP case drops significantly further and faster than that in the OPA case, and the OPA case stabilizes at around 70% of the nominal flow.

The TR locked rotor loop (e.g., Loop 4) mass flow as a fraction of the nominal flow is shown in Figure 4-8-A and Figure 4-8-B. The LOOP and OPA RELAP5-3D runs decrease more slowly than the FSAR run and ends up with a reverse flow of a significantly smaller magnitude. These figures show a small difference between the LOOP and the 2OPA. The reverse flow in the LOOP case is of slightly lower magnitude than in the OPA case.

The TR PRZ pressure is shown in Figure 4-9-A and Figure 4-9-B. From Figure 4-9-A, the LOOP RELAP5-3D run begins to pressurize ~1 second after the FSAR run and reaches a slightly lower peak, but otherwise follows a very similar TR. From Figure 4-9-B, the OPA RELAP5-3D run also begins to pressurize ~1 second after the FSAR run, but also reaches a significantly lower peak pressure. The FSAR run depressurizes much faster. These figures show some difference between the LOOP and the OPA. In

the OPA case, the pumps continuing to run allow significantly more heat transfer through the SG, and thus, a lower and shorter pressurization.

The TR average rod heat flux is shown in Figure 4-10-A and Figure 4-10-B. The RELAP5-3D runs have a slightly lower peak heat flux than the FSAR runs, and the heat flux decreases more quickly throughout the RELAP5-3D TRs. These figures show no appreciable difference between the LOOP and the OPA.

The TR hot rod heat flux is shown in Figure 4-11-A and Figure 4-11-B. The RELAP5-3D runs suddenly drop significantly, and then have a smooth increase for a bit before decreasing throughout the rest of the TR. In both cases, they are nothing like the FSAR runs. It is theorized that RELAP5-3D is switching to a heat transfer mode with a significantly decreased HTC. These figures show no appreciable difference between the LOOP and the OPA.

The TR core power as a fraction of the nominal power is shown in Figure 4-12-A and Figure 4-12-B. The RELAP5-3D runs have a similar core power TR to the FSAR runs, but with a lower peak. These figures show no appreciable difference between the LOOP and the OPA.

The TR maximum clad temperature is shown in Figure 4-13-A and Figure 4-13-B. The RELAP5-3D runs have significantly lower peak temperature than the FSAR runs. It is unclear why this is the case, but it is theorized that the fuel rod geometry or material properties could be contributing. These figures show no appreciable difference between the LOOP and the OPA.

The TR cladding oxidation at the peak power location of the hot rod is shown in Figure 4-14-A and Figure 4-14-B. There are no FSAR plots for comparison, but this value is a tabular result in the FSAR, as discussed in the following section. From Figure 4-14-A and Figure 4-14-B, the RELAP5-3D runs both experience similar progression of oxidation, which is consistent with their similar max cladding temperature plots.

The TR departure from nucleate boiling ratio (DNBR) at the peak power location of the hot rod is shown in Figure 4-15-A and Figure 4-15-B. There are no FSAR plots for comparison, but this value is listed as an acceptance criterion in the FSAR. From Figure 4-15-A and Figure 4-15-B, the RELAP5-3D runs both experience similar progression of DNBR, which show that after a small initial decrease, the DNBR shoots very high, quickly drops back down, and then gradually increases for the remainder of the TR. It is noted that the large, sudden changes in DNBR occur at a similar time to the large, sudden changes in heat flux, lending further credibility to the possibility that a change in HT mode is causing the heat flux change.

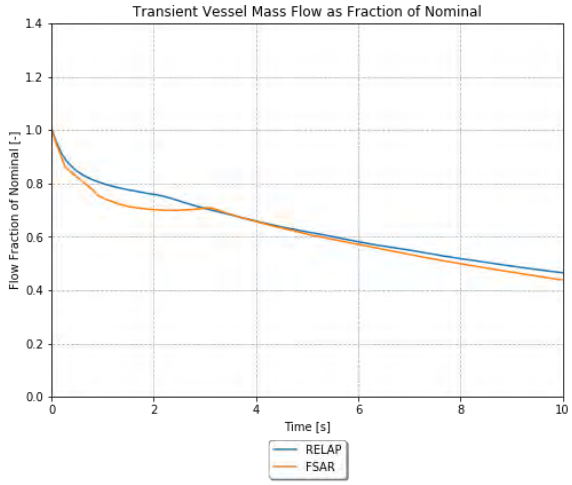

A

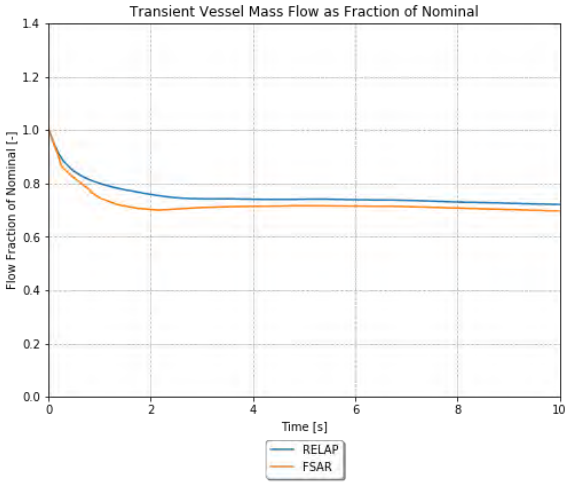

B

Figure 4-7. TR Vessel Mass Flow as a fraction of nominal for the locked rotor scenario (e.g., both the LOOP and the OPA).

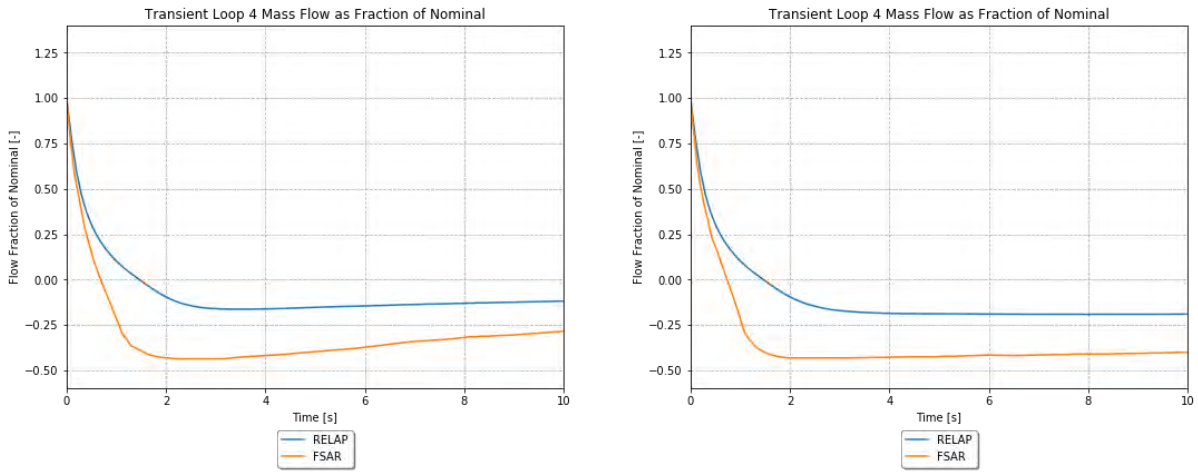

A **B**

Figure 4-8. TR Loop 4 Mass Flow as a fraction of nominal for the locked rotor scenario (e.g., both the LOOP and the OPA).

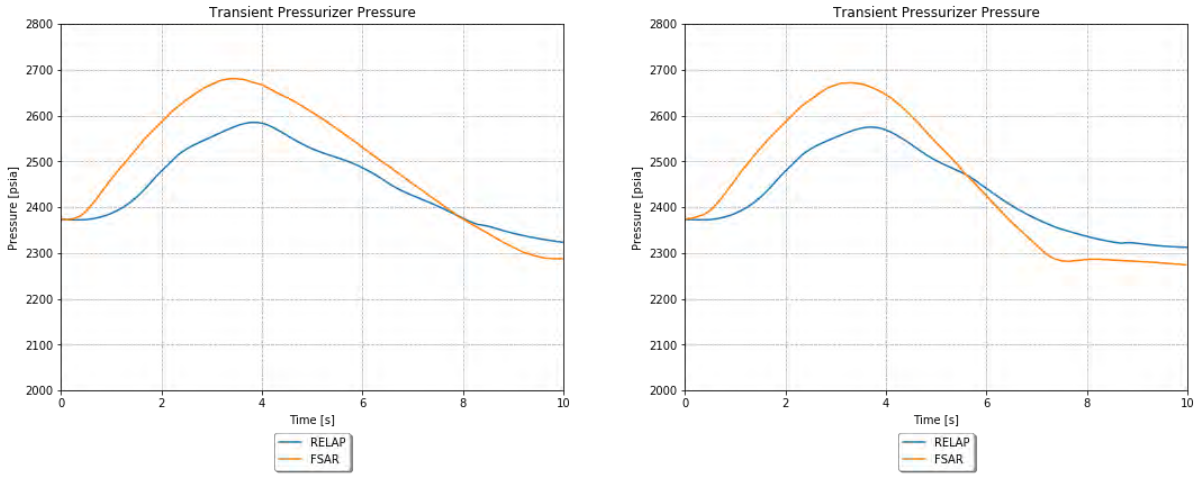

A **B**

Figure 4-9. TR PRZ Pressure for the locked rotor scenario (e.g., both the LOOP and the OPA).

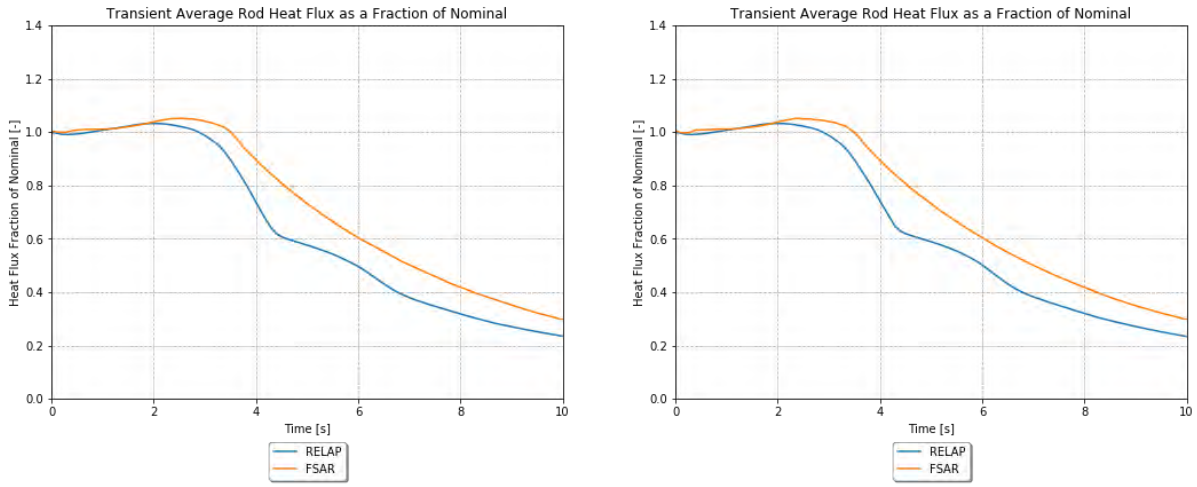

A **B**

Figure 4-10. TR Average Rod Heat Flux as a fraction of nominal for the locked rotor scenario (e.g., both the LOOP and the OPA).

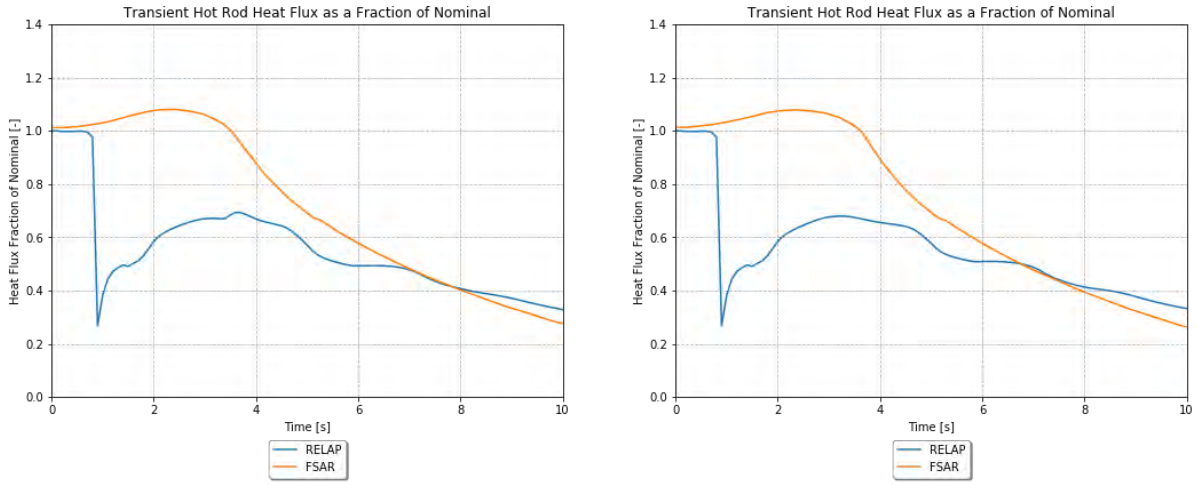

A **B**

Figure 4-11. TR Hot Rod Heat Flux as a fraction of nominal for the locked rotor scenario (e.g., both the LOOP and the OPA).

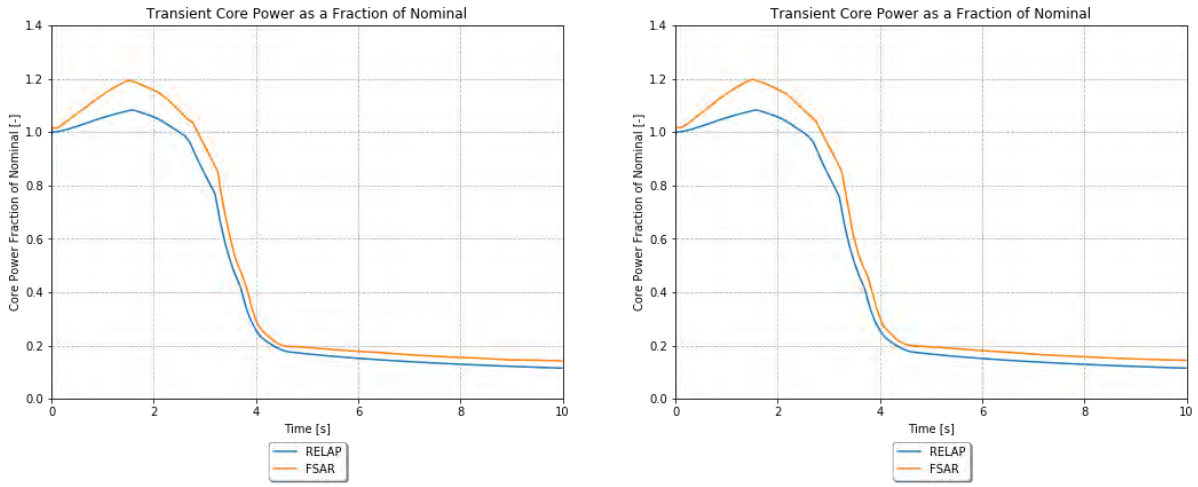

A **B**

Figure 4-12. TR Core Power as a fraction of nominal for the locked rotor scenario (e.g., both the LOOP and the OPA).

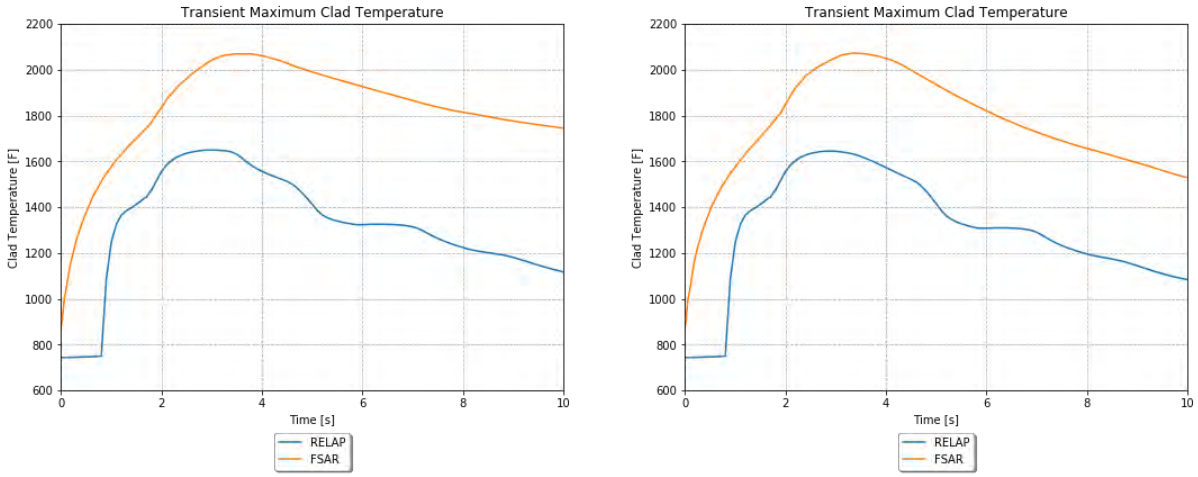

A **B**

Figure 4-13. TR Maximum Clad Temperature for the locked rotor scenario (e.g., both the LOOP and the OPA).

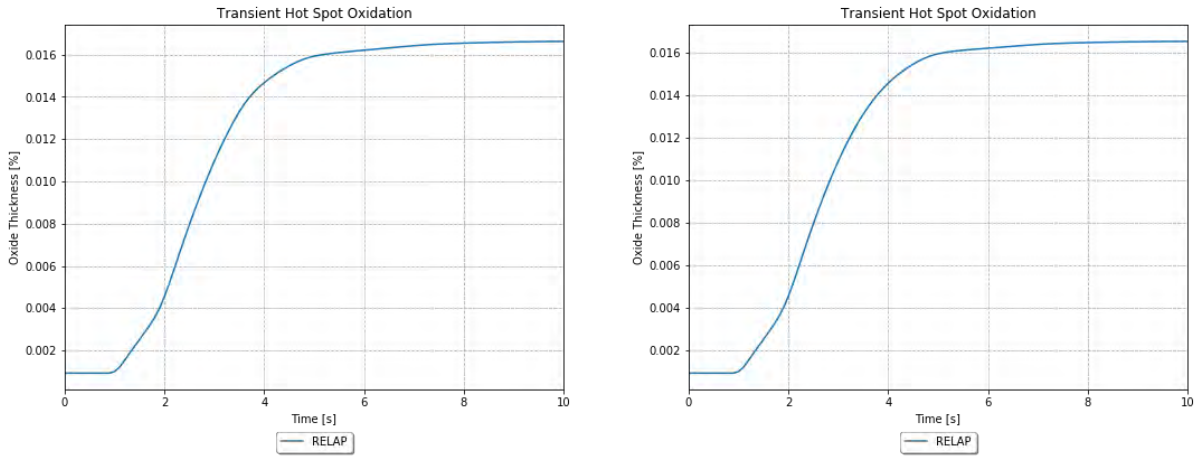

A **B**

Figure 4-14. TR Cladding Oxidation at the peak power location for the locked rotor scenario (e.g., both the LOOP and the OPA).

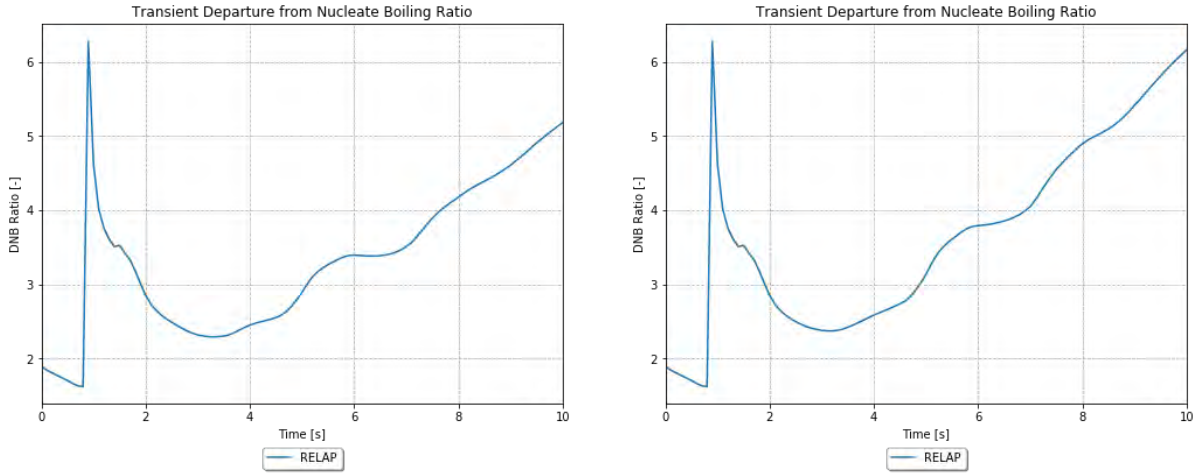

A **B**

Figure 4-15. TR DNBR for the locked rotor scenario (e.g., both the LOOP and the OPA).

4.5.6 Adherence to Acceptance Criteria

The final results for the locked rotor TRs are compared to the results from the FSAR and the acceptance criteria in Table 4-6. The acceptance criteria are based on examination of the FSAR and the applicable sections of the standard review plan.

Table 4-6. Locked rotor final results.

Result	FSAR (OPA)	FSAR (LOOP)	RELAP5-3D (OPA)	RELAP5-3D (LOOP)	Acceptance Criterion
Maximum RCS Pressure [psia]	2669	2669	2585	2590	2750
Maximum Clad Temperature [°F]	2048	2054	1612	1612	2375
Zr-H_2O reaction [% by weight]	0.6	0.7	0.0166%	0.0168%	-
Minimum DNBR [-]	-	-	1.7	1.5	1.24

The RELAP5-3D simulations meet all acceptance criteria for the locked rotor scenario. Some of the potential input differences between the FSAR simulations and the RELAP5-3D simulations are discussed in following section. These may drive some of the differences in results between the FSAR analysis and the RELAP5-3D simulations, in addition to code differences.

4.5.7 Scenario Specific Limitations and Conditions for Usage

The following limitations apply specifically to the locked rotor case:

- The main steam and feedwater flow are assumed to ramp to 0 over 1 second after trip. It is unclear what the base analysis assumptions are, but given that the TR is 10 seconds, this assumption could have a significant effect.
- The MSSVs are modeled to open at the set pressure and ramp to be fully open over 5 psi above each set pressure. There is insufficient detail in the FSAR to know if this is consistent with the modeling in the FSAR analysis.
- The PRZ safety valve is modeled to linearly ramp flow from none at 2500 psia to maximum at 2575 psia. There is insufficient detail in the FSAR to know if this is consistent with the modeling in the FSAR analysis.
- The reactivity feedback model has two major simplifications:
  - A single value for MDC based on an approximate average temperature is used to develop the table of reactivity vs. density, while the FSAR indicates that the MDC will vary with temperature. It is likely that this is a small effect.
  - The FSAR analysis uses a doppler power coefficient (DPC), and modeling DPC is not supported by RELAP5-3D. As such, a generic fuel temperature coefficient (FTC) table from Section 4.4 was used. This is a valid source, but may cause a small deviation from the FSAR analysis.
- The power shape used may be inconsistent with that in the FSAR analysis, but it is confirmed that the FQ value is consistent.

4.6 Steam System Piping Failure (Main Steam line Break)

Steam system piping failure is an ANS Condition IV incident and is commonly referred to as a main steam line break/rupture (MSLB).

The steam release arising from a rupture of a main steam line will result in an initial increase in steam flow that decreases during the accident as the steam pressure falls. The energy removal from the RCS causes a reduction of coolant temperature and pressure. In the presence of a negative moderator temperature coefficient, the cooldown results in an insertion of positive reactivity. If the most reactive RCCA is assumed stuck in its fully withdrawn position after a reactor trip, there is an increased possibility that the core will become critical and return to power. A return to power following a steam line rupture is a potential problem mainly because of the high-power peaking factors that exist, assuming the most reactive RCCA to be stuck in its fully withdrawn position. The core is ultimately shut down by the boric acid solution delivered by the SI system and accumulators.

According to the FSAR, numerous combinations of break sizes and power level were run to determine the limiting cases. For the purposes of this work, the limiting cases presented in the FSAR section are re-created. This includes:

- HZP operation assuming the LOOP
- HZP operation assuming the OPA
- Hot full power (HFP) operation (e.g., no information is provided on LOOP vs. OPA).

The HZP cases have identical input, except for pump behavior defined in the TR input files, and the SI delay defined in the RAVEN distributions.

The HFP case has substantially different input. LOOP is arbitrarily assumed.

4.6.1 Scenario-Specific Inputs in the TR Input File

4.6.1.1 Hot Zero Power Cases

The TR input file is defined as follows:

- Upfront cards are included, which specify that this is a restart TR run using the last available printout in the restart file.
- The end time is set to 600 seconds, consistent with the analysis in the reference plant FSAR. The max time step is set to 0.05 seconds, as this is a value that is reasonable for a relatively stable simulation such as this.
- The minor edits are used to specify the variables used in the plots.
- CV 405 (reactivity controller) is listed as a constant value of 0.0 $. This is done as a placeholder for RAVEN to substitute in the actual end of SS value of CV 405 using RAVEN variable “ssreact”. This step is necessary to turn off the reactivity controller but make the SS reactivity adder persist.
- The pump inputs are specified differently depending on LOOP vs OPA:
  - For the OPA, the pump CVs are used to impose the desired conditions. These CVs are specified in the TR input file as constants. CVs 419, 420, 421, and 422 are set as constant values consistent with the end of SS Pump Speed, and these values will be replaced by RAVEN using the variable ‘sspmpvel.’ This causes the pumps to simply continue operating like normal SS. Variable Trips 450 through 453 must remain true, as this will cause the pumps to continue using CVs 419 through 422. Therefore, these trips need not be specified in the TR input file.
  - For the LOOP, in order to model the motor trip, Variable Trips 450 through 453 are set to be false, so the motor trip takes precedence. This is done by setting them to trip at a time greater than or equal to 1E9 seconds in the TR input file. The motor trip specifications from the steady state file already perform the desired motor trip behavior, so nothing needs to be specified in the TR input file.
  - CVs 435 through 438 (e.g., the steam valve position) are changed to be functions of General Table 650. This allows them to be set to the SS valve position prior to the reactor trip or SI signal, and then close based on the specified delay and ramp times.
- CVs 459 through 462 (e.g., the MFW flow rate) are listed as constant values of 1118.9 lbm/sec. This is done as a placeholder for RAVEN to substitute in the actual end of SS values of CVs 459 through 462 using RAVEN variable ‘ssmfw.’
- CV 472 is listed as a constant value of 0.0. This is used to turn off the SS charging flow.
- CV 473 is listed as a constant value of 0.0. This is used to turn off the SS letdown flow.
- CV 482 is listed as a constant value of 0.0. This is used to turn off the SS PRZ heater.
- CV 483 is listed as a constant value of 0.0. This is used to turn off the SS PRZ spray.
- CV 641 is listed as a constant value of 0.0. This is used to disable the PRZ PORV.
- General Table 640 is listed with values identical to the SS input. This input does not necessarily need to be here, but it is generically listed in the TR input files to allow the analyst to change the trip used for MFW.

- General Table 650 is listed with values identical to the SS input. This input needs to be here so that the first three valve position entries in the table can be replaced with the end of SS values using RAVEN variable 'ssstmvlv.' This step is necessary to turn off the steam flow controller, but have the SS steam flow persist.
- Component 483 is present in this file so that the steam valve can be replaced with a single junction. The area of this junction is set equal to the break size, based on the FSAR (1.4 ft^2).
- Component 484 is present in this file to change the break pressure boundary from one based on the condenser to the atmospheric conditions.
- Component 481 is present because the AFW flow is credited for the intact SGs, but not the broken SG. As such, the existing SS inputs can be used for Loops 1 through 3, but the easiest way to shut off Loop 4 AFW is to simply specify the component in the TR input file with 0 flow at all points.

4.6.1.2 Hot Full Power Case

The TR input file differs from the HZP LOOP case as follows:

- The end time is set to 35 seconds, which is consistent with the analysis in the reference plant FSAR.
- The minor edits are different, because the plot package is different between the HFP and HZP cases.
- The PRZ low pressure reactor trip setpoint (e.g., Variable Trip 410) is added to the TR input file for this case; however, it is changed to instead trip at a time consistent with the FSAR case reactor trip. The FSAR case has reactor trip triggered by the overpower ΔT (OPΔT) reactor trip setpoint, but insufficient information exists in the FSAR to implement the OPΔT logic in the RELAP5-3D model. As such, reactor trip is simply triggered at a consistent time.
- The area for component 483 is changed to 0.8 ft^2 to reflect the FSAR analysis break area.
- The AFW assumptions are the same for all SGs in this case, so the specification of Component 481 in the HZP case is removed for this case.

4.6.2 Scenario-Specific RAVEN Inputs

The RAVEN distribution means are set as shown in Table 4-7. The inputs are consistent with the FSAR, as described below. The remaining inputs are assumptions that are not specifically mentioned in the FSAR.

Table 4-7. Summary of RAVEN inputs for steam system piping failure (e.g., main steam line break [MSLB]).

Distribution	Description	Unit	Mean (HZP LOOP)	Mean (HFP)
cltempdist	Cold Leg Temperature	°F	560	557.2
corepdist	Core Power	W	1	3.657E+09
fwtempdist	Feedwater Temperature	°F	448.7	448.7
hltempdist	Hot Leg Temperature	°F	560	621.6
przleveldist	PRZ Level	ft.	19	29.4
przpressdist	PRZ Pressure	psia	2250.1	2263
rcsflowdist	RCS Volumetric Flow	gpm	93600	93600
rcsmflodist	RCS Mass Flow	lbm/sec	9684.028	9684.028
rcsmflorrdist	RCS Mass Flow in Vessel	lbm/sec	-9684.028	-9684.028
sgleveldist	SG Level	ft.	32	40.1

Distribution	Description	Unit	Mean (HZP LOOP)	Mean (HFP)
stmpressdist	SG Steam Pressure	psia	941	941
sgflowdist	SG Flow Rate	lbm/sec	1132.639	1132.639
dpvessdist	Vessel Pressure Drop	psi	46.5	46.5
dphldist	Hot Leg Pressure Drop	psi	1.2	1.2
dpxldist	Crossover Leg Pressure Drop	psi	3.1	3.1
dpcldist	Cold Leg Pressure Drop	psi	3.3	3.3
dpsgdist	SG Primary Pressure Drop	psi	45.5	45.5
corbypdist	Core Bypass Flow	%	5	5
przphirxtdist	High PRZ Pressure Reactor Trip Setpoint	psia	5000	5000
przplorxtdist	Low PRZ Pressure Reactor Trip Setpoint	psia	1	1
rcsflolorxtdist	High PRZ Level Reactor Trip Setpoint	ft.	100	100
rcsflolorxtdist	Low RCS Flow Rate Reactor Trip Setpoint	lbm/sec	-1.0E9	-1.0E9
sglevlorxtdist	Low SG Level Reactor Trip Setpoint	ft.	-1	-1
mfwdeltimedist	MFW Delay Time	sec	2	2
mfwramptimedist	MFW Ramp Time	sec	7	7
afwdeltimedist	AFW Delay Time	sec	7	7
afwramptimedist	AFW Ramp Time	sec	8	8
afwflodist	AFW Flow Rate	lbm/sec	105.65	105.65
pmpmotdeldist	Pump Motor Trip Delay Time	sec	2	2
achfluxdist	Average Channel Maximum SS Heat Flux	BTU/sec-ft^2	99.954	99.954
hchfluxdist	Hot Channel Maximum SS Heat Flux	BTU/sec-ft^2	164.93	164.93
initreactdist	Initial Reactivity	$	-1.7333	0
mdcdist	Moderator Density Coefficient	$\Delta k/g/cm^3$	0.5	0.5
accbordist	Accumulator Boron Concentration	Mass Frac	0.0019	0.0019
chgbordist	Charging Boron Concentration	Mass Frac	0.0024	0.0024
accvoldist	Accumulator Water Volume	ft^3	900	900
acctempdist	Accumulator Temperature	°F	120	120
accpressdist	Accumulator Pressure	psia	600	600
sitrplspdist	Low Steam Pressure SI Signal	psia	800	800
sitrpdeldist	SI Signal Delay Time	sec	42	42
msivdeldist	MSIV Delay Time	sec	5	5
msivrampdist	MSIV Ramp Time	sec	10	10

Distribution	Description	Unit	Mean (HZP LOOP)	Mean (HFP)
rccadeldist	RCCA Delay Time	sec	8	8
rcpheatdist	RCP Heat Generation	MW	4.25	0.00001
przsafdist	PRZ Safety Valve Open Pressure	psia	2500	2500
rcsbordist	RCS Initial Boron Concentration	Mass Frac	0	0

4.6.2.1 Hot Zero Power Cases

- The SS conditions are generally set to nominal values, with the following exceptions:
  - Core power, which is set to 1 W, since RELAP5-3D does not allow a lower number.
  - RCS temperatures, which are set to a constant 560°F, as there is insufficient power to reach a higher temperature or a significant gradient between hot and cold.
  - The SG and PRZ levels are set lower than the other nominal cases, as the convergence logic was having difficulty with higher values.
- The reactor trip setpoints are all set to impossible values. This is because in the HZP cases, there is no reactor trip (rods are already inserted).
- For the HZP cases, the MFW is ramped down over 5 seconds, starting again after a delay of 2 seconds after the SI signal. The AFW starts ramping up 7 seconds after the SI signal and then reaches full flow at 8 seconds after the SI signal.
- For the HZP LOOP case, the RCP begins coast-down 2 seconds after the SI signal.
- For the HZP cases, the initial reactivity is set to a value consistent with the -1.3 Δk/k from the FSAR.
- The accumulator and charging SI boron concentrations are set to 1900 ppm and 2400 ppm, respectively.
- For the HZP cases, the low steam pressure SI signal is set to 800 psia, as this results in timing consistent with the FSAR analysis. This approach was taken because no information could be located in the FSAR about this actual setpoint value in ft. It is generally expressed as a percentage of span, but the boundaries of the span were not available.
- The SI delay values are set to 27 seconds for the OPA case and 42 seconds for the LOOP case.
- For the HZP cases, the main steam is ramped down over 5 seconds, starting again after a delay of 5 seconds after the SI signal.

4.6.2.2 Hot Full Power Case

- The SS conditions are generally set to nominal conditions.
- The reactor trip setpoints are all set to impossible values. For the HFP case, the trip is forced at a certain time, as discussed in the following section.
- For the HFP case, the MFW is ramped down over 5 seconds, starting again after a delay of 2 seconds after the reactor trip. The AFW starts ramping up 7 seconds after the reactor trip and then reaches full flow at 8 seconds after the reactor trip.
- For the HFP case, the RCP begins coast-down 2 seconds after the reactor trip.
- For the HFP case, the initial reactivity is set to 0.

- For the HFP case, a conservatively large positive MDC of 0.5 $\Delta k/g/cm^3$ is used.
- The accumulator and charging SI boron concentrations are set to 1900 ppm and 2400 ppm, respectively.
- For the HFP case, a low steam pressure SI setpoint of -800 psia is used, to prevent the SI actuation.
- The RCCAs begin to drop 8 seconds after reactor trip.

4.6.3 Steady State Results

The steady state observations for the steam main line break are explained in detail in the FY-2020 report [2].

4.6.4 TR Boundary Conditions

The TR boundary conditions for the steam main line break are explained in detail in the FY-2020 report [2].

4.6.5 TR Results

The RELAP5-3D results are compared to the MSLB runs from the FSAR in the subsections below. Note that the figures labeled with -A are for the LOOP and the figures labeled with -B are for the OPA. The HZP and HFP cases are discussed separately.

4.6.5.1 Hot Zero Power Cases

The TR vessel mass flow as a fraction of the nominal flow is shown in Figure 4-16-A and Figure 4-16-B. The LOOP RELAP5-3D run matches the FSAR run closely. The OPA RELAP5-3D run initially increases similarly to the FSAR run for the first ~50 seconds, but the FSAR run then increases significantly more. This timing seems to coincide with the much more significant re-criticality observed in RELAP5-3D, as discussed below.

The TR PRZ pressure is shown in Figure 4-17-A and Figure 4-17-B. The RELAP5-3D runs de-pressurize significantly more slowly than the FSAR run. At approximately the same time of re-criticality, the pressure begins to increase significantly in the RELAP5-3D runs, while it continues to decrease in the FSAR runs. Note that the pressure increase in the LOOP run is a little slower than the OPA run due to the slower increase in power. These differences suggest that the significantly higher power excursion in the RELAP5-3D run drives a major difference in RCS conditions.

The TR average rod heat flux is shown in Figure 4-18-A and Figure 4-18-B, and the core power as a fraction of nominal is shown in Figure 4-19-A and Figure 4-19-B. From these figures, in both cases, the power excursion is significantly higher in the RELAP5-3D runs than in the FSAR runs. In the LOOP cases, both the FSAR and RELAP5-3D runs have a power excursion that is lower in peak, but longer in duration than the OPA case. As the kinetics model is sensitive to small changes, and the FSAR inputs were simplified a bit for entry into RELAP5-3D, it is not surprising that there are significant differences between the RELAP5-3D power results and the FSAR results.

The TR maximum clad temperature is shown in Figure 4-20-A and Figure 4-20-B. There are no equivalent figures in the FSAR, but these results are still of interest. Neither the LOOP nor the OPA case experience any significant heat up.

The TR feedwater flow is shown in Figure 4-21-A and Figure 4-21-B. The RELAP5-3D runs start with no MFW flow, then the AFW comes on and goes to a level consistent with that in the FSAR run. The FSAR runs start with a normal MFW flow, but as discussed in the SS sections, this is due to the difficulties in obtaining a good HZP SS with this model.

The TR steam flow is shown in Figure 4-22-A and Figure 4-22-B. The RELAP5-3D steam flow values are very similar initially. In the LOOP case, the RELAP5-3D steam flow continues to be very

similar to the FSAR run until about 250 seconds. In the OPA case, there is a significant deviation starting at about 50 seconds, and then the RELAP5-3D run steam flow ceases by about 100 seconds. All things considered, the differences between the RELAP5-3D runs and the FSAR runs are fairly minimal.

The TR SG pressure is shown in Figure 4-23-A and Figure 4-23-B. The broken SG pressure follows nearly identical trends to the steam flow. The intact SGs appear to initialize from substantially lower pressure in the FSAR run, but they converge to similar pressures with the RELAP5-3D runs.

The TR average core temperature is shown in Figure 4-24-A and Figure 4-24-B. RELAP5-3D runs decrease in temperature significantly more slowly than the FSAR run. At approximately the time of re-criticality, the temperature begins to increase in the RELAP5-3D runs, while it continues to decrease in the FSAR runs. These differences suggest that the significantly higher power excursion in the RELAP5-3D run drives a major difference in RCS conditions.

The TR vessel inlet temperature is shown in Figure 4-25-A and Figure 4-25-B. The intact loops have a fairly similar TR between the RELAP5-3D run and the FSAR run, and the faulted loop is very similar until about 80 seconds for the OPA and 150 seconds for the LOOP. At that point, the RELAP5-3D run experiences a rapid increase in temperature. This is likely due to the larger power excursion in RELAP5-3D and runs decrease in temperature significantly more slowly than the FSAR run. From Figure 4-26-B, in all four RELAP5-3D loops, the temperature barely decreases, then stays nearly the same for the last 500 seconds. The FSAR runs have a sustained, significant decrease in temperature in all loops. This is likely due to the larger power excursion in RELAP5-3D.

The TR PRZ water volume is shown in Figure 4-27-A and Figure 4-27-B. RELAP5-3D runs decrease in PRZ water volume significantly more slowly than the FSAR run. At approximately the time of re-criticality, the temperature begins to increase in the RELAP5-3D runs, while it continues to decrease in the FSAR runs. These differences suggest that the significantly higher power excursion in the RELAP5-3D run drives a major difference in RCS conditions.

The TR reactivity is shown in Figure 4-28-A and Figure 4-28-B. RELAP5-3D runs have an initial increase in reactivity, which results in the large re-criticality of the run. Once this decrease, the FSAR runs decrease more quickly, which explains the much lower power.

The TR core boron concentration is shown in Figure 4-29-A and Figure 4-29-B. RELAP5-3D runs experience a very similar increase in core boron concentration. This is strange, since the RCPs continued operation would be expected to promote the movement of boron to the core more rapidly. This is reflected in the FSAR run.

The TR DNBR is shown in Figure 4-29-A and Figure 4-29-B. RELAP5-3D runs show a value of 0 for the entire TR. In RELAP5-3D, this indicates that the heat structure is in an HT mode, which does not even calculate CHF (i.e., single-phase liquid). This is thus interpreted as a very high DNBR value.

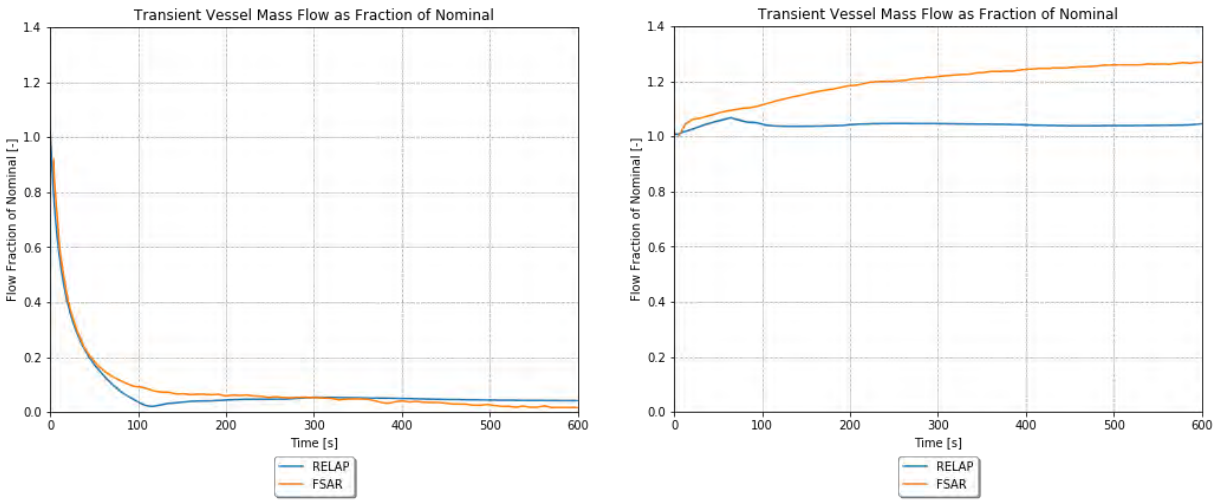

A **B**

Figure 4-16. TR vessel mass flow as a fraction of nominal for the MSLB scenario (e.g., HZP for both the LOOP and the OPA).

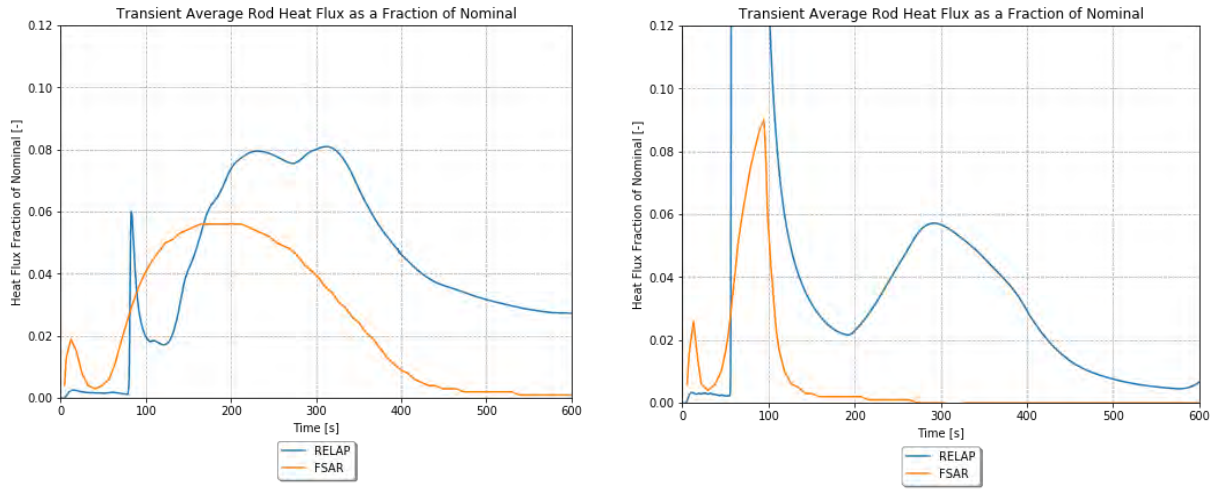

A **B**

Figure 4-17. TR PRZ pressure for the MSLB scenario (e.g., HZP for both the LOOP and the OPA).

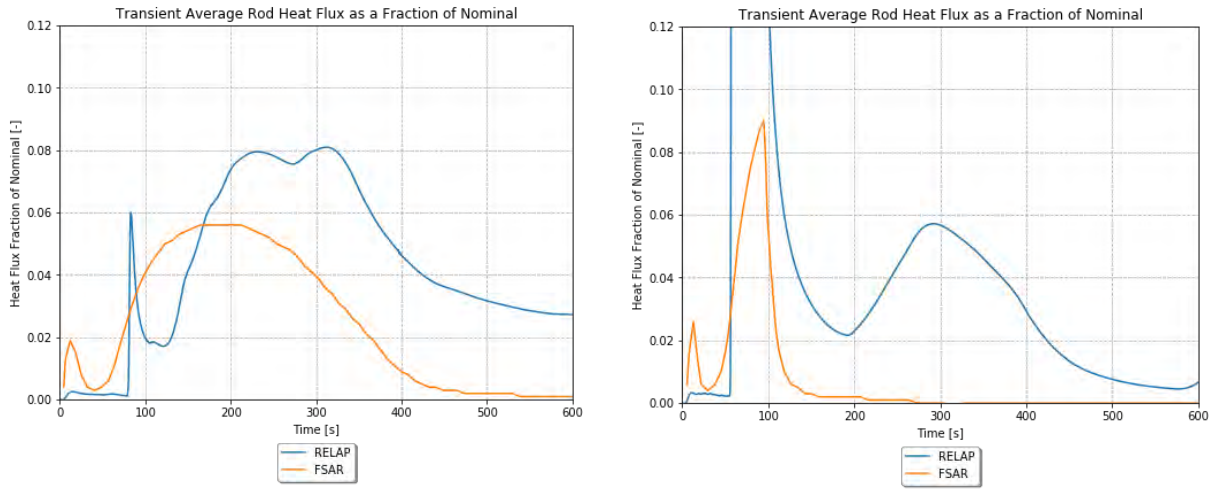

A **B**

Figure 4-18. TR average rod heat flux as a fraction of nominal for the MSLB scenario (e.g., HZP for both the LOOP and the OPA).

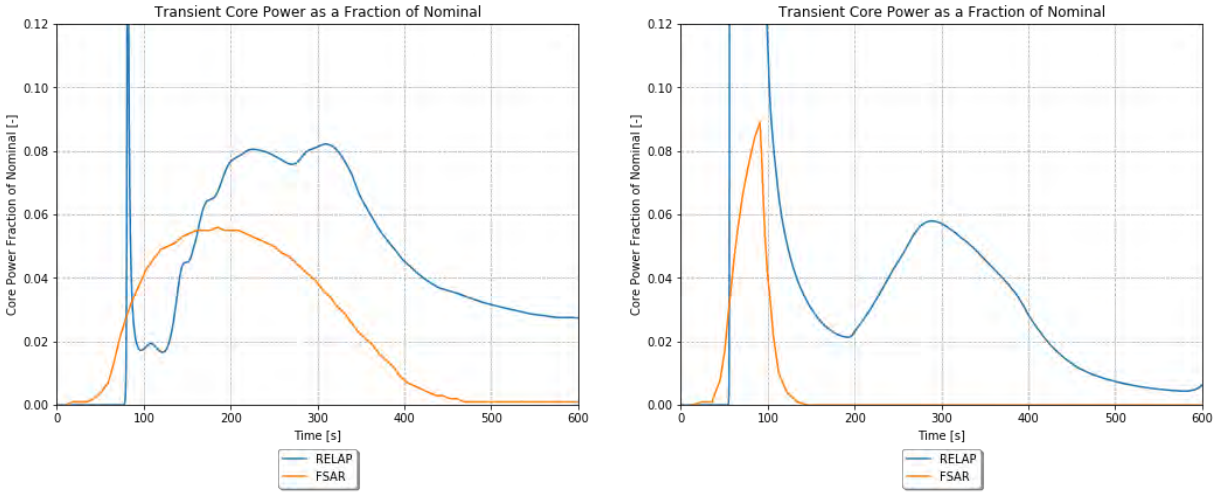

A **B**

Figure 4-19. TR core power as a fraction of nominal for the MSLB scenario (e.g., HZP for both the LOOP and the OPA).

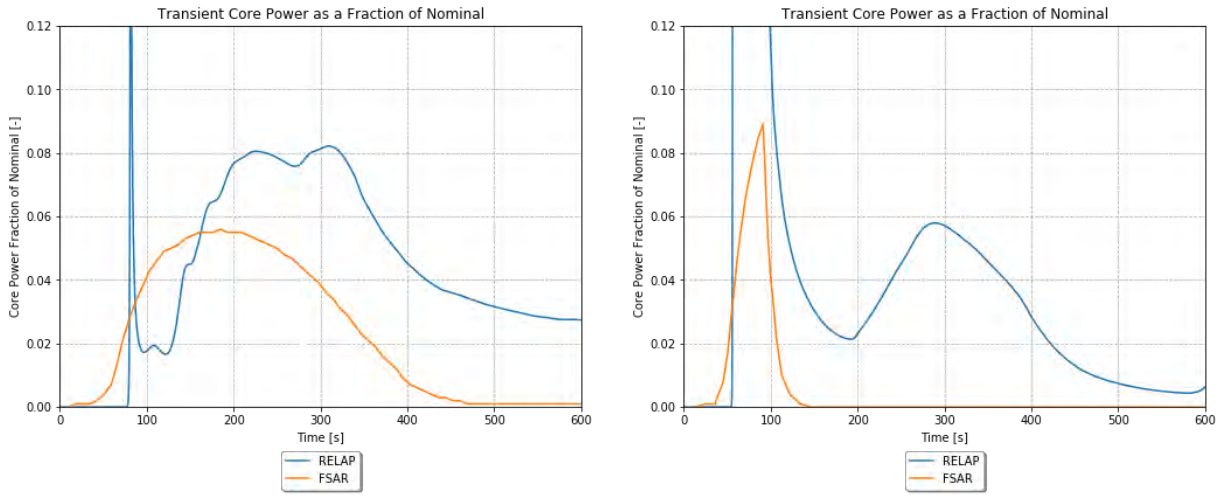

A **B**

Figure 4-20. TR maximum clad temperature for the MSLB scenario (e.g., HZP for both the LOOP and the OPA).

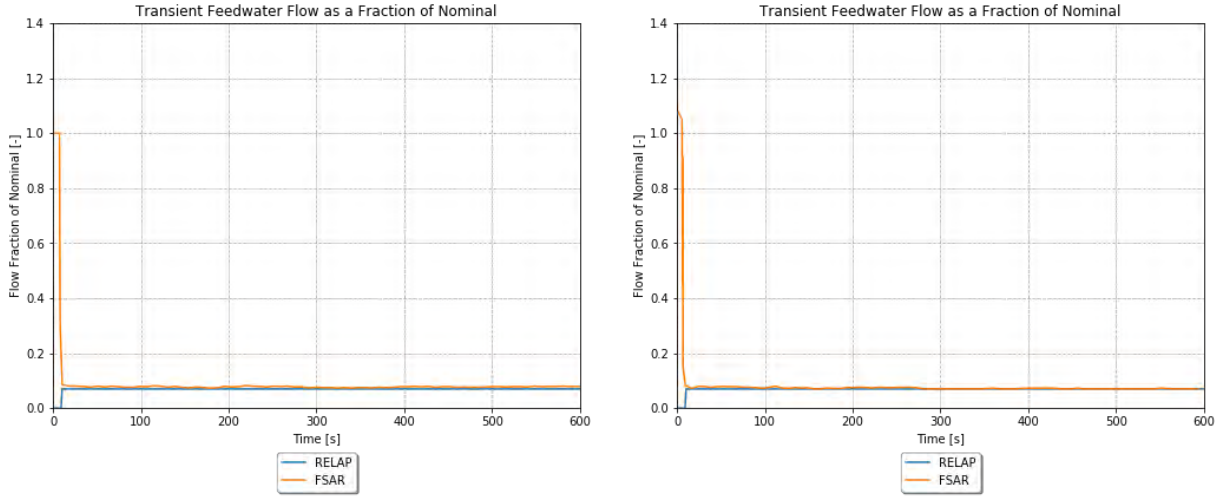

A **B**

Figure 4-21. TR feedwater flow for the MSLB scenario (e.g., HZP for both the LOOP and the OPA).

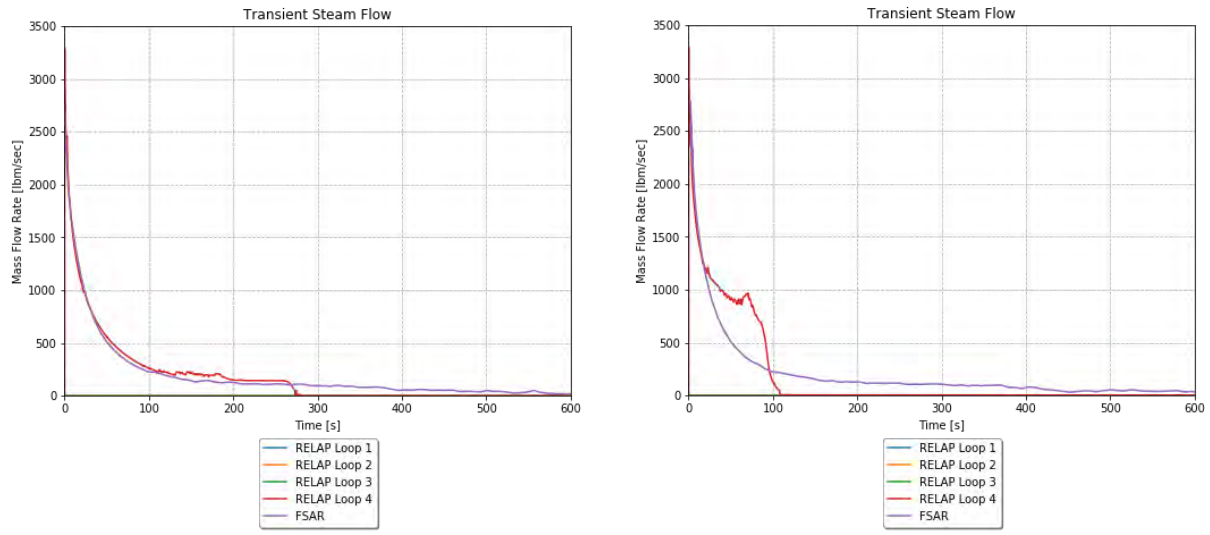

A **B**

Figure 4-22. TR steam flow for the MSLB scenario (e.g., HZP for both the LOOP and the OPA).

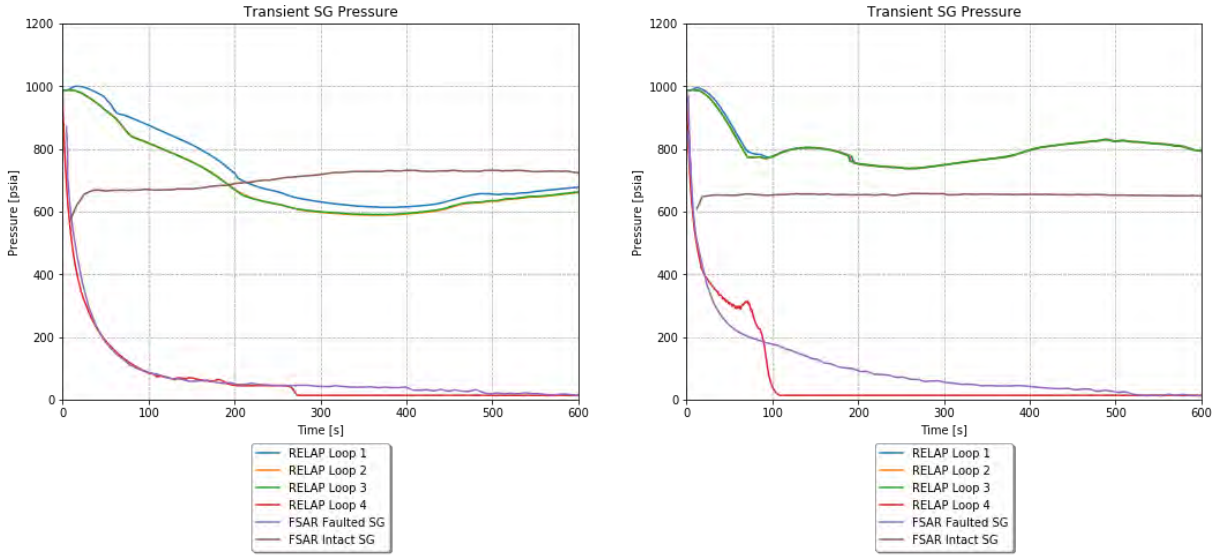

A **B**

Figure 4-23. TR SG pressure for the MSLB scenario (e.g., HZP for both the LOOP and the OPA).

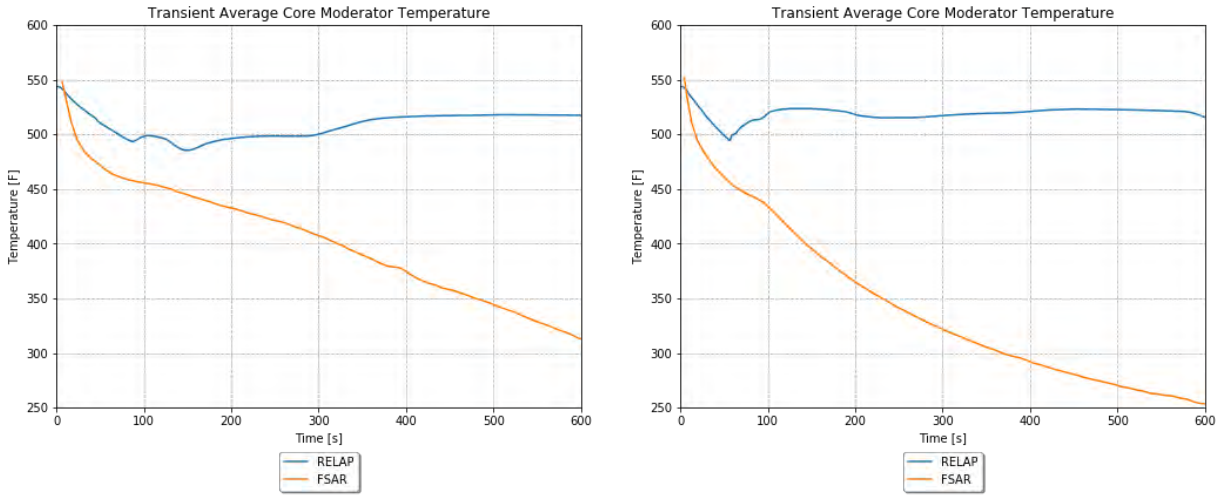

A **B**

Figure 4-24. TR core average temperature for the MSLB scenario (e.g., HZP for both the LOOP and the OPA).

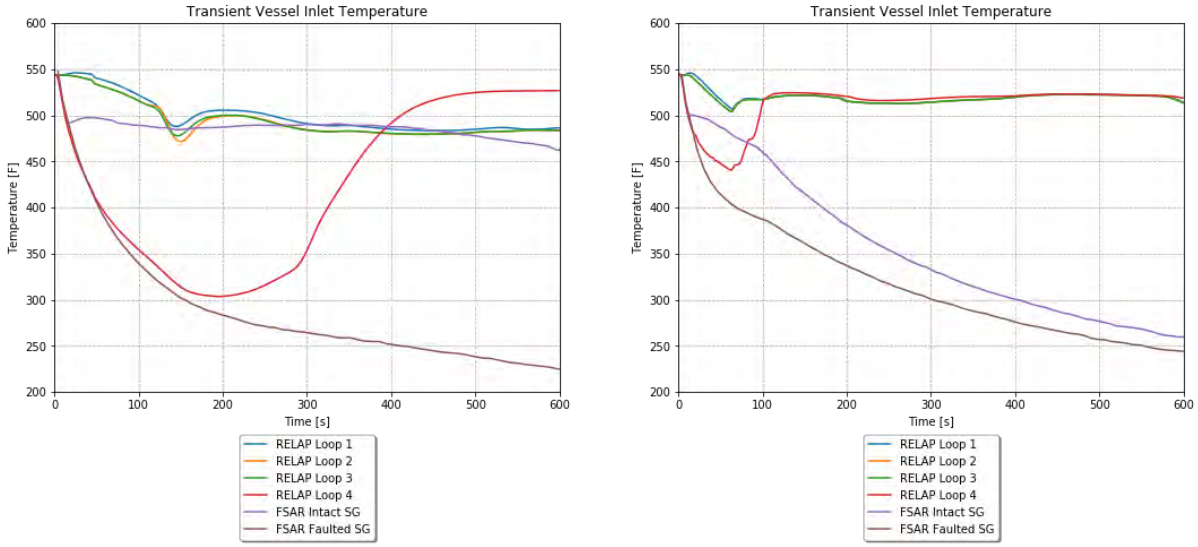

A **B**

Figure 4-25. TR vessel inlet temperature for the MSLB scenario (e.g., HZP for both the LOOP and the OPA).

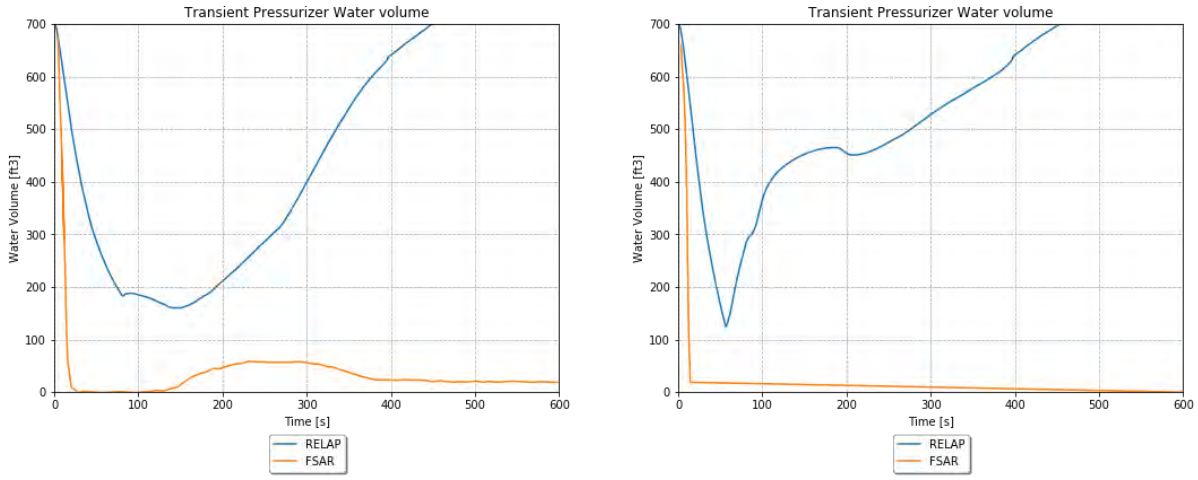

A **B**

Figure 4-26. TR PRZ water volume for the MSLB scenario (e.g., HZP for both the LOOP and the OPA).

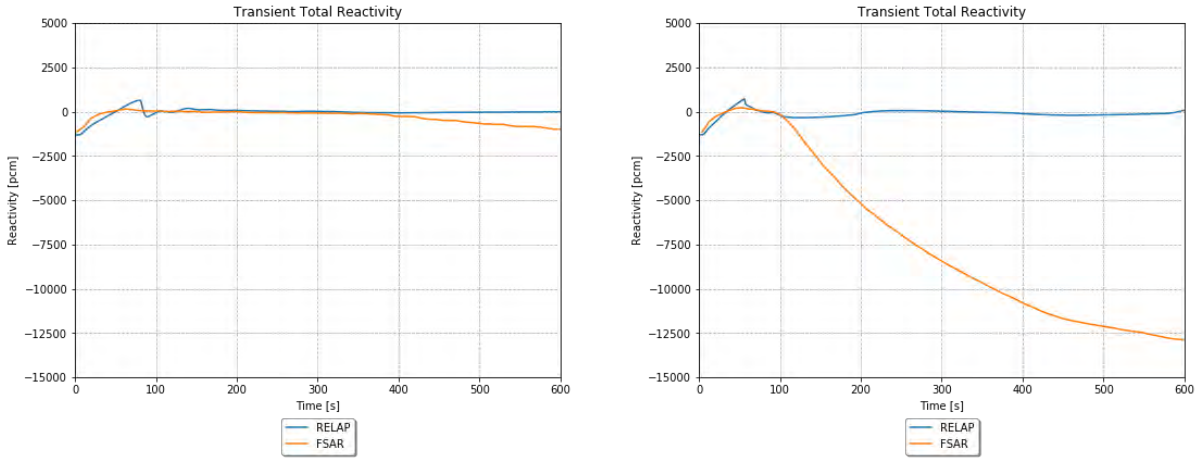

A **B**

Figure 4-27. TR total reactivity for the MSLB scenario (e.g., HZP for both the LOOP and the OPA).

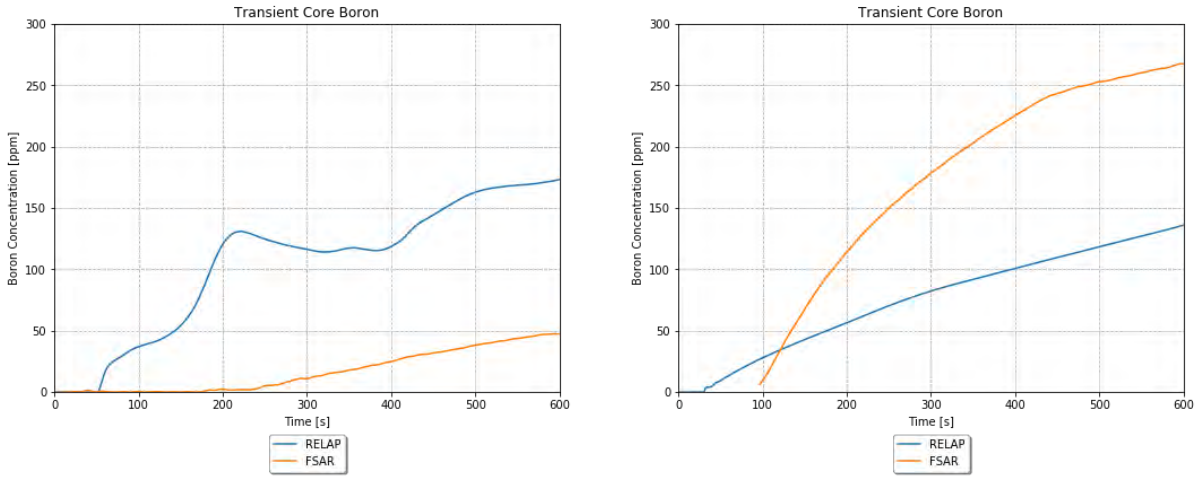

A **B**

Figure 4-28. TR core boron concentration for the MSLB scenario (e.g., HZP for both the LOOP and the OPA).

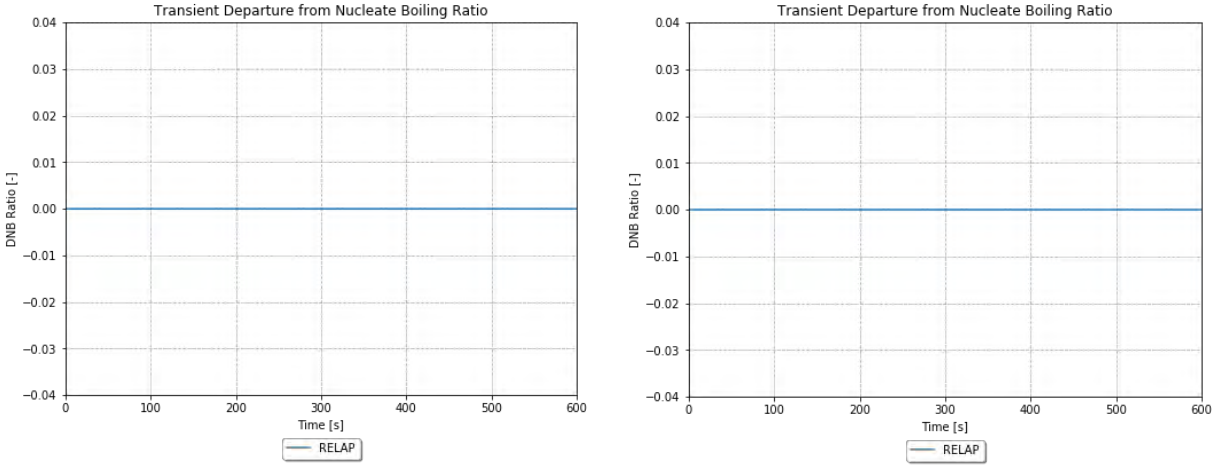

A **B**

Figure 4-29. TR DNBR for the MSLB scenario (e.g., HZP for both the LOOP and the OPA).

4.6.5.2 Hot Full Power Case

The TR PRZ pressure is shown in Figure 4-30. The RELAP5-3D run depressurizes a bit initially. At approximately the time of re-criticality, the pressure begins to increase again, and then at the time of scram, it drops significantly. Note that this plot should have an FSAR curve to compare it to; however, there is an error in the FSAR, where these figures are instead replaced with the figures from the previous page (i.e., there are two pages in a row with identical figures, when the second page should have three new figures on it).

The TR average rod heat flux is shown in Figure 4-31 and the core power as a fraction of nominal is shown in Figure 4-32. From these figures, it is apparent that RELAP5-3D does have a power excursion, but it is very small compared to that in the FSAR analysis. As the kinetics model is sensitive to small changes, and the FSAR inputs were simplified a bit for entry into RELAP5-3D, it is not surprising that there are significant differences between the RELAP5-3D power results and the FSAR results. Note that

Figure 4-32 should have an FSAR curve to compare to; however, there is an error in the FSAR, where these figures are instead replaced with the figures from the previous page.

The TR maximum clad temperature is shown in Figure 4-33. There are no equivalent figures in the FSAR, but these results are still of interest. The RELAP5-3D run experiences a significant heatup that terminates shortly after the reactor scrams.

The TR SG pressure is shown in Figure 4-34. The broken SG pressure in RELAP5-3D follows a very similar trend to that from the FSAR, other than the last 5 seconds or so. The intact SG pressures in RELAP5-3D stay about the same, until a sudden pressurization after scram, while in the FSAR, they decrease very similar to the broken SG prior to the pressurization after scram.

The TR average core temperature is shown in Figure 4-35. The temperature stays fairly consistent through the RELAP5-3D TR, while the FSAR run decreases significantly. The TR vessel inlet temperature is shown in Figure 4-36. The intact loops stay more or less the same until a decrease after reactor scram. The broken loop shows a cooldown fairly similar to the FSAR results.

The TR PRZ water volume is shown in Figure 4-37. The RELAP5-3D run shows a fairly slow and steady decrease in PRZ water volume for the first 15 seconds or so. It then begins a very gradual increase until reactor scram causes it to start deceasing very quickly. Note that this figure should have an FSAR curve to compare to; however, there is an error in the FSAR, where these figures are instead replaced with the figures from the previous page.

The TR steam flow as a fraction of nominal is shown in Figure 4-38. The RELAP5-3D steam flow initially increases to almost 20% higher than nominal, then rapidly drops to about 10% higher than nominal, and slowly drops after that. Once the reactor trips, it drops very quickly. This trend is very similar to the FSAR run, except that the FSAR run ends up with a much higher sustained flow rate.

The TR DNBR is shown in Figure 4-39. the RELAP5-3D run shows a significant margin in the beginning, and then around 14 seconds, the DNBR drops sharply and goes to 0. In RELAP5-3D, a value of 0 may indicate that the heat structure is in an HT mode, which does not even calculate CHF (i.e., single-phase liquid) or it may be in CHF. Since this happens approximately when the clad temperature excursion occurs, it is presumed that this plot is showing that DNBR is below 1 starting at around 16 seconds.

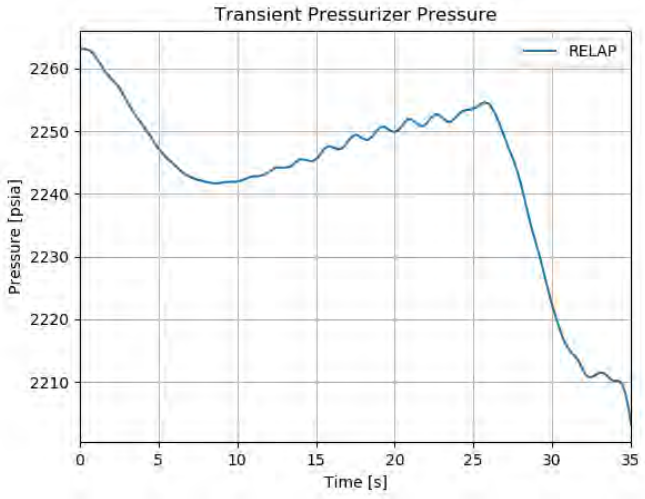

Figure 4-30. TR PRZ pressure for the MSLB scenario (e.g., HFP).

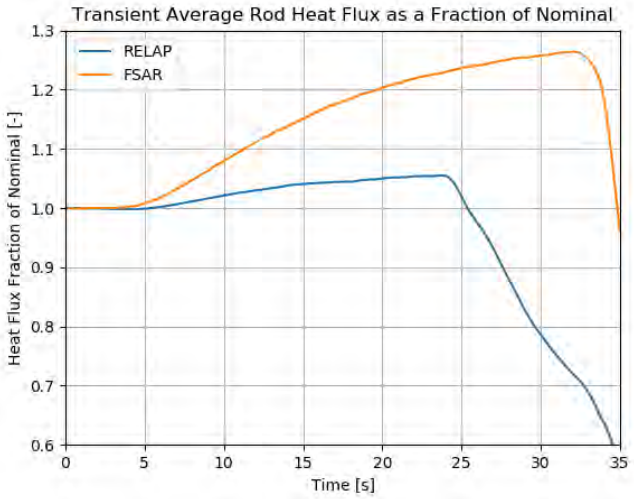

Figure 4-31. TR average rod heat flux for the MSLB scenario (e.g., HFP).

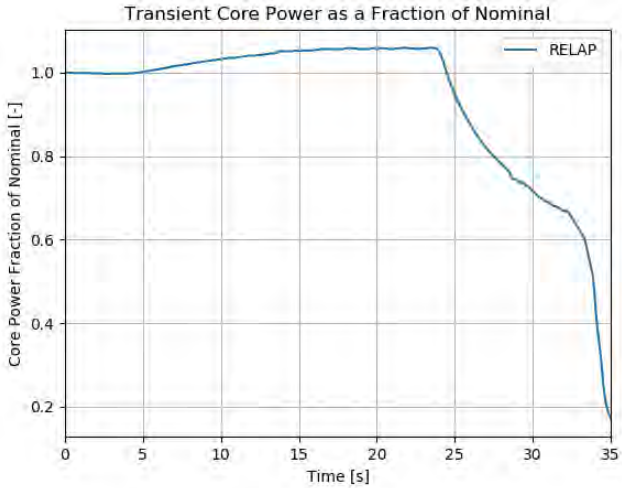

Figure 4-32. TR core power as a fraction of nominal for the MSLB scenario (e.g., HFP).

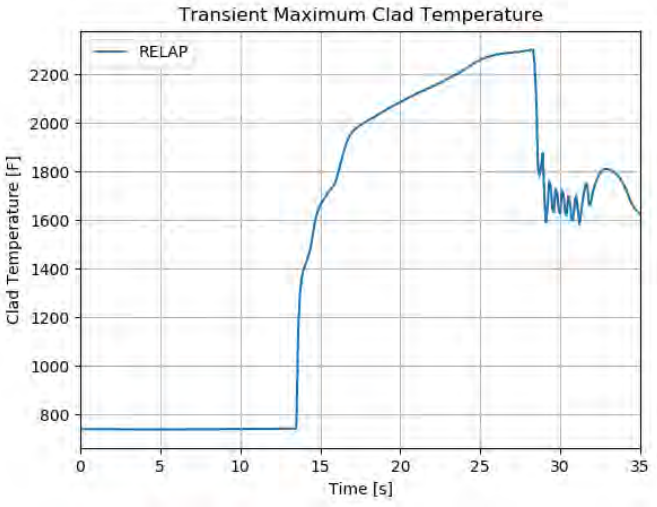

Figure 4-33. TR maximum clad temperature for the MSLB scenario (e.g., HFP).

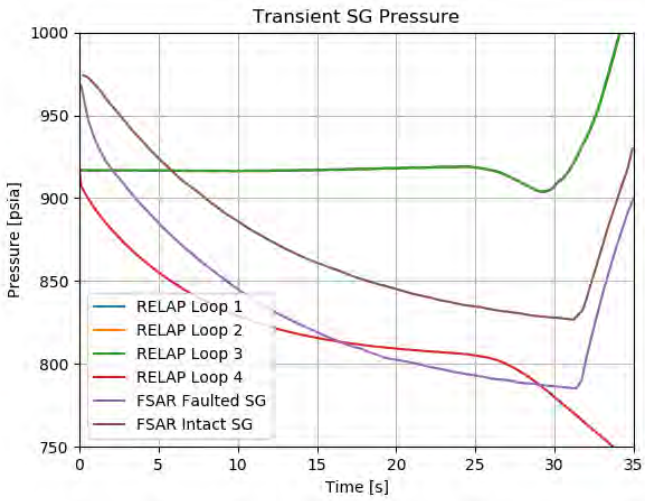

Figure 4-34. TR PRZ pressure for the MSLB scenario (e.g., HFP).

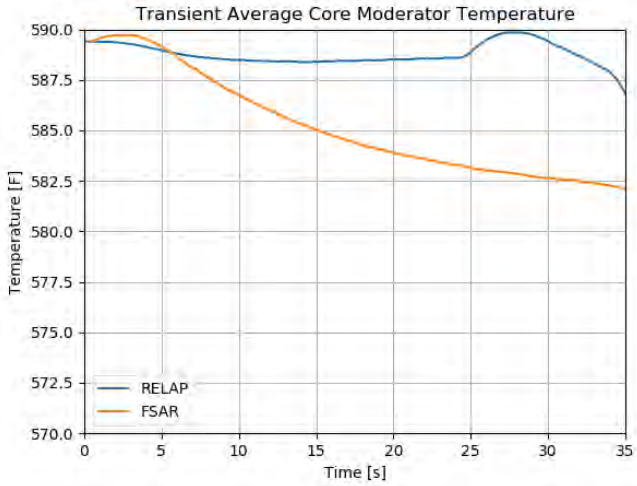

Figure 4-35. TR average core temperature for the MSLB scenario (e.g., HFP).

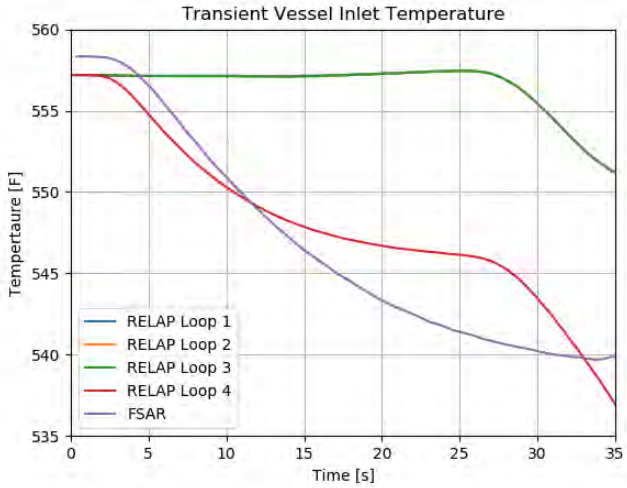

Figure 4-36. TR vessel inlet temperature for the MSLB scenario (e.g., HFP).

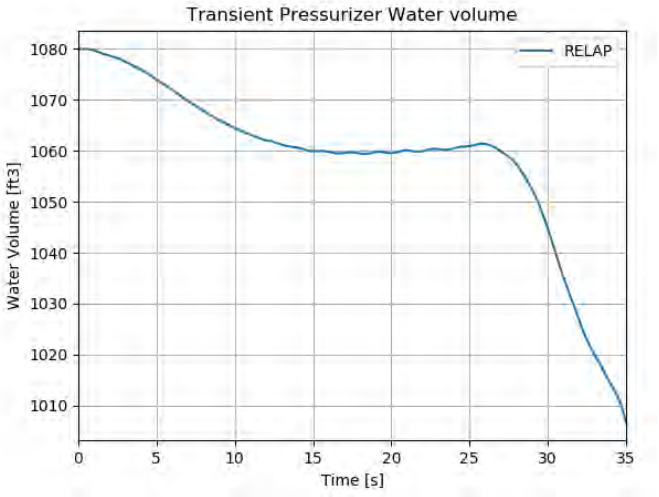

Figure 4-37. TR PRZ pressure for the MSLB scenario (e.g., HFP).

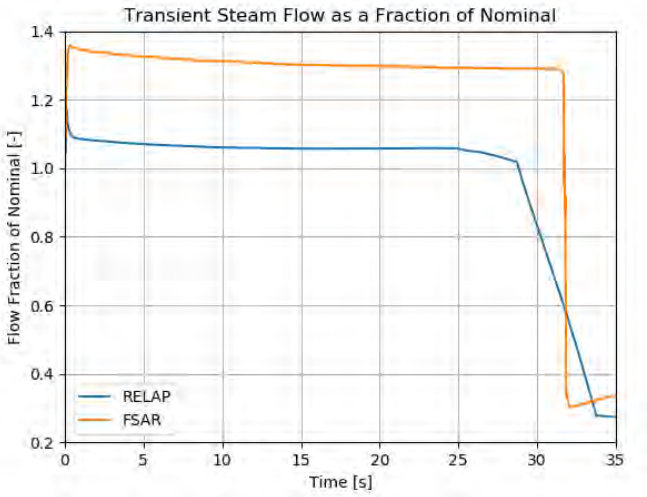

Figure 4-38. TR steam flow for the MSLB scenario (e.g., HFP).

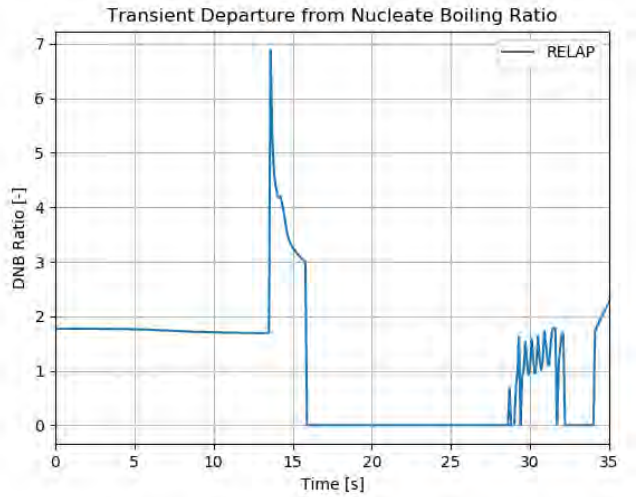

Figure 4-39. TR DNBR for the MSLB scenario (e.g., HFP).

4.6.6 Adherence to Acceptance Criteria

The final results for the MSLB TRs are compared to the results from the FSAR and the acceptance criteria in Table 4-8. The acceptance criteria are based on examination of the FSAR sections, and the applicable sections of the standard review plan.

The RELAP5-3D simulations meet all acceptance criteria for the MSLB scenario, except the HFP run violates the clad temperature and DNBR criteria. Some of the potential input differences between the FSAR simulations and the RELAP5-3D simulations are discussed in following section. These may drive some of the differences in results between the FSAR analysis and the RELAP5-3D simulations, in addition to code differences.

Table 4-8. MSLB final results.

Result	FSAR (HZP OPA)	FSAR (HZP LOOP)	FSAR (HFP)	RELAP5-3D (HZP OPA)	RELAP5-3D (HZP LOOP)	RELAP5-3D (HFP)	Acceptance Criterion
Maximum RCS Pressure [psia]	~2250	~2250	-	2505	2508	2263	2750
Maximum Clad Temperature [°F]	-	-	-	573	602	2305	2200
Minimum DNBR [-]	> 1.24	> 1.24	> 1.24	∞	∞	< 1	1.24

4.6.7 Scenario-Specific Limitations and Conditions for Usage

The following limitations apply specifically to the main steamline break case.

- There is no Moody choked flow model in RELAP5-3D, so Ransom-Trapp is used instead. It is unknown what kind of effect this might have.
- The containment conditions in the FSAR analysis are unknown, so it is assumed that atmospheric conditions exist.
- There is minimal information about the RCCA insertion specific to the FSAR analysis, so the same information from the locked rotor analysis is used. This may cause a slight deviation.
- The reactivity feedback model has two major simplifications:
  - A single value of 0.5 $\Delta k/g/cm^3$ was used for all cases, even though the HZP cases used a different figure altogether. Initial runs with an MDC based on that figure resulted in no power excursion.
  - The FSAR analysis uses a DPC, but modeling DPC is not supported by RELAP5-3D. As such, a generic FTC table from Section 4.4 was used. This is a valid source, but may cause a small deviation from the FSAR analysis.
- Due to the lack of information, the base file charging flows and refueling water storage tank (RWST) conditions are used for this analysis. This may have a significant effect.
- Due to a lack of information, the actual low steam pressure SI signal setpoint is unknown. A value is used to duplicate the timing from the FSAR analysis.
- The OvertemperatureΔ (OTΔT) reactor trip setpoint could not be modeled appropriately, so a trip was forced at the time observed in the FSAR analysis.
- The RCP heat is added to the RCS using pump heat structures with arbitrary geometry.
- The power shape used may be inconsistent with that in the FSAR analysis, but it is confirmed that the FQ value is consistent.

4.7 Turbine Trip

For a turbine trip event, the reactor trips directly from a signal derived from the turbine stop signals—unless the reactor is operating below approximately 40 percent power. Steam flow to the turbine stops abruptly upon stop valve closure initiation, Sensors on the stop valve detect the turbine trip and initiate turbine bypass through steam dump valves and, if above 40 percent power, a reactor trip. The loss of steam flow results in an almost immediate rise in secondary system temperature and pressure with a resultant increase in primary system temperature and pressure.

The automatic turbine bypass system would accommodate up to 40 percent of rated steam flow. Reactor coolant temperatures and pressure do not increase significantly if the turbine bypass system and the PRZ pressure control system are functioning properly. If the condenser was not available, the excess steam generation would be relieved to the atmosphere, and MFW flow would be lost. For this situation, feedwater flow would be maintained by the AFW system to ensure adequate residual and decay heat removal capability. A turbine trip is classified as an ANS Condition II event, fault of moderate frequency.

The turbine trip scenario presents four cases in the FSAR:

1. Maximum moderator feedback without PRZ spray and PORV.
2. Maximum moderator feedback with PRZ spray and PORV.
3. Minimum moderator feedback without PRZ spray and PORV.
4. Minimum moderator feedback with PRZ spray and PORV.

There are minor changes in the TR input files for the changes to the PRZ controls, and there are minor changes to the RAVEN distributions for the moderator feedback changes. Also note that there are some changes to both files for TR-specific reactor trip modeling.

4.7.1 Scenario-Specific Inputs in the TR Input File

The TR input files are defined as follows:

- Upfront cards are included that specify this is a restart TR run, which uses the last available printout in the restart file.
- The end time is set to 100 seconds, consistent with the analysis in the reference plant FSAR. The max time step is set to 0.05 seconds, as this is a value that is reasonable for a relatively stable simulation such as this.
- The minor edits are used to specify the variables used in the plots.
- CV 405 (e.g., the reactivity controller) is listed as a constant value of 0.0 $. This is done as a placeholder for RAVEN to substitute in the actual end of SS value of CV 405 using the RAVEN variable “ssreact.” This step is necessary to turn off the reactivity controller, but make the SS reactivity adder persist.
- CVs 419, 420, 421, and 422 (e.g., the pump inputs) are set as constant values consistent with the end of SS pump speed, and these values will be replaced by RAVEN using the variable “sspmpvel.” This causes the pumps to simply continue operating like normal SS.
- CVs 435 through 438 (e.g., the steam valve position) are changed to be functions of General Table 650. This allows them to be set to the SS valve position prior to the reactor trip or SI signal, and then close based on the specified delay and ramp times.
- CVs 459 through 462 (e.g., the MFW flow rate) are listed as constant values of 1118.9 lbm/sec. This is done as a placeholder for RAVEN to substitute in the actual end of SS values of CVs 459 through 462 using the RAVEN variable “ssmfw.”
- CV 472 is listed as a constant value of 0.0. This is used to turn off the SS charging flow.
- CV 473 is listed as a constant value of 0.0. This is used to turn off the SS letdown flow.
- CV 482 is listed as a constant value of 0.0. This is used to turn off the SS PRZ heater.
- The PRZ spray is specified differently depending on the case:
  - For the cases without the PRZ controls, CV 483 is listed as a constant value of 0.0. This is used to turn off the SS PRZ spray.

- For the cases crediting the PRZ controls, CV 483 is omitted from the TR input file. Instead, General Table 481 is specified to update the spray to kick on at 10 psia above the PRZ pressure setpoint, rather than the SS controls that make it come on as soon as the pressure goes above 10 psia.

- The PRZ PORV is specified differently depending on the case:
  - For the cases without PRZ controls, CV 641 is listed as a constant value of 0.0. This is used to disable the PRZ PORV.
  - For the cases crediting PRZ controls, CV 641 is simply omitted. The PORV logic is in the SS model, so this allows it to function as intended.
- The reactor trip is specified differently depending on the case:
  - For cases that use reactor trips based on forcing at a certain time, Variable Trip 411 is specified as a trip when time is greater than the intended value. This includes:
    - In the FSAR case with maximum feedback and crediting pressure controls, the low-low SG level setpoint is reached at 40.9 seconds. Insufficient information exists in the FSAR to determine the actual SG level in ft. for the RELAP5-3D model. As such, reactor trip is simply triggered at a consistent time.
    - In the FSAR case with minimum feedback and crediting pressure controls, the overtemperature ΔT (OTΔT) setpoint is reached at 8.9 seconds. Insufficient information exists in the FSAR to implement the OTΔT logic in the RELAP5-3D model. As such, reactor trip is simply triggered at a consistent time.
- General Table 640 is listed, with a change to have the table trip removed, so that the specified MFW delay and ramp time will simply be based on the TR time.
- General Table 650 is listed, with a change to have the table trip removed, so that the specified MSIV delay and ramp time will simply be based on the TR time. This input also needs to be here so that the first three valve position entries in the table can be replaced with the end of SS values using the RAVEN variable "ssstmvlv."

4.7.2 Scenario-Specific RAVEN Inputs

The RAVEN distribution means are set as shown in Table 4-9. The inputs are consistent with the FSAR, as described below. The remaining inputs are assumptions that are not specifically mentioned in the FSAR:

- The SS conditions are generally set to nominal values.
- The reactor trip setpoints are set as follows:
  - In both cases crediting pressure controls, the low-low SG level setpoint is set to -1.0 in the RAVEN input. This is because the trip time is hardcoded for these cases, as discussed in the following section, and with the base value for this input, the reactor trip was occurring too early.
  - In both cases not crediting pressure controls, the high PRZ pressure setpoint causes reactor trip, and it is set to actuate at 2439.7 psia.
- The MFW is immediately ramped down over 0.1 seconds from the reactor trip time, and the AFW never comes on.
- The RCP motors trip 2 seconds after reactor trip.

- The MDC is set as follows:
  - For the minimum feedback cases, it is set to -0.042 $\Delta k/g/cm^3$.
  - For the maximum feedback cases, it is set to 0.5 $\Delta k/g/cm^3$.
- The MSIV is immediately ramped down over 0.1 seconds from the reactor trip time.
- The RCCAs begin to drop 2 seconds after reactor trip.
- The PRZ safety valve is set to open at 2550 psia.
- All inputs related to ECCS flows and timing are irrelevant to this case.

Table 4-9. Summary of RAVEN inputs for turbine trip.

Distribution	Description	Unit	Mean
cltempdist	Cold Leg Temperature	°F	556.2
corepdist	Core Power	W	3.626E+09
fwtempdist	Feedwater Temperature	°F	448.7
hltempdist	Hot Leg Temperature	°F	620.6
przleveldist	PRZ Level	ft.	34.3
przpressdist	PRZ Pressure	psia	2250
rcsflowdist	RCS Volumetric Flow	gpm	93600
rcsmflodist	RCS Mass Flow	lbm/sec	9684.028
rcsmflorrdist	RCS Mass Flow in Vessel	lbm/sec	-9684.028
sgleveldist	SG Level	ft.	40.1
stmpressdist	SG Steam Pressure	psia	941
sgflowdist	SG Flow Rate	lbm/sec	1132.639
dpvessdist	Vessel Pressure Drop	psi	46.5
dphldist	Hot Leg Pressure Drop	psi	1.2
dpxldist	Crossover Leg Pressure Drop	psi	3.1
dpcldist	Cold Leg Pressure Drop	psi	3.3
dpsgdist	SG Primary Pressure Drop	psi	45.5
corbypdist	Core Bypass Flow	%	5
przphirxtdist	High PRZ Pressure Reactor Trip Setpoint	psia	2439.7
przplorxtdist	Low PRZ Pressure Reactor Trip Setpoint	psia	1714.7
przlhirxtdist	High PRZ Level Reactor Trip Setpoint	ft.	48.9
rcsflolorxtdist	Low RCS Flow Rate Reactor Trip Setpoint	lbm/sec	8425.08
sglevlorxtdist	Low SG Level Reactor Trip Setpoint	ft.	-1.0 or 27.1
mfwdeltimedist	MFW Delay Time	sec	0.001
mfwramptimedist	MFW Ramp Time	sec	0.1
afwdeltimedist	AFW Delay Time	sec	1E+08
afwramptimedist	AFW Ramp Time	sec	1.1E+08
afwflodist	AFW Flow Rate	lbm/sec	105.65
pmpmotdeldist	Pump Motor Trip Delay Time	sec	2
achfluxdist	Average Channel Maximum SS Heat Flux	BTU/sec-ft^2	99.954

Distribution	Description	Unit	Mean
hchfluxdist	Hot Channel Maximum SS Heat Flux	BTU/sec-ft^2	164.93
initreactdist	Initial Reactivity	$	0
mdcdist	Moderator Density Coefficient	Δk/g/cm^3	0.5 or -0.042
accbordist	Accumulator Boron Concentration	Mass Frac	0.0019
chgbordist	Charging Boron Concentration	Mass Frac	0.0024
accvoldist	Accumulator Water Volume	ft^3	900
acctempdist	Accumulator Temperature	°F	120
accpressdist	Accumulator Pressure	psia	600
sitrplspdist	Low Steam Pressure SI Signal	psia	800
sitrpdeldist	SI Signal Delay Time	sec	42
msivdeldist	MSIV Delay Time	sec	0.001
msivrampdist	MSIV Ramp Time	sec	0.1
rccadeldist	RCCA Delay Time	sec	2
rcpheatdist	RCP Heat Generation	MW	0.00001
przsafdist	PRZ Safety Valve Open Pressure	psia	2550
rcsbordist	RCS Initial Boron Concentration	Mass Frac	0

4.7.3 Steady State Results

The steady state observations for the turbine trip are explained in detail in FY-2020 [2].

4.7.4 TR Boundary Conditions

The TR boundary conditions for the turbine trip are explained in detail in FY-2020 [2].

4.7.5 TR Results

The RELAP5-3D results are compared to the turbine trip runs from the FSAR in the subsections that follow.

4.7.5.1 Maximum Moderator Feedback without PRZ Controls

The TR PRZ pressure is shown in Figure 4-40. The RELAP5-3D response is extremely similar to the FSAR run.

The TR core power as a fraction of the nominal power is shown in Figure 4-41. RELAP5-3D predicts a slightly higher power excursion, and very similar behavior after scram to the FSAR run.

The TR clad temperature is shown in Figure 4-42. There is a significant heatup around the time of the power excursion.

The TR oxidation at the hot rod peak power location is shown in Figure 4-43. The oxidation increases coincident with the significant heatup from Figure 4-42, and then flattens out once the clad temperature drops back down.

The TR core average moderator temperature is shown in Figure 4-44. The RELAP5-3D response is extremely similar to the FSAR run.

The TR vessel inlet temperature is shown in Figure 4-45. The RELAP5-3D response is extremely similar to the FSAR run.

The TR PRZ water volume is shown in Figure 4-46. The RELAP5-3D response is similar to the FSAR run but has more exaggerated changes.

The TR DNBR is shown in Figure 4-47. The RELAP5-3D response is very different from the FSAR run, though they indicate a similar trend. The RELAP5-3D run shows an increasing DNBR that suddenly drops to 0. In RELAP5-3D, this can indicate that the heat structure is in an HT mode, which does not even calculate CHF (i.e., single-phase liquid). This is thus interpreted as a very high DNBR value. The FSAR shows a consistent increase in DNBR.

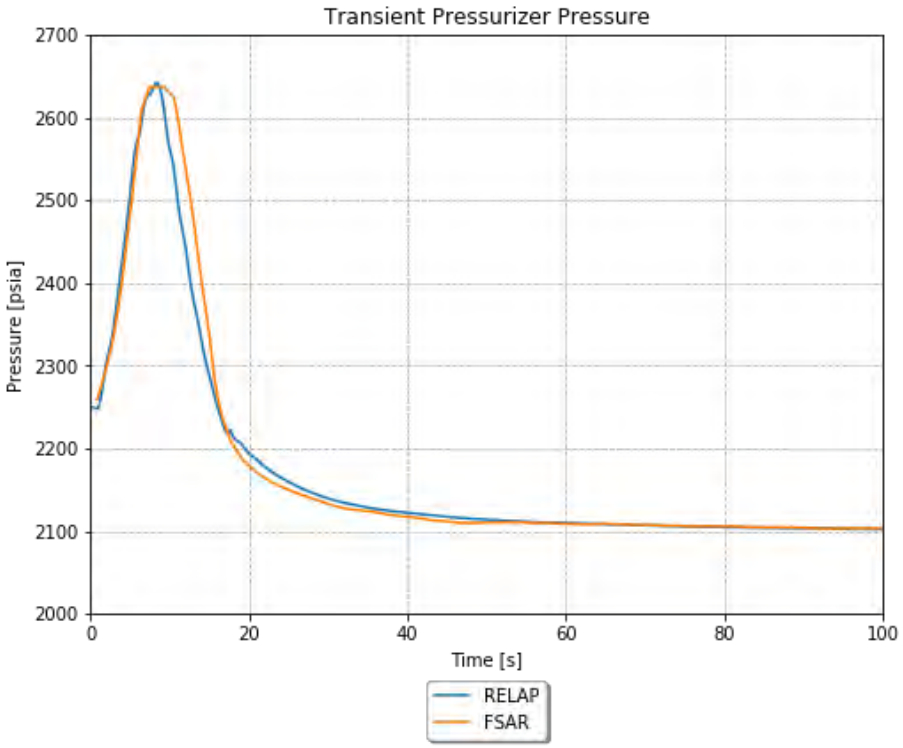

Figure 4-40. TR PRZ pressure for the turbine trip scenario (e.g., maximum moderator feedback without PRZ controls).

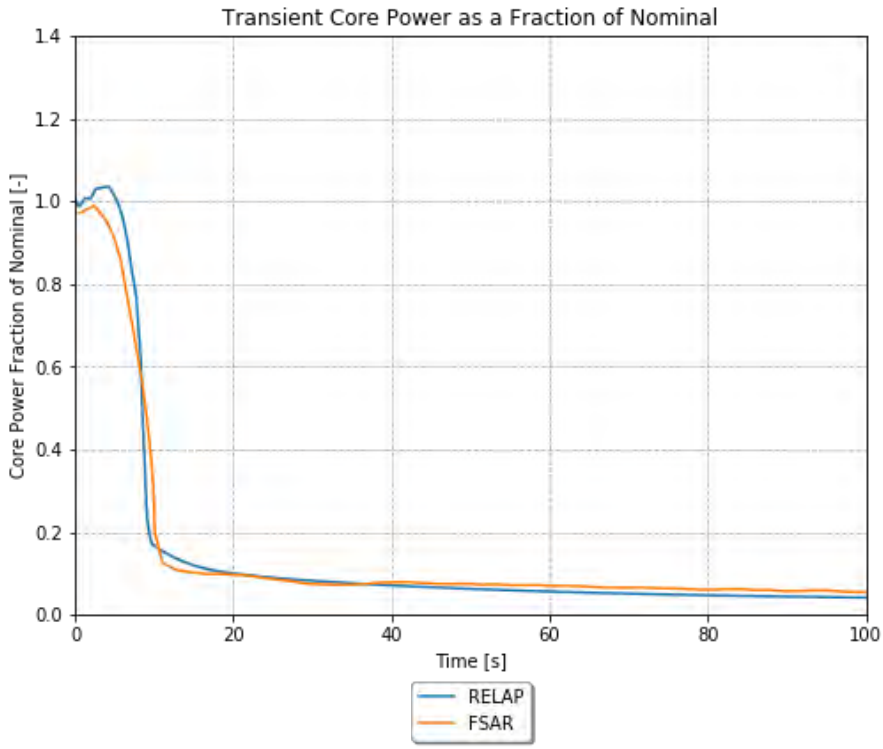

Figure 4-41. TR core power as a fraction of the nominal power for the turbine trip scenario (e.g., maximum moderator feedback without PRZ controls).

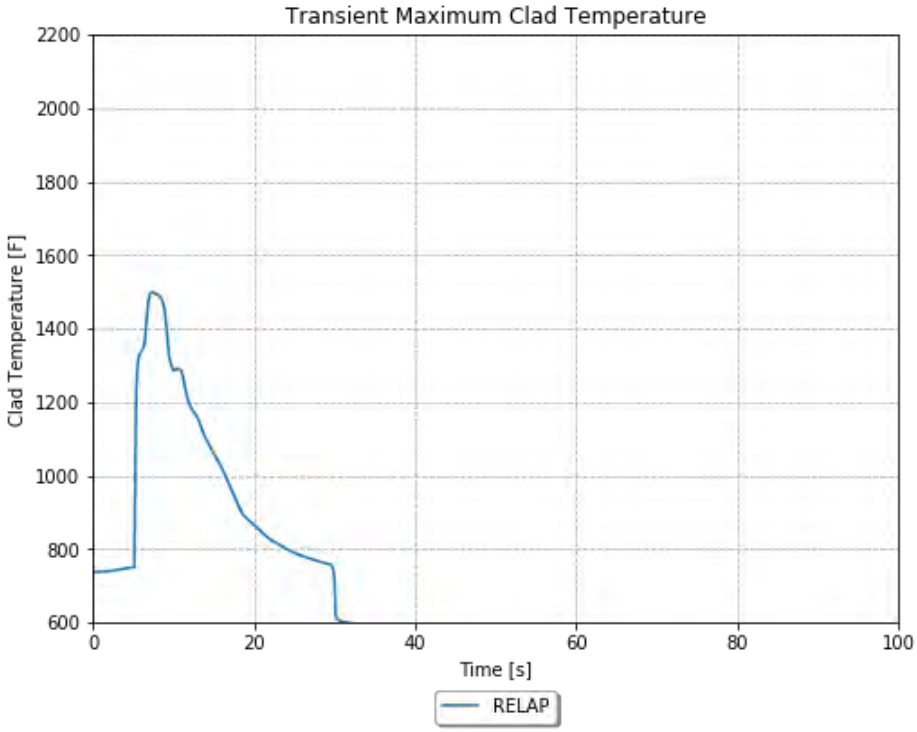

Figure 4-42. TR maximum clad temperature for the turbine trip scenario (e.g., maximum moderator feedback without PRZ controls).

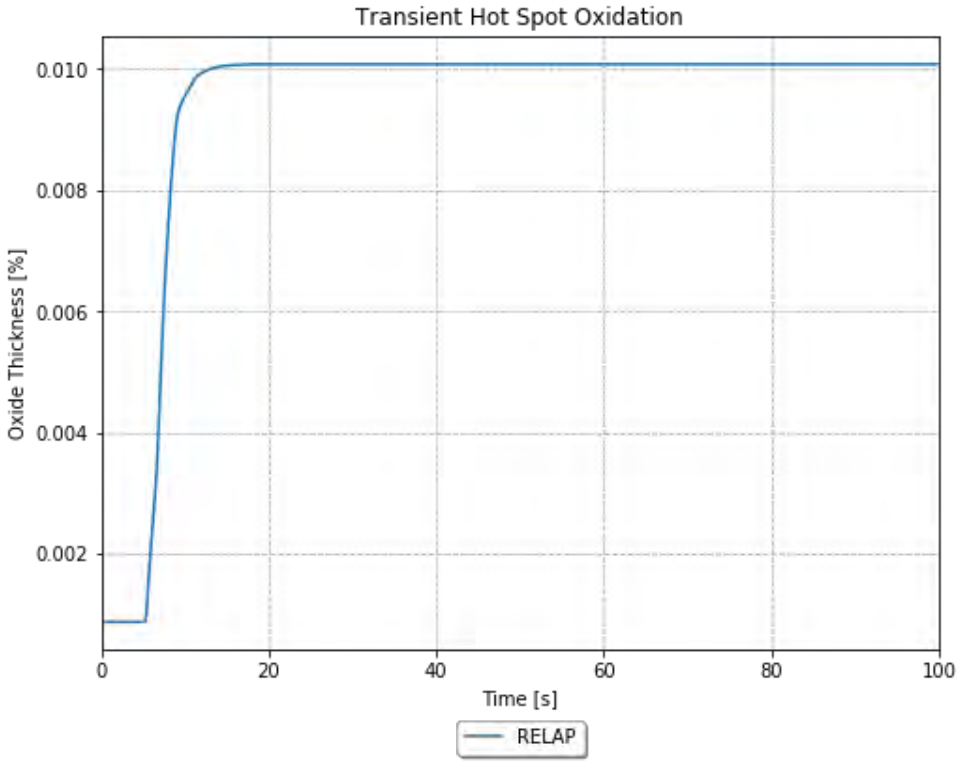

Figure 4-43. TR oxidation at the hot rod peak power location for the turbine trip scenario (e.g., maximum moderator feedback without PRZ controls).

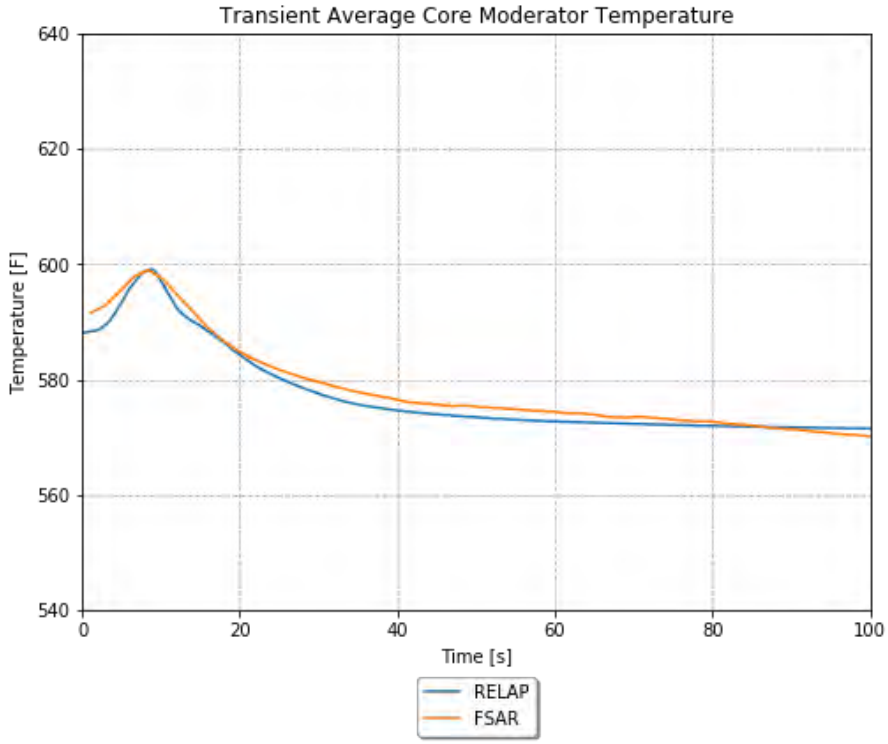

Figure 4-44. TR core average moderator temperature for the turbine trip scenario (e.g., maximum moderator feedback without PRZ controls).

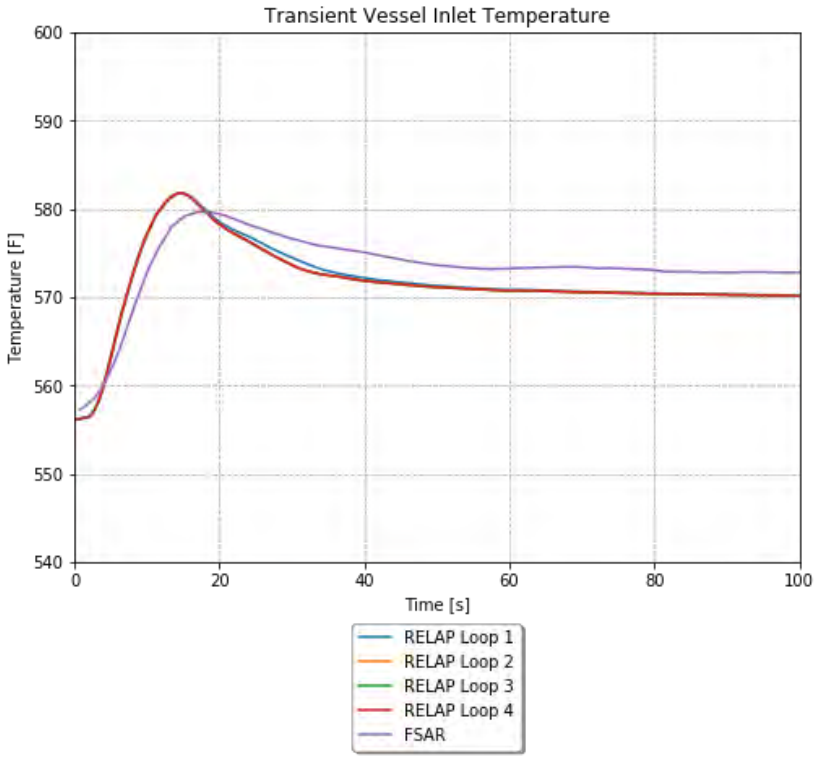

Figure 4-45. TR vessel inlet temperature for the turbine trip scenario (e.g., maximum moderator feedback without PRZ controls).

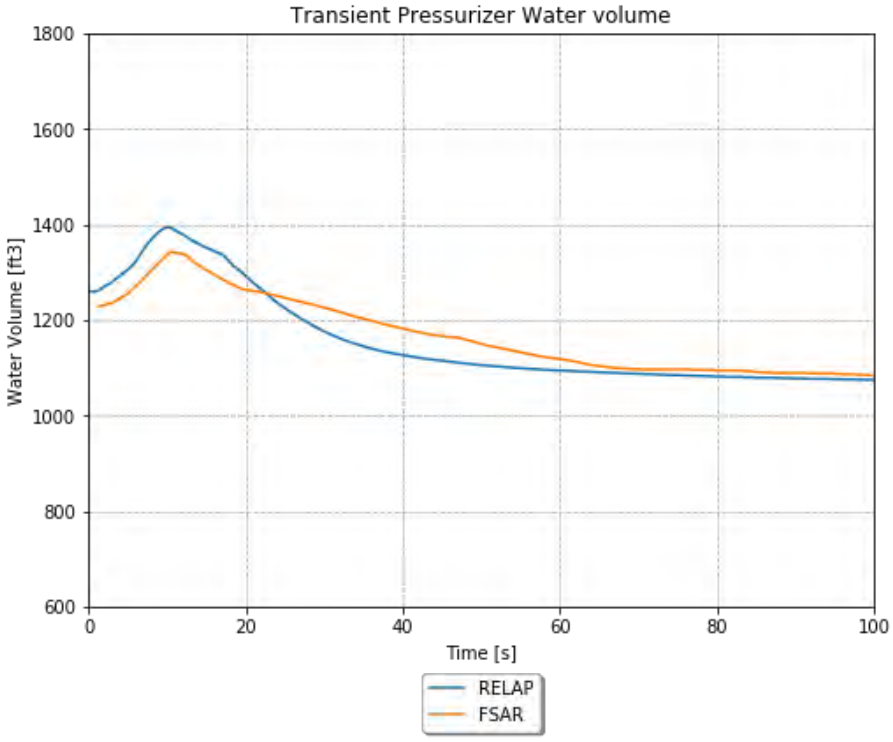

Figure 4-46. TR PRZ water volume for the turbine trip scenario (e.g., maximum moderator feedback without PRZ controls).

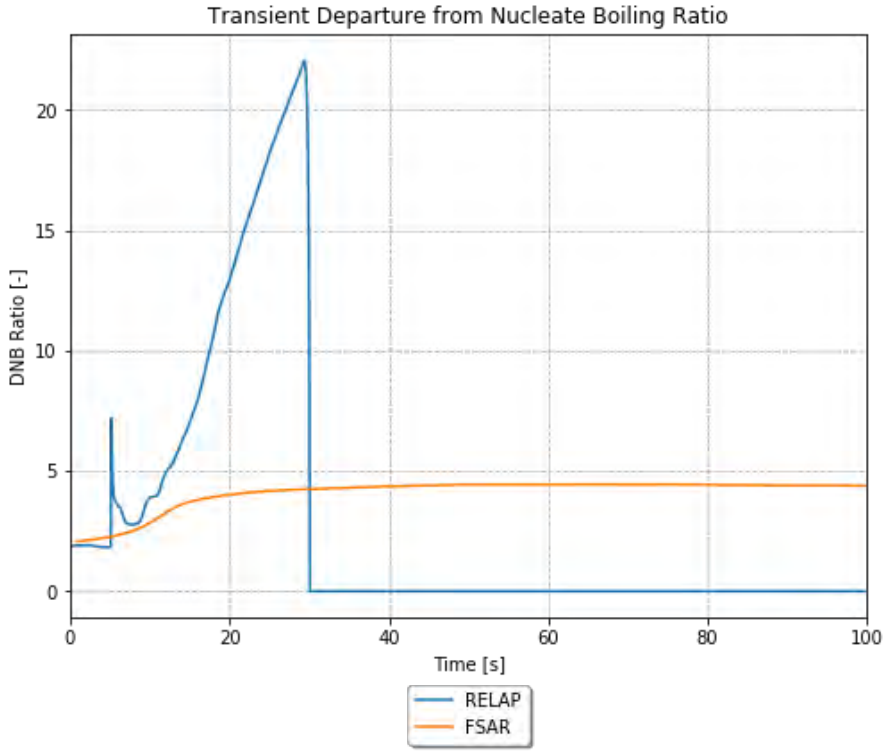

Figure 4-47. TR DNBR for the turbine trip scenario (e.g., maximum moderator feedback without PRZ controls).

4.7.5.2 Maximum Moderator Feedback with PRZ Controls

The TR PRZ pressure is shown in Figure 4-48. The RELAP5-3D response shows a similar trend to the FSAR run, but the initial pressurization is much higher. The pressure does settle close to the FSAR value. The larger increase in pressure indicates that the modeled spray flow and PORV flow may be inadequate.

The TR core power as a fraction of the nominal power is shown in Figure 4-49. RELAP5-3D predicts a slightly higher initial power excursion, and very similar behavior after scram to the FSAR run. The power plateau between ~10-40 seconds is a bit lower for RELAP5-3D, but still fairly close.

The TR clad temperature is shown in Figure 4-50. There is a significant heatup around the time of the power excursion.

The TR oxidation at the hot rod peak power location is shown in Figure 4-51. The oxidation increases coincident with the significant heatup from Figure 4-50, and then flattens out once the clad temperature drops back down.

The TR core average moderator temperature is shown in Figure 4-52. The RELAP5-3D response is similar to the FSAR run. There is a major difference that RELAP5-3D is lower during the period when the power plateau is lower, which is consistent.

The TR vessel inlet temperature is shown in Figure 4-53. The RELAP5-3D response is similar to the FSAR run. There is a major difference that RELAP5-3D is lower during the period when the power plateau is lower, which is consistent.

The TR PRZ water volume is shown in Figure 4-54. The RELAP5-3D response is similar to the FSAR run for the first 20 seconds, but is then lower for the remainder of the TR.

The TR DNBR is shown in Figure 4-55. The RELAP5-3D response is very different from the FSAR run, though they indicate a similar trend. The RELAP5-3D run shows an increasing DNBR that suddenly drops to 0. In RELAP5-3D, this can indicate that the heat structure is in a HT mode that does not even calculate CHF (i.e., single-phase liquid). This is thus interpreted as a very high DNBR value. The FSAR shows a consistent increase in DNBR.

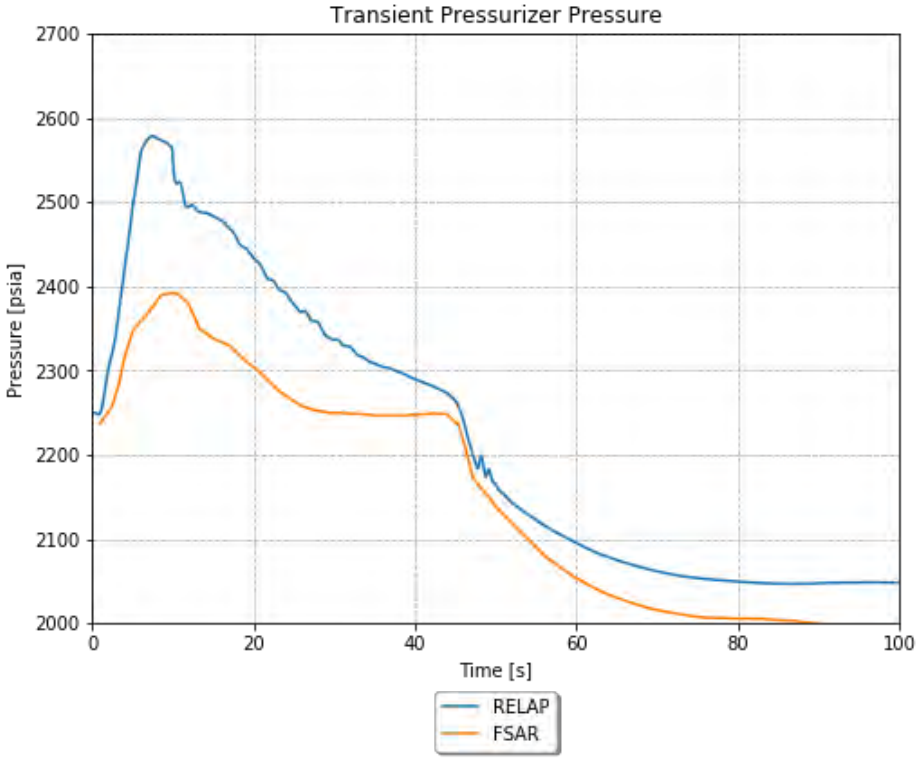

Figure 4-48. TR PRZ pressure for the turbine trip scenario (e.g., maximum moderator feedback with PRZ controls).

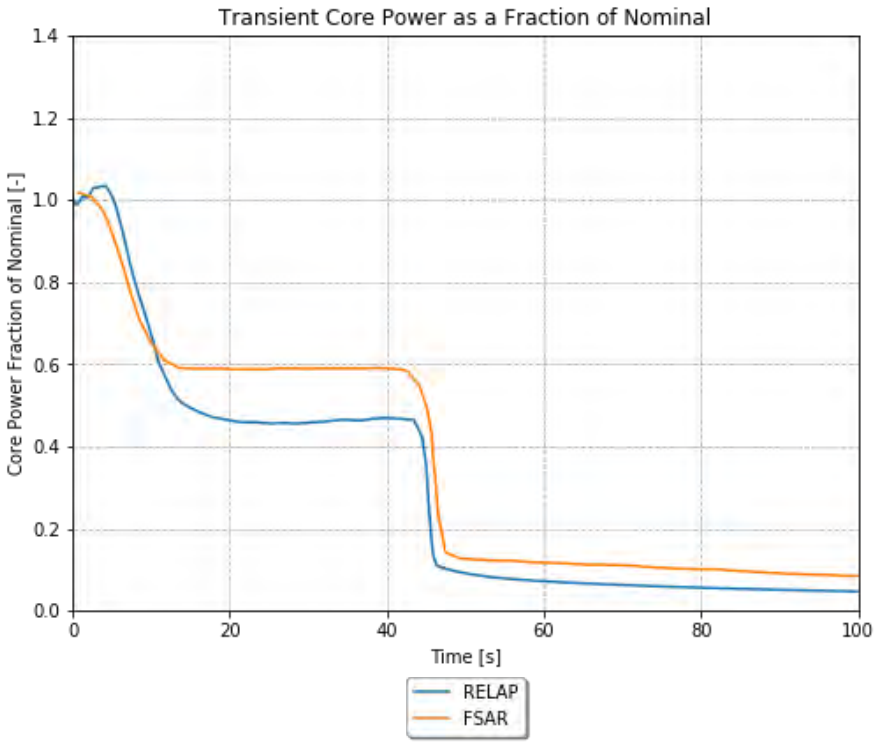

Figure 4-49. TR core power as a fraction of the nominal power for the turbine trip scenario (e.g., maximum moderator feedback with PRZ controls).

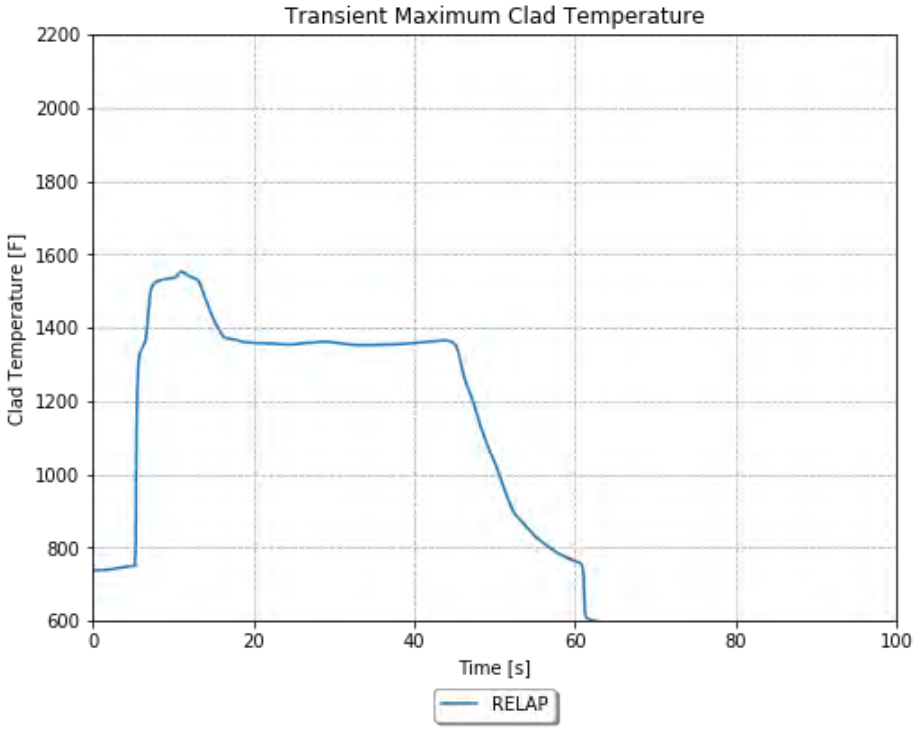

Figure 4-50. TR maximum clad temperature for the turbine trip scenario (e.g., maximum moderator feedback with PRZ controls).

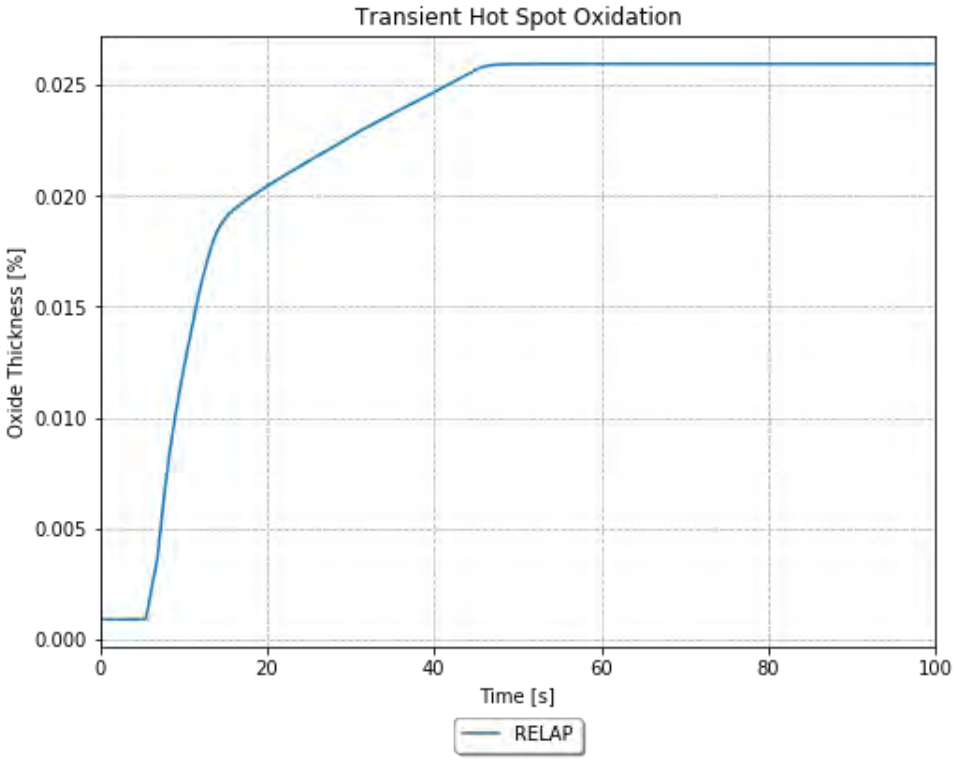

Figure 4-51. TR oxidation at the hot rod peak power location for the turbine trip scenario (e.g., maximum moderator feedback with PRZ controls).

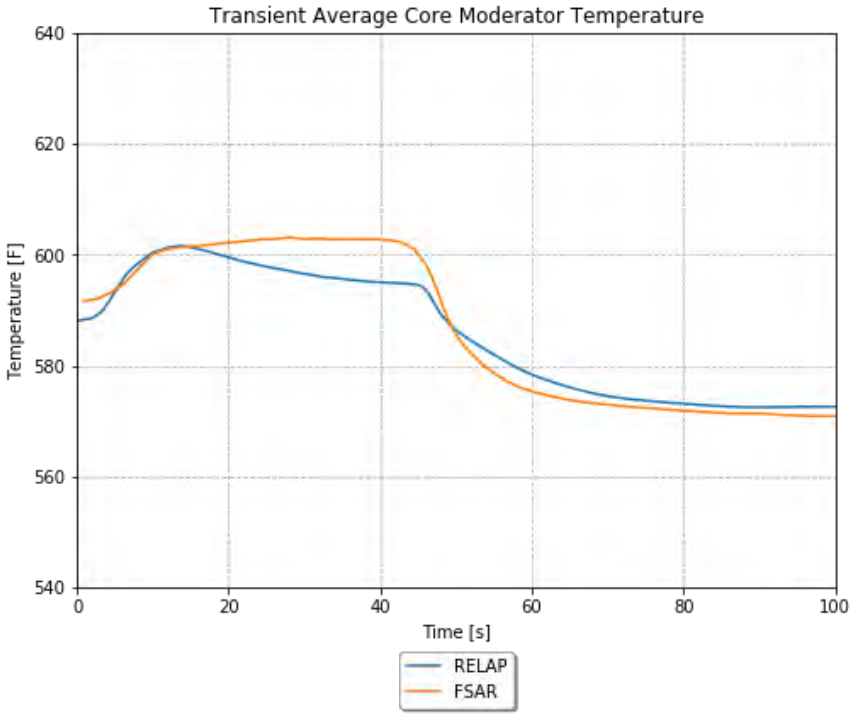

Figure 4-52. TR core average moderator temperature for the turbine trip scenario (e.g., maximum moderator feedback with PRZ controls).

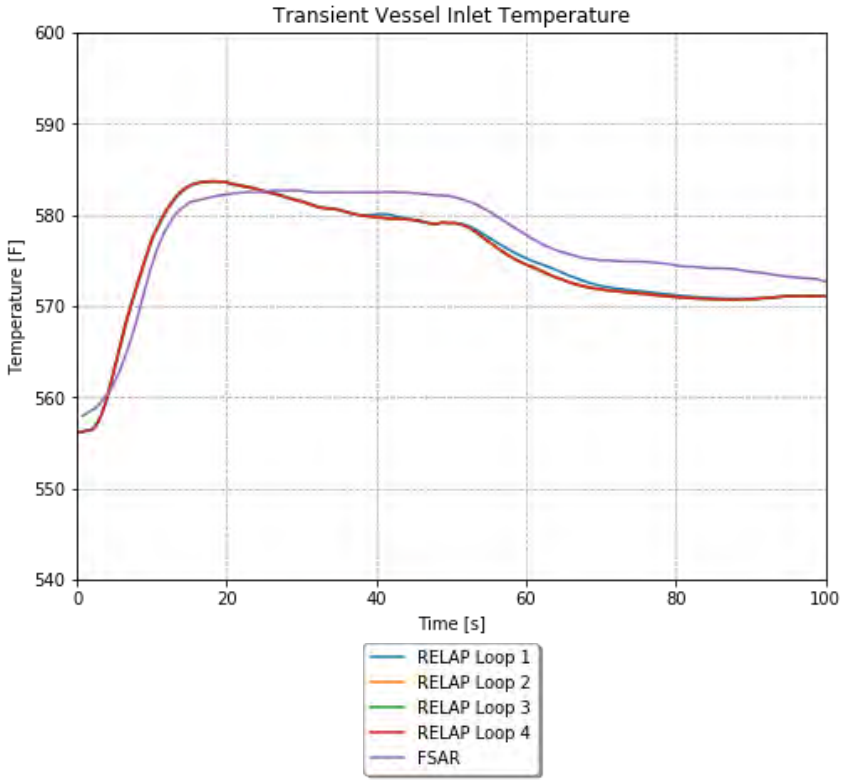

Figure 4-53. TR vessel inlet temperature for the turbine trip scenario (e.g., maximum moderator feedback with PRZ controls).

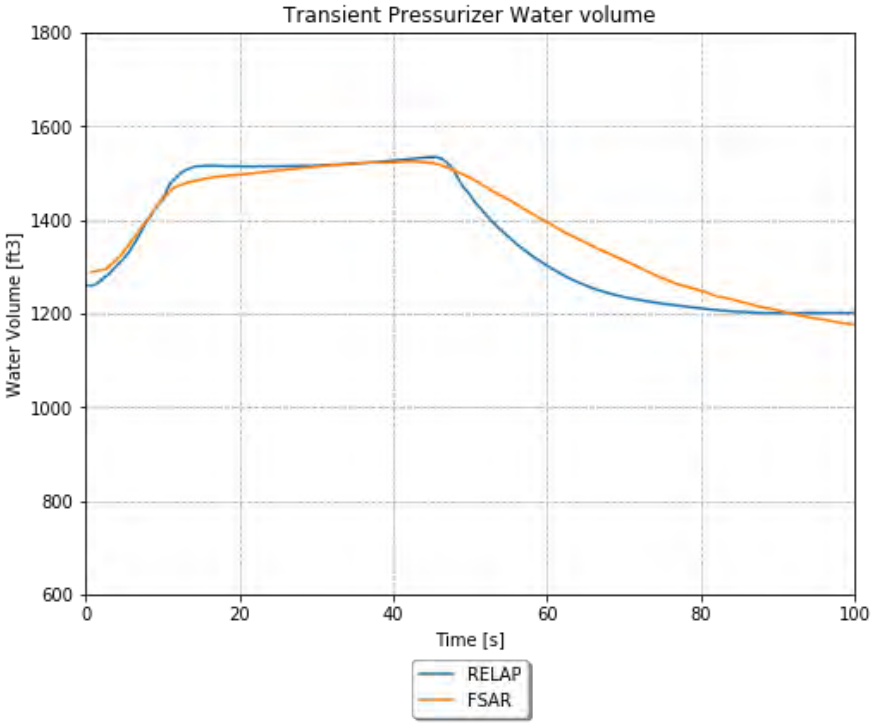

Figure 4-54. TR PRZ water volume for the turbine trip scenario (e.g., maximum moderator feedback with PRZ controls).

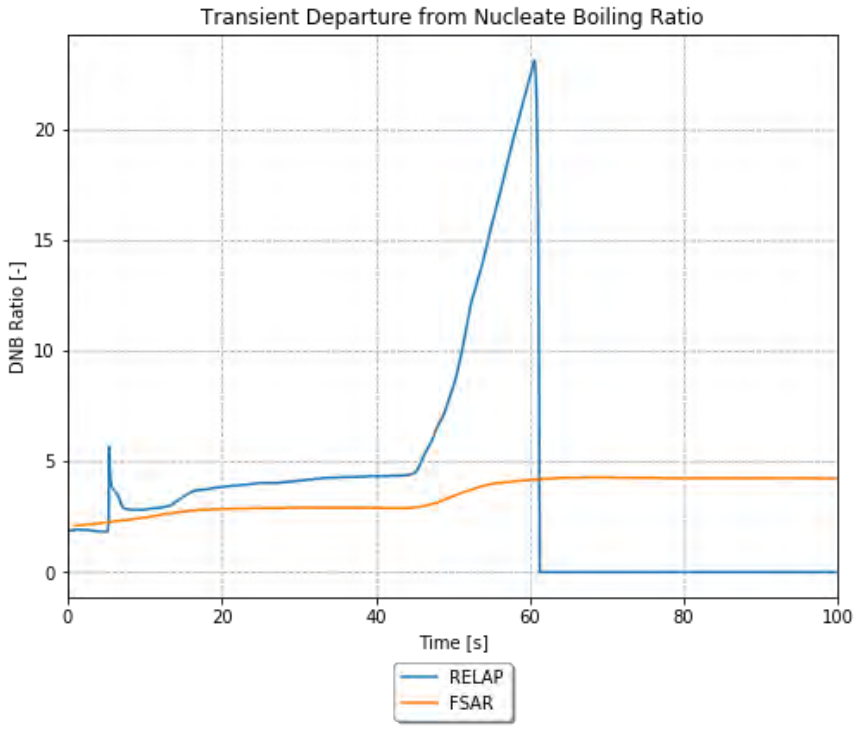

Figure 4-55. TR PRZ water volume for the turbine trip scenario (e.g., maximum moderator feedback with PRZ controls).

4.7.5.3 Minimum Moderator Feedback without PRZ Controls

The TR PRZ pressure is shown in Figure 4-56. The RELAP5-3D response is extremely similar to the FSAR run.

The TR core power as a fraction of the nominal power is shown in Figure 4-57. RELAP5-3D predicts a slightly higher power excursion, and very similar behavior after scram to the FSAR run.

The TR clad temperature is shown in Figure 4-58. There is a significant heatup around the time of the power excursion.

The TR oxidation at the hot rod peak power location is shown in Figure 4-59. The oxidation increases coincident with the significant heatup from Figure 4-58, and then flattens out once the clad temperature drops back down.

The TR core average moderator temperature is shown in Figure 4-60. The RELAP5-3D response is extremely similar to the FSAR run.

The TR vessel inlet temperature is shown in Figure 4-61. The RELAP5-3D response is extremely similar to the FSAR run.

The TR PRZ water volume is shown in Figure 4-62. The RELAP5-3D response is similar to the FSAR run, but is drops more quickly after reactor trip, although the converge on a similar value by the end of the TR.

The TR DNBR is shown in Figure 4-63. The RELAP5-3D response is very different from the FSAR run, though they indicate a similar trend. The RELAP5-3D run shows an increasing DNBR which suddenly drops to 0. In RELAP5-3D, this can indicate that the heat structure is in a HT mode which does not even calculate CHF (i.e., single-phase liquid). This is thus interpreted as a very high DNBR value. The FSAR shows a consistent increase in DNBR.

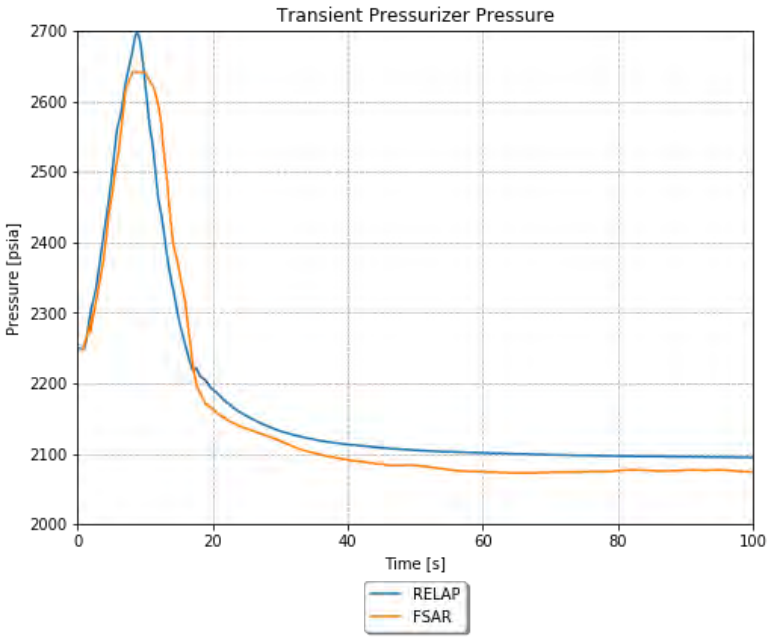

Figure 4-56. TR PRZ pressure for the turbine trip scenario (e.g., minimum moderator feedback without PRZ controls).

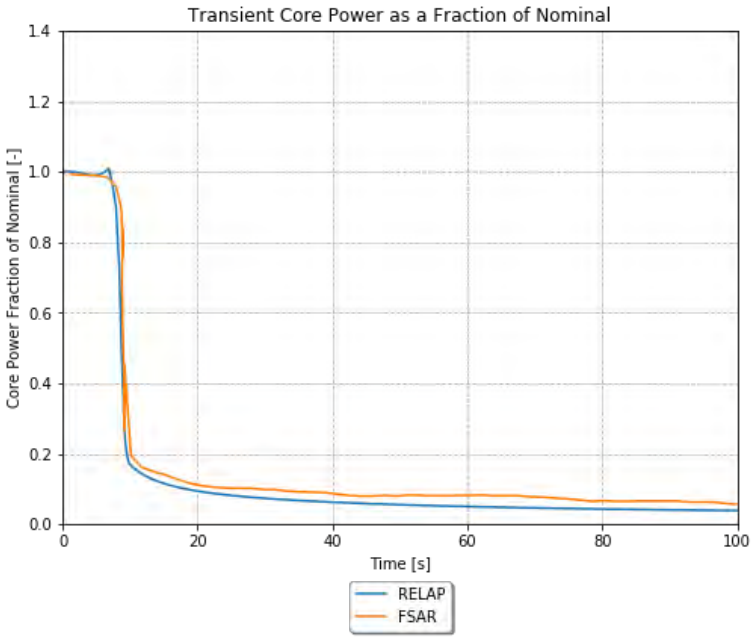

Figure 4-57. TR core power as a fraction of the nominal power for the turbine trip scenario (e.g., minimum moderator feedback without PRZ controls).

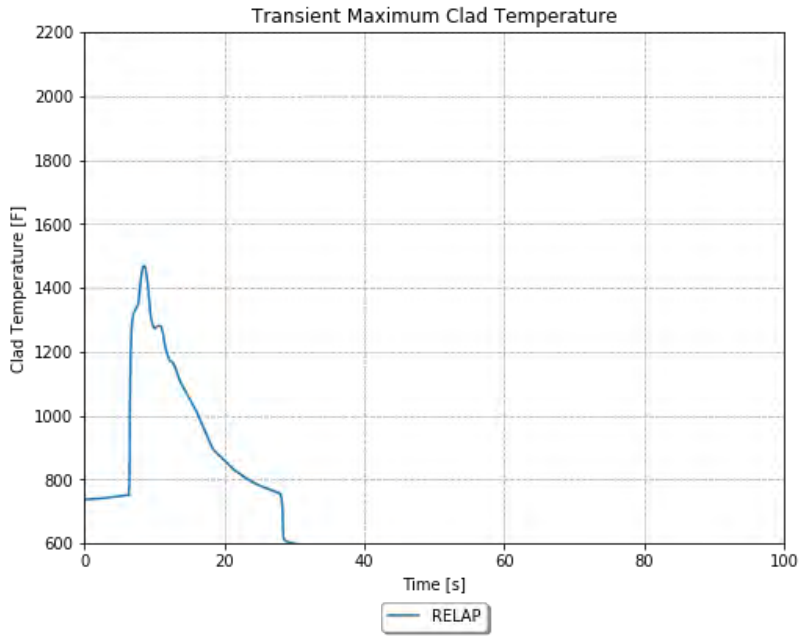

Figure 4-58. Tr maximum clad temperature for the turbine trip scenario (e.g., minimum moderator feedback without PRZ controls).

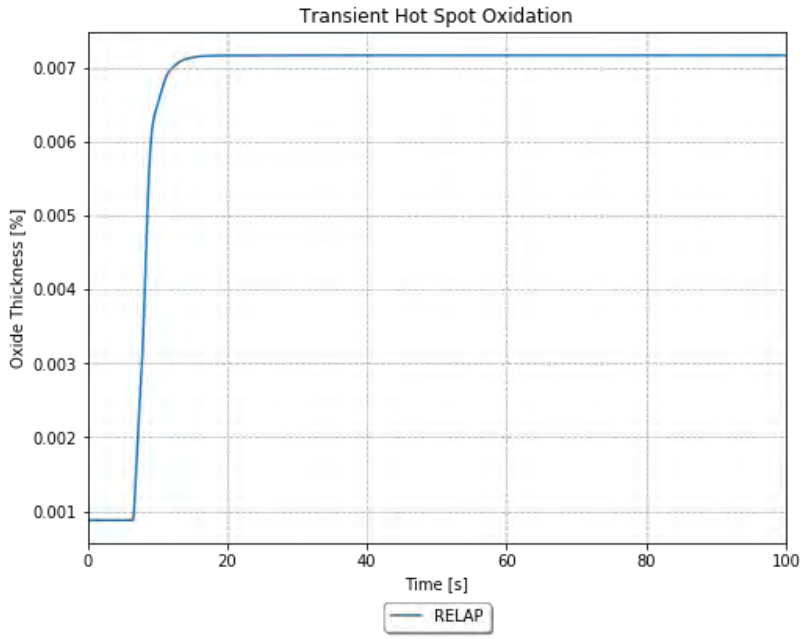

Figure 4-59. TR oxidation at the hot rod peak power location for the turbine trip scenario (e.g., minimum moderator feedback without PRZ controls).

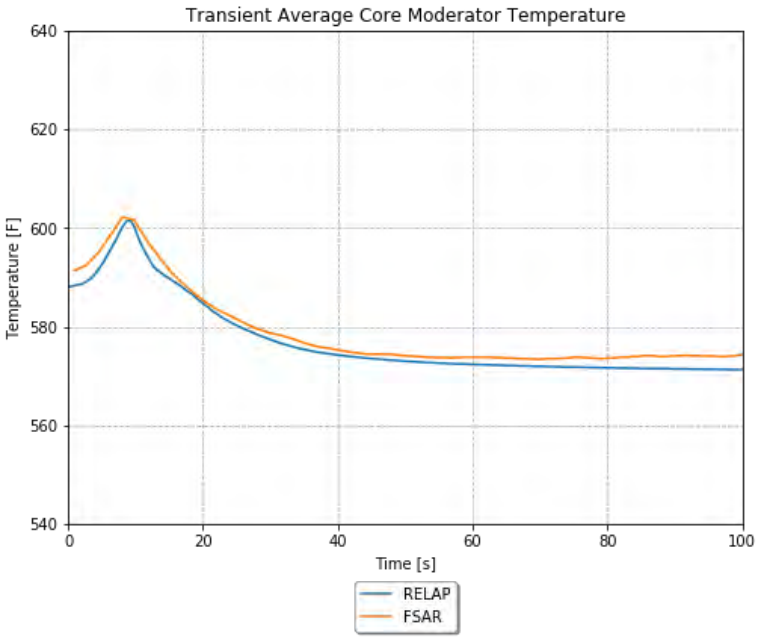

Figure 4-60. TR core average moderator temperature for the turbine trip scenario (e.g., minimum moderator feedback without PRZ controls).

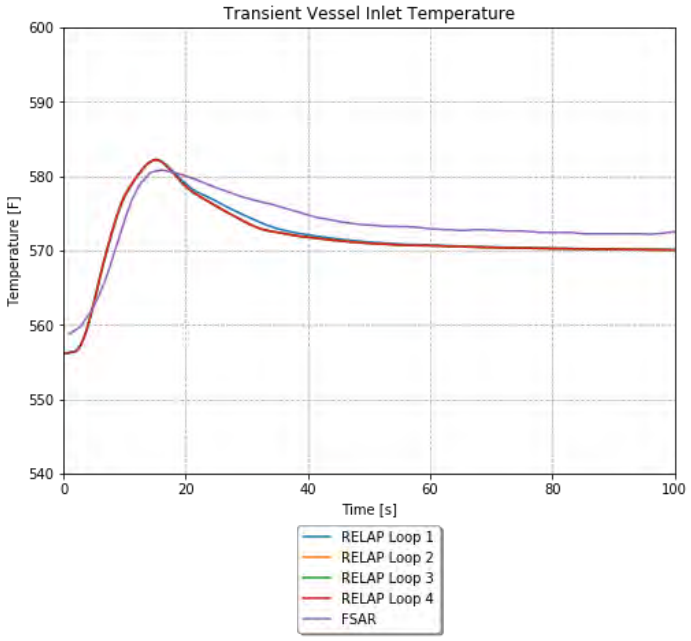

Figure 4-61. TR vessel inlet temperature for the turbine trip scenario (e.g., minimum moderator feedback without PRZ controls).

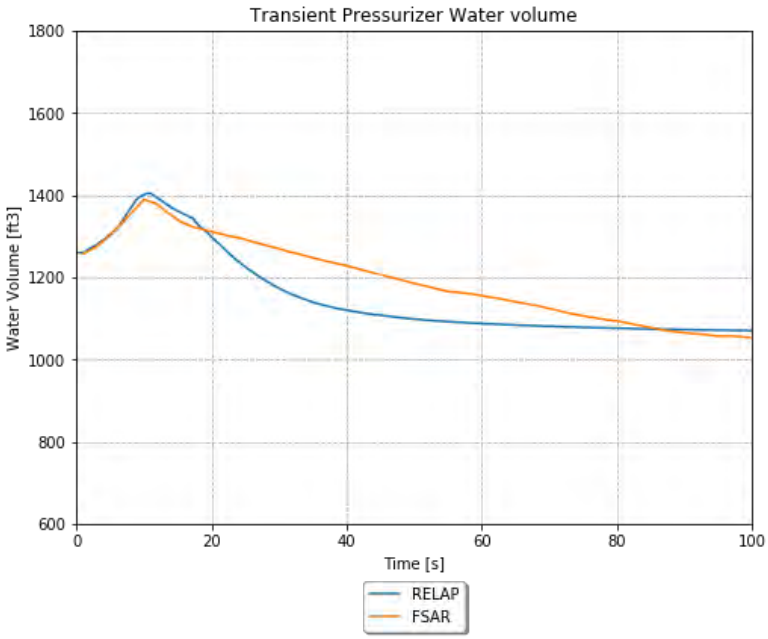

Figure 4-62. TR PRZ water volume for the turbine trip scenario (e.g., minimum moderator feedback without PRZ controls).

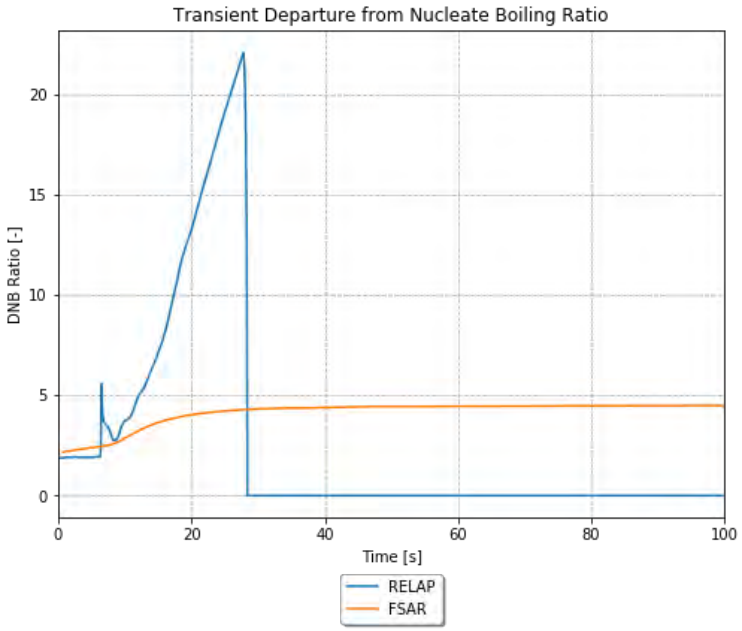

Figure 4-63. TR DNBR for the turbine trip scenario (e.g., minimum moderator feedback without PRZ controls).

4.7.5.4 Minimum Moderator Feedback with PRZ Controls

The TR PRZ pressure is shown in Figure 4-64. The RELAP5-3D response shows a similar trend to the FSAR run, but the initial pressurization is much higher. This indicates that the modeled spray flow and PORV flow may be inadequate.

The TR core power as a fraction of the nominal power is shown in Figure 4-65. RELAP5-3D predicts a large initial power excursion, and very similar behavior after scram to the FSAR run.

The TR clad temperature is shown in Figure 4-66. There is a significant heatup around the time of the power excursion.

The TR oxidation at the hot rod peak power location is shown in Figure 4-67. The oxidation increases coincident with the significant heatup from Figure 4-66, and then flattens out once the clad temperature drops back down.

The TR core average moderator temperature is shown in Figure 4-68. The RELAP5-3D response is very similar to the FSAR run.

The TR vessel inlet temperature is shown in Figure 4-69. The RELAP5-3D response is similar to the FSAR run.

The TR PRZ water volume is shown in Figure 4-70. The RELAP5-3D response is similar to the FSAR run, but it both increases and decreases much faster.

The TR DNBR is shown in Figure 4-71. The RELAP5-3D response is very different from the FSAR run, though they indicate a somewhat similar trend. Initially, the RELAP5-3D run shows an increase in DNBR, which then rapidly drops around the power excursion. When the RELAP5-3D run goes to zero at this point, this is interpreted to mean that DNB occurs. The FSAR run shows a slight decrease in DNBR at this time. After the power excursion, the RELAP5-3D run shows an increasing DNBR that suddenly drops to 0. In RELAP5-3D, this can indicate that the heat structure is in a HT mode that does not even calculate CHF (i.e., single-phase liquid). This is thus interpreted as a very high DNBR value. The FSAR shows a consistent increase in DNBR.

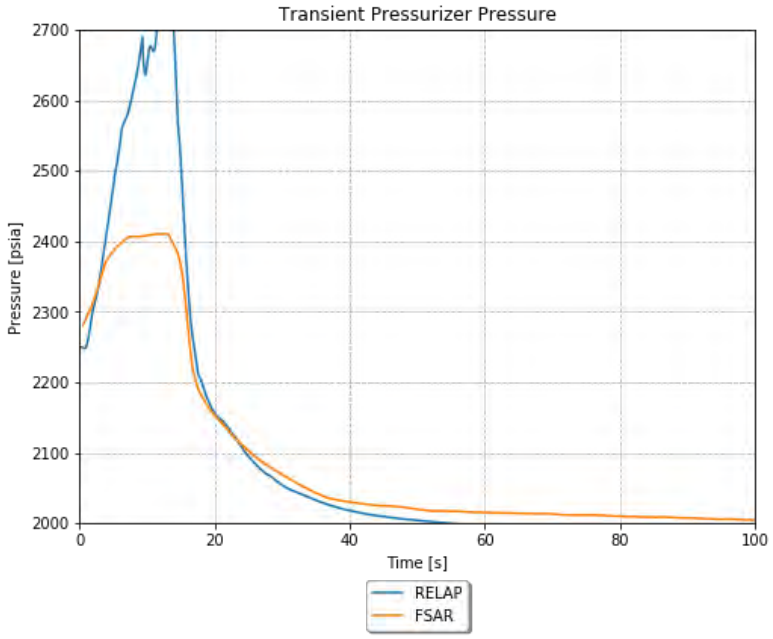

Figure 4-64. TR PRZ pressure for the turbine trip scenario (e.g., minimum moderator feedback with PRZ controls).

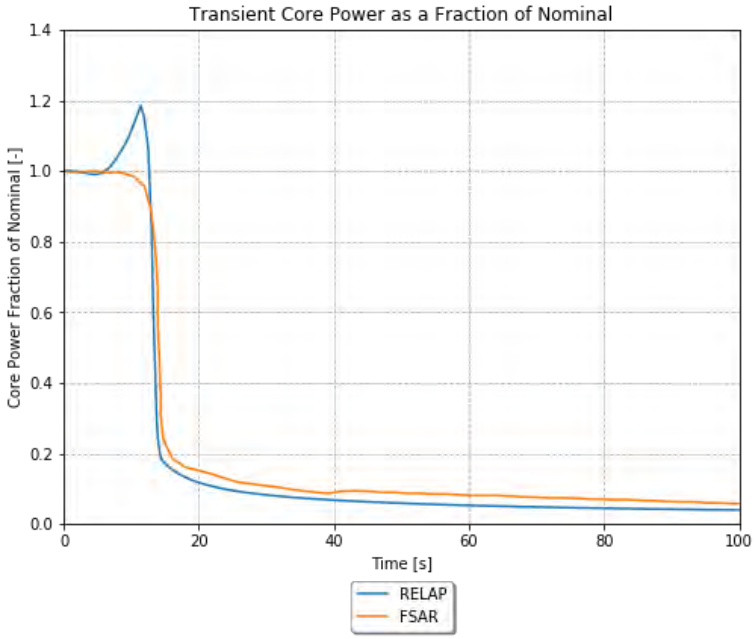

Figure 4-65. TR core power as a fraction of the nominal power for the turbine trip scenario (e.g., minimum moderator feedback with PRZ controls).

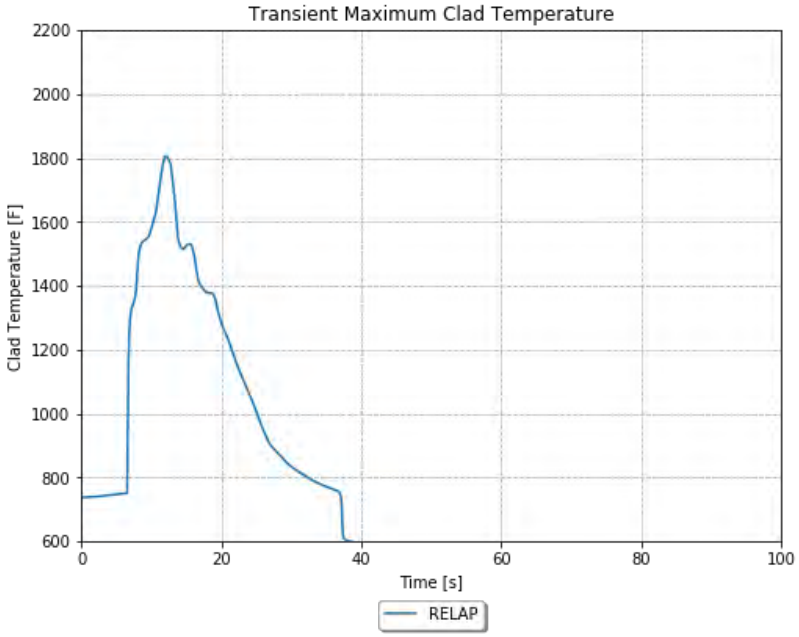

Figure 4-66. TR maximum clad temperature for the turbine trip scenario (e.g., minimum moderator feedback with PRZ controls).

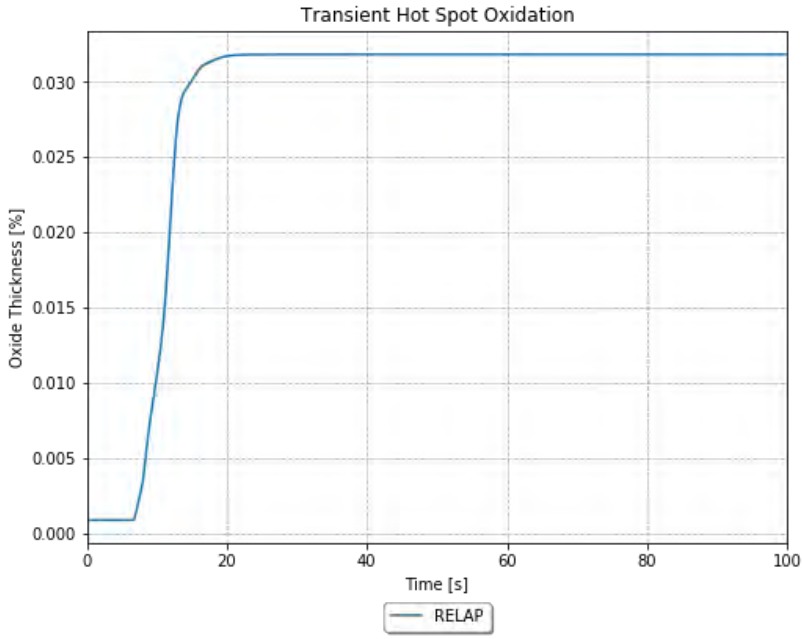

Figure 4-67. TR oxidation at the hot rod peak power location for the turbine trip scenario (e.g., minimum moderator feedback with PRZ controls).

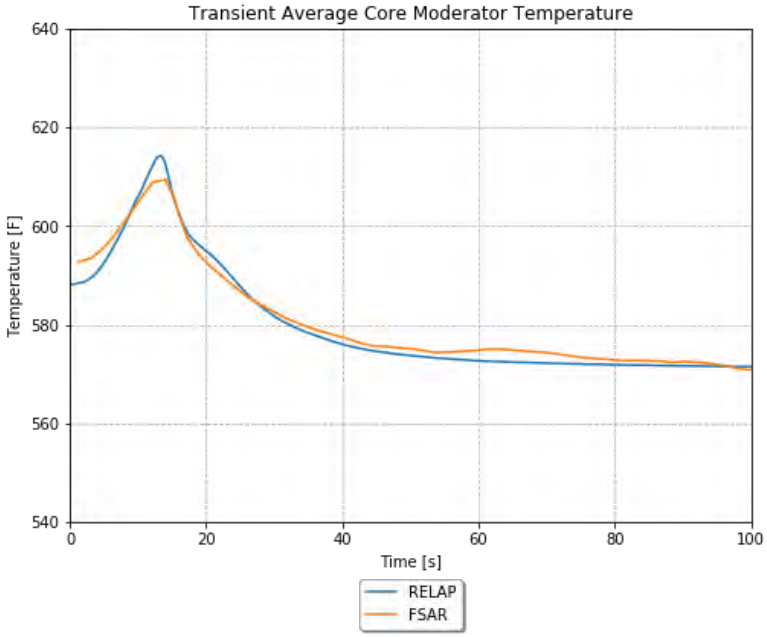

Figure 4-68. TR core average moderator temperature for the turbine trip scenario (e.g., minimum moderator feedback with PRZ controls).

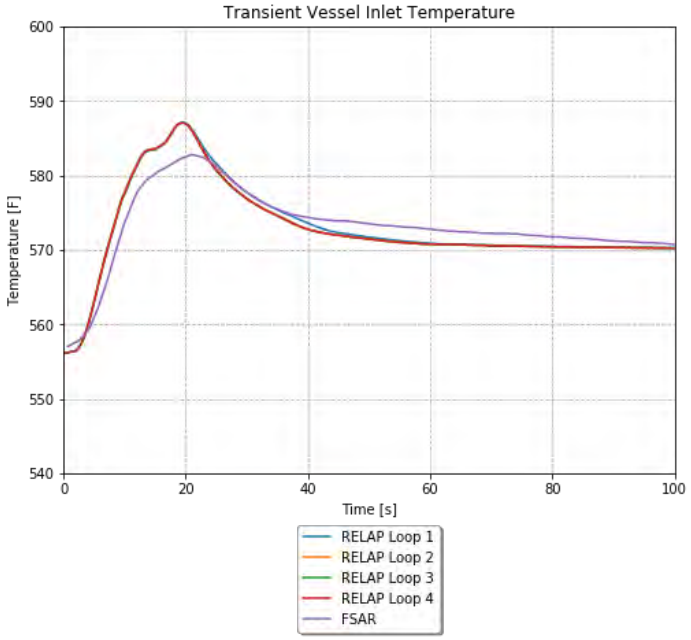

Figure 4-69. TR vessel inlet temperature for the turbine trip scenario (e.g., minimum moderator feedback with PRZ controls).

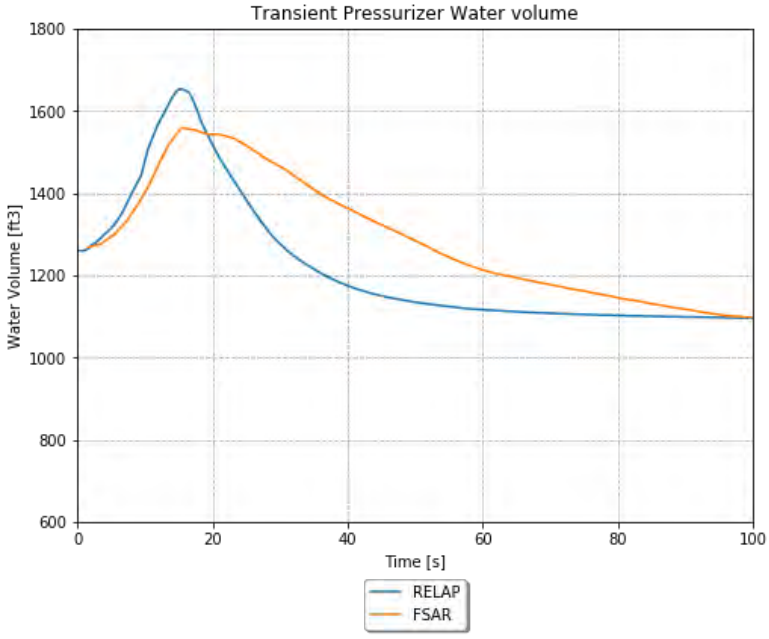

Figure 4-70. TR PRZ water volume for the turbine trip scenario (e.g., minimum moderator feedback with PRZ controls).

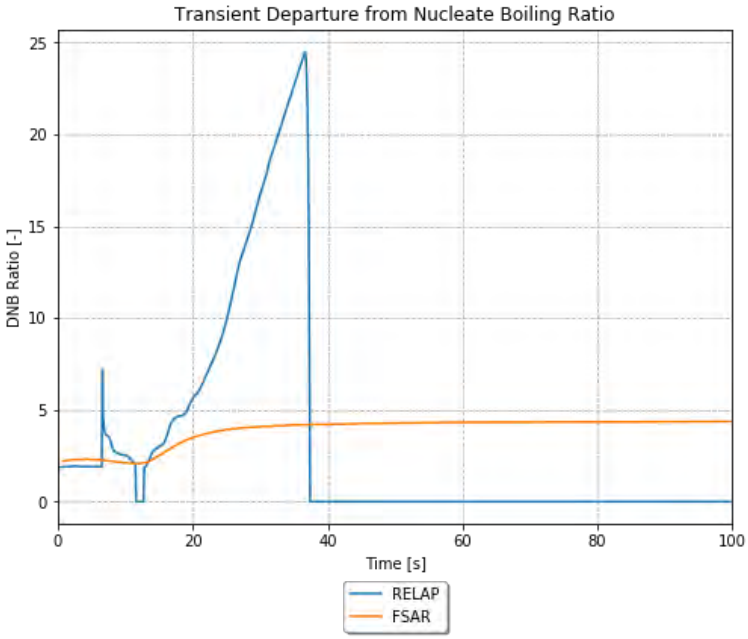

Figure 4-71. TR DNBR for the turbine trip scenario (e.g., minimum moderator feedback with PRZ controls).

4.7.6 Adherence to Acceptance Criteria

The final results for the turbine trip TRs are compared to the results from the FSAR and the acceptance criteria in Table 4-10. The acceptance criteria are based on examination of the FSAR sections, and the applicable sections of the standard review plan.

Table 4-10. Turbine trip rotor final results.

Result	Maximum Moderator Feedback				Minimum Moderator Feedback				Acceptance Criteria
	PRZ Contr.		No PRZ Contr.		PRZ Contr.		No PRZ Contr.		
	FSAR	RELAP 5-3D	FSAR	RELAP 5-3D	FSAR	RELAP 5-3D	FSAR	RELAP 5-3D	
Maximum RCS Pressure [psia]	~2390	2580	~2640	2642	~2410	2715	~2640	2700	2750
Minimum DNBR [-]	~2	~2	~2	~2	~2	< 1	~2	~2	1.24

The RELAP5-3D simulations meet all acceptance criteria for the turbine trip scenario, except the minimum moderator feedback run with PRZ controls, which encounters DNB. Some of the potential input differences between the FSAR simulations and the RELAP5-3D simulations are discussed in the following section. These may drive some of the differences in results between the FSAR analysis and the RELAP5-3D simulations, in addition to code differences.

4.7.7 Scenario-Specific Limitations and Conditions for Usage

The following limitations apply specifically to the turbine trip case:

- The main steam and feedwater flow are assumed to ramp to 0 over 1 second after trip. It is unclear what the base analysis assumptions are, but given that the TR is 10 seconds, this assumption could have a significant effect.
- The MSSVs are modeled to open at the set pressure and ramp to be fully open over 5 psi above each set pressure. There is insufficient detail in the FSAR to know if this is consistent with the modeling in the FSAR analysis.
- The PRZ safety valve is modeled to linearly ramp flow from none at 2500 psia to maximum at 2575 psia. There is insufficient detail in the FSAR to know if this is consistent with the modeling in the FSAR analysis.
- The reactivity feedback model has two major simplifications:
  - A single value for MDC based on an approximate average temperature is used to develop the table of reactivity vs. density, while the FSAR indicates that the MDC will vary with temperature. It is likely that this is a small effect.
  - The FSAR analysis uses a DPC, and modeling DPC is not supported by RELAP5-3D. As such, a generic FTC table from Chapter 4 was used. This is a valid source, but may cause a small deviation from the FSAR analysis.
- The power shape used may be inconsistent with that in the FSAR analysis, but it is confirmed that the FQ value is consistent.

4.8 Loss of Nonemergency AC Power to the Plant Auxiliaries

A complete loss of nonemergency alternating current (AC) power (also called a LOOP) may result in the loss of all power to the plant auxiliaries (i.e., the RCPs, condensate pumps, etc.). This loss of power may be caused by a complete loss of the offsite grid accompanied by a turbine-generator trip at the plant or by a loss of the onsite AC distribution system.

This TR is more severe than the turbine trip event analyzed in Section 4.7 because for this case, the decrease in heat removal by the secondary system is accompanied by a flow coast-down, which further reduces the capacity of the primary coolant to remove heat from the core.

Following a loss of AC power with turbine and reactor trips, the sequence described below will occur:

1. Plant vital instruments are supplied from emergency direct current (DC) power sources.
2. As the steam system pressure rises following the trip, the SG power-operated relief valves may be automatically opened to the atmosphere. The condenser is assumed not to be available for turbine bypass. If the steam flowrate through the power-operated relief valves is not available, the SG safety valves may lift to dissipate the sensible heat of the fuel and the coolant plus the residual decay heat produced in the reactor.
3. As the no-load temperature is approached, the SG power-operated relief valves—or safety valves, if the power-operated relief valves are not available—are used to dissipate the residual decay heat and to maintain the plant at the hot shutdown condition.
4. The standby diesel generators, which started on the loss of voltage on the plant emergency buses, begin to supply plant vital loads.
5. The auxiliary feedwater system is started automatically, and is designed to supply rated flow within 1 minute of the initiating signal, even if a loss of all nonemergency AC power occurs simultaneously with loss of normal feedwater.

Following the reactor coolant pump coast-down caused by the loss of AC power, the natural circulation capability of the RCS will remove residual and decay heat from the core, aided by auxiliary feedwater in the secondary system.

A LOOP is classified as an ANS Condition II event, fault of moderate frequency.

The LOOP scenario presents three cases in the FSAR:

1. Base LOOP.
2. LOOP with the AFW assumption changed due to a TMI concern related to PRZ overfill. This assumption is to have no AFW delivered to two SGs.
3. LOOP with charging flow on to check for PRZ overfill.

There are minor changes in the TR input files and the RAVEN distributions for the changes to the AFW and charging flow.

4.8.1 Scenario-Specific Inputs in the TR Input File

The TR input files are defined as follows:

- Upfront cards are included that specify this is a restart TR run, which uses the last available printout in the restart file.
- The end time is set to 7200 seconds for the base case and the altered AFW case, which is seemingly slightly longer than the reference plant FSAR runs. The end time is set to 600 seconds for the run with charging flows. The max time step is set to 0.05 seconds, as this is a value that is reasonable for a relatively stable simulation such as this.
- The minor edits are used to specify the variables used in the plots.
- CV 405 (e.g., the reactivity controller) is listed as a constant value of 0.0 $. This is done as a placeholder for RAVEN to substitute in the actual SS value end of CV 405 using the RAVEN variable, “ssreact.” This step is necessary to turn off the reactivity controller, but make the SS reactivity adder persist.
- CVs 419, 420, 421, and 422 (e.g., the pump inputs) are set as constant values consistent with the end of SS Pump Speed, and these values will be replaced by RAVEN using the variable “sspmpvel.” Note that this is in the TR input file but is unimportant to the run, as the pumps are tripped. Later in the file, Variable Trips 450 through 453 are specified to be false, so that the RCP motor trips are used.
- CVs 435 through 438 (e.g., the steam valve position) are changed to be functions of General Table 650. This allows them to be set to the SS valve position prior to the reactor trip or SI signal, and then close based on the specified delay and ramp times.
- CVs 459 through 462 (e.g., the MFW flow rate) are listed as constant values of 1118.9 lbm/sec. This is done as a placeholder for RAVEN to substitute in the actual end of SS values of CVs 459 through 462 using the RAVEN variable “ssmfw.”
- CV 472 is listed as a constant value of 0.0. This is used to turn off the SS charging flow.
- CV 473 is listed as a constant value of 0.0. This is used to turn off the SS letdown flow.
- The reactor trip is forced at a time consistent with the FSAR run (e.g., 56.5 seconds). Variable Trip 411 is specified as a trip when time is greater than the intended value. In the FSAR case, the low-low SG level setpoint is used. Insufficient information exists in the FSAR to determine the actual SG level in ft. for the RELAP5-3D model. As such, reactor trip is simply triggered at a consistent time. Nothing is mentioned in the FSAR for reactor trip for the altered AFW run or the run with charging flows, so the same assumption is used.

- The base case has a large slightly higher power spike than the other two cases around 55 seconds causing the cladding temperature to reach impossible temperatures causing a failure in the simulation. Therefore, the Variable Trip 411 is changed from 56.5 seconds to 51.5 seconds to reduce the power spike. It is recommended that this be re-evaluated in the next phase.
- General Table 481 is specified to update the spray to kick on 10 psia above the PRZ pressure setpoint—rather than the SS controls that make it come on as soon as the pressure goes above 10 psia.
- Currently, the spray lines are modeled using a time-dependent volume. For all three LOOP TRs, this component is replaced with a branch (e.g., BRANCH 157) that has four pipes (e.g., PIPES 190, 290, 390, and 490) connected to it that each are connected with their respective cold legs (e.g., PIPES 114, 214, 314, and 414) to.
- CV 641 is omitted from the input file, so the PORV is operational. The PORV logic is in the SS model, so this allows it to function as intended.
- General Table 640 is listed with a change to have the table trip removed so that the specified MFW delay and ramp time will simply be based on the TR time.
- General Table 650 is listed, with input identical to the SS. This input needs to be here so that the first three valve position entries in the table can be replaced with the end of the SS values using the RAVEN variable "ssstmvlv."
- In the run with the altered AFW for TMI concerns, AFW time-dependent junctions 381 and 481 are added to the TR input file, with the liquid flow changed to 0.0 lbm/sec at all times.
- In the run with charging flows, the simplest way to turn on the charging flow without causing Logical Trip 640 to activate is to update Trip 631 in the TR input file so that it is triggered by Variable Trip 471 AND Variable Trip 402 (always true) and updating Trip 471 so that it is time greater than or equal to 1 second. This value is used because the "TIMEOF" Trip 630 is initialized to -1 and remains at that value until Trip 630 trips. The SI trip delay time variable is added to the "TIMEOF" Trip 630, so this will function to make Variable Trip 471 turn true at 0.1 seconds. Combined with the always true trip, this will result in Logical Trip 631 activating at 0.1 seconds into the TR, as desired.

4.8.2 Scenario-Specific RAVEN Inputs

The RAVEN distribution means are set as shown in Table 4-11. The inputs are consistent with the FSAR, as described below. The remaining inputs are assumptions that are not specifically mentioned in the FSAR:

- The SS conditions are set as follows:
  - For the base run, the initial conditions are generally set to nominal values, except the core power, the PRZ pressure, and the RCS temperatures, which are skewed high.
  - The run with altered AFW flow for TMI concerns, the initial conditions are set to nominal values.
- As discussed in the previous section, the reactor trip is forced at a time consistent with the FSAR run. As such, the setpoints set in the distributions are irrelevant except for the low-low SG level, which is set to an impossible value so that it won't trip before the intended time.
- The MFW is ramped down over 5 seconds with a delay of 5 seconds from the reactor trip time, and the AFW comes on with a 75 second delay time, and a ramp time of 2 seconds.
- The AFW flow rate is set to a mass flow rate consistent with 255 gpm/SG, which is the flow rate given in the FSAR. This is consistent in all runs; however, note that the case with altered AFW flow for TMI concerns models AFW to only 2 SGs—so effectively half the total AFW flow.
- The RCP motors trip 4 seconds after the reactor trip.

- The MDC is set consistent with the locked rotor case (-0.042 $\Delta k/g/cm^3$).
- The MSIV is immediately ramped down over 0.1 seconds from the reactor trip time.
- The RCCAs begin to drop 2 seconds after reactor trip.
- The inputs related to SI flows are set as follows:
  - For the base run and the run with altered AFW flows, all inputs related to ECCS flows and timing are irrelevant to this case. The SI signal setpoint is set to a value that isn't reached.
  - For the charging SI run, the SI delay time is set to 1.1 seconds, and the trip is set to go off immediately.

Table 4-11. Summary of RAVEN input loss of nonemergency AC power to the plant auxiliaries.

Distribution	Description	Unit	Mean
cltempdist	Cold Leg Temperature	°F	562.2 or 556.2
corepdist	Core Power	W	3.653E+09
fwtempdist	Feedwater Temperature	°F	448.7
hltempdist	Hot Leg Temperature	°F	626.6 or 620.6
przleveldist	PRZ Level	ft.	34.3
przpressdist	PRZ Pressure	psia	2250
rcsflowdist	RCS Volumetric Flow	gpm	93600
rcsmflodist	RCS Mass Flow	lbm/sec	9684.028
rcsmflorrdist	RCS Mass Flow in Vessel	lbm/sec	-9684.028
sgleveldist	SG Level	ft.	40.1
stmpressdist	SG Steam Pressure	psia	941
sgflowdist	SG Flow Rate	lbm/sec	1132.639
dpvessdist	Vessel Pressure Drop	psi	46.5
dphldist	Hot Leg Pressure Drop	psi	1.2
dpxldist	Crossover Leg Pressure Drop	psi	3.1
dpcldist	Cold Leg Pressure Drop	psi	3.3
dpsgdist	SG Primary Pressure Drop	psi	45.5
corbypdist	Core Bypass Flow	%	5
przphirxtdist	High PRZ Pressure Reactor Trip Setpoint	psia	2439.7
przplorxtdist	Low PRZ Pressure Reactor Trip Setpoint	psia	1714.7
przlhirxtdist	High PRZ Level Reactor Trip Setpoint	ft.	48.9
rcsflolorxtdist	Low RCS Flow Rate Reactor Trip Setpoint	lbm/sec	8425.08
sglevlorxtdist	Low SG Level Reactor Trip Setpoint	ft.	-1
mfwdeltimedist	MFW Delay Time	sec	5
mfwramptimedist	MFW Ramp Time	sec	10
afwdeltimedist	AFW Delay Time	sec	75
afwramptimedist	AFW Ramp Time	sec	77
afwflodist	AFW Flow Rate	lbm/sec	35.3
pmpmotdeldist	Pump Motor Trip Delay Time	sec	4
achfluxdist	Average Channel Maximum SS Heat Flux	BTU/sec-ft^2	99.954

Distribution	Description	Unit	Mean
hchfluxdist	Hot Channel Maximum SS Heat Flux	BTU/sec-ft^2	164.93
initreactdist	Initial Reactivity	$	0
mdcdist	Moderator Density Coefficient	$\Delta k/g/cm^3$	-0.042
accbordist	Accumulator Boron Concentration	Mass Frac	0.0019
chgbordist	Charging Boron Concentration	Mass Frac	0.0024
accvoldist	Accumulator Water Volume	ft^3	900
acctempdist	Accumulator Temperature	°F	120
accpressdist	Accumulator Pressure	psia	600
sitrplspdist	Low Steam Pressure SI Signal	psia	800
sitrpdeldist	SI Signal Delay Time	sec	42 or 1.1
msivdeldist	MSIV Delay Time	sec	0.001
msivrampdist	MSIV Ramp Time	sec	0.1
rccadeldist	RCCA Delay Time	sec	2
rcpheatdist	RCP Heat Generation	MW	0.00001
przsafdist	PRZ Safety Valve Open Pressure	psia	2474.7
rcsbordist	RCS Initial Boron Concentration	Mass Frac	0

4.8.3 Steady State Results

The steady state observations for the LOOP cases are explained in detail in FY-2020 [2].

4.8.4 TR Boundary Conditions

The TR boundary conditions for the LOOP are explained in detail in FY-2020 [2].

4.8.5 TR Results

The RELAP5-3D results are examined in the subsections below.

4.8.5.1 LOOP Base Case

The TR PRZ pressure is shown in Figure 4-72. The trends in the RELAP5-3D response are fairly similar to the FSAR run. The RELAP5-3D run has much more subdued changes.

The TR core power as a fraction of the nominal power is shown in Figure 4-73. RELAP5-3D the base case predicts a small power excursion prior to reactor trip, followed by normal decay heat.

The TR clad temperature is shown in Figure 4-74. There is a significant heatup around the time of the power excursion.

The TR oxidation at the hot rod peak power location is shown in Figure 4-75. The oxidation increases coincident with the significant heatup from Figure 4-74, and then flattens out once the clad temperature drops back down.

The TR SG pressures are shown in Figure 4-76. The trends in the RELAP5-3D response are fairly similar to the FSAR run. The FSAR run has much more subdued changes.

The TR PRZ water volume is shown in Figure 4-77. The trends in the RELAP5-3D response are fairly similar to the FSAR run. The FSAR run has much more subdued changes.

The TR DNBR is shown in Figure 4-78. The RELAP5-3D DNBR is 0 for a vast majority of the TR, other than right around the power excursion. Because of the extremely fast cladding heatup, it is presumed that the DNBR is under 1 at this point.

The TR hot leg, cold leg, and saturation temperatures are shown in Figure 4-79. The saturation temperatures are very close throughout the TR. The hot leg and cold leg temperature are fairly close through about 3000 seconds. After that point, the RELAP5-3D temperatures continue down, while the FSAR temperatures plateau.

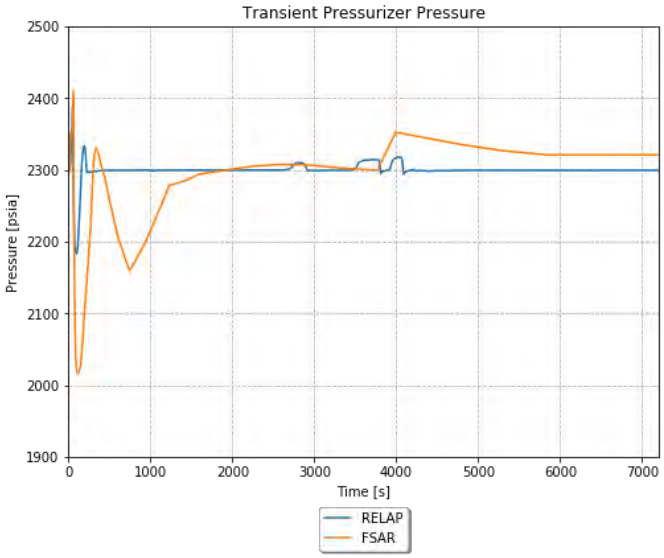

Figure 4-72. TR PRZ pressure for the loop scenario (e.g., base case).

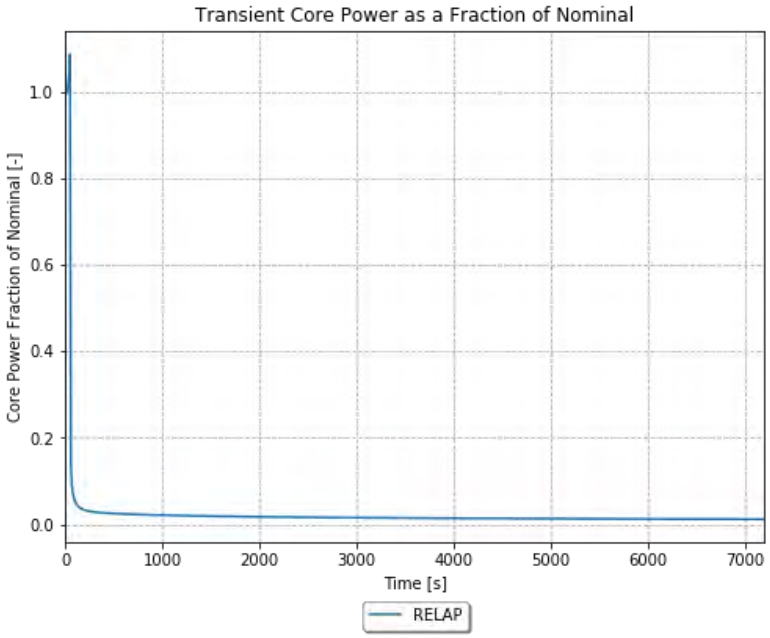

Figure 4-73. TR core power as a fraction of nominal power for the LOOP scenario (e.g., base case).

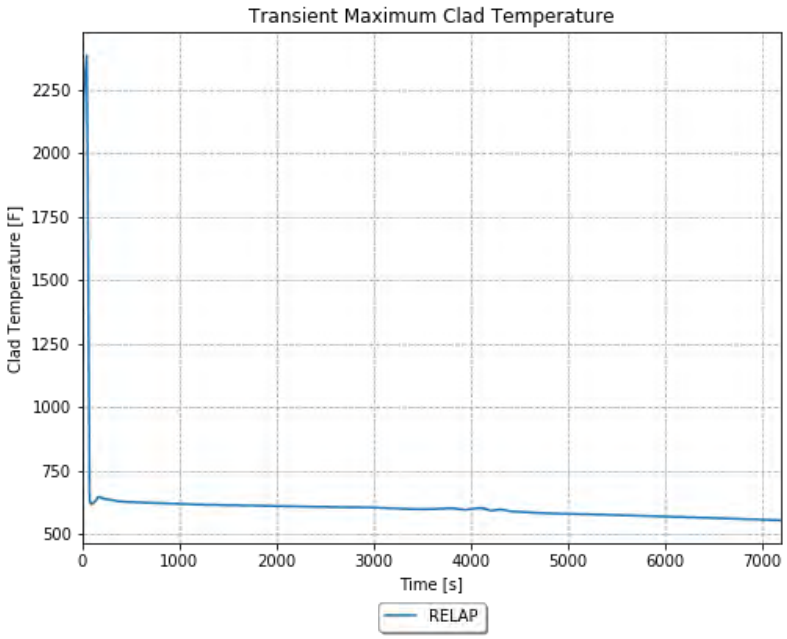

Figure 4-74. TR maximum clad temperature for the LOOP scenario (e.g., base case).

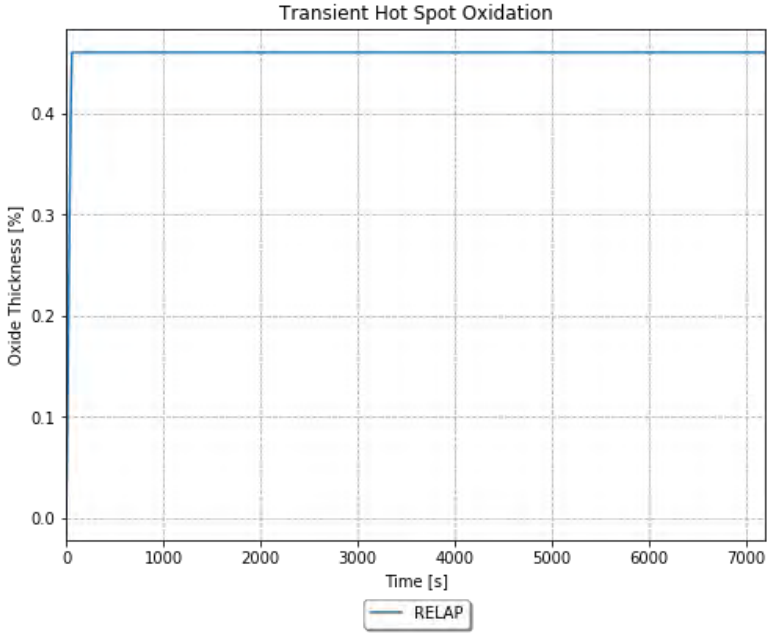

Figure 4-75. TR oxidation at the hot rod peak power location for the LOOP scenario (e.g., base case).

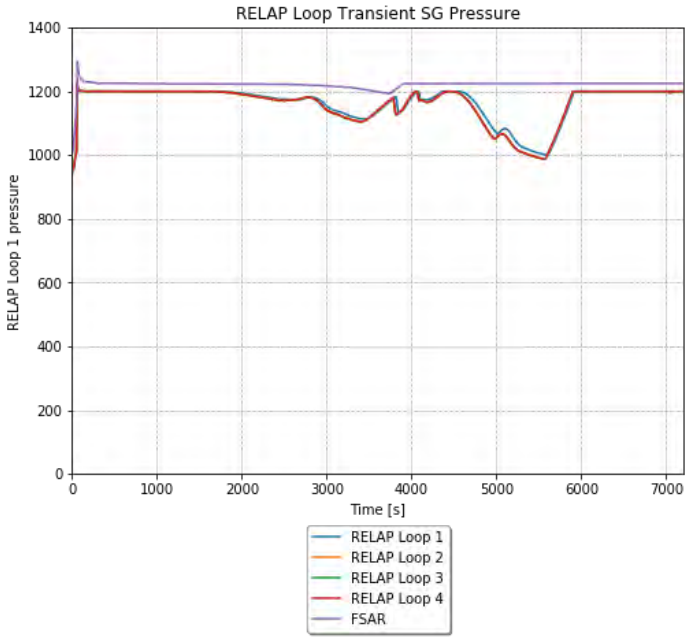

Figure 4-76. TR SG pressure for the LOOP scenario (e.g., base case).

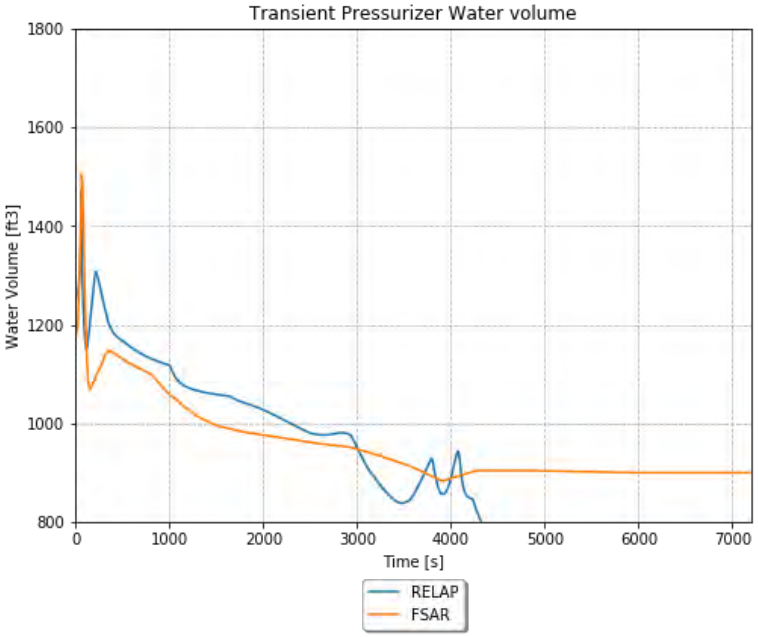

Figure 4-77. TR PRZ water volume for the LOOP scenario (e.g., base case).

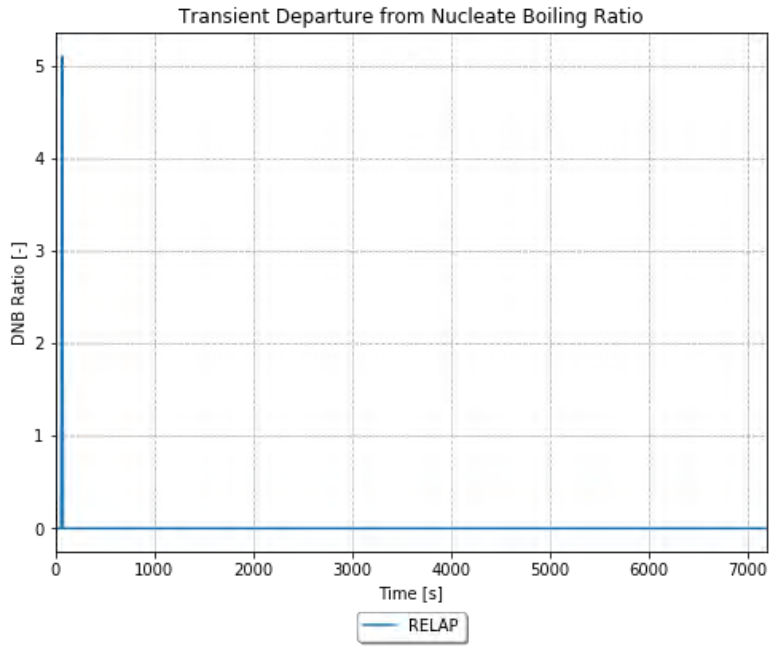

Figure 4-78. TR DNBR for the LOOP scenario (e.g., base case).

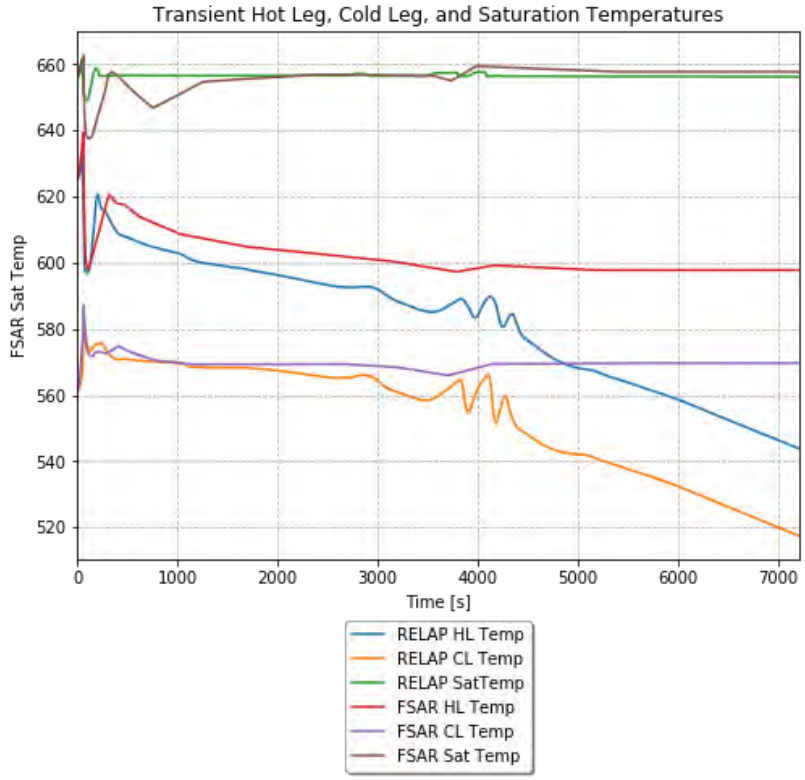

Figure 4-79. TR hot leg, cold leg, and saturation temperatures for the LOOP scenario (e.g., base case).

4.8.5.2 LOOP Case with Charging SI Flows

This case is run specifically to check the PRZ water volume. The pressure is also examined for relevance to the boundary conditions.

The TR PRZ pressure is shown in Figure 4-80. This response is fairly different as the large depressurization observed in the base case does not occur; a large pressurization occurs at the end of the charging case—presumably due to the PRZ becoming water solid. Note that the PORV and PRZ safety valve are set to have steam flow and not liquid flow, so this pressurization is non-physical. However, the purpose of this run is to determine if the PRZ becomes water solid, which it does, so the run can be considered to not meet the acceptance criteria at that point.

The TR PRZ water volume is shown in Figure 4-81. The PRZ water volume increases significantly throughout the TR and does become water solid at about 450 seconds.

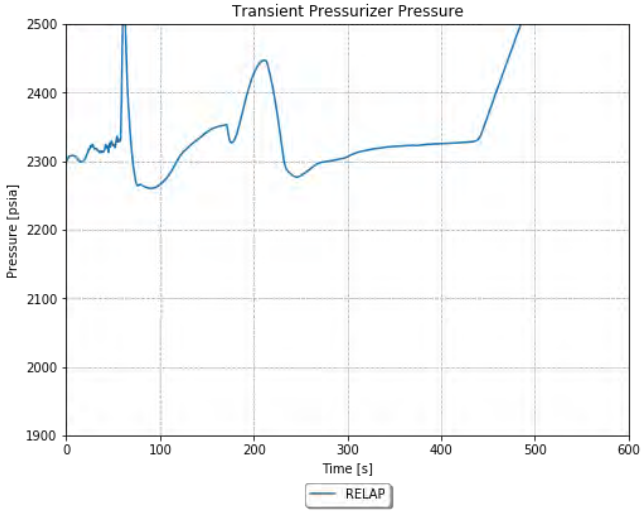

Figure 4-80. TR PRZ pressure for the LOOP scenario (e.g., the case with charging flows).

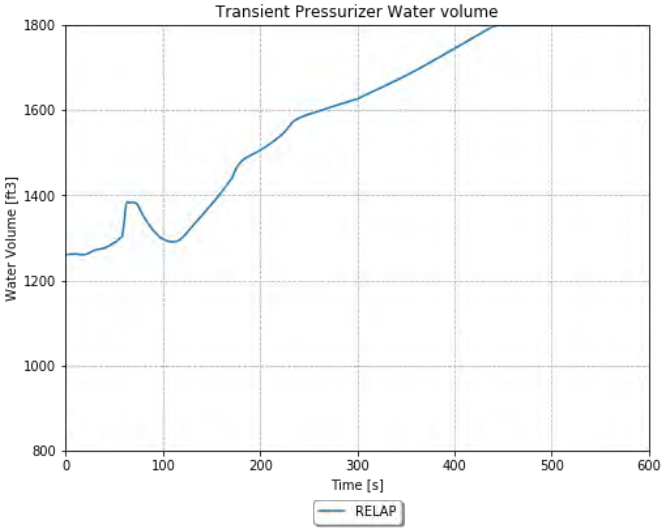

Figure 4-81. TR PRZ water volume for the LOOP scenario (e.g., the case with charging flows).

4.8.5.3 LOOP Case with Altered AFW Flows for TMI Concerns

This case is run specifically to check the PRZ water volume. The pressure is also examined for relevance to the boundary conditions.

The TR PRZ pressure is shown in Figure 4-82. This response is very similar to the base case.

The TR PRZ water volume is shown in Figure 4-83. The PRZ water volume is increased significantly above the base case, but it does not go over 1800 ft^3.

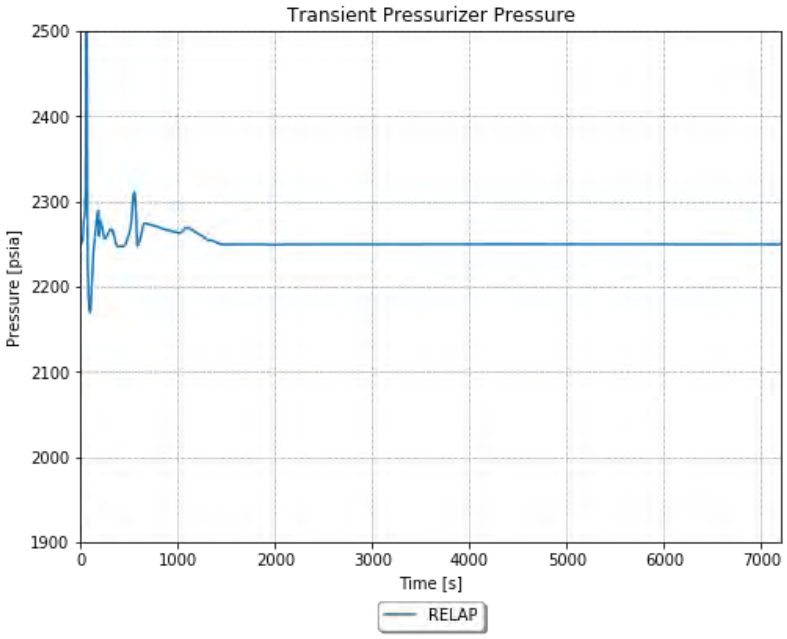

Figure 4-82. TR PRZ pressure for the LOOP scenario (e.g., the case with altered AFW flow for TMI concerns).

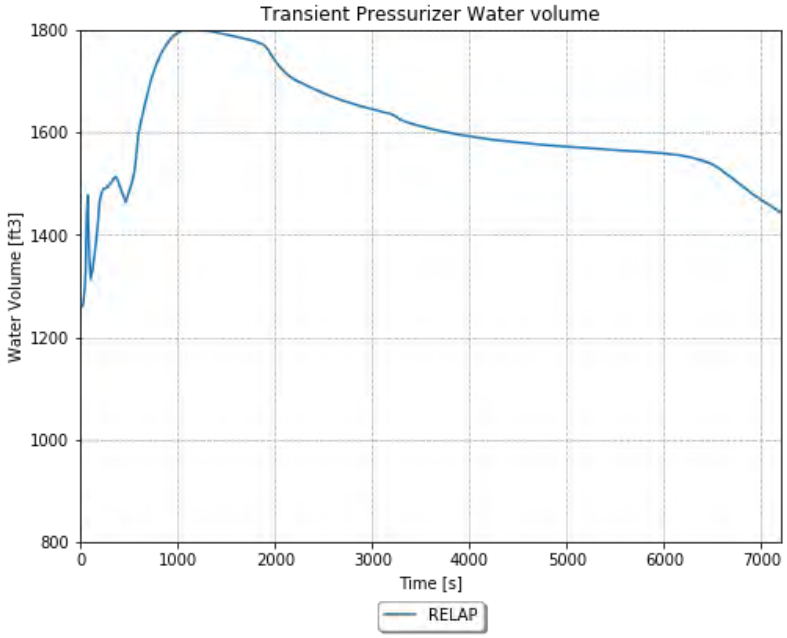

Figure 4-83. TR PRZ water volume for the LOOP scenario (e.g., the case with altered AFW flow for TMI concerns).

4.8.6 Adherence to Acceptance Criteria

The final results for the LOOP TRs are compared to the results from the FSAR and the acceptance criteria in Table 4-12. The acceptance criteria are based on the examination of the FSAR sections, as well as the applicable sections of the standard review plan.

Table 4-12. LOOP final results.

Result	FSAR (Base)	RELAP5-3D (Base)	RELAP5-3D (Charging)	RELAP5-3D (TMI)	Acceptance Criteria
Maximum RCS Pressure [psia]	~2400	2340	-	-	2750
Minimum DNBR [-]	-	< 1	-	-	1.24
Maximum PRZ Water Volume [ft^3]	~1500	~1350	~1800	~1800	~1800*

*This value is based on the input file total PRZ volume.

The RELAP5-3D simulations meet all acceptance criteria for the turbine trip scenario, except the base run briefly fails the DNBR criteria, and the run with charging SI fails the PRZ water volume criteria. Some of the potential input differences between the FSAR simulations and the RELAP5-3D simulations are discussed in the following section. These may drive some of the differences in results between the FSAR analysis and the RELAP5-3D simulations, in addition to code differences.

4.8.7 Scenario-Specific Limitations and Conditions for Usage

The following limitations apply specifically to the LOOP case:

- The reactivity feedback model has two major simplifications:
  - A single value for MDC based on an approximate average temperature is used to develop the table of reactivity vs. density, while the FSAR indicates that the MDC will vary with temperature. It is likely that this is a small effect.
  - The FSAR analysis uses a DPC, and modeling DPC is not supported by RELAP5-3D. As such, a generic FTC table from Chapter 4 was used. This is a valid source, but may cause a small deviation from the FSAR analysis.
- Due to a lack of information, the actual low-low SG level reactor trip setpoint is unknown. A value is used to duplicate the timing from the FSAR analysis.
- The turbine trip and steam flow behavior is not clearly described in the FSAR, so it was assumed to occur coincidentally with the reactor trip.
- Due to the lack of information, the base file charging flows and RWST conditions are used for this analysis. This may have a significant effect.
- The power shape used may be inconsistent with that in the FSAR analysis, but it is confirmed that the FQ value is consistent.

4.9 Chemical and Volume Control System Malfunction that Results in a Decrease in the Boron Concentration in the Reactor Coolant

Feeding primary grade water into the RCS via the reactor makeup portion of the CVCS adds reactivity to the core. Boron dilution is a manual operation under strict administrative controls with procedures calling for a limit on the rate and duration of dilution. A boric acid blend system permits the operator to match the boron concentration of reactor coolant makeup water during normal charging to that in the RCS. Even under various postulated failure modes, the CVCS design limits the potential dilution rate to a value that gives the operator sufficient time to correct the situation in a safe and orderly manner.

The opening of the primary water makeup control valve supplies water to the RCS that can dilute the reactor coolant. Inadvertent dilution can be readily terminated by closing one of the valves in the makeup pathway. In order to add makeup water to the RCS at pressure, at least one charging pump in addition to the primary makeup water pumps must be running. Normally, only one primary water supply pump is operating while the other is on standby.

The boric acid from the boric acid tank blends with primary grade water at the mixing tee; the preset flowrates of boric acid and primary grade water on the control board determine the composition.

To cover all phases of the plant operation, the reference plant FSAR analysis considers boron dilution during refueling, cold shutdown, hot shutdown, hot standby, startup, and power operation. The analysis assumes conservative values for the critical parameters (i.e., high RCS critical boron concentrations, most negative boron worth, minimum shutdown margins, and small RCS volumes). These result in conservative calculations of the time available for the operator to determine the cause of the addition and take corrective action before shutdown margin is lost. Although not explicitly stated, the analyses described for refueling, cold shutdown, hot shutdown, and hot standby appear to be done with some simplified hand calculation, and not a simulation.

It is unclear if simulations are even performed for the startup and full power operation analyses, but the following simulations are run:

- Dilution during startup or full power with manual control.
- Dilution during full power operation with automatic reactor control.

The assumptions for the automatic reactor control case are the same as the manual reactor control case, except that letdown flow is considered. This results in a change to only the TR input file. The objective of this analysis is to find the time when the RCS boron concentration drops to 300 ppm below the initial condition.

4.9.1 Scenario-Specific Inputs in the TR Input File

The TR input file is defined as follows:

- Upfront cards are included that specify this is a restart TR run, which uses the last available printout in the restart file.
- The end time is set to 3600 seconds, as this value bounds the objective time considerably (e.g., the RCS boron concentration drops by 300 ppm well before 3600 seconds). The max time step is set to 0.05 seconds, as this is a value that is reasonable for a relatively stable simulation such as this.
- The minor edits are used to specify the variables used in the plots.
- CV 405 (e.g., the reactivity controller) is listed as a constant value of 0.0 $. This is done as a placeholder for RAVEN to substitute in the actual end of the SS value of CV 405 using the RAVEN variable “ssreact.” This step is necessary to turn off the reactivity controller, but makes the SS reactivity adder persist.
- CVs 419, 420, 421, and 422 (e.g., the pump inputs) are set as constant values consistent with the end of the SS Pump Speed, and these values will be replaced by RAVEN using the variable “sspmpvel.” This causes the pumps to simply continue operating like normal SS.
- CVs 435 through 438 (e.g., the steam valve position) are changed to be functions of General Table 650. This allows them to be set to the SS valve position prior to the reactor trip or SI signal, and then close based on the specified delay and ramp times.
- CVs 459 through 462 (e.g., the MFW flow rate) are listed as constant values of 1118.9 lbm/sec, which act as a placeholder for RAVEN to substitute in the actual SS end values of CVs 459 through 462 using the RAVEN variable “ssmfw.”

- CV 472 is listed as a constant value of 0.0. This is used to turn off the SS charging flow.
- CV 473 is listed as a constant value of 0.0. This is used to turn off the SS letdown flow.
- CV 482 is listed as a constant value of 0.0. This is used to turn off the SS PRZ heater.
- Variable Trip 411 is specified so that the reactor trip occurs at the onset of the TR. This is done by setting it to be at time greater than or equal to 0.0 seconds.
- General Table 481 is specified to update the spray to kick on 10 psia above the PRZ pressure setpoint rather than the SS controls that make it come on as soon as the pressure goes above 10 psia.
- General Table 650 is listed with identical SS input values, which need to be included so the first three valve position entries can be replaced with the SS end values using the RAVEN variable "ssstmvlv." This step is necessary to turn off the steam flow controller, but allow the SS steam flow to persist.
- All four charging SI time-dependent junctions are included in the file, so that they can be set to a constant dilution flow consistent with 242 gpm.
- In the run with automatic reactor controls, the letdown valve is also included in the TR input file, so that it can be set to a constant flow rate consistent with 130 gpm.

4.9.2 Scenario-Specific RAVEN Inputs

The RAVEN distribution means are set as shown in Table 4-13. Inputs are consistent with the FSAR, as described below. Remaining inputs are assumptions not specifically mentioned in the FSAR:

- The SS conditions are set to nominal values, other than the PRZ level, which is set to 1 ft to minimize the RCS inventory, making it easier to dilute.
- The reactor trip setpoints as irrelevant, as a trip is forced at the onset of the TR.
- The MFW is ramped down over 5 seconds with a 5 second delay from the reactor trip time, while the AFW comes on 60 seconds after the reactor trip time, with a 5 second ramp up to full flow.
- The RCP motors trip 4 seconds after reactor trip.
- The charging boron concentration is set to 0 ppm.
- The MSIV is ramped down over 5 seconds with a 5 second delay from the reactor trip time.
- The RCCAs begin to drop 0.001 seconds after reactor trip.
- The initial RCS boron concentration is set to 2.1E-3 kg/kg (2100 ppm).

Table 4-13. Summary of RAVEN inputs for CVCS malfunction.

Distribution	Description	Unit	Mean
cltempdist	Cold Leg Temperature	°F	556.2
corepdist	Core Power	W	3.626E+09
fwtempdist	Feedwater Temperature	°F	448.7
hltempdist	Hot Leg Temperature	°F	620.6
przleveldist	PRZ Level	ft.	1
przpressdist	PRZ Pressure	psia	2250
rcsflowdist	RCS Volumetric Flow	gpm	93600
rcsmflodist	RCS Mass Flow	lbm/sec	9684.028
rcsmflorrdist	RCS Mass Flow in Vessel	lbm/sec	-9684.028
sgleveldist	SG Level	ft.	40.1

Distribution	Description	Unit	Mean
stmpressdist	SG Steam Pressure	psia	941
sgflowdist	SG Flow Rate	lbm/sec	1132.639
dpvessdist	Vessel Pressure Drop	psi	46.5
dphldist	Hot Leg Pressure Drop	psi	1.2
dpxldist	Crossover Leg Pressure Drop	psi	3.1
dpcldist	Cold Leg Pressure Drop	psi	3.3
dpsgdist	SG Primary Pressure Drop	psi	45.5
corbypdist	Core Bypass Flow	%	5
przphirxtdist	High PRZ Pressure Reactor Trip Setpoint	psia	2439.7
przplorxtdist	Low PRZ Pressure Reactor Trip Setpoint	psia	1714.7
przlhirxtdist	High PRZ Level Reactor Trip Setpoint	ft.	48.9
rcsflolorxtdist	Low RCS Flow Rate Reactor Trip Setpoint	lbm/sec	8425.08
sglevlorxtdist	Low SG Level Reactor Trip Setpoint	ft.	-1
mfwdeltimedist	MFW Delay Time	sec	5
mfwramptimedist	MFW Ramp Time	sec	10
afwdeltimedist	AFW Delay Time	sec	60
afwramptimedist	AFW Ramp Time	sec	65
afwflodist	AFW Flow Rate	lbm/sec	105.65
pmpmotdeldist	Pump Motor Trip Delay Time	sec	4
achfluxdist	Average Channel Maximum SS Heat Flux	BTU/sec-ft^2	99.954
hchfluxdist	Hot Channel Maximum SS Heat Flux	BTU/sec-ft^2	164.93
initreactdist	Initial Reactivity	$	0
mdcdist	Moderator Density Coefficient	Δk/g/cm^3	-0.042
accbordist	Accumulator Boron Concentration	Mass Frac	0.0019
chgbordist	Charging Boron Concentration	Mass Frac	0
accvoldist	Accumulator Water Volume	ft^3	900
acctempdist	Accumulator Temperature	°F	120
accpressdist	Accumulator Pressure	psia	200
sitrplspdist	Low Steam Pressure SI Signal	psia	800
sitrpdeldist	SI Signal Delay Time	sec	42
msivdeldist	MSIV Delay Time	sec	5
msivrampdist	MSIV Ramp Time	sec	5
rccadeldist	RCCA Delay Time	sec	0.001
rcpheatdist	RCP Heat Generation	MW	0.00001
przsafdist	PRZ Safety Valve Open Pressure	psia	2474.7
rcsbordist	RCS Initial Boron Concentration	Mass Frac	0.0021

4.9.3 Steady State Results

The steady state observations for the CVCS are explained in detail in FY-2020 [2].

4.9.4 TR Boundary Conditions

The TR boundary conditions for the CVCS are explained in detail in FY-2020 [2].

4.9.5 TR Results

The RELAP5-3D results are compared to each other in the paragraphs below, as there are no FSAR results given, other than the RCS dilution time. Note that the figures labeled with -A are for manual reactor control and the figures labeled with -B are for automatic reactor control.

The TR PRZ pressure is shown in

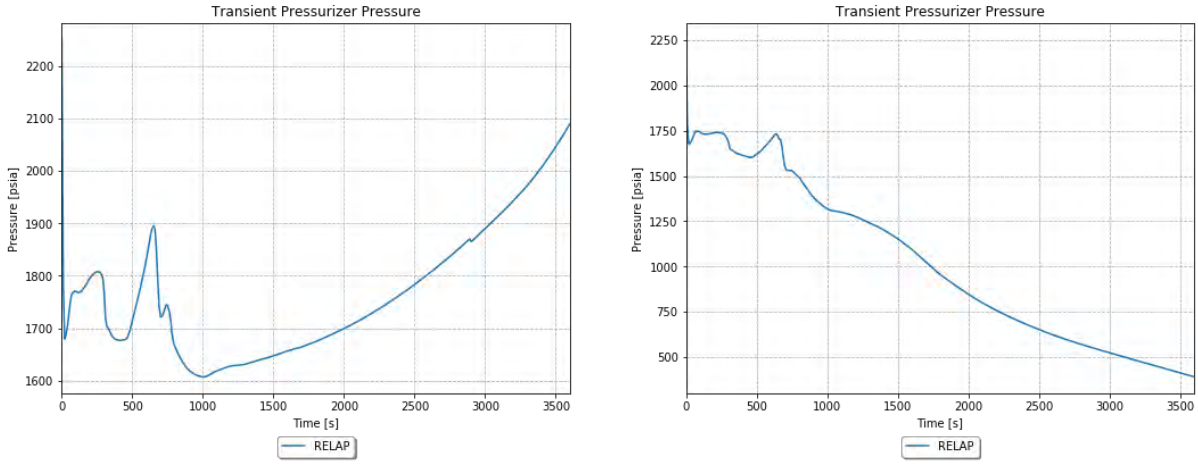

A **B**

Figure 4-84-A and

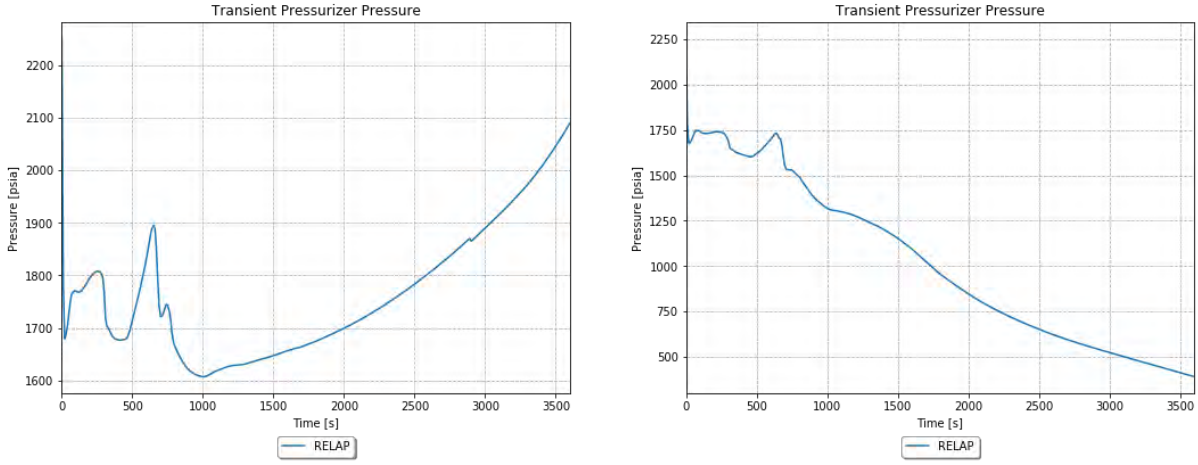

A **B**

Figure 4-84-B. The RELAP5-3D run with manual reactor control, as shown in

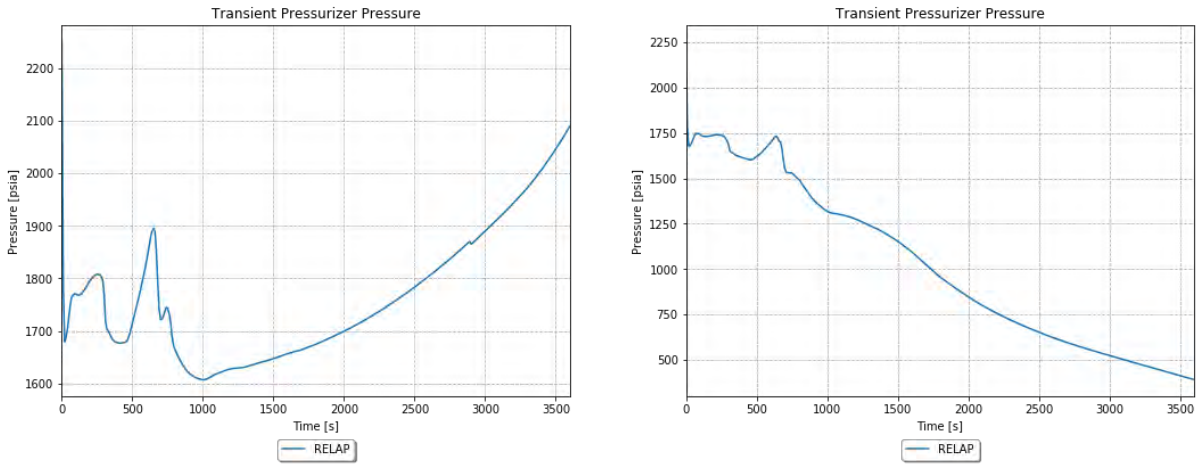

A **B**

Figure 4-84-A, has significant depressurization early in the TR. However, as the PRZ begins to refill, the pressure starts to rise again. The RELAP5-3D run with automatic reactor control, as observed in

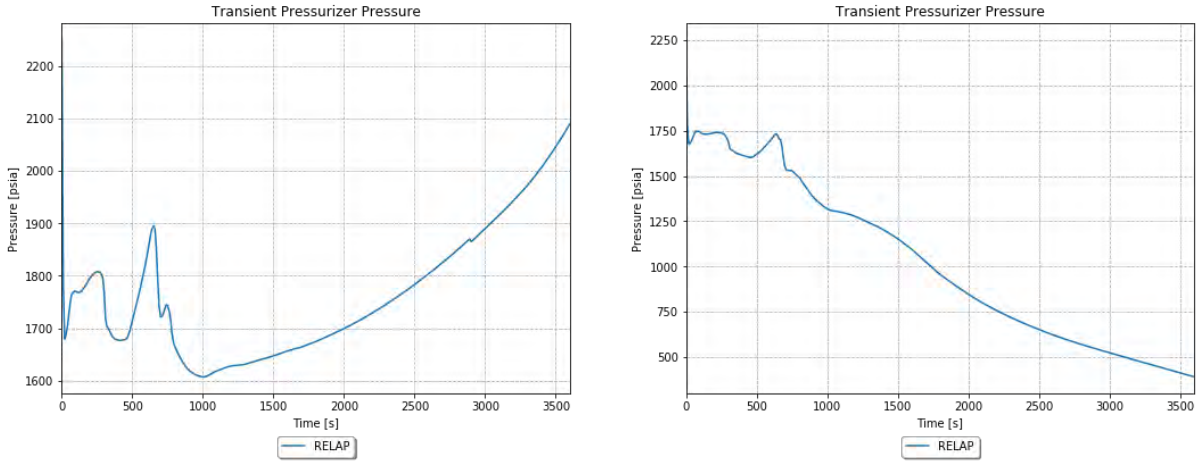

A **B**

Figure 4-84-B, depressurizes consistently throughout the TR, due to the letdown flow.

The TR core power as a fraction of the nominal power is shown in

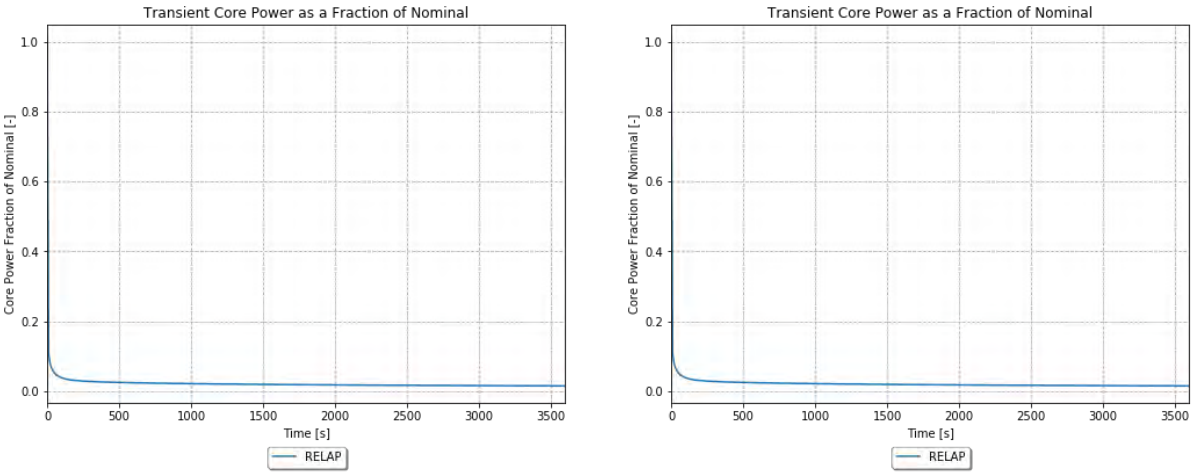

A **B**

Figure 4-85-A and

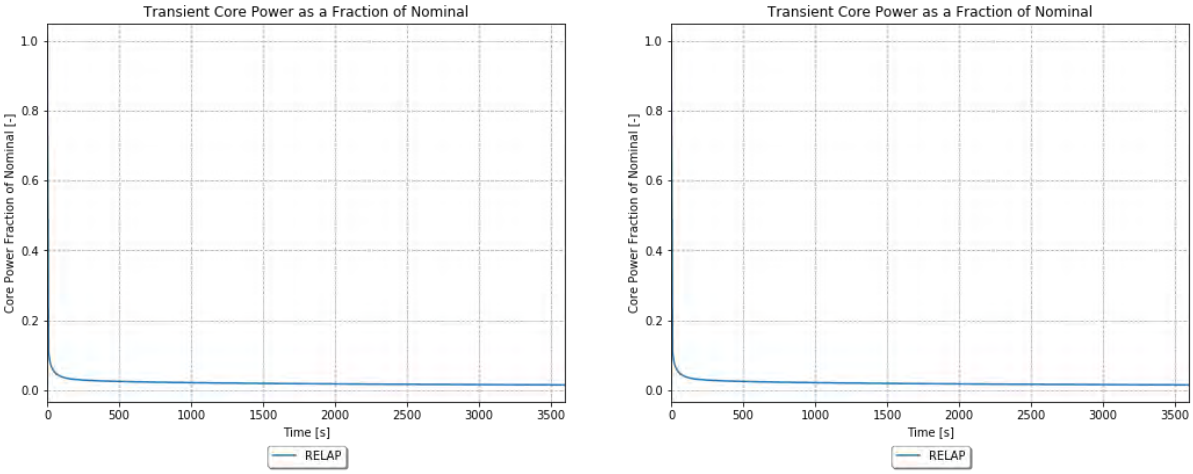

A **B**

Figure 4-85-B. The RELAP5-3D runs have a similar core power TR, which show a standard reduction from operating power to just decay heat.

The TR maximum clad temperature is shown in

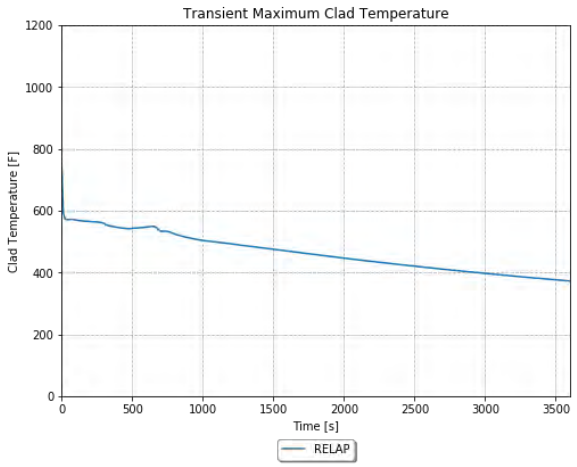

A

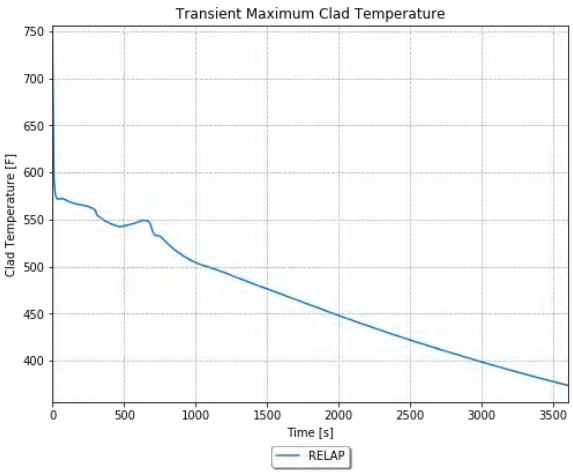

B

Figure 4-86-A and

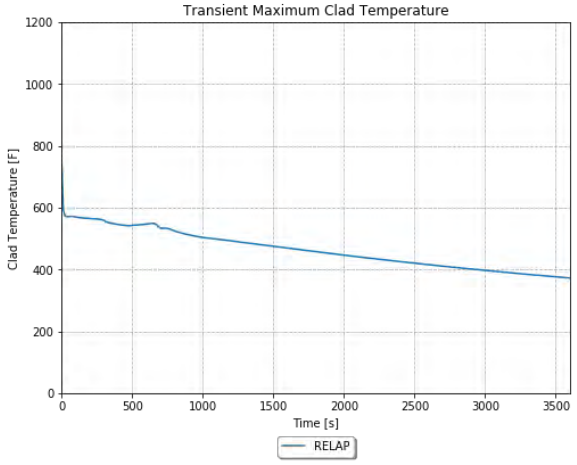

A

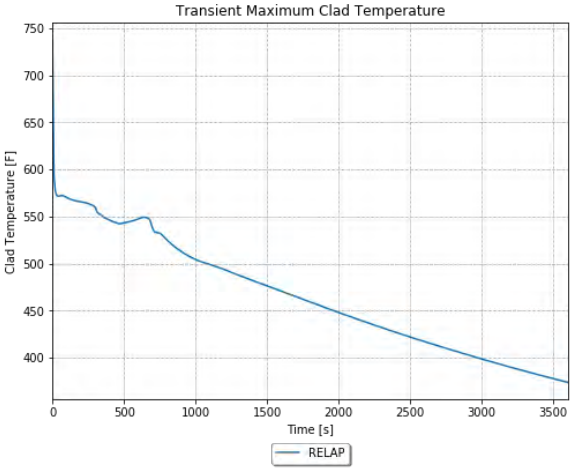

B

Figure 4-86-B, where both runs have a consistent reduction in peak temperature.

The TR cladding oxidation at the peak power location of the hot rod is shown in

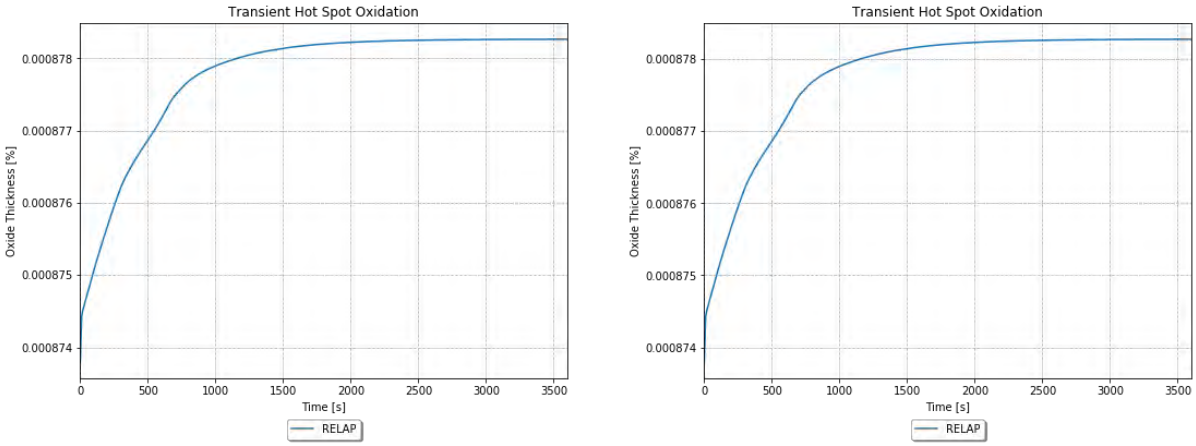

A **B**

Figure 4-87-A and

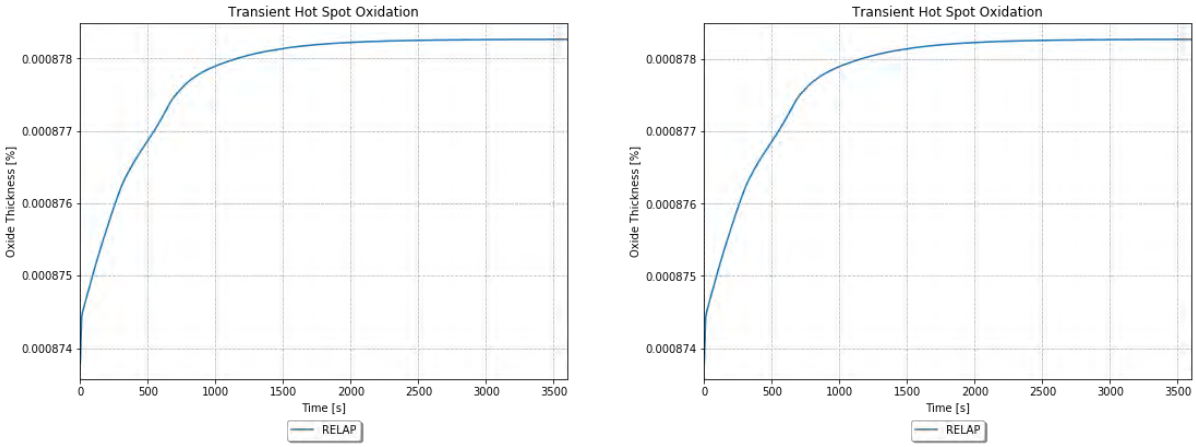

A **B**

Figure 4-87-B. The RELAP5-3D runs both experience consistent and negligible oxidation.

The TR SG pressure is shown in

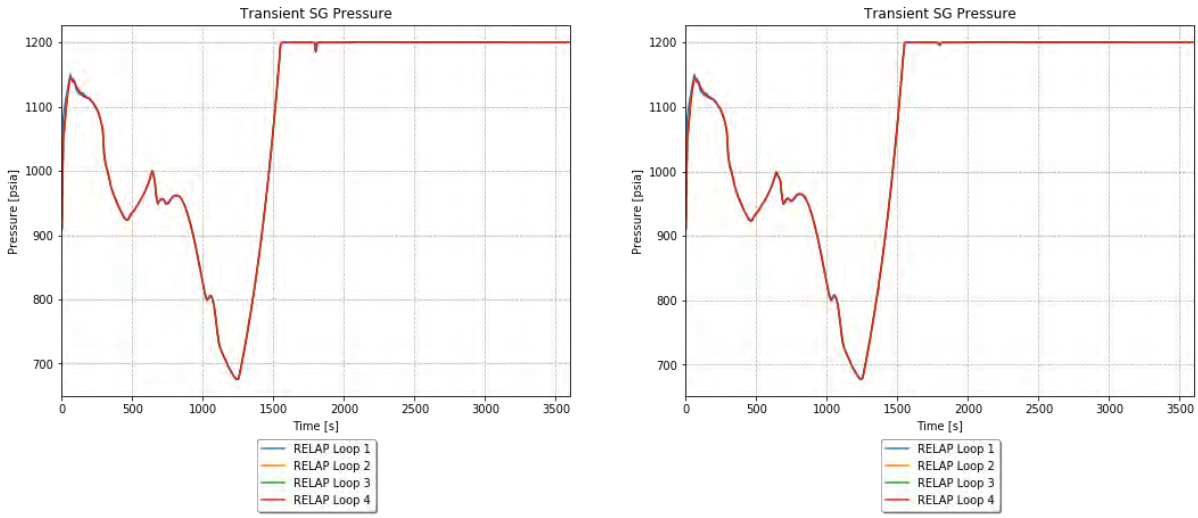

A **B**

Figure 4-88-A and

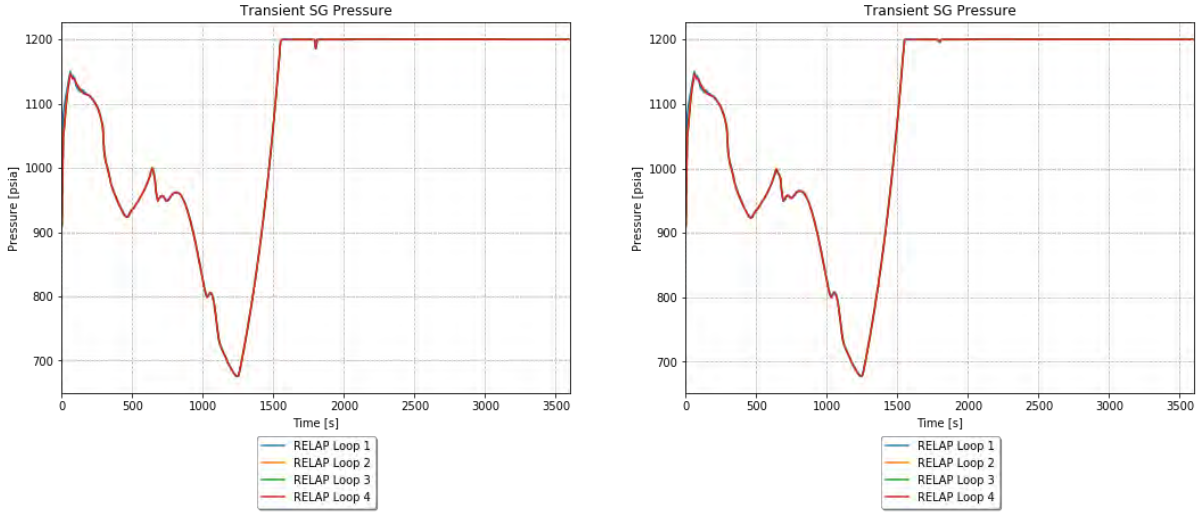

A **B**

Figure 4-88-B. The RELAP5-3D runs both experience an initial large decrease in steam pressure, likely due to the reduction in heat from the core. However, at about 1200 seconds, the pressure starts rapidly increasing. This is presumably due to the continuous operation of the AFW.

The TR PRZ water volume is shown in

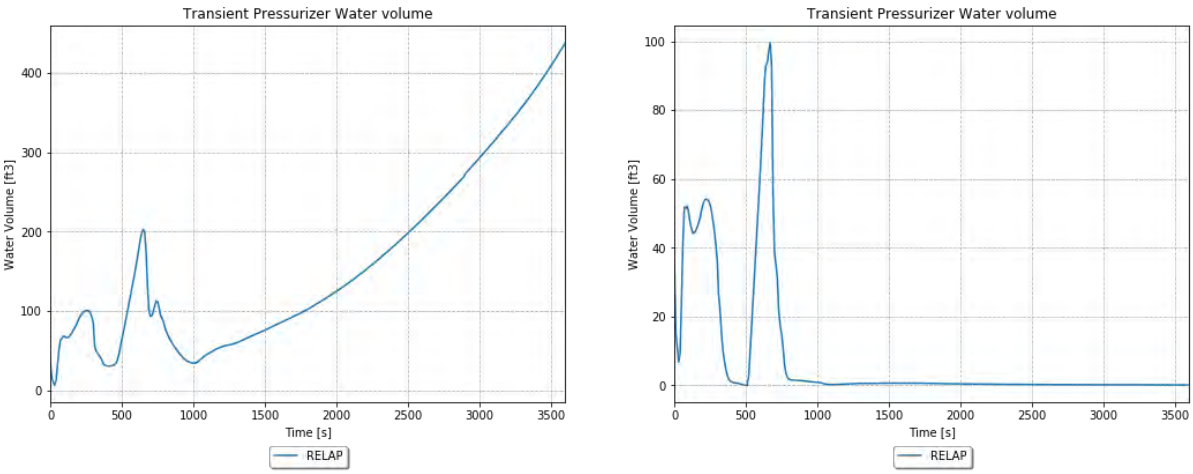

A **B**

Figure 4-89-A and

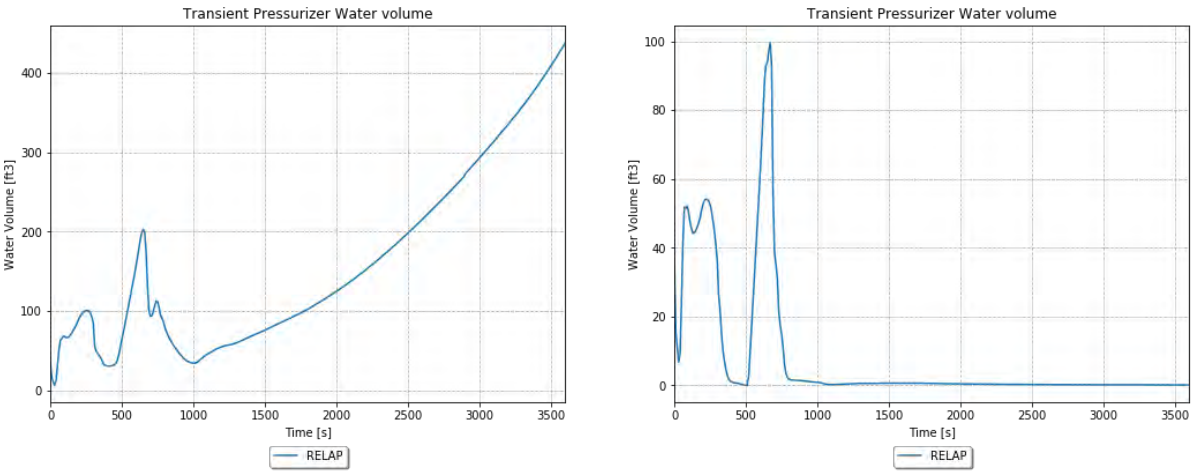

A **B**

Figure 4-89-B. The RELAP5-3D run with manual reactor control, as shown in

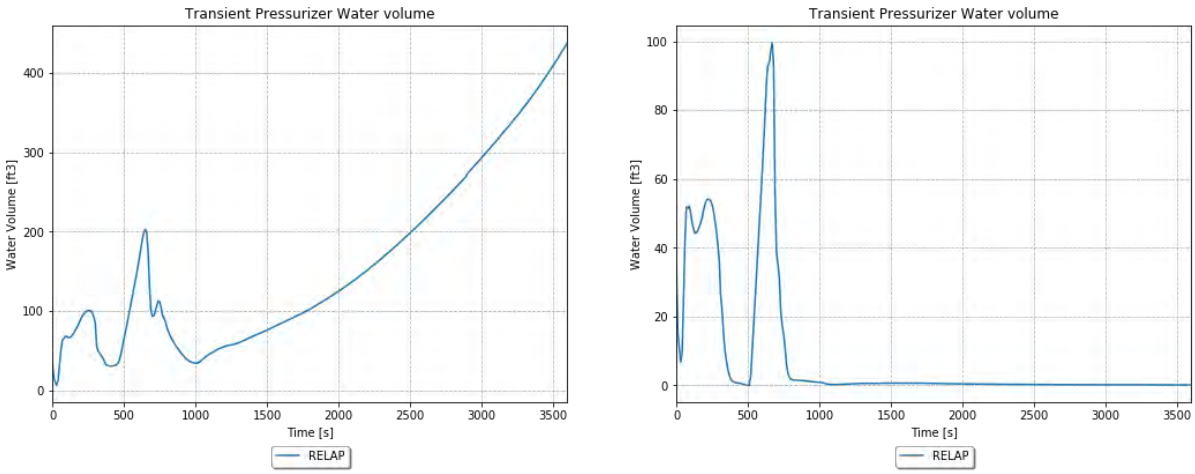

A **B**

Figure 4-89-A, has minimal water volume early in the TR, but eventually begins to refill. The RELAP5-3D run with automatic reactor control, as observed in

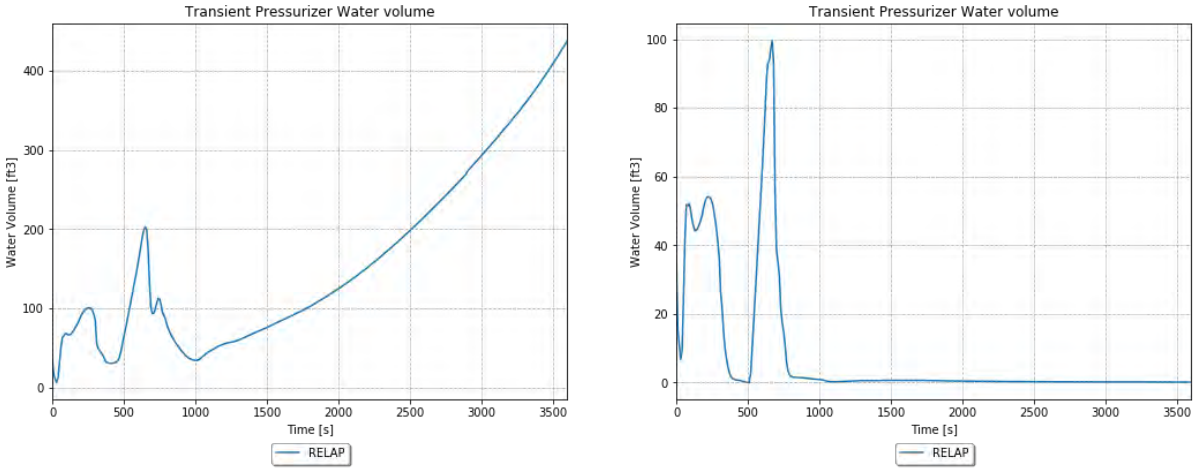

A **B**

Figure 4-89-B, has a similar amount of water volume at the beginning, but quickly becomes insignificant. The water volume stays minimal for the rest of the simulation due to the continuous letdown flow.

The TR core boron concentration and critical concentration is shown in

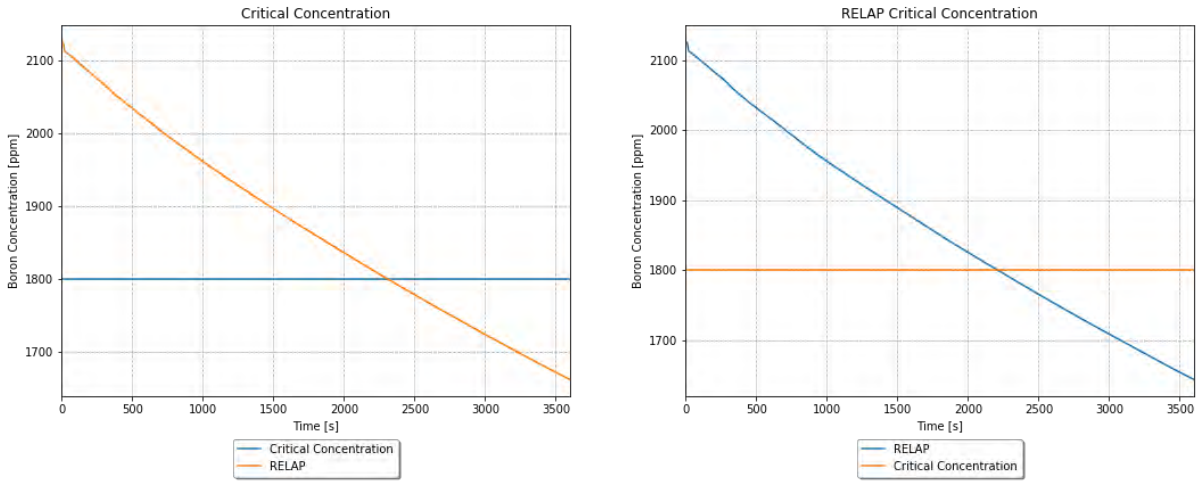

A **B**

Figure 4-90-A and

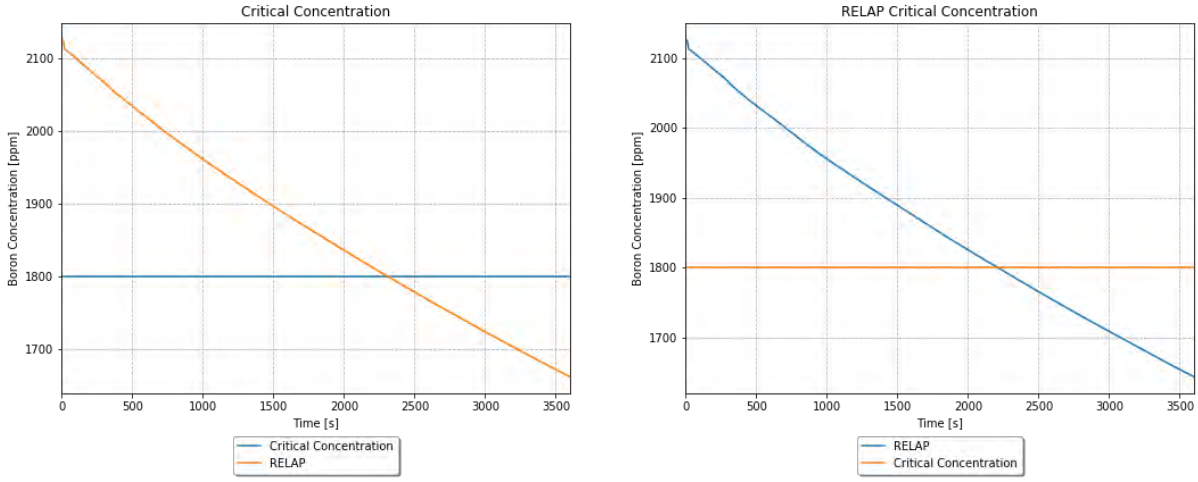

A **B**

Figure 4-90-B. The RELAP5-3D run with manual reactor control, as shown in

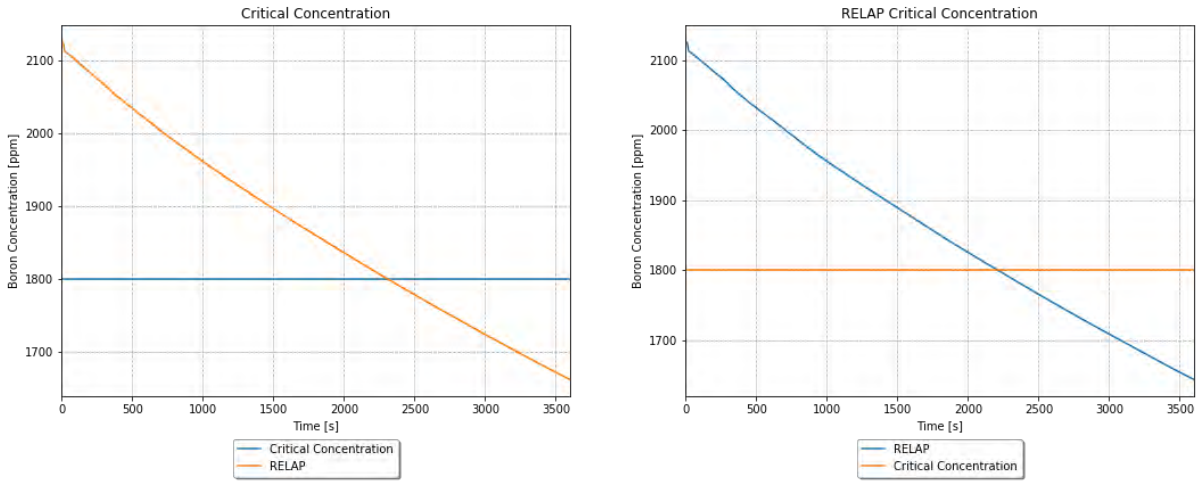

A **B**

Figure 4-90-A, crosses the critical concentration line at about 2300 seconds. The RELAP5-3D run with manual reactor control, as observed in

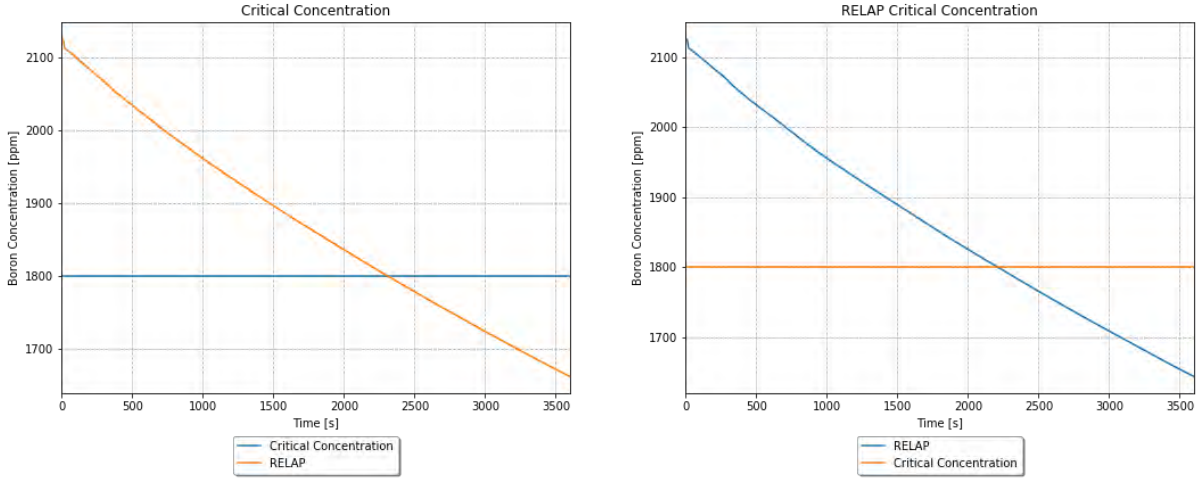

A **B**

Figure 4-90-B, crosses the critical concentration line at about 2200 seconds.

The TR DNBR is shown in

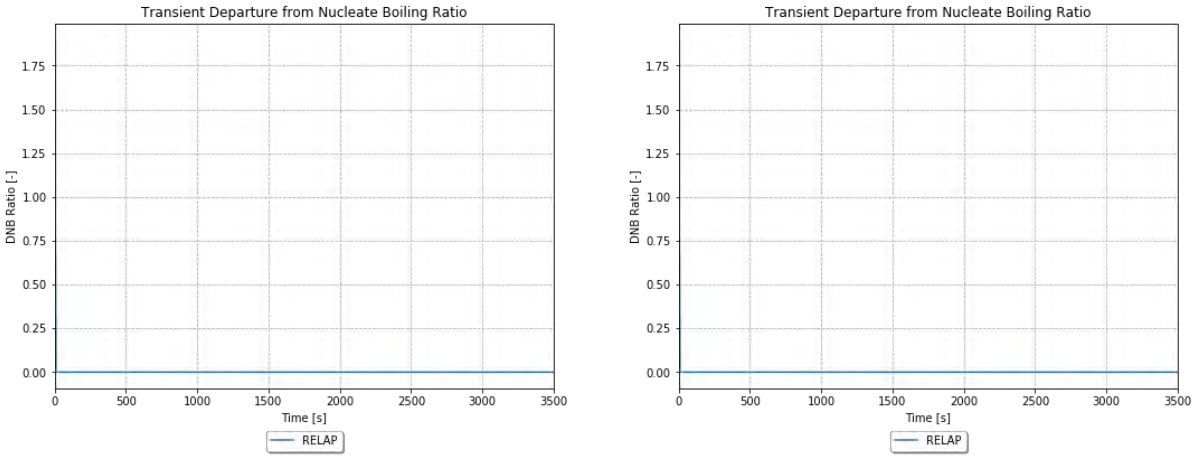

A **B**

Figure 4-91-A and

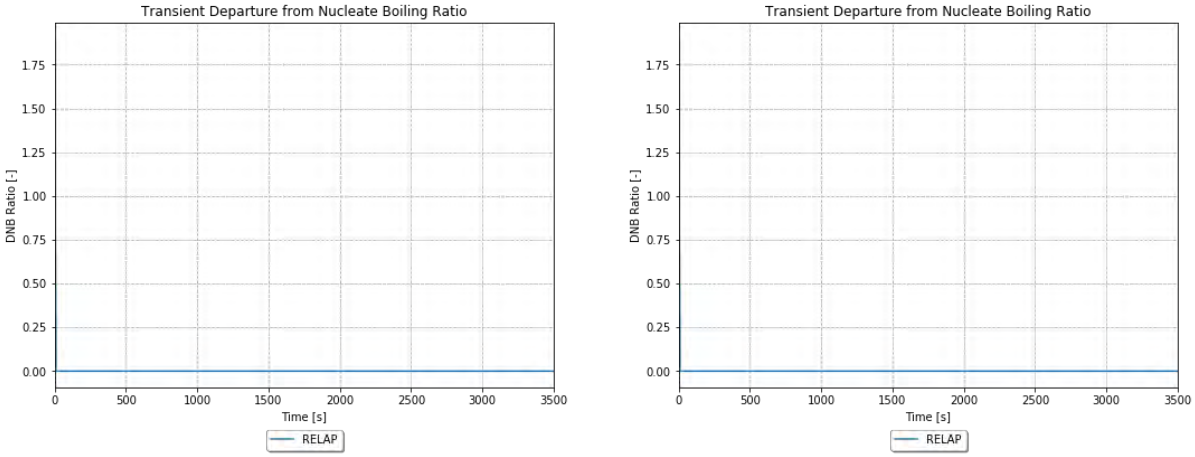

A **B**

Figure 4-91-B, where both runs have a consistent DNBR of 0 throughout the TRs, which is interpreted to mean a very high value.

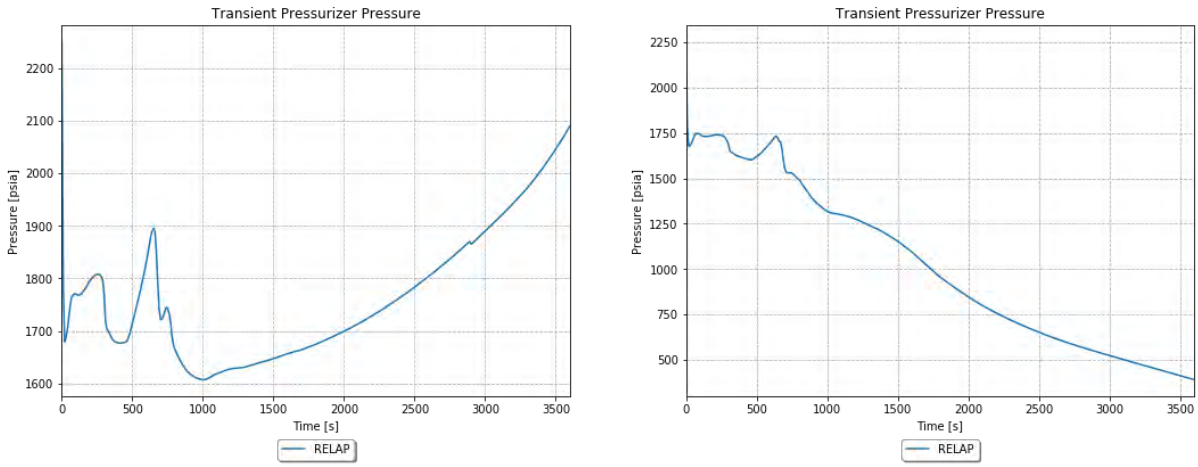

A **B**

Figure 4-84. TR PRZ pressure for the CVCS malfunction scenario (e.g., both manual and automatic controls).

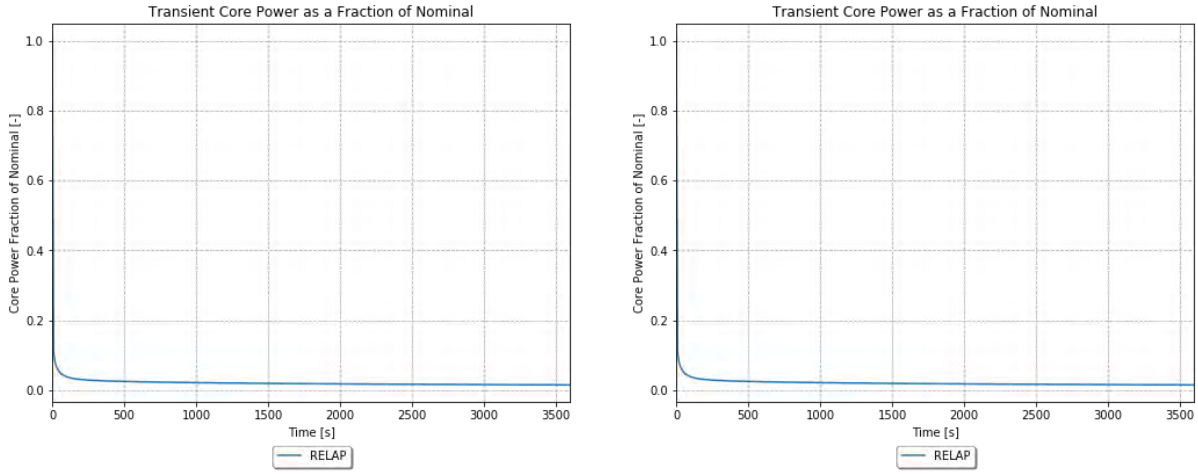

A **B**

Figure 4-85. TR core power as a fraction of the nominal power for the CVCS malfunction scenario (e.g., both manual and automatic controls).

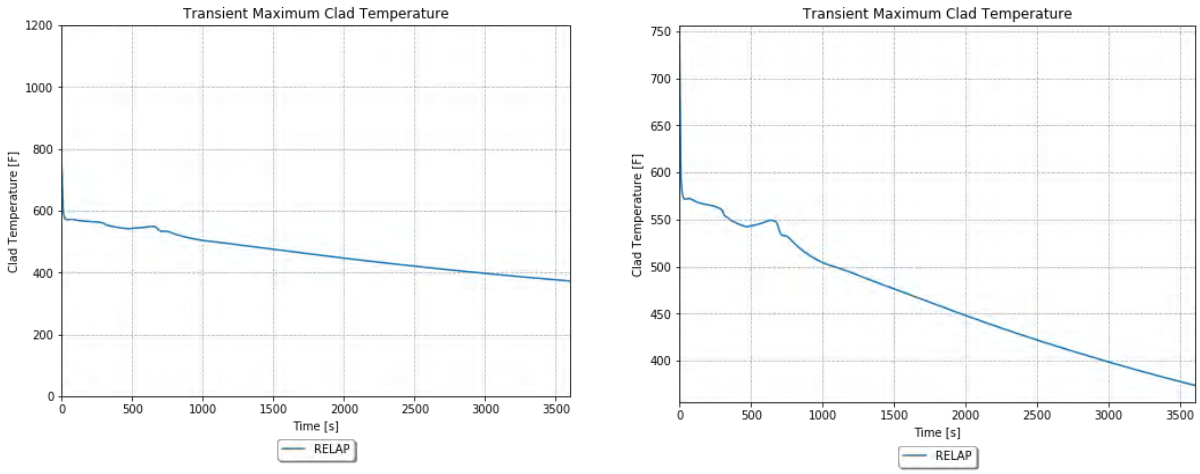

A **B**

Figure 4-86. TR maximum clad temperature for the CVCS malfunction scenario (e.g., both manual and automatic controls).

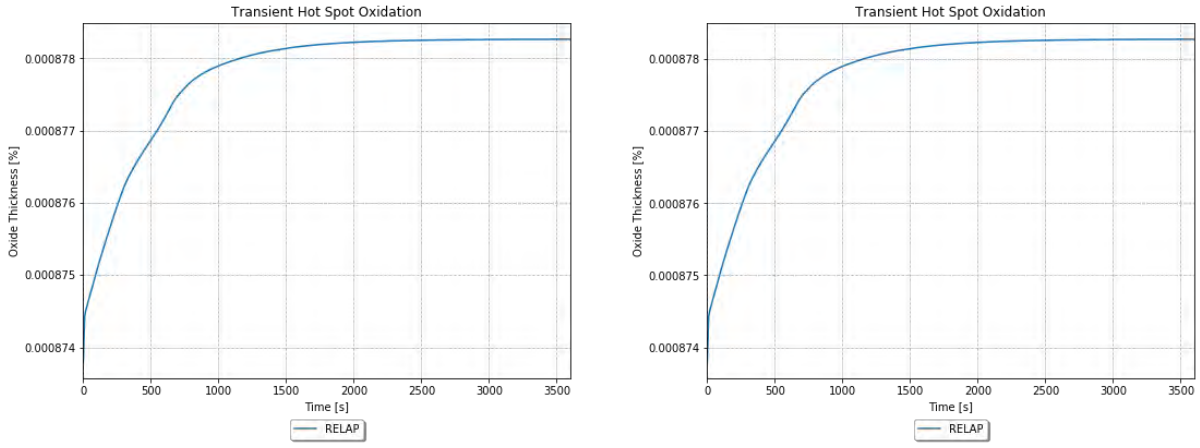

A **B**

Figure 4-87. TR cladding oxidation at the peak power location for the CVCS malfunction scenario (e.g., both manual and automatic controls).

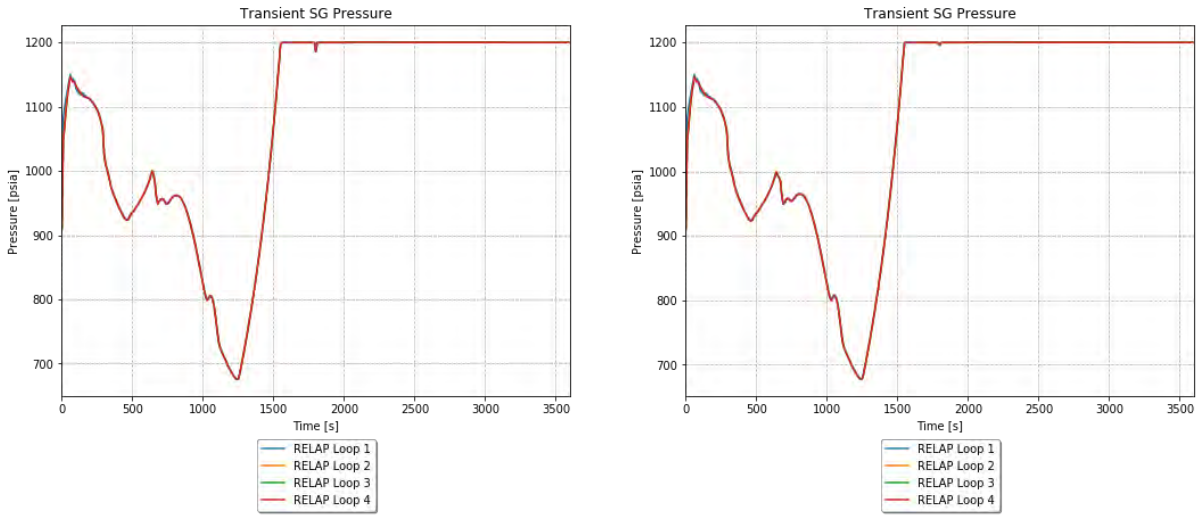

A **B**

Figure 4-88. TR SG pressure for the CVCS malfunction scenario (e.g., both manual and automatic controls).

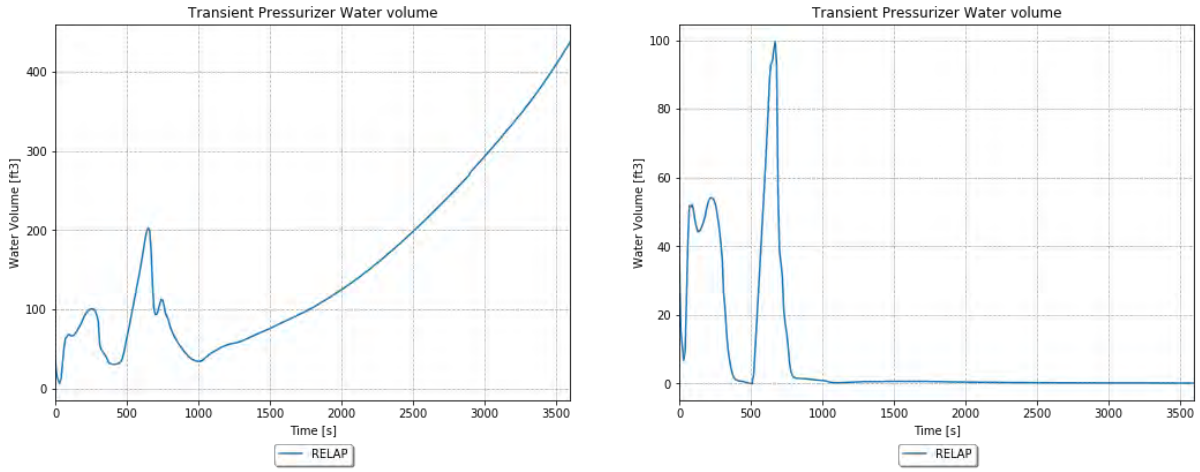

A **B**

Figure 4-89. TR PRZ water volume for the CVCS malfunction scenario (e.g., both manual and automatic controls).

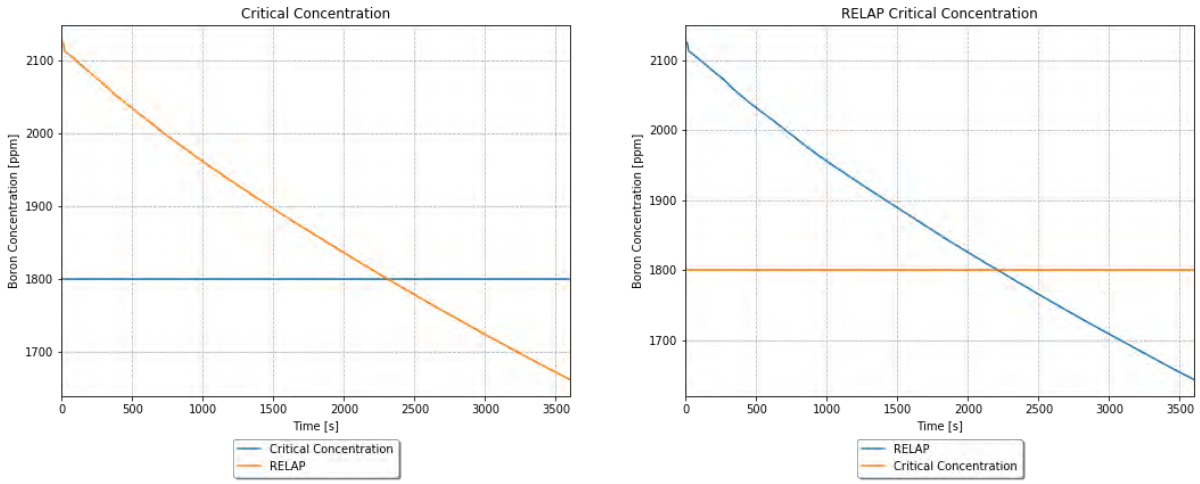

A **B**

Figure 4-90. TR core boron concentration for the CVCS malfunction scenario (e.g., both manual and automatic controls).

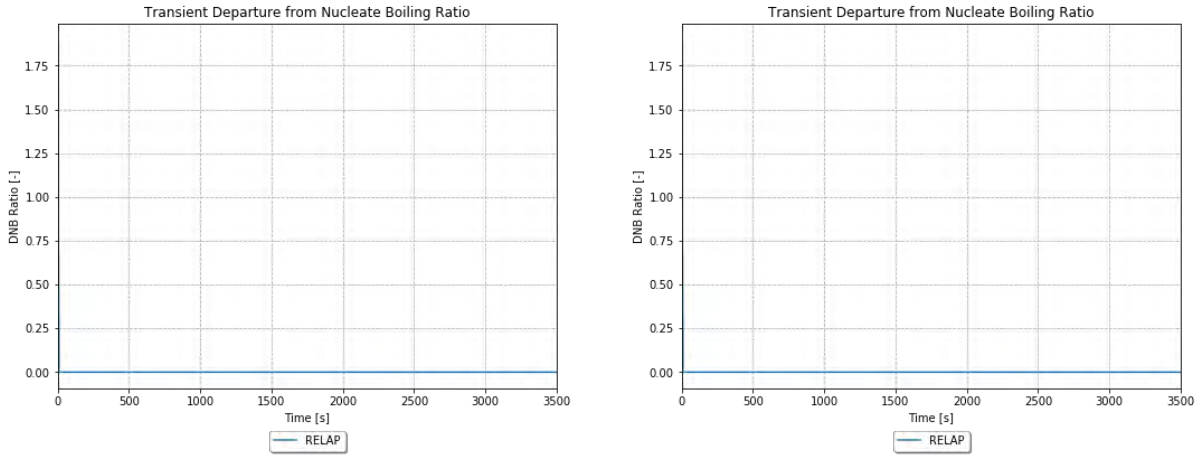

A **B**

Figure 4-91. TR DNBR for the CVCS malfunction scenario (e.g., both manual and automatic controls).

4.9.6 Adherence to Acceptance Criteria

The final results for the CVCS malfunction are compared to the results from the FSAR and the acceptance criteria in Table 4-14. The acceptance criteria are based on examination of the FSAR sections, and the applicable sections of the standard review plan.

Table 4-14. CVCS malfunction final results.

Result	FSAR (Manual)	FSAR (Automatic)	RELAP5-3D (Manual)	RELAP5-3D (Automatic)	Acceptance Criteria
Maximum RCS Pressure [psia]	-	-	2090	1750	2750
Minimum DNBR [-]	-	-	∞	∞	1.24
Minimum Critical Concentration Time [sec]	1860	3560	~2300	~2200	900

4.9.7 Scenario-Specific Limitations and Conditions for Usage

The following limitations apply specifically to the boron dilution due to the CVCS malfunction case:

- The power assumptions associated with the dilution during startup analysis is not described in the FSAR, so this case is not explicitly simulated. It is instead considered to be covered by the full power with manual reactor control case, since all assumptions other than power are apparently the same.
- The minimum RCS volume is not modeled exactly, as the 10% tube plugging would require SS changes, and the PRZ needs a small amount of water for the SS control logic to function.
- Most of the assumptions used for the RCS and SG control are not mentioned in the FSAR, so assumed conditions were created. This likely affects the simulation, potentially significantly.

4.10 Loss of Coolant Accidents

A LOCA is the result of a pipe rupture of the RCS pressure boundary. For the analyses reported here, a major pipe break (e.g., large break, [LB]) is defined as a rupture with a total cross-sectional area equal to or greater than 1.0 ft^2. This event is considered a limiting fault—an ANS Condition IV event—in that it is not expected to occur during the lifetime of the plant, but is postulated as a conservative design basis.

A minor pipe break (e.g., small break, [SB]), as considered in this subsection, is defined as a rupture of the reactor coolant pressure boundary with a total cross-sectional area less than 1.0 ft^2, in which the normally operating charging system flow is not sufficient to sustain PRZ level and pressure. This is considered a Condition III event in that it is an infrequent fault that may occur during the life of the plant.

Both the limiting LB and SB cases are simulated.

4.10.1 LBLOCA Development Process

From FY-2020 activity, the LBLOCA was found to be the most limiting case and would not even successfully run without a huge reverse form loss applied at the break nozzle in the TR input. The updated RELAP5-3D MULTID model shows huge improvements, but the case still failed when the form loss nominal value of the four-junction connection point, 1.783, was applied. The case failed at ~43 seconds and it was due to the cladding temperature being too high. This is due to the core becoming uncovered around the failure time. RELAP5-3D BEPU version allows the manipulation of the interfacial friction using a multiplier input. It is important to note that this value varies globally, but by reducing the value and thus reducing the interfacial drag coefficient, downcomer liquid penetration should be easier to achieve. While the probability of liquid reaching to the lower plenum and core region is increased, the ability to effectively cover the core is in question due to the multiplier being applied in the core components. Reducing the drag here may effectively hold the liquid in the lower cells, and therefore, cause high cladding temperatures in the higher axial levels.

The model was rerun using the RELAP5-3D BEPU version with an interfacial friction value set to 0.5 and 0.1. Both cases failed due to high cladding temperature values. This results from an increase in reactivity. Because the fidelity of this model is not deemed sufficient to predict reflood re-criticality, the reactor is tripped, and control rods are used at the beginning of the TR. Therefore, the reactivity is more negative, and the power is reduced immediately, whereas the original model saw a slower decrease, and in addition, no power spikes are experienced. The same two RELAP5-3D BEPU version cases were rerun, the 0.5 case fails at 102 seconds and the 0.1 case runs successfully. Therefore, for this section, the 0.1 case will be used for the discussion. All three updates (e.g., MULTID, decrease interfacial friction, attribute control rods) were required for the LBLOCA event. It is noted that through separate investigation in relevant integral effect tests (IETs), a multiplier on the order of 0.1 may be appropriate; however, this requires additional investigation.

4.10.2 Scenario-Specific Inputs in the TR Input File

The TR input file is defined as follows:

- Upfront cards are included that specify this is a restart TR run, which uses the last available printout in the restart file.
- The end time is set to 300 seconds for LBLOCA and 4000 seconds for small break loss of coolant accident (SBLOCA), consistent with the analysis in the reference plant FSAR. For the LBLOCA, the max time step is set to 0.001 seconds due to the large instability of the actual event. It was found reducing the max time step was largely beneficial to the simulation. The max time step for the SBLOCA is set to 0.05 seconds, as this is a value that is reasonable for a relatively stable simulation such as this.
- The minor edits are used to specify the variables used in the plots.
- CV 405 (e.g., the reactivity controller) is listed as a constant value of 0.0 $. This is done as a placeholder for RAVEN to substitute in the actual end of SS value of CV 405 using the RAVEN variable “ssreact.” This step is necessary to turn off the reactivity controller, but make the SS reactivity adder persist.
- The pump inputs are specified as follows. Variable Trips 450 through 453 are set to be false immediately, so the motor trip takes precedence. This is done by setting them to trip at time greater than or equal to 1E9 seconds in the TR input file. In addition, CVs 419 through 422 (e.g., the pump speeds) are specified as a constant value that is replaced using the RAVEN variable “sspmpvel.” It is noted that the specifications of these CVs are not necessary, as Trips 450 through 453 immediately make them not be used, but they are left in as they have no negative effect.
- CVs 435 through 438 (e.g., the steam valve position) are changed to be functions of General Table 650. This allows them to be set to the SS valve position prior to the reactor trip or SI signal, and then close based on the specified delay and ramp times.
- CVs 459 through 462 (e.g., the MFW flow rate) are listed as constant values of 1118.9 lbm/sec. This is done as a placeholder for RAVEN to substitute in the actual end of SS values of CVs 459 through 462 using the RAVEN variable “ssmfw.”
- CV 472 is listed as a constant value of 0.0. This is used to turn off the SS charging flow.
- CV 473 is listed as a constant value of 0.0. This is used to turn off the SS letdown flow.
- CV 482 is listed as a constant value of 0.0. This is used to turn off the SS PRZ heater.
- CV 483 is listed as a constant value of 0.0. This is used to turn off the SS PRZ spray.
- CV 641 is listed as a constant value of 0.0. This is used to disable the PRZ PORV.
- Trip 470 is listed to trip at a time greater than or equal to 2 seconds for LBLOCA and 28 seconds for SBLOCA. This is defined this way because the FSAR analyses use the low PRZ pressure SI signal, but it is unknown what the setpoint is. As a result, the times of the trips from the FSAR analyses are forced.
- General Table 640 is listed with values identical to the SS input. This input does not necessarily need to be here, but it is generically listed in the TR input files to allow the analyst to change the trip used for MFW.
- General Table 650 is listed with values identical to the SS input. This input needs to be here so that the first three valve position entries in the table can be replaced with the end of the SS values using the RAVEN variable “ssstmvlv.” This step is necessary to turn off the steam flow controller, but have the SS steam flow persist.

- The hydraulic components are listed as follows for LBLOCA:
  - Component 417 (e.g., the cold leg nozzle for the broken loop) is included in the file. This component is included so that the reverse loss coefficient can be varied. In FY-2020, it was found that a non-physical value (e.g., 500) was required to allow the run to execute [2]. With the RELAP5-3D MULTID update, this value was found to be not needed, but higher than true values were still required.
  - The interfacial friction multiplier is varied using the BEPU version of RELAP5-3D for the LBLOCA case. This value must be entered during the steady state portion, but it is expected to largely impact only the TR portion of the run. The value is set to 0.1, but it must be noted that this is a global modifier; therefore, other components such as the core components will have unwanted effects from a low interfacial drag coefficient. As such, an updated version of the BEPU version is requested so that the interfacial friction can be varied in specific locations (mainly the downcomer portion of the MULTID).
  - Components 144, 244, 344, and 444 are included to set the TR-specific SI flows.
  - Component 461 is included to set the break area and discharge coefficients. Note that this component is used to connect the pump-side cold leg to the break, using the area of a single cold leg.
  - Component 415 is included to change the connection from the pump-side cold leg to the vessel side cold leg to instead be from the vessel side cold leg to the break. The break area and discharge coefficients are set consistent with Component 461. Note that this change and the last one was necessary because the base model was set up as a split break type, and a double-ended guillotine (DEG) break was desired.
  - Component 462 is included to set the time-dependent pressure boundary for the break. The boundary conditions are set using pressure and quality. A constant quality of 1 is set so that there is zero chance of liquid ending from this location. This is set based on the FSAR analysis.
- The hydraulic components are listed as follows for the SBLOCA:
  - Components 144, 244, 344, and 444 are included to set the TR-specific SI flows. Note that these are different from the LBLOCA.
  - Component 461 is included to trip open and set the break area. Note that the break area used is different from the FSAR analysis, because the depressurization was much too fast using an area consistent with the FSAR analysis.

4.10.3 Scenario-Specific RAVEN Inputs

The RAVEN distribution means are set as shown in Table 4-15. The inputs are consistent with the FSAR, as described below. The remaining inputs are assumptions that are not specifically mentioned in the FSAR.

- The SS conditions are generally set to analysis-specific values from the FSAR.
- The PRZ low pressure reactor trip setpoint is set to 1884.7 psia.
- The pump motors for the non-locked rotor loops trip 0.1 seconds after reactor trip, to trigger immediate coast-down.
- The SI delay time is set to 40 seconds.

- The RCCA behavior is set as follows:
  - For LBLOCA, the delay time to rod drop is set to 1.0e9 seconds, so that rods are not credited. Using this method, the void effects were not enough to force a large enough negative reactivity and the simulation saw cladding temperature failures. Therefore, for the current LBLOCA model, rods are credited, and the delay time is set to 1.0 seconds.
  - For SBLOCA, the delay time is set to 1.0 seconds.
- The MDC is set to allow shutdown by voiding.
- The MSIV is immediately ramped down over 1 second from the reactor trip time.
- The MFW is set to ramp down over 5 seconds after reactor trip or SI signal, and then the AFW ramps up over 5 seconds after the MFW is off.

Table 4-15. Summary of RAVEN inputs for LOCA.

Distribution	Description	Unit	Mean
cltempdist	Cold Leg Temperature	°F	537.6
corepdist	Core Power	W	3.636E+09
fwtempdist	Feedwater Temperature	°F	448.7
hltempdist	Hot Leg Temperature	°F	603.8
przleveldist	PRZ Level	ft.	29.4
przpressdist	PRZ Pressure	psia	2250
rcsflowdist	RCS Volumetric Flow	gpm	9.36E+04
rcsmflodist	RCS Mass Flow	lbm/sec	9684.028
rcsmflorrdist	RCS Mass Flow in Vessel	lbm/sec	-9684.028
sgleveldist	SG Level	ft.	40.1
stmpressdist	SG Steam Pressure	psia	817
sgflowdist	SG Flow Rate	lbm/sec	1126.389
dpvessdist	Vessel Pressure Drop	psi	47.8
dphldist	Hot Leg Pressure Drop	psi	1.3
dpxldist	Crossover Leg Pressure Drop	psi	3.4
dpcldist	Cold Leg Pressure Drop	psi	3.6
dpsgdist	SG Primary Pressure Drop	psi	41.3
corbypdist	Core Bypass Flow	%	5
przphirxtdist	High PRZ Pressure Reactor Trip Setpoint	psia	2514.7
przplorxtdist	Low PRZ Pressure Reactor Trip Setpoint	psia	1884.7
przlhirxtdist	High PRZ Level Reactor Trip Setpoint	ft.	48.9
rcsflolorxtdist	Low RCS Flow Rate Reactor Trip Setpoint	lbm/sec	8425.08
sglevlorxtdist	Low SG Level Reactor Trip Setpoint	ft.	0.1
mfwdeltimedist	MFW Delay Time	sec	0.001
mfwramptimedist	MFW Ramp Time	sec	5
afwdeltimedist	AFW Delay Time	sec	5.001
afwramptimedist	AFW Ramp Time	sec	10
afwflodist	AFW Flow Rate	lbm/sec	105.65

Distribution	Description	Unit	Mean
pmpmotdeldist	Pump Motor Trip Delay Time	sec	0.1
achfluxdist	Average Channel Maximum SS Heat Flux	BTU/sec-ft^2	99.954
hchfluxdist	Hot Channel Maximum SS Heat Flux	BTU/sec-ft^2	164.93
initreactdist	Initial Reactivity	$	0
mdcdist	Moderator Density Coefficient	Δk/g/cm^3	0.042
accbordist	Accumulator Boron Concentration	Mass Frac	1.90E-03
chgbordist	Charging Boron Concentration	Mass Frac	2.40E-03
accvoldist	Accumulator Water Volume	ft^3	900
acctempdist	Accumulator Temperature	°F	120
accpressdist	Accumulator Pressure	psia	611.3
sitrplspdist	Low Steam Pressure SI Signal	psia	100
sitrpdeldist	SI Signal Delay Time	sec	40
msivdeldist	MSIV Delay Time	sec	0.001
msivrampdist	MSIV Ramp Time	sec	0.1
rccadeldist	RCCA Delay Time	sec	1.0 (SB) 1.0 (LB)
rcpheatdist	RCP Heat Generation	MW	1.00E-05
przsafdist	PRZ Safety Valve Open Pressure	psia	2500
rcsbordist	RCS Initial Boron Concentration	Mass Frac	0

4.10.4 Steady State Results

The steady state observations for the LOCA cases are explained in detail in FY-2020 [2].

4.10.5 TR Boundary Conditions

The TR boundary conditions for the LOCA cases are explained in detail in FY-2020 [2].

4.10.6 TR Results

The LBLOCA results from FY-2020 showed that the model was not able to accurately simulate LBLOCA type events. The results from the 1D model and the model with the MULTID component are shown below.

4.10.6.1 LBLOCA

The TR PRZ pressure is shown in Figure 4-92. The FSAR run depressurizes much more rapidly than the RELAP5-3D run because of the change in the broken loop cold leg nozzle reverse loss coefficient. The updated model shows an improvement in the depressurization and RELAP5-3D value coming much closer to the FSAR results.

The TR core power as a fraction of nominal is shown in Figure 4-93. The FSAR run shuts down much more rapidly due to two factors. The first is that the 1971 decay heat model exhibits a normal exponential decay that accounts for some residual fission, while RELAP5-3D explicitly calculates residual fission. This is amplified by the fact that the RELAP5-3D run depressurizes much more slowly, and thus shuts down the residual fissions via voiding much more slowly. This is a known issue that should be corrected downstream when the depressurization is fixed, although some amount of slower

decrease may persist due to the calculation of residual fission. The updated model currently has control rods drop with a delay time of 1 sec. This change is likely improving the rapid decrease in power as well.

The TR maximum clad temperature is shown in Figure 4-94. The FSAR run shows a very typical LB TR, with a period of distinct blowdown heatup followed by some cooling, then a rapid heatup during refill, and a more gradual heatup through reflood, until the heatup is terminated and slow cooling begins. The 1D RELAP5-3D TR shows somewhat similar behavior, although generally much more exaggerated heatups and cooldowns. The updated RELAP5-3D immediately drops in cladding temperature, followed by rapid heat up around 50 seconds, and once there, slowly decreases for the rest of the TR. These results might also be attributed to the low interfacial friction multiplier. It is suggested to allow the value to be reduced only in the downcomer and allow the core—and other components—to use default values.

The TR hot spot oxidation is shown in Figure 4-95. There is no FSAR plot for this. The 1D plot shows that the RELAP5-3D run produces a result of ~0.23%, and most of this oxidation accumulates over the period of significant reflood heatup. The updated RELAP5-3D model shows an instant increase and an additional small increase when the reheat up at 50 seconds occurs. The total amount appears to be much less than the 1D simulation, which is expected due to the lower cladding temperature observed during the updated RELAP5-3D simulation.

The TR liquid levels in the downcomer and core are shown in Figure 4-96. For the 1D model, the core levels show a similar trend between RELAP5-3D and the FSAR, although the RELAP5-3D case has a consistently lower level. The downcomer level is initially somewhat similar, but the FSAR case retains significant inventory through the TR, while the RELAP5-3D case expels significant inventory. The updated RELAP5-3D case shows much stronger agreement for both the core and downcomer liquid levels. The overall trends are very close to the FSAR, but the RELAP5-3D results do tend to be slightly below the FSAR results.

The TR containment pressure is shown in Figure 4-97. This plot shows that the RELAP5-3D boundary condition was specified consistent with the FSAR analysis.

The TR core inlet and outlet mass flow rates are shown in Figure 4-98. The 1D RELAP5-3D results show that the normal flow path is maintained, and that no reverse flow is observed. This is due to the large reverse loss coefficient at the broken loop cold leg nozzle. The updated RELAP5-3D model trends much closer to the FSAR than the 1D model. Since there is no large loss coefficient, reverse flow is observed as it was in the FSAR. The updated model of removal of the large loss coefficient shows a huge improvement in the capability of RELAP5-3D to simulate core mass flow.

The TR HTC is shown in Figure 4-99. The 1D RELAP5-3D results differ significantly from the FSAR results. The updated RELAP5-3D results are closer, but still differ from the FSAR. This is not investigated further, as the TR results will change significantly in downstream analyses.

The TR vapor temperature at the hot spot is shown in Figure 4-100. The RELAP5-3D results differ significantly from the FSAR results, but this is not investigated further, as the TR results will change significantly in the downstream analyses. The initial increase in temperature is observed with the updated RELAP5-3D simulation, but the temperature immediately drops down while the FSAR plateaus.

The TR break mass flow rate is shown in Figure 4-101. The RELAP5-3D run has significantly lower break flow, consistent with the much slower depressurization. This is due to the large reverse loss coefficient at the broken loop cold leg nozzle. While the updated RELAP5-3D model does not have the large reverse loss coefficient, the results still differ significantly from the FSAR.

The TR break energy release rate is shown in Figure 4-102. The RELAP5-3D run has a significantly lower energy release rate, consistent with the break flow.

The TR fluid quality at the peak cladding temperature (PCT) elevation is shown in Figure 4-103. The RELAP5-3D results differ significantly from the FSAR results, but this is not investigated further, as the TR results will change significantly in the downstream analyses.

The TR mass flux at the PCT elevation is shown in Figure 4-104. The 1D RELAP5-3D results differ significantly from the FSAR results, consistent with the difference in core mass flow. The core mass flow for the updated RELAP5-3D model showed values similar to the FSAR, but the TR mass flux shows values much closer to the FSAR as well. Note the variability of the updated model appears to be very large.

The TR accumulator mass flow rate during blowdown is shown in Figure 4-105. This shows that the RELAP5-3D run does not even have accumulator injection in this time frame, consistent with depressurization. The updated model does show accumulator injection with a 6 second delay. This is a massive improvement over the 1D model.

The TR combined SI mass flow rate is shown in Figure 4-106. This shows that the 1D RELAP5-3D run has accumulator flow shortly after ~40 seconds. By this point, the FSAR accumulators are nearly empty, and the flow quickly falls to the purely SI level. Once the RELAP5-3D accumulators empty, the RELAP5-3D SI produces flow at a similar level to the FSAR run. The updated RELAP5-3D model matches the FSAR very closely.

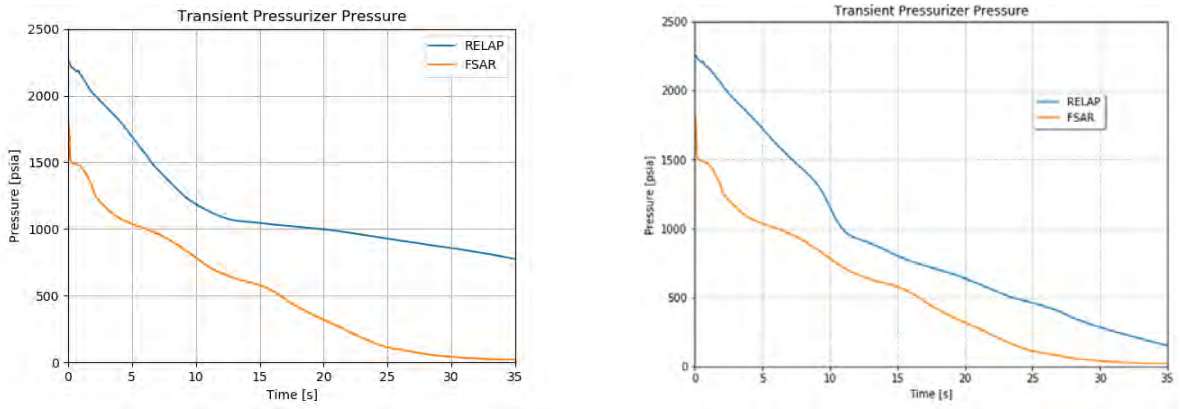

1D Model **MULTID Model**

Figure 4-92. TR PRZ pressure for the LBLOCA scenario.

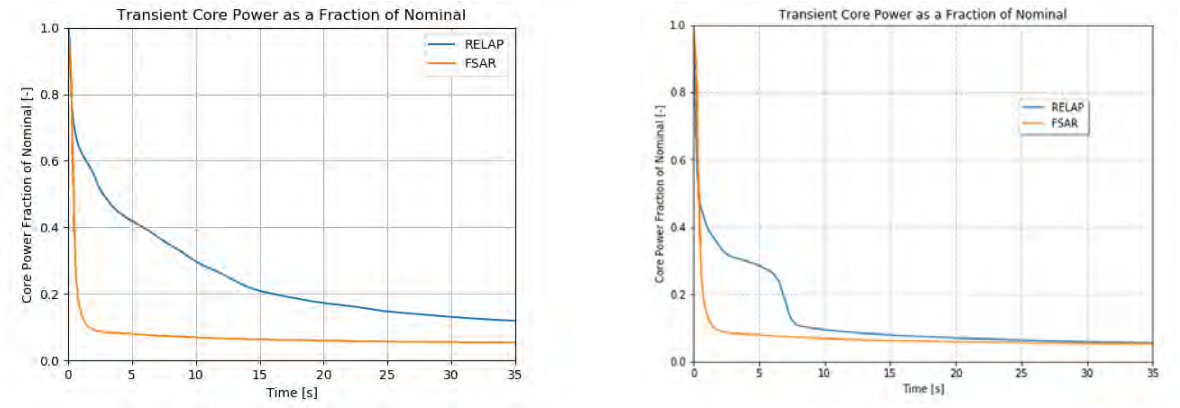

1D Model **MULTID Model**

Figure 4-93. TR core power as a fraction of nominal for the LBLOCA scenario.

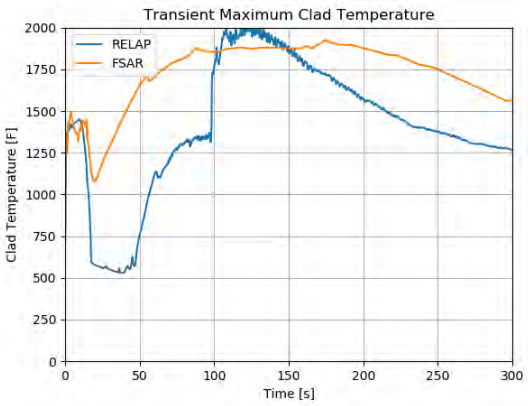

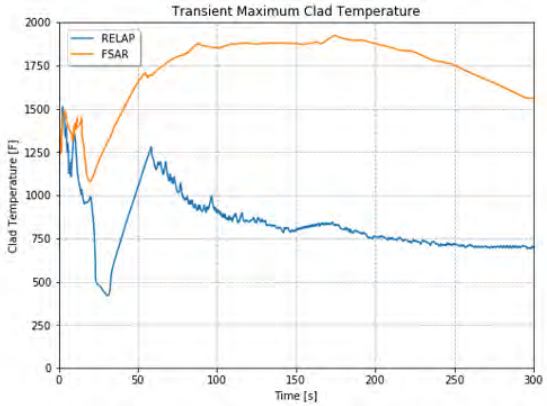

1D Model **MULTID Model**

Figure 4-94. TR maximum clad temperature for the LBLOCA scenario.

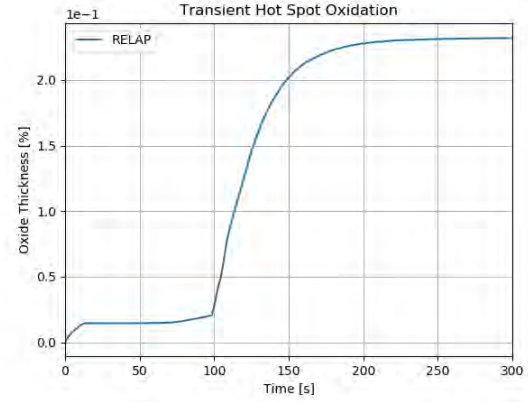

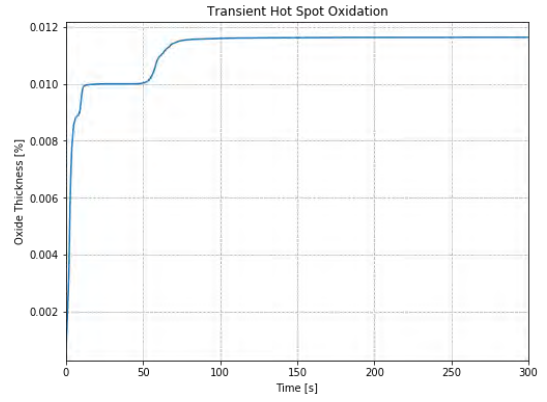

1D Model **MULTID Model**

Figure 4-95. TR hot spot oxidation for the LBLOCA scenario.

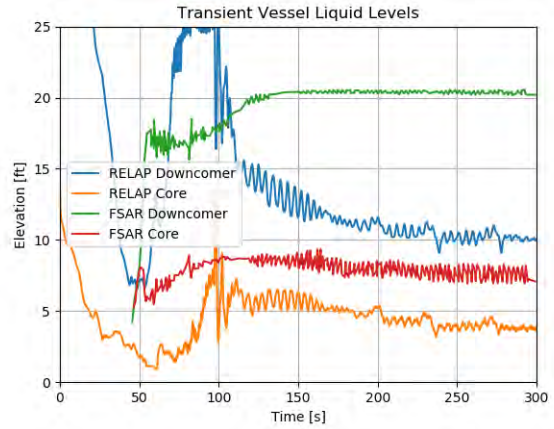

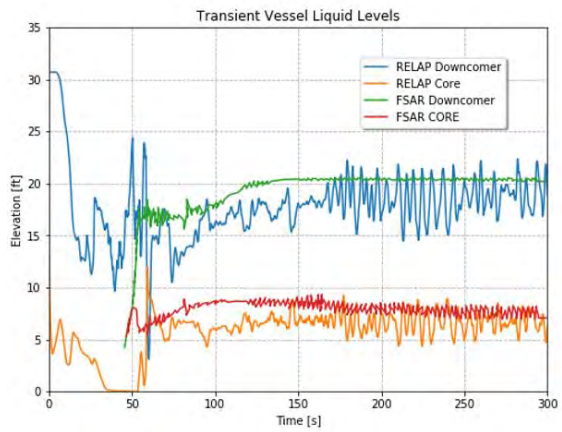

1D Model **MULTID Model**

Figure 4-96. TR vessel liquid levels for the LBLOCA scenario.

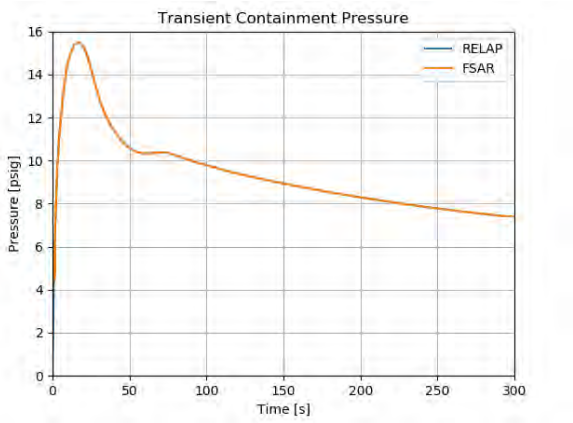

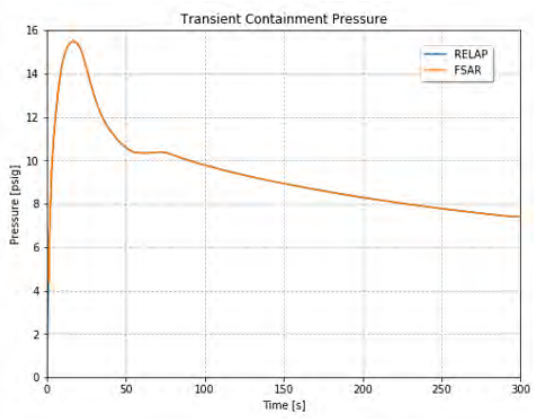

1D Model **MULTID Model**

Figure 4-97. TR containment pressure for the LBLOCA scenario.

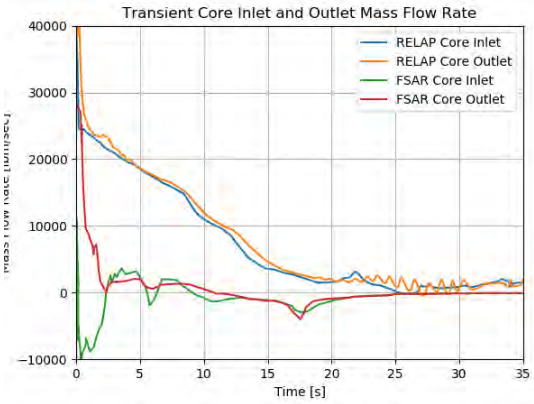

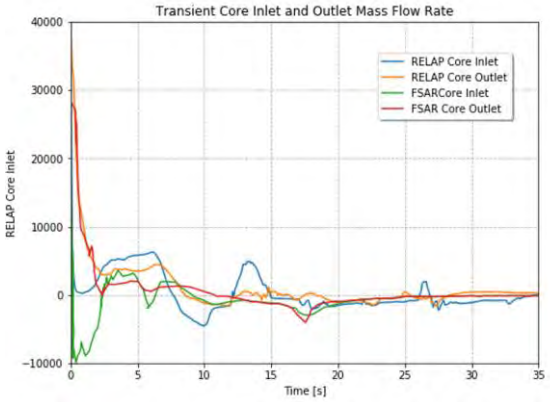

1D Model **MULTID Model**

Figure 4-98. TR core inlet and outlet mass flow rate for the LBLOCA scenario.

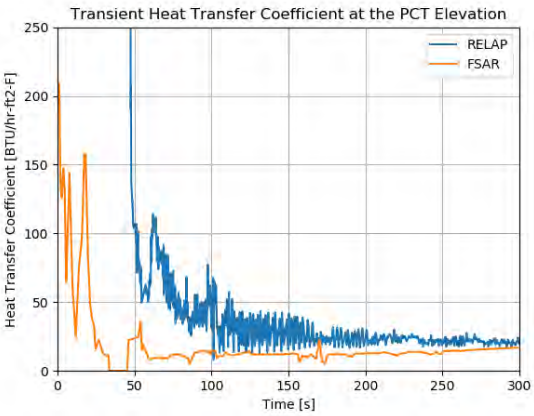

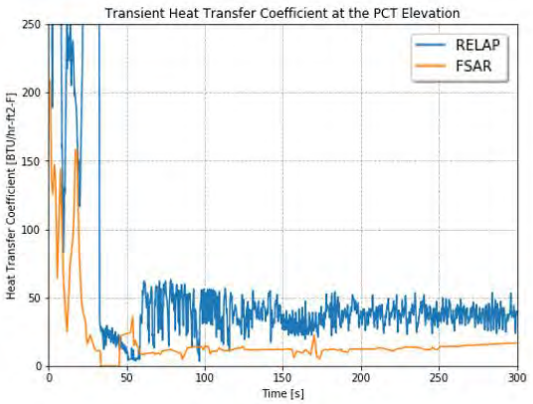

1D Model **MULTID Model**

Figure 4-99. TR HTC at the PCT elevation for the LBLOCA scenario.

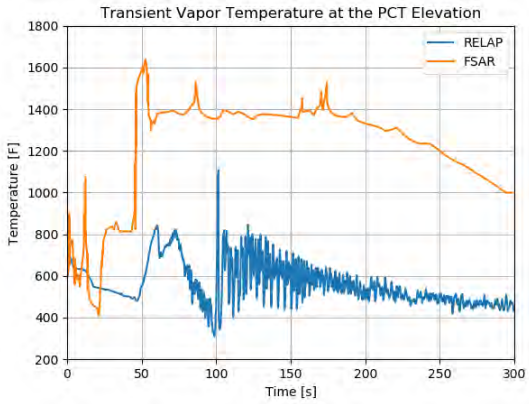

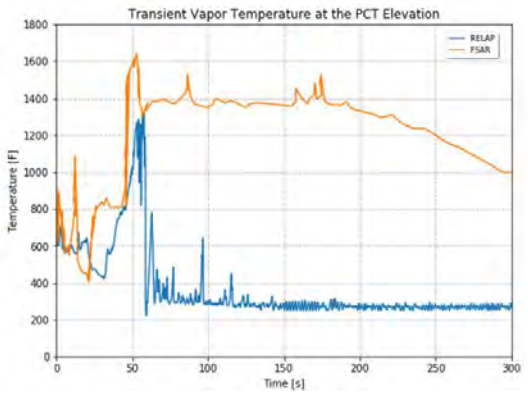

1D Model **MULTID Model**

Figure 4-100. TR vapor temperature at the PCT elevation for the LBLOCA scenario.

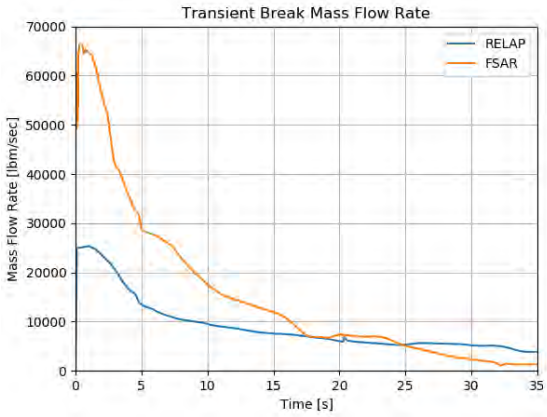

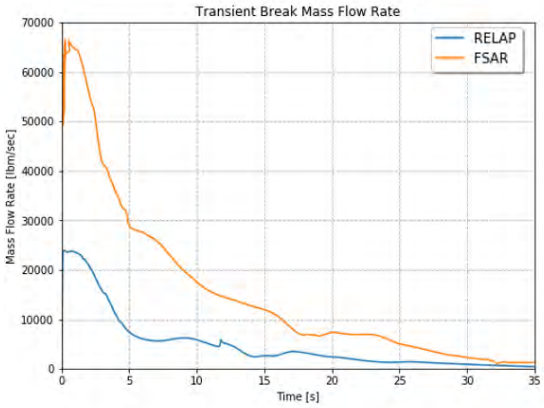

1D Model **MULTID Model**

Figure 4-101. TR break mass flow rate for the LBLOCA scenario.

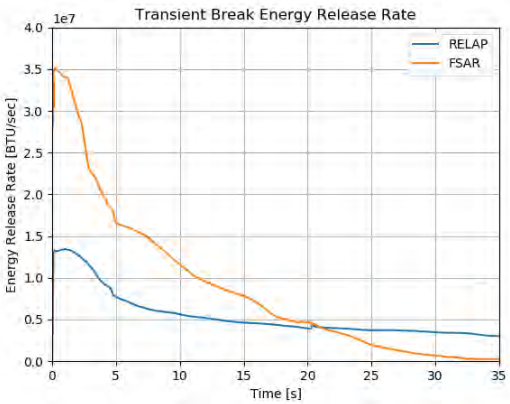

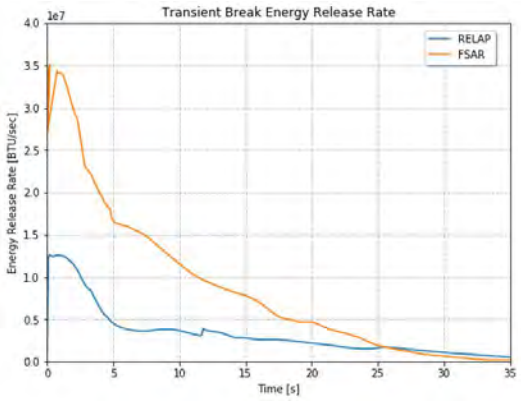

1D Model **MULTID Model**

Figure 4-102. TR break energy release rate for the LBLOCA scenario.

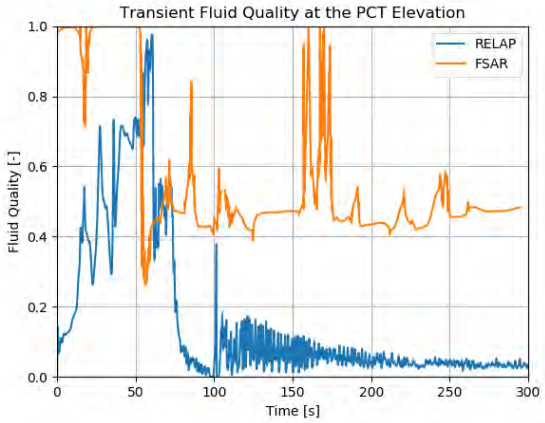

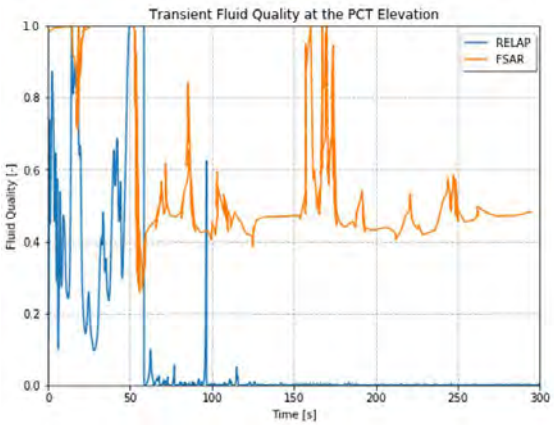

1D Model **MULTID Model**

Figure 4-103. TR fluid quality at the PCT elevation for the LBLOCA scenario.

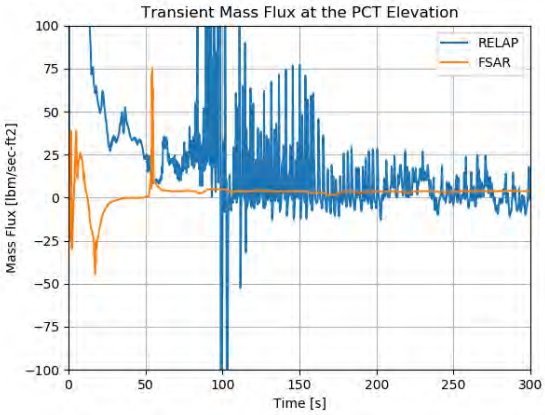

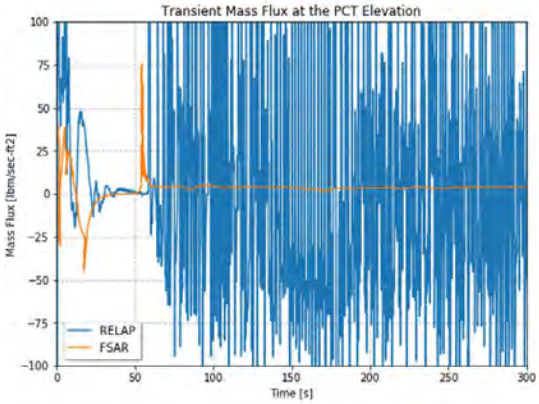

1D Model **MULTID Model**

Figure 4-104. TR mass flux at the PCT elevation for the LBLOCA scenario.

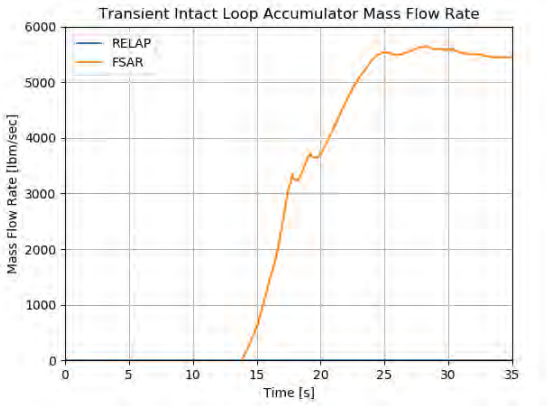

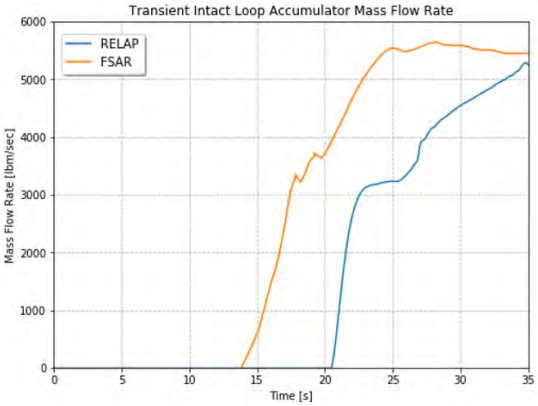

1D Model **MULTID Model**

Figure 4-105. TR intact loop accumulator mass flow rate for the LBLOCA scenario.

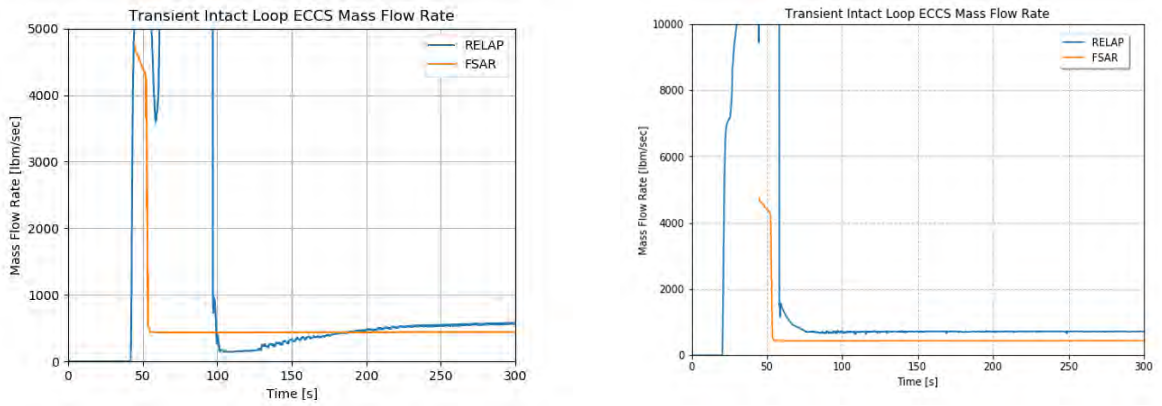

1D Model **MULTID Model**

Figure 4-106. TR intact loop ECCS mass flow rate for the LBLOCA scenario.

4.10.6.2 SBLOCA

The TR PRZ pressure is shown in Figure 4-107. The FSAR and RELAP5-3D runs follow a somewhat similar depressurization path. The FSAR results lower much more quickly initially, but then plateau by about 200 seconds. This is likely due to the loop seal formation. The RELAP5-3D run shows slower depressurization, but it is not apparent that a loop seal forms at all.

The TR core power as a fraction of nominal is shown in Figure 4-108. There is no FSAR plot for this. This plot shows that the reactor is shut down almost immediately and follows a reasonably looking decay heat curve.

The TR clad temperature is shown in Figure 4-109. The RELAP5-3D run shows no heatup, while the FSAR run shows a significant heatup. This is due to the core not uncovering in the RELAP5-3D run. This is likely due to a number of issues with the RELAP5-3D model. The lack of loop seal formation likely contributes to this, as does the inconsistent break flow model. More investigation should be done downstream.

The TR oxidation at the hot spot is shown in Figure 4-110. There is no FSAR plot for this. This shows negligible oxidation accrual throughout the TR, consistent with a lack of heatup.

The TR core liquid level is shown in Figure 4-111. There is no FSAR plot for this, although this is a surrogate for the TR mixture level plot shown in the FSAR. The RELAP5-3D options for mixture level tracking did not appear to work correctly, and this should be investigated downstream. From the RELAP5-3D results presented, however, it is apparent that the mixture level would not have dropped below the top of the core, as there is only a very brief decrease from being liquid solid. As the mixture level includes a two-phase region, it is extremely unlikely that the small drop in liquid level shown in this figure indicates a mixture level below the top of the core.

The TR core outlet steam mass flow rate is shown in Figure 4-112. The RELAP5-3D run shows no steam mass flow, other than the short period where the level dropped below the top of the core. This is because the core remains purely liquid otherwise, so there is no steam flow.

The TR HTC at the PCT elevation is shown in Figure 4-113. This shows a fairly consistent heat transfer level throughout the TR, notably missing the period of little to no heat transfer during core uncover.

The TR vapor temperature at the PCT elevation is shown in Figure 4-114. This follows the same trend as the clad temperature.

The TR intact loops SI mass flow rate is shown in Figure 4-115. The RELAP5-3D flows are very similar to the FSAR flows, and the differences largely follow the pressure differences.

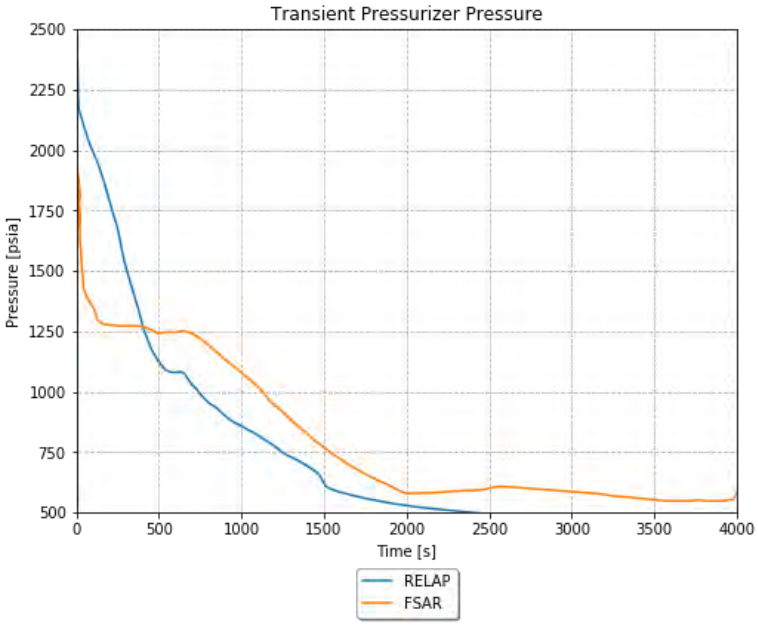

Figure 4-107. TR PRZ pressure for the SBLOCA scenario.

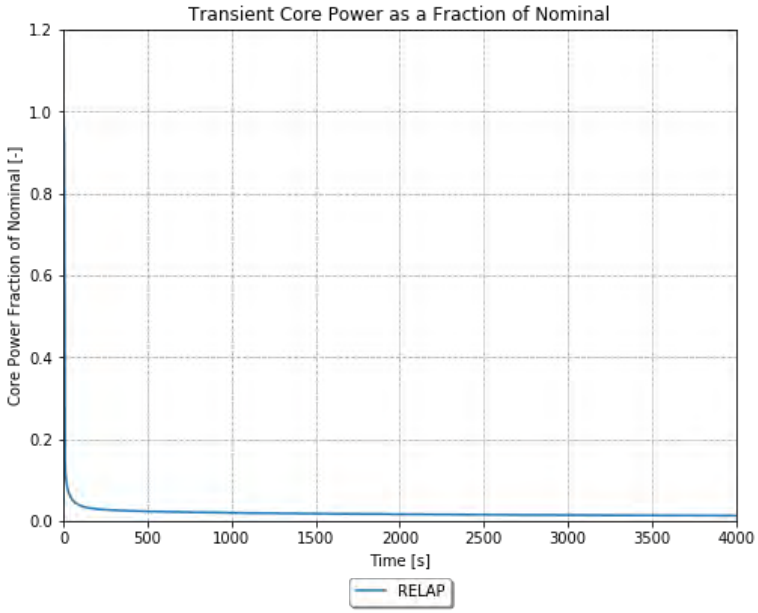

Figure 4-108. TR core power as a fraction of nominal for the SBLOCA scenario.

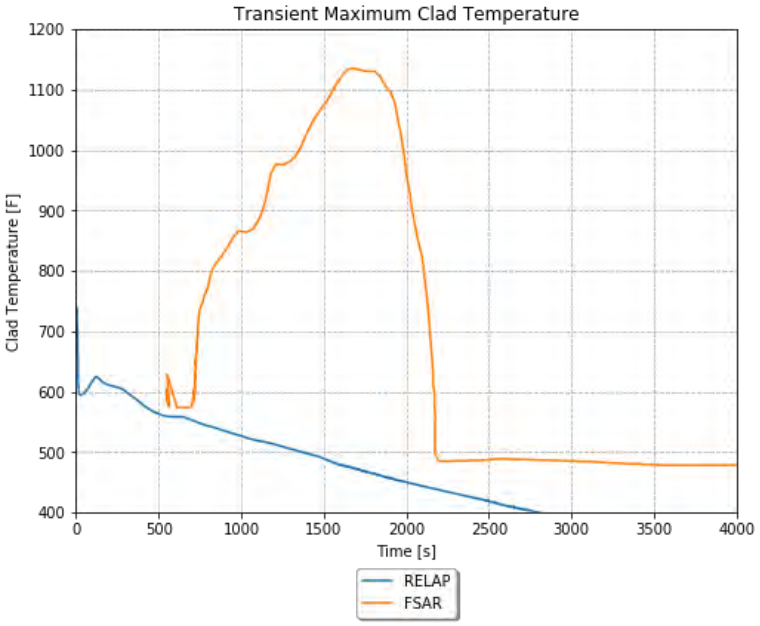

Figure 4-109. TR maximum clad temperature for the SBLOCA scenario.

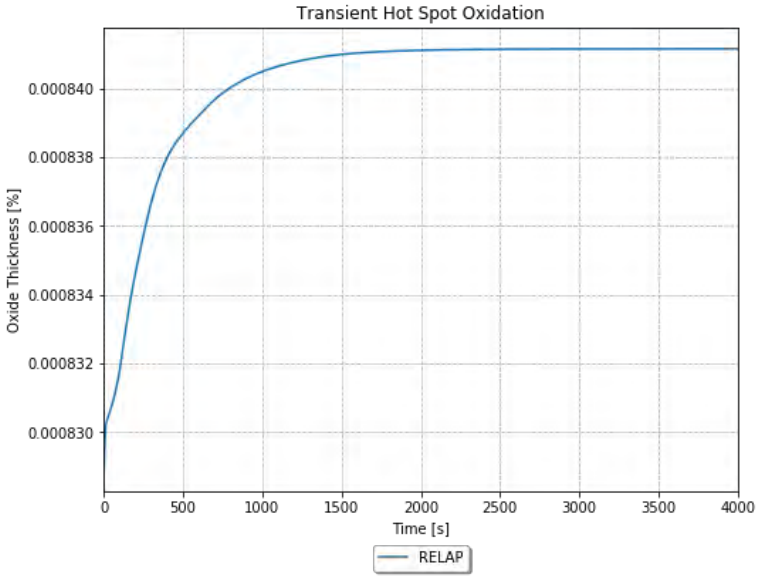

Figure 4-110. TR hot spot oxidation for the SBLOCA scenario.

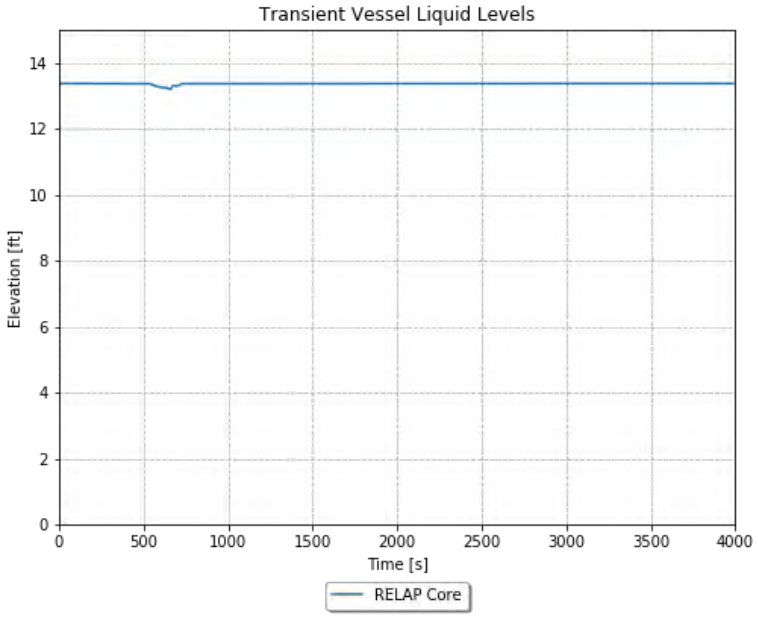

Figure 4-111. TR vessel liquid levels for the SBLOCA scenario.

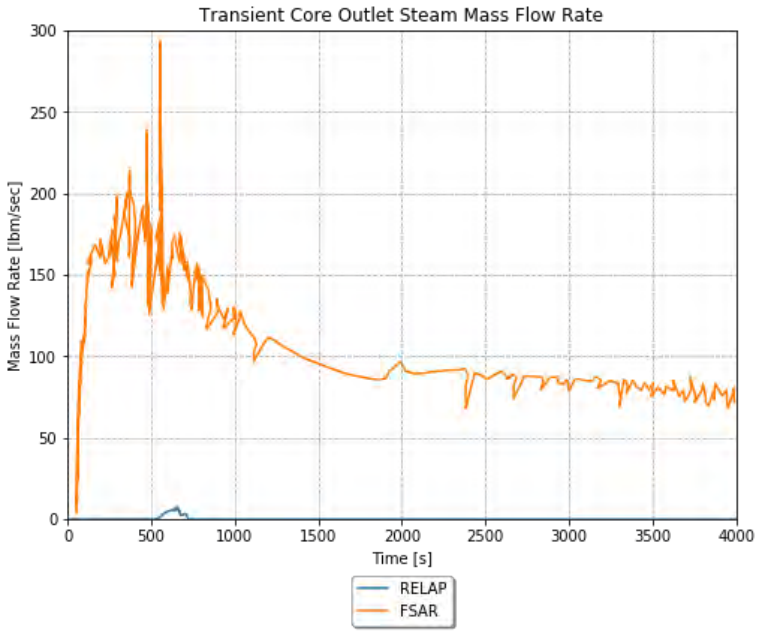

Figure 4-112. TR core outlet steam mass flow rate for the SBLOCA scenario.

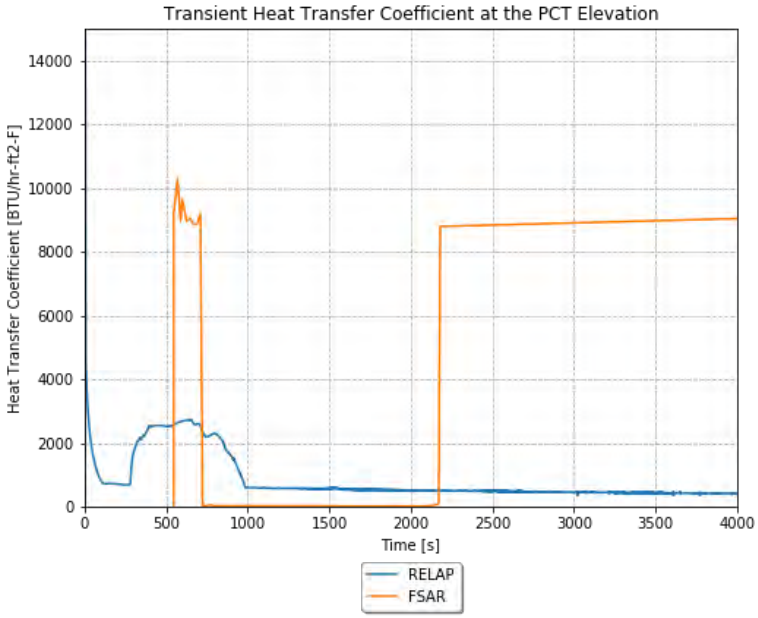

Figure 4-113. TR HTC at the pct elevation for the SBLOCA scenario.

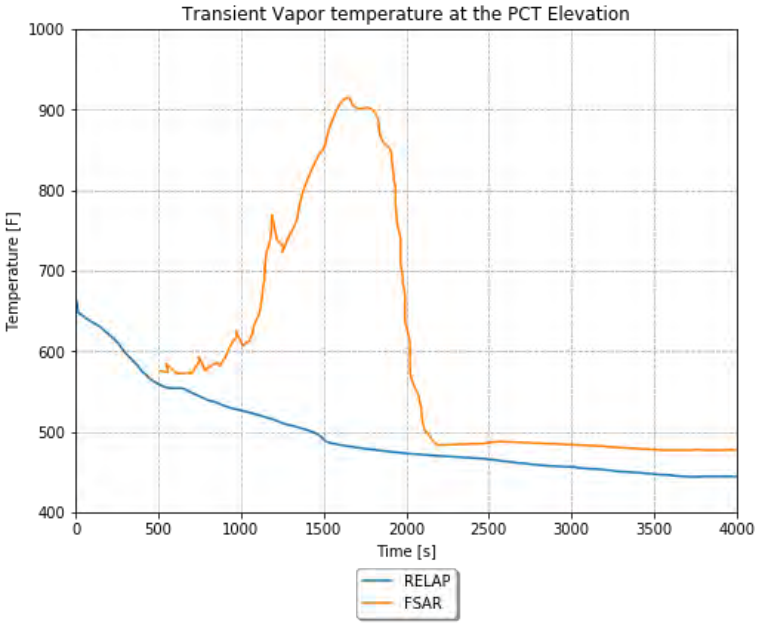

Figure 4-114. TR vapor temperature at the PCT elevation for the SBLOCA scenario.

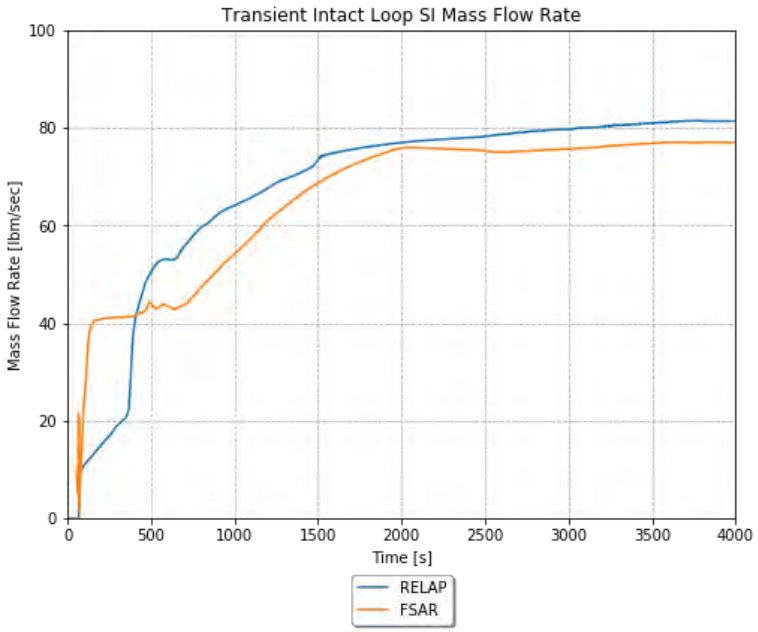

Figure 4-115. TR intact loop SI mass flow rate for the SBLOCA scenario.

4.10.7 Adherence to Acceptance Criteria

The final results for the LOCA TRs are compared to the results from the FSAR and the acceptance criteria in Table 4-16. The acceptance criteria are based on examination of the FSAR sections, and the applicable sections of the standard review plan.

The RELAP5-3D simulations meet all acceptance criteria for the LOCA scenario. Some of the potential input differences between the FSAR simulations and the RELAP5-3D simulations are discussed in following section. These may drive some of the differences in results between the FSAR analysis and the RELAP5-3D simulations, in addition to code differences.

Table 4-16. LOCA final results.

Result	FSAR (LB)	RELAP5-3D (LB)	FSAR (SB)	RELAP5-3D (SB)	Acceptance Criteria
Peak Cladding Temperature [°F]	1936.3	1252	1138	735	2200
Maximum Local Oxidation [%]	N/A	0.011	N/A	0.00085	17

4.10.8 Scenario-Specific Limitations and Conditions for Usage

The following limitations apply specifically to the large break LOCA case:

- No containment model is made, and the backpressure curve from the FSAR analysis is used instead.
- The pump trip and coast-down behavior of the FSAR analysis is unknown.
- The low PRZ pressure SI signal setpoint is unknown, so a time of SI signal consistent with the FSAR analysis is forced.
- The main steam flow is assumed to ramp to 0 over 0.1 second after trip. It is unclear what the base analysis assumptions are.
- No information is given on feedwater timing, so assumed values for delays and ramping are used.

- The SG tube plugging value of 10% is not modeled herein. This is expected to be a small effect.
- The FQ value of 2.55 from the base model is used, while the FSAR analysis uses 2.50.
- The power shape used is inconsistent with that in the FSAR analysis.
- Several initial conditions believed to be of low importance are set to arbitrary values.
- The vessel noding of the current core model is likely two coarse and may be causing run failures due to high PCT values.

The following limitations apply specifically to the small break LOCA case:

- The pump trip and coast-down behavior of the FSAR analysis is unknown.
- The low PRZ pressure SI signal setpoint is unknown, so a time of SI signal consistent with the FSAR analysis is forced.
- The main steam flow is assumed to ramp to 0 over 0.1 second after trip. It is unclear what the base analysis assumptions are.
- No information is given on the feedwater timing, so assumed values for delays and ramping are used.
- The MDC and FTC of reactivity are not given in the FSAR. Reasonable values are used.
- The SG tube plugging value of 10% is not modeled herein. This is expected to be a small effect.
- The FQ value of 2.55 from the base model is used, while the FSAR analysis uses 2.58.
- The power shape used is inconsistent with that in the FSAR analysis.
- Several initial conditions believed to be of low importance are set to arbitrary values.
- Using a break area consistent with the FSAR analysis produced depressurization that was much too fast. Therefore, a smaller break size was used to obtain a more similar depressurization. The break flow model should be investigated for suitability.

4.11 Inadvertent Operation of the ECCS During Power Operation

Inadvertent operation of the ECCS at power could be caused by operator error, test sequence error, or a false electrical actuation signal. A spurious signal initiated after the logic circuitry in one solid-state protection system train for any of the following engineered safety feature (ESF) functions could cause this incident by actuating the ESF equipment associated with the affected train:

- High containment pressure.
- Low PRZ pressure.
- Low steam line pressure.

Following the actuation signal, the suction of the coolant charging pumps diverts from the volume control tank to the refueling water storage tank. Simultaneously, the valves isolating the injection header from the charging pumps open and the normal charging line isolation valves close. The charging pumps force the borated water from the RWST through the pump discharge header, the injection line, and into the cold leg of each loop. The SI pumps also start automatically but provide no flow when the RCS is at normal pressure. The passive accumulator tank SI and low head system are available. However, they do not provide flow when the RCS is at normal pressure.

A SI signal normally results in a direct reactor trip and a turbine trip. However, any single fault that actuates the ECCS will not necessarily produce a reactor trip. If an SI signal generates a reactor trip, the operator should determine if the signal is spurious. If the SI signal is determined to be spurious, the operator should terminate SI and maintain the plant in the hot standby condition as determined by

appropriate recovery procedures. If repair of the ESF actuation system instrumentation is necessary, future plant operation will be in accordance with the technical specifications.

If the reactor protection system does not produce an immediate trip as a result of the spurious SI signal, the reactor experiences a negative reactivity addition due to the injected boron, which causes a decrease in reactor power. The power mismatch causes a drop in the reactor coolant average temperature (TAVG) and consequent coolant shrinkage. The PRZ pressure and water level decrease. Load decreases due to the effect of reduced steam pressure on load after the turbine throttle valve is fully open. If automatic rod control is used, these effects will lessen until the rods have moved out of the core. The TR is eventually terminated by the reactor protection system low PRZ pressure trip or by manual trip.

The limiting cases presented in the FSAR section are recreated. This includes:

- A case for analysis of DNBR.
- A case for analysis of PRZ filling using low TAVG.
- A case for analysis of PRZ filling using high TAVG.

4.11.1 Scenario-Specific Inputs in the TR Input File

The TR input file is defined as follows:

- Upfront cards are included that specify this is a restart TR run, which uses the last available printout in the restart file.
- The end times are set as shown below, consistent with the analyses in the reference plant FSAR. The max time step is set to 0.05 seconds, as this is a value that is reasonable for a relatively stable simulation such as this:
  - DNBR case: 600 seconds
  - PRZ filling with low TAVG: 700 seconds
  - PRZ filling with low TAVG: 800 seconds.
- The minor edits are used to specify the variables used in the plots.
- CV 405 (e.g., the reactivity controller) is listed as a constant value of 0.0 $. This is done as a placeholder for RAVEN to substitute in the actual end of SS value of CV 405 using the RAVEN variable “ssreact.” This step is necessary to turn off the reactivity controller, but make the SS reactivity adder persist.
- The pump inputs are specified by including CVs 419 through 422 (e.g., the pump speed), specified as a constant value that is replaced using the RAVEN variable “sspmpvel.”
- CVs 435 through 438 (e.g., the steam valve position) are changed to be functions of General Table 650. This allows them to be set to the SS valve position prior to the reactor trip or SI signal, and then close based on the specified delay and ramp times.
- CVs 459 through 462 (e.g., the MFW flow rate) are listed as constant values of 1118.9 lbm/sec. This is done as a placeholder for RAVEN to substitute in the actual end of SS values of CVs 459 through 462 using the RAVEN variable “ssmfw.”
- CV 472 is listed as a constant value of 0.0. This is used to turn off the SS charging flow.
- CV 473 is listed as a constant value of 0.0. This is used to turn off the SS letdown flow.
- CV 482 is listed as a constant value of 0.0. This is used to turn off the SS PRZ heater.
- CV 483 is listed as a constant value of 0.0. This is used to turn off the SS PRZ spray.

- For the PORV behavior:
  - For the DNBR case, the PORV is simply not included in the TR file to evoke the base behavior.
  - For the PRZ filling cases, General Table 690 is copied from the SS file into the TR file. The trip value is changed to be 501. In addition, a new trip 501 is added and is specified to trip at a time greater than or equal to 590 seconds for the low TAVG case. This is changed to 625 seconds in the high TAVG case. These times are based on the FSAR analysis.
- For the PRZ safety valve:
  - Trip 660 is used as the PRZ safety valve component trip; thus, the valve is open when Trip 660 is true. Trip 660 is true when Trip 503 is true and when Trip 661 is true.
  - Variable Trip 502 is true CV 180 (e.g., pressure) is less than or equal to 2425 psia.
  - Variable Trip 503 is true CV 180 (e.g., pressure) is greater than or equal to 2300 psia.
  - Trip 661 is true when Trip 502 is false, or Trip 660 is true.
  - General Table 670 is copied from the SS file, and the trip input is altered to be 661. Also, the upper pressure limit is set to 2425 psia instead of 2575 psia, as it appears that the FSAR run immediately opens to full flow.
  - This results in the PRZ safety valve opening initially when the PRZ pressure is greater than 2425 psia, then not closing until pressure is less than 2300 psia, and then staying closed until it hits 2425 psia again.
- Trip 470 is listed to trip at time greater than or equal to 0.0 seconds, as this initiates the SI at the onset of the TR, which is part of the definition of the scenario.
- General Table 640 is listed with values identical to the SS input. This input does not necessarily need to be here, but it is generically listed in the TR input files to allow the analyst to change the trip used for MFW.
- Unique to the DNBR case, General Table 650 is listed, with the trip changed to 613, to prevent main steam from tripping at the onset of the TR.
- General Table 650 is also listed for all cases so that the first three valve position entries in the table can be replaced with the end of the SS values using the RAVEN variable “ssstmvlv.” This step is necessary to turn off the steam flow controller, but have the SS steam flow persist.
- Unique to the PRZ filling cases, Trip 410 is added to the trip at the onset of the TR. This causes an immediate reactor trip, consistent with the FSAR cases.

4.11.2 Scenario-Specific RAVEN Inputs

The RAVEN distribution means are set as shown in Table 4-17. Inputs are consistent with the FSAR, as described below. Remaining inputs are assumptions that are not specifically mentioned in the FSAR:

- The SS conditions are set as follows:
  - For the DNBR case, they are set based on the revised thermal design procedure (RTDP) conditions with high TAVG, and an additional 5°F increase in RCS temperatures for uncertainty.
  - For the PRZ filling high (PF H) TAVG case, they are set based on RTDP conditions with high TAVG.
  - For the PRZ filling low (PF L) TAVG case, they are set based on RTDP conditions with low TAVG. Some additional parameters are adjusted for TAVG, including steam pressure and RCS pressure drops.

- The PRZ low pressure reactor trip setpoint is set to 1935 psia.
- The SI delay time is set to 0.1 seconds so that SI immediately comes on in the TR.
- The PRZ safety valve opening pressure is set to 2300 psia.
- The charging boron distribution is set as follows:
  - For the DNBR case, it is set to 2600 ppm (2.6e-3 kg/kg).
  - For the PRZ filling cases, the boron concentrations are irrelevant because the reactor trips at the onset of the TR; therefore, it is set to 0 ppm.
- The RCS boron distribution is set as follows:
  - For the DNBR case, it is set to 882 ppm (8.82e-4 kg/kg).
  - For the PRZ filling cases, the boron concentrations are irrelevant because the reactor trips at the onset of the TR; therefore, it is set to 0 ppm.
- The MSIV is immediately ramped down over 0.1 seconds from the reactor trip time.
- The MFW is set to ramp down over 5 seconds after the SI signal, and then the AFW never starts.

Table 4-17. Summary of RAVEN inputs for inadvertent operation of the ECCS during power operation.

Distribution	Description	Unit	Mean (DNBR)	Mean (PF H)	Mean (PF L)
cltempdist	Cold Leg Temperature	°F	561.9	556.9	539.2
corepdist	Core Power	W	3.657E+09	3.657E+09	3.657E+09
fwtempdist	Feedwater Temperature	°F	448.7	448.7	448.7
hltempdist	Hot Leg Temperature	°F	624.9	619.9	602.2
przleveldist	PRZ Level	ft.	29.4	29.4	29.4
przpressdist	PRZ Pressure	psia	2250	2250	2250
rcsflowdist	RCS Volumetric Flow	gpm	9.56E+04	9.56E+04	9.56E+04
rcsmflodist	RCS Mass Flow	lbm/sec	-9684.028	9684.028	9684.028
rcsmflorrdist	RCS Mass Flow in Vessel	lbm/sec	-9684.028	-9684.028	-9684.028
sgleveldist	SG Level	ft.	40.1	40.1	40.1
stmpressdist	SG Steam Pressure	psia	941	941	817
sgflowdist	SG Flow Rate	lbm/sec	1132.639	1132.639	1132.639
dpvessdist	Vessel Pressure Drop	psi	46.5	46.5	47.8
dphldist	Hot Leg Pressure Drop	psi	1.2	1.2	1.3
dpxldist	Crossover Leg Pressure Drop	psi	3.1	3.1	3.4
dpcldist	Cold Leg Pressure Drop	psi	3.3	3.3	3.6
dpsgdist	SG Primary Pressure Drop	psi	45.5	45.5	41.3
corbypdist	Core Bypass Flow	%	5	5	5
przphirxtdist	High PRZ Pressure Reactor Trip Setpoint	psia	2514.7	3514.7	3514.7
przplorxtdist	Low PRZ Pressure Reactor Trip Setpoint	psia	1935	1935	1935
przlhirxtdist	High PRZ Level Reactor Trip Setpoint	ft.	48.9	500	500

Distribution	Description	Unit	Mean (DNBR)	Mean (PF H)	Mean (PF L)
rcsflolorxtdist	Low RCS Flow Rate Reactor Trip Setpoint	lbm/sec	8425.08	8425.08	8425.08
sglevlorxtdist	Low SG Level Reactor Trip Setpoint	ft.	1	1	1
mfwdeltimedist	MFW Delay Time	sec	0.001	0.001	0.001
mfwramptimedist	MFW Ramp Time	sec	5	5	5
afwdeltimedist	AFW Delay Time	sec	1.00E+08	1.00E+08	1.00E+08
afwramptimedist	AFW Ramp Time	sec	1.10E+08	1.10E+08	1.10E+08
afwflodist	AFW Flow Rate	lbm/sec	105.65	105.65	105.65
pmpmotdeldist	Pump Motor Trip Delay Time	sec	2	2	2
achfluxdist	Average Channel Maximum SS Heat Flux	BTU/sec-ft^2	99.954	99.954	99.954
hchfluxdist	Hot Channel Maximum SS Heat Flux	BTU/sec-ft^2	164.93	164.93	164.93
initreactdist	Initial Reactivity	$	0	0	0
mdcdist	Moderator Density Coefficient	Δk/g/cm^3	-0.084	-0.084	-0.084
accbordist	Accumulator Boron Concentration	Mass Frac	1.90E-03	1.90E-03	1.90E-03
chgbordist	Charging Boron Concentration	Mass Frac	2.60E-03	0.00E+00	0.00E+00
accvoldist	Accumulator Water Volume	ft^3	900	900	900
acctempdist	Accumulator Temperature	°F	120	120	120
accpressdist	Accumulator Pressure	psia	600	600	600
sitrplspdist	Low Steam Pressure SI Signal	psia	800	1	1
sitrpdeldist	SI Signal Delay Time	sec	0.1	0.1	0.1
msivdeldist	MSIV Delay Time	sec	0.001	0.001	0.001
msivrampdist	MSIV Ramp Time	sec	0.1	0.1	0.1
rccadeldist	RCCA Delay Time	sec	1	1	1
rcpheatdist	RCP Heat Generation	MW	1.00E-05	1.00E-05	1.00E-05
przsafdist	PRZ Safety Valve Open Pressure	psia	2300	2300	2300
rcsbordist	RCS Initial Boron Concentration	Mass Frac	8.82E-04	0	0.00E+00

4.11.3 Steady State Results

The steady state observations for the inadvertent operation of the ECCS at power are explained in detail in FY-2020 [2].

4.11.4 TR Boundary Conditions

The TR boundary conditions for the inadvertent operation of the ECCS at power are explained in detail in FY-2020 [2].

4.11.5 TR Results

The RELAP5-3D results are compared to the runs from the FSAR in the paragraphs below.

4.11.5.1 DNBR Case Results

The TR PRZ pressure is shown in Figure 4-116. The FSAR run depressurizes slightly more than the RELAP5-3D run, but the behavior is similar. After the initial re-pressurization, the RELAP5-3D run goes through two cycles of the PRZ safety valve while the FSAR run does not. This is likely due to the unknown exact nature of the PRZ pressure control modeling.

The TR core power as a fraction of nominal is shown in Figure 4-117. The power is very similar, with the RELAP5-3D run staying slightly higher for slightly longer.

The TR maximum clad temperature is shown in Figure 4-118. There is no FSAR plot for this. The cladding temperature immediately drops significantly, and then more or less flattens out after reactor trip.

The TR hot spot oxidation is shown in Figure 4-119. There is no FSAR plot for this. There is no appreciable oxidation accrual during the TR.

The TR average core moderator temperature is shown in Figure 4-120. The FSAR run decreases slightly more than the RELAP5-3D run and takes longer to increase, but the behavior is generally similar.

The TR PRZ water volume is shown in Figure 4-121. The TRs are very similar until about 250 seconds, at which point the FSAR increases significantly above the RELAP5-3D run.

The TR steam flow as a fraction of nominal is shown in Figure 4-122. The TRs are very similar, with the main difference being due to the timing of reactor trip.

The TR DNBR is shown in Figure 4-123. The behavior is similar for about 50 seconds, at which time the RELAP5-3D run drops to 0. In RELAP5-3D, this indicates that the heat structure is in a HT mode which does not even calculate CHF (i.e., single-phase liquid). As such, this is consistent with the very high DNBR observed in the FSAR run.

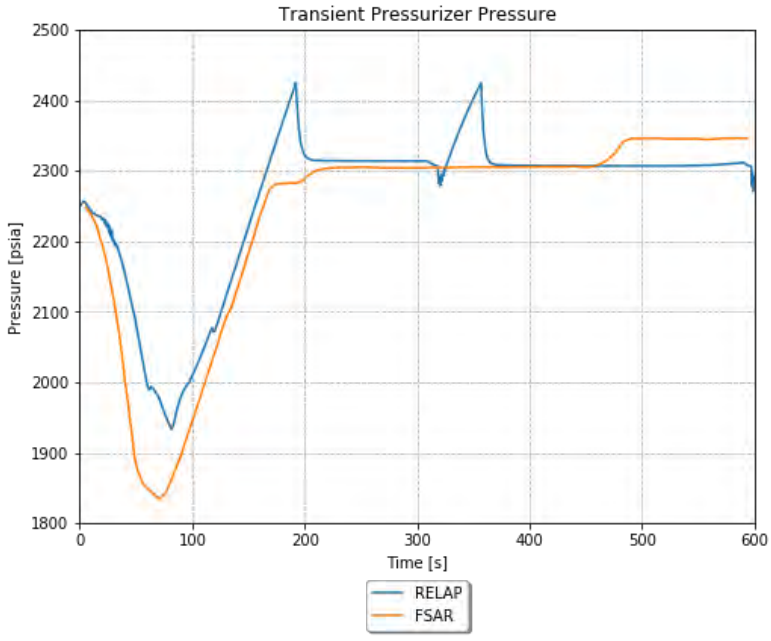

Figure 4-116. TR PRZ pressure for the inadvertent operation of the ECCS scenario (e.g., the DNBR case).

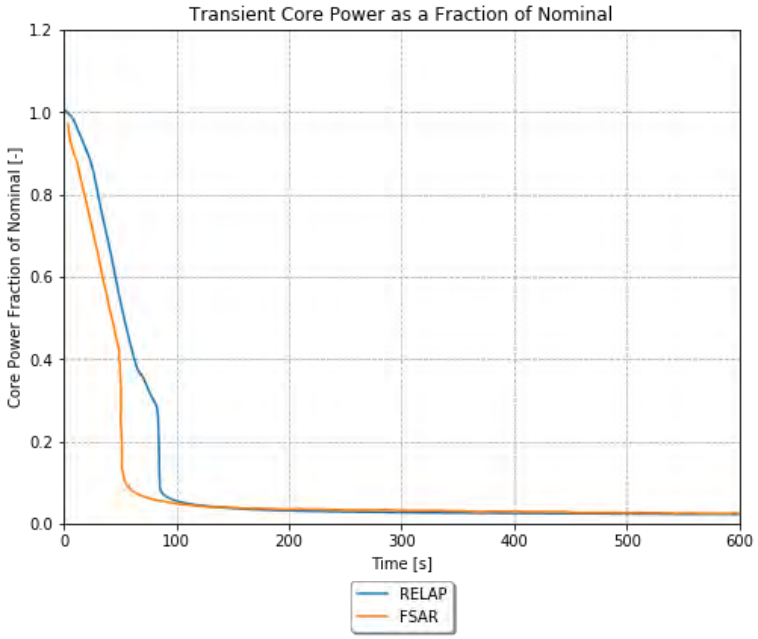

Figure 4-117. TR core power as a fraction of nominal for the inadvertent operation of the ECCS scenario (e.g., the DNBR case).

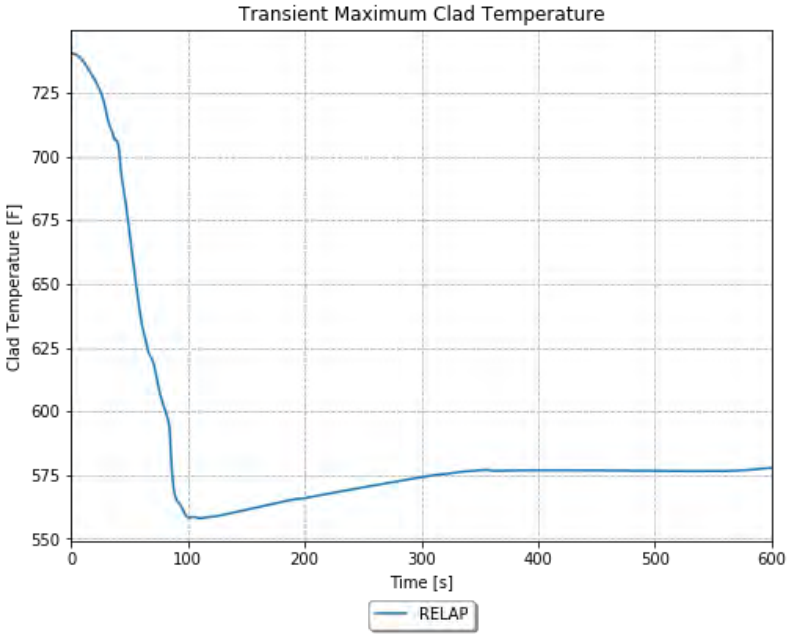

Figure 4-118. TR maximum cladding temperature for the inadvertent operation of the ECCS scenario (e.g., the DNBR case).

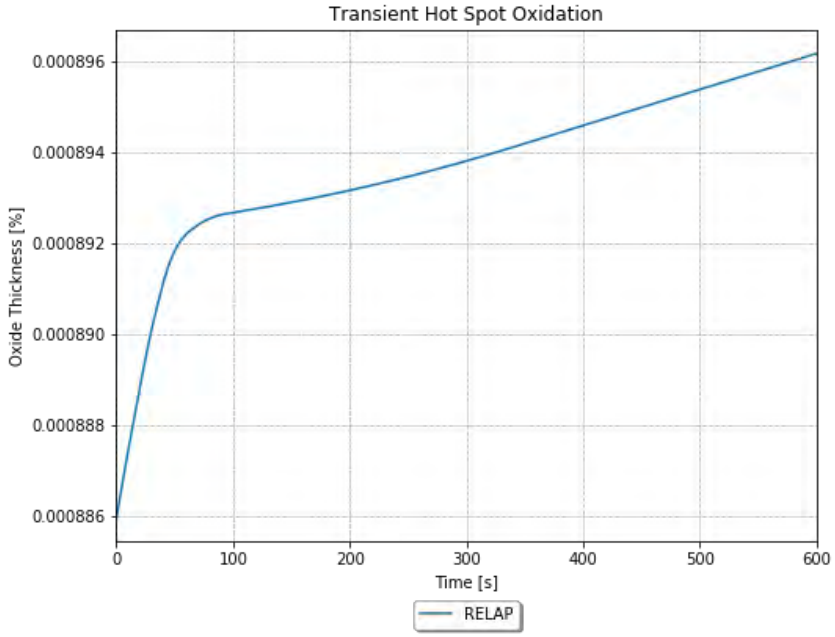

Figure 4-119. TR hot spot oxidation for the inadvertent operation of the ECCS scenario (e.g., the DNBR case).

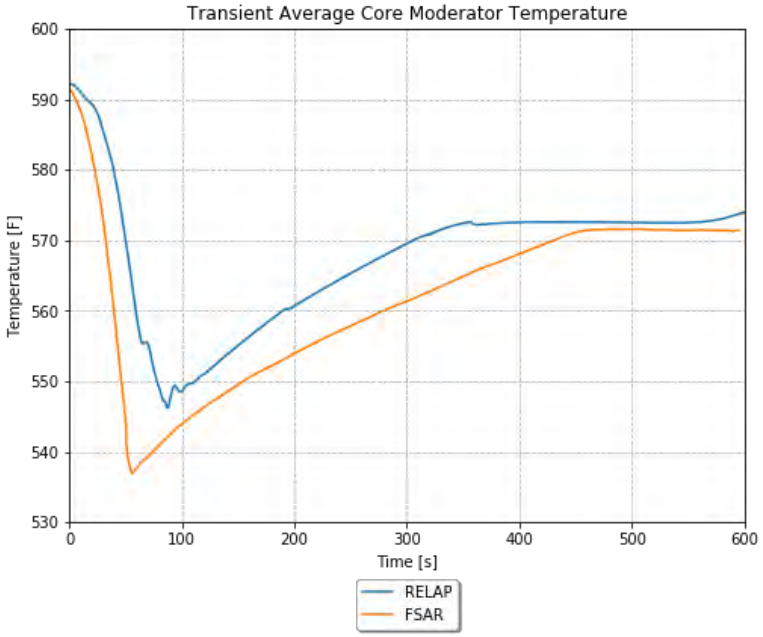

Figure 4-120. TR average core moderator temperature for the inadvertent operation of the ECCS scenario (e.g., the DNBR case).

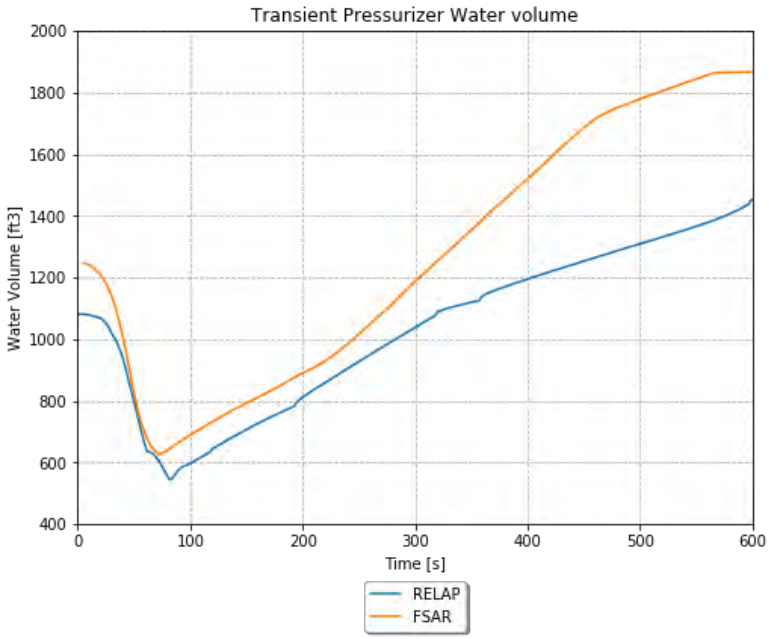

Figure 4-121. TR PRZ water volume for the inadvertent operation of the ECCS scenario (e.g., the DNBR case).

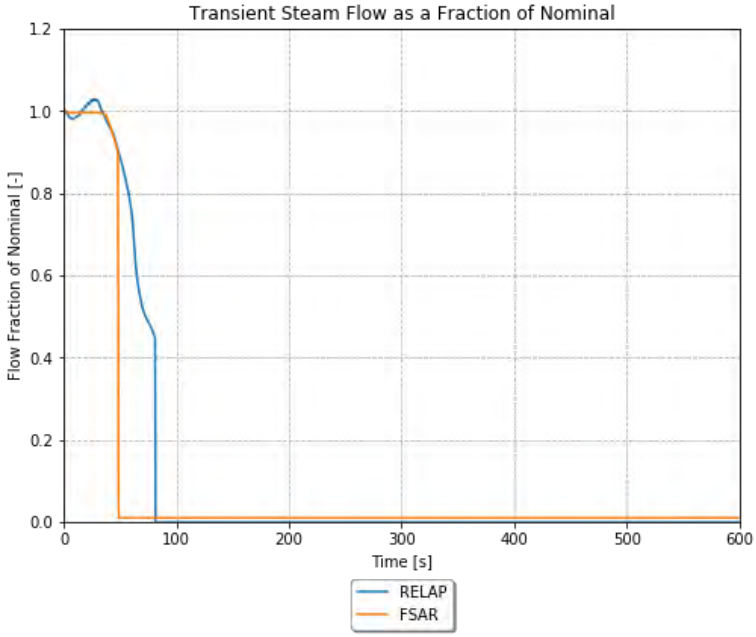

Figure 4-122. TR steam flow as a fraction of nominal for the inadvertent operation of the ECCS scenario (e.g., the DNBR case).

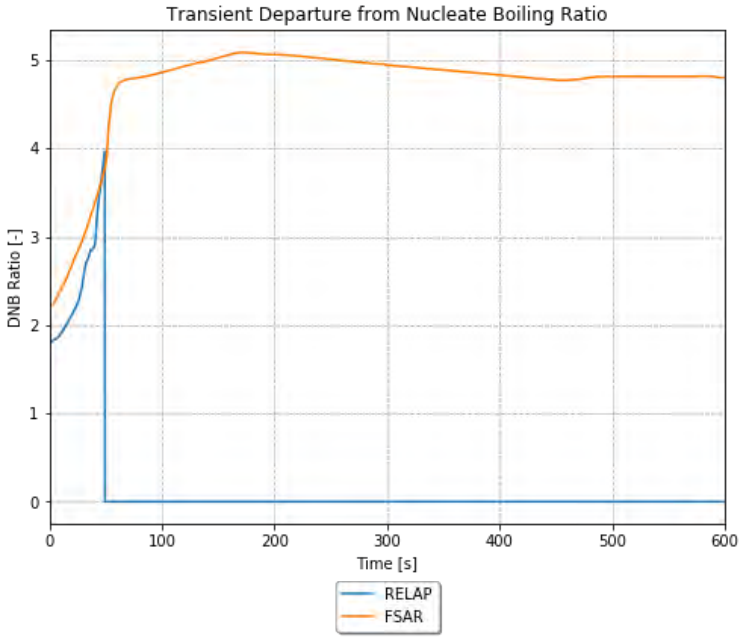

Figure 4-123. TR DNBR for the inadvertent operation of the ECCS scenario (e.g., the DNBR case).

4.11.5.2 PF H TAVG Case Results

The TR PRZ pressure is shown in Figure 4-131. After the initial decrease, the RELAP5-3D run repressurizes much faster and quickly goes through two cycles of the PRZ safety valve. The FSAR run pressure flattens out for several hundred seconds before going through its PRZ safety valve cycles.

The TR core power as a fraction of nominal is shown in Figure 4-125. The power is nearly identical between RELAP5-3D and the FSAR.

The TR maximum clad temperature is shown in Figure 4-126. There is no FSAR plot for this. The cladding temperature immediately drops significantly, and then more or less flattens out after the reactor trip.

The TR hot spot oxidation is shown in Figure 4-127. There is no FSAR plot for this. There is no appreciable oxidation accrual during the TR.

The TR average core moderator temperature is shown in Figure 4-128. The RELAP5-3D run decreases slightly more than the FSAR run and flattens out at a lower temperature.

The TR PRZ water volume is shown in Figure 4-129. A fairly significant difference develops in the first 20–30 seconds, and this difference more or less persists throughout the TR. The slope of increase is very similar through the TR.

The TR steam flow as a fraction of nominal is shown in Figure 4-130. The TRs are the same, with the steam being turned off immediately due to immediate reactor trip.

The TR DNBR is shown in Figure 4-131. There is no FSAR plot for this. The RELAP5-3D run immediately goes to 0. In RELAP5-3D, this indicates that the heat structure is in a HT mode, which does not even calculate CHF (i.e., single-phase liquid).

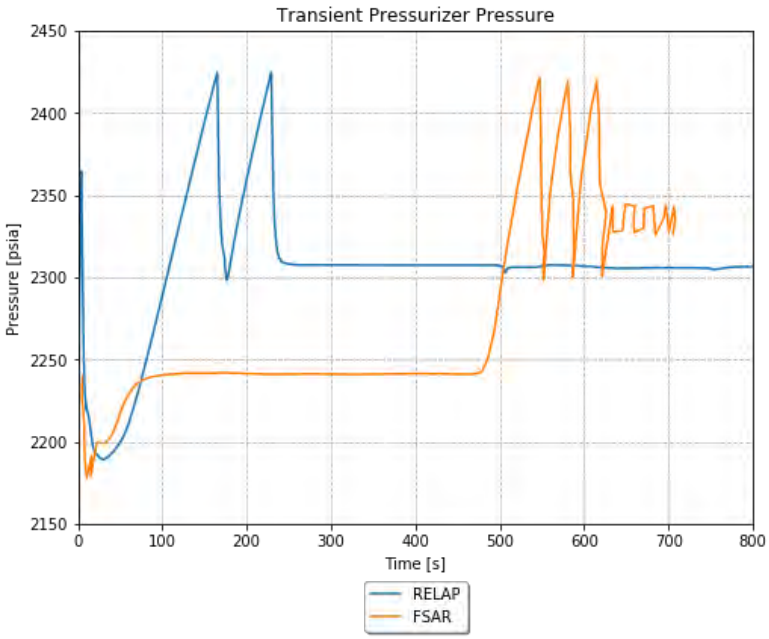

Figure 4-124. TR PRZ pressure for the inadvertent operation of the ECCS scenario (e.g., the PF H TAVG case).

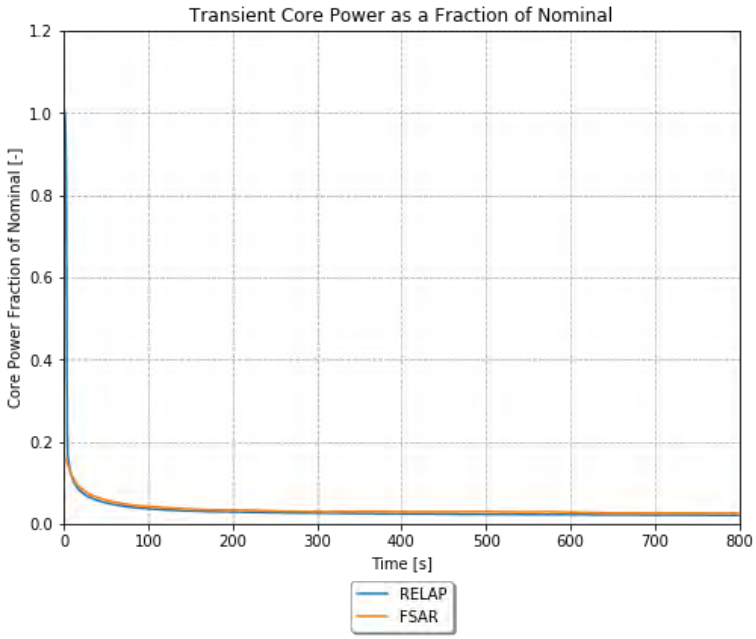

Figure 4-125. TR core power as a fraction of nominal for the inadvertent operation of the ECCS scenario (e.g., the PF H TAVG case).

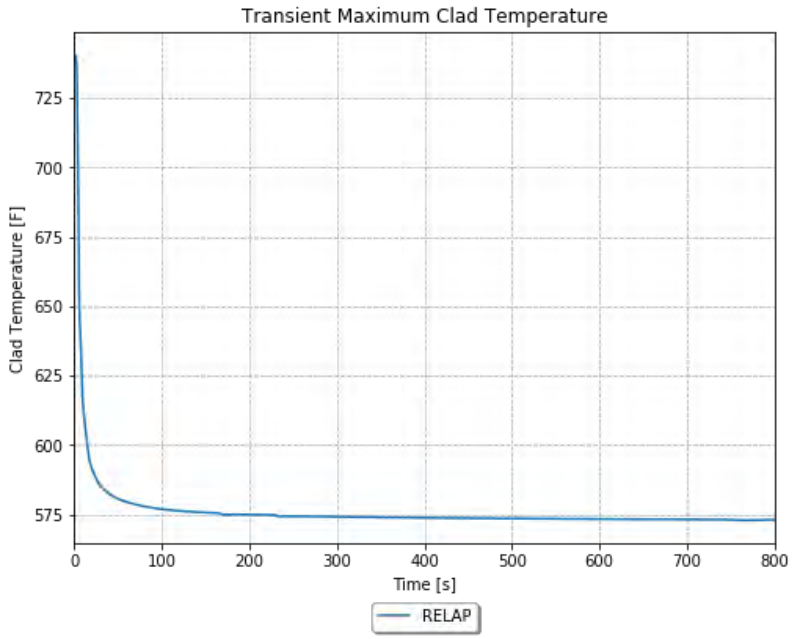

Figure 4-126. TR maximum cladding temperature for the inadvertent operation of the ECCS scenario (e.g., the PF H TAVG case).

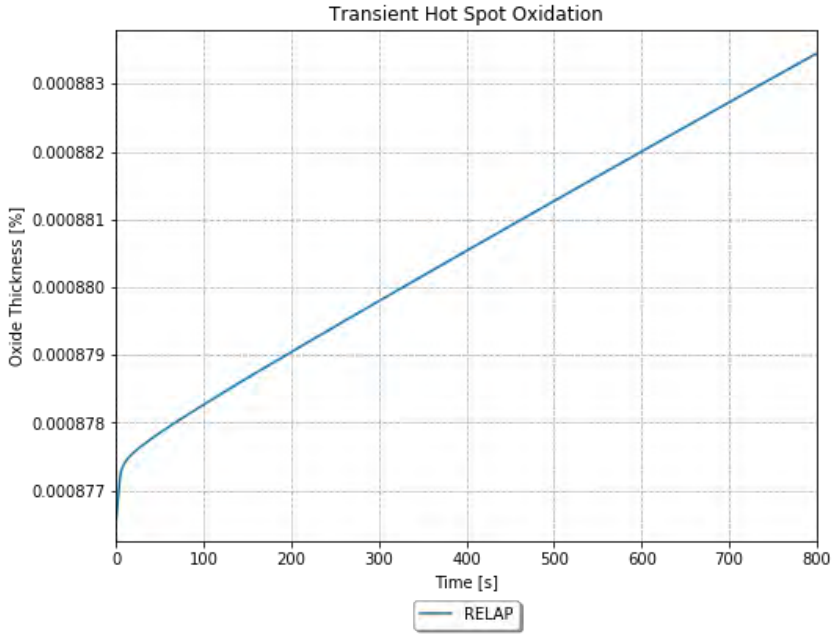

Figure 4-127. TR hot spot oxidation for the inadvertent operation of the ECCS scenario (e.g., the PF H TAVG case).

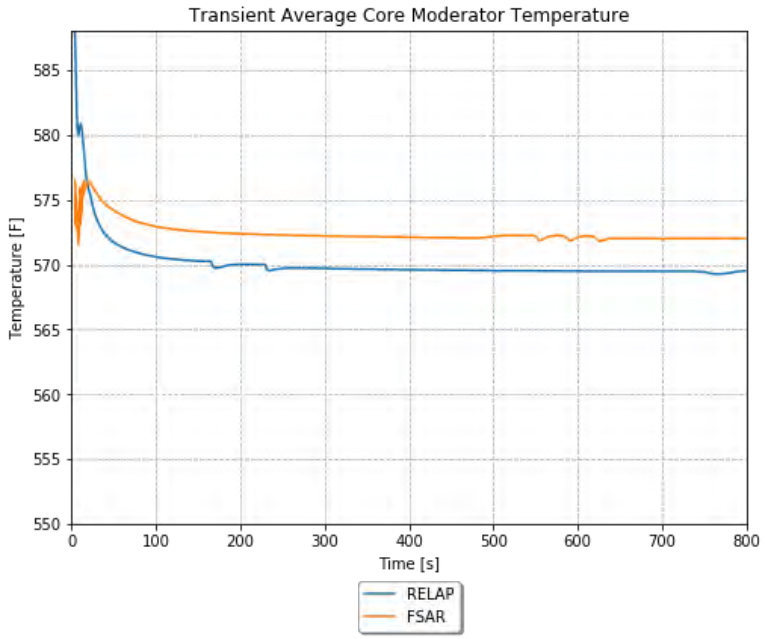

Figure 4-128. TR average core moderator temperature for the inadvertent operation of the ECCS scenario (e.g., the PF H TAVG case).

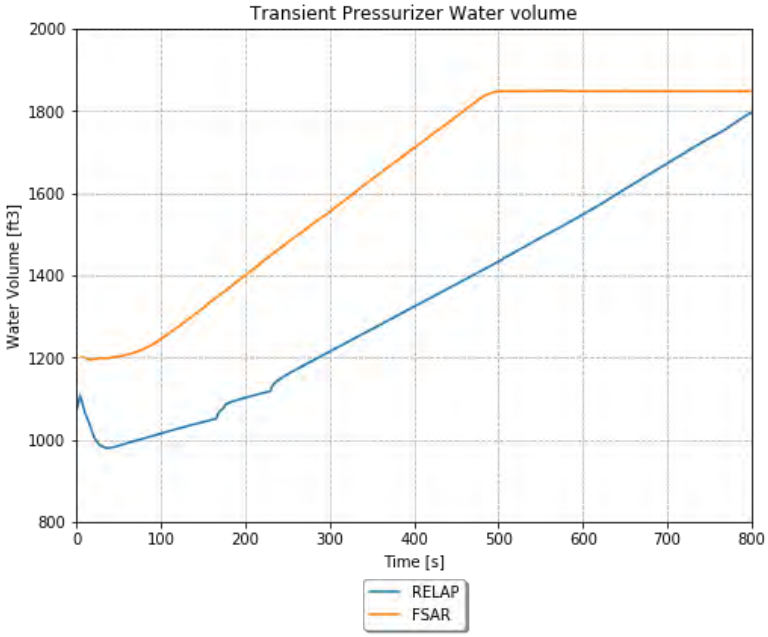

Figure 4-129. TR PRZ water volume for the inadvertent operation of the ECCS scenario (e.g., the PF H TAVG case).

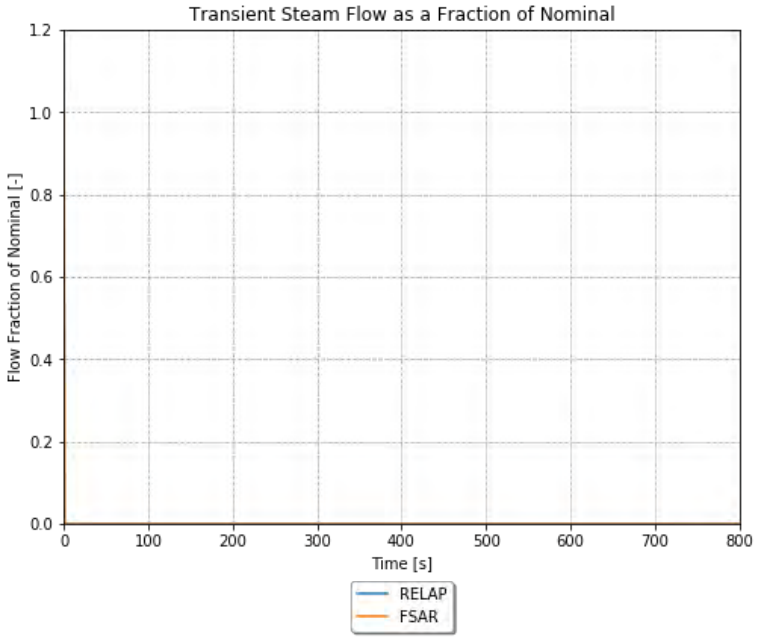

Figure 4-130. TR steam flow as a fraction of nominal for the inadvertent operation of the ECCS scenario (e.g., the PF H TAVG case).

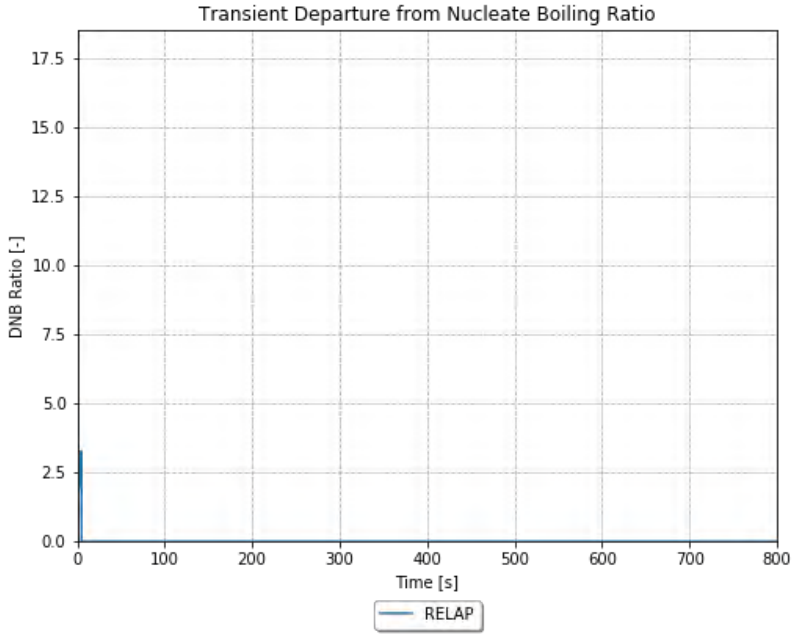

Figure 4-131. TR DNBR for the inadvertent operation of the ECCS scenario (e.g., the PF H TAVG case).

4.11.5.3 PF L TAVG Case Results

The TR PRZ pressure is shown in Figure 4-132. After the initial decrease, the RELAP5-3D run repressurizes and then depressurizes greatly and stays under pressure compared to the FSAR until roughly 350 seconds when it goes through a cycle of the PRZ safety valve. The FSAR run pressure flattens out for several hundred seconds before going through its PRZ safety valve cycles. The large dip in pressure greatly effects the runs and is seen in all the following plots as well.

The TR core power as a fraction of nominal is shown in Figure 4-133. The power is nearly identical between RELAP5-3D and the FSAR.

The TR maximum clad temperature is shown in Figure 4-134. There is no FSAR plot for this. The cladding temperature immediately drops significantly, and then more or less flattens out after reactor trip.

The TR hot spot oxidation is shown in Figure 4-135. There is no FSAR plot for this. There is no appreciable oxidation accrual during the TR.

The TR average core moderator temperature is shown in Figure 4-136. The RELAP5-3D run initially decreases significantly more than the FSAR run and then also increases significantly less, resulting in it never really flattening out, and staying at a consistently lower temperature.

The TR PRZ water volume is shown in Figure 4-137. A fairly significant difference develops in the first 200 seconds, which sees the RELAP5-3D run with significantly less volume. The FSAR run increases much faster. This results in the FSAR run hitting maximum volume and the RELAP5-3D run never hits the maximum.

The TR steam flow as a fraction of nominal is shown in Figure 4-138. The TRs are the same with the steam being turned off immediately due to immediate reactor trip.

The TR DNBR is shown in Figure 4-139. There is no FSAR plot for this. The RELAP5-3D run goes to 0 in the first couple of seconds. In RELAP5-3D, this indicates that the heat structure is in a HT mode, which does not even calculate CHF (i.e., single-phase liquid). As such, this is consistent with the very high DNBR observed in the FSAR run.

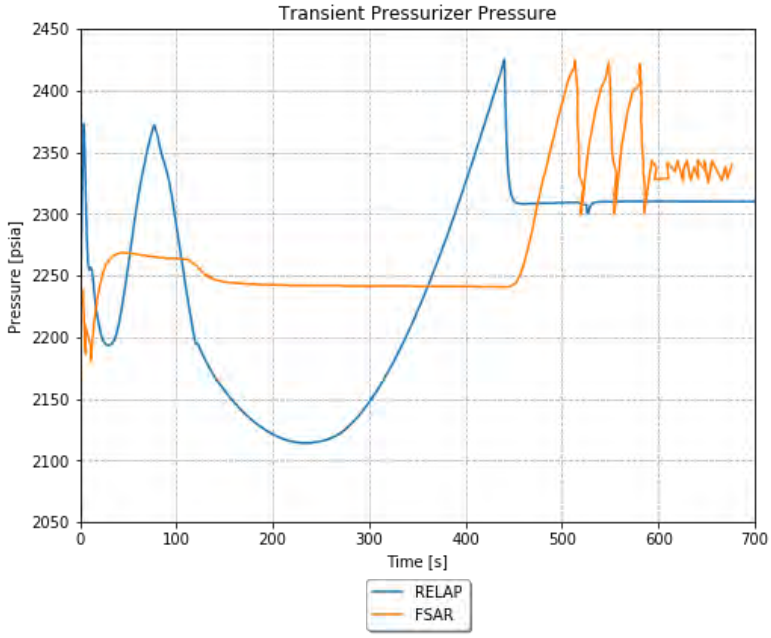

Figure 4-132. TR PRZ pressure for the inadvertent operation of the ECCS scenario (e.g., the PF L TAVG case).

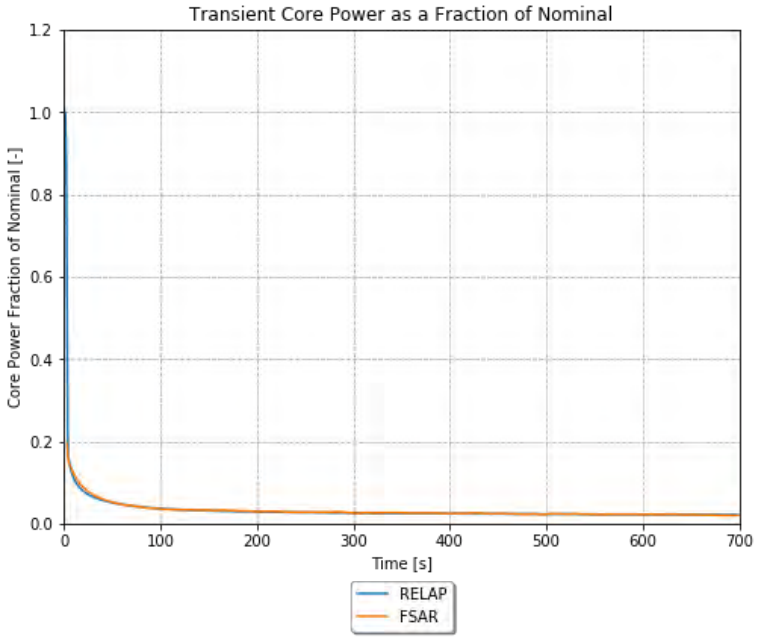

Figure 4-133. TR core power as a fraction of nominal for the inadvertent operation of the ECCS scenario (e.g., the PF L TAVG case).

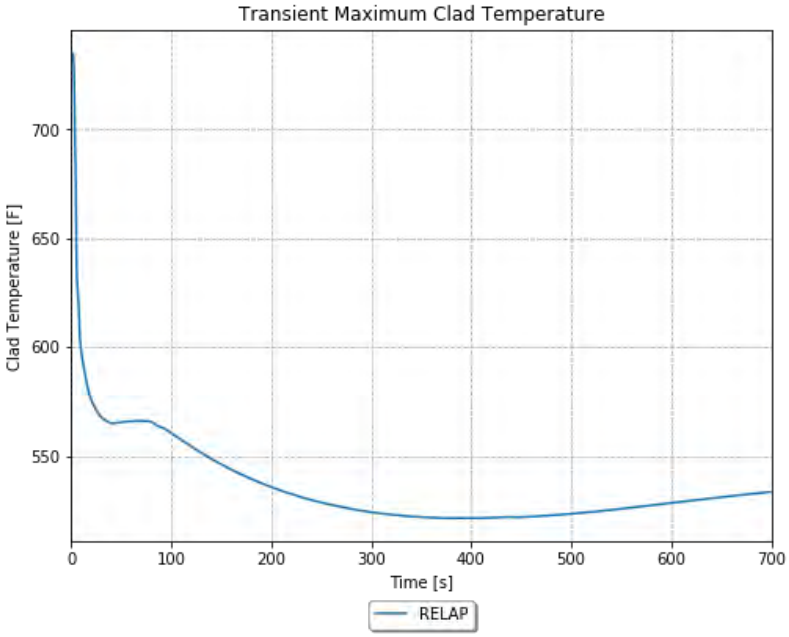

Figure 4-134. TR maximum cladding temperature for the inadvertent operation of the ECCS scenario (e.g., the PF L TAVG case).

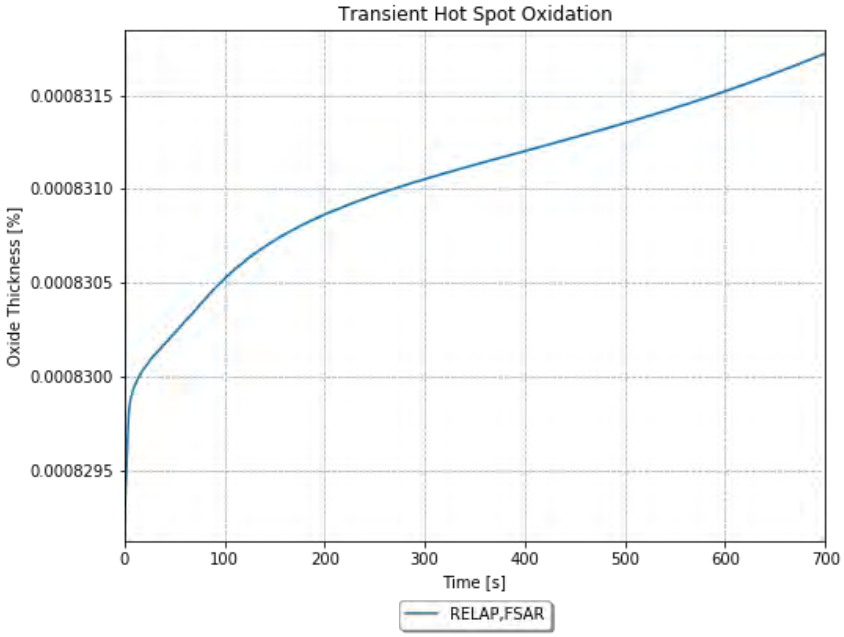

Figure 4-135. TR hot spot oxidation for the inadvertent operation of the ECCS scenario (e.g., the PF L TAVG case).

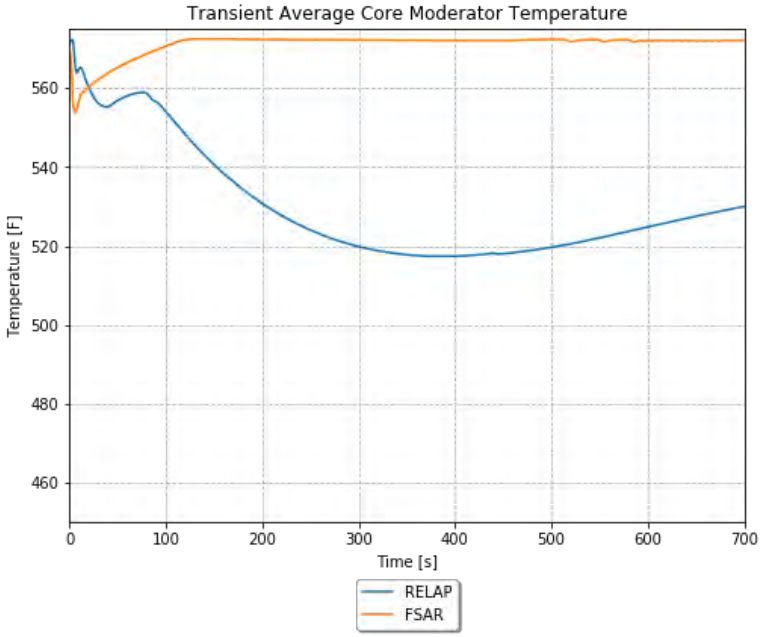

Figure 4-136. TR average core moderator temperature for the inadvertent operation of the ECCS scenario (e.g., the PF L TAVG case).

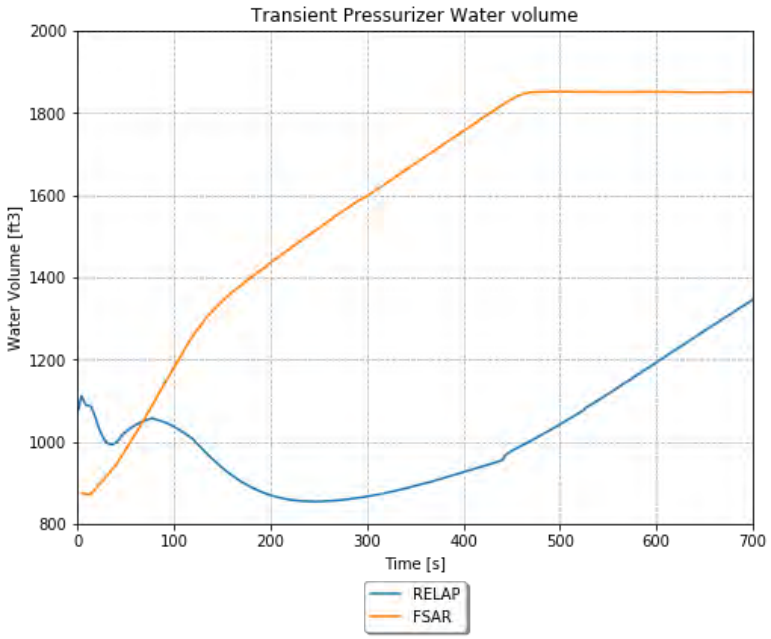

Figure 4-137. TR PRZ water volume for the inadvertent operation of the ECCS scenario (e.g., the PF L TAVG case).

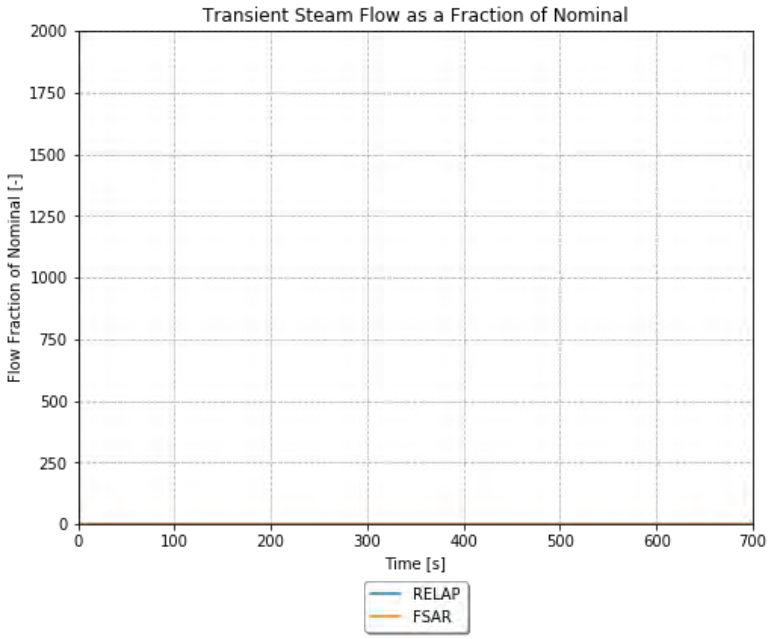

Figure 4-138. TR steam flow as a fraction of nominal for the inadvertent operation of the ECCS scenario (e.g., the PF L TAVG case).

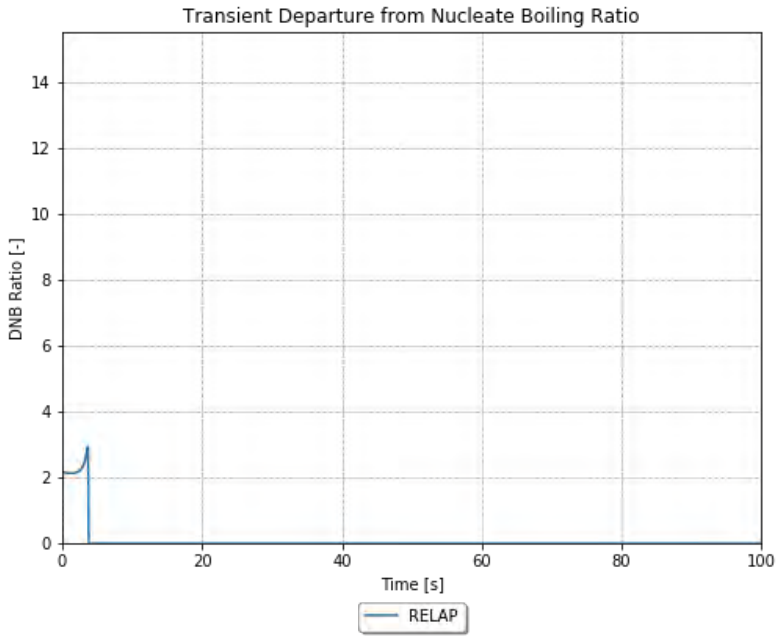

Figure 4-139. TR DNBR for the inadvertent operation of the ECCS scenario (e.g., the PF L TAVG case).

4.11.6 Adherence to Acceptance Criteria

The final results for the inadvertent operation of the ECCS TRs are compared to the results from the FSAR and the acceptance criteria in Table 4-18. The acceptance criteria are based on examination of the FSAR sections, and the applicable sections of the standard review plan.

Table 4-18. Inadvertent operation of the ECCS final results.

Result	FSAR (DNBR)	RELAP5-3D (DNBR)	FSAR (PF H)	RELAP5-3D (PF H)	FSAR (PF L)	RELAP5-3D (PF L)	Acceptance Criteria
Maximum RCS Pressure [psia]	~2320	2425	~2440	2435	~2400	2450	2750
Minimum DNBR [-]	~2.2	~2	~2	~2	N/A	~2	1.24
PSV Cycles [-]	0	2	3	2	3	2	3

The RELAP5-3D simulations meet all acceptance criteria for this scenario. Some of the potential input differences between the FSAR simulations and the RELAP5-3D simulations are discussed in the following section. These may drive some of the differences in results between the FSAR analysis and the RELAP5-3D simulations, in addition to code differences.

4.11.7 Scenario-Specific Limitations and Conditions for Usage

The following limitations apply specifically to the inadvertent operation of the ECCS case:

- No information is given on the feedwater or flow rates, so assumed values for delays and ramping are used. In addition, no AFW is modeled.
- The MDC and FTC of reactivity are adjusted to give reasonable core power prediction.
- The PRZ PORV and safety valve are both modeled to only remove vapor. This is ordinarily not a problem, but it causes the PRZ pressure to rapidly increase once the PRZ is liquid solid. This should be updated in the future.

- The initial boron concentrations of the RCS and RWST are unknown, so reasonable values are assumed.

4.12 Feedwater System Malfunctions that Result in an Increase in Feedwater Flow

The addition of excessive feedwater will cause an increase in core power by decreasing reactor coolant temperature. The thermal capacity of the secondary plant and the RCS attenuates such TRs. The SG high-high water level signal terminates the excessive feedwater flow. It also initiates a turbine trip that results in a reactor trip and trips of the SG feedwater pumps. Should the turbine trip not initiate a reactor trip, the subsequent reduction in SG water level will initiate a reactor trip on the SG low-low level.

The full opening of a feedwater regulating valve due to a feedwater control system malfunction or an operator error may cause excessive feedwater flow. At power conditions, this excess flow causes a greater load demand on the RCS due to increased subcooling in the SG. With the plant at no-load conditions, the addition of cold feedwater may cause a decrease in RCS temperature, and thus. a reactivity insertion because of the negative moderator temperature coefficient of reactivity.

The SG high-high water level ESF signal does the following:

- Closes the feedwater valves.
- Closes the feedwater pump discharge valves.
- Trips the turbine.
- Trips the main feedwater pumps.
- Prevents the continuous addition of excessive feedwater.
- The turbine trip signal initiates a reactor trip.

Feedwater system malfunctions that result in an increase in feedwater flow are classified as ANS Condition II events, fault of moderate frequency.

4.12.1 Scenario-Specific Inputs in the TR Input File

The TR input file is defined as follows:

- Upfront cards are included that specify this is a restart TR run, which uses the last available printout in the restart file.
- The end time is set to 200 seconds, consistent with the analysis in the reference plant FSAR. The max time step is set to 0.05 seconds, as this is a value that is reasonable for a relatively stable simulation such as this.
- The minor edits are used to specify the variables used in the plots.
- CV 405 (e.g., the reactivity controller) is listed as a constant value of 0.0 $. This is done as a placeholder for RAVEN to substitute in the actual end of SS value of CV 405 using the RAVEN variable “ssreact.” This step is necessary to turn off the reactivity controller, but makes the SS reactivity adder persist.
- The pump inputs are specified using CVs 419 through 422 (e.g., the pump speed), which are set to a constant value that is replaced using the RAVEN variable “sspmpvel.”
- CVs 435 through 438 (e.g., the steam valve position) are changed to be functions of General Table 650. This allows them to be set to the SS valve position prior to the reactor trip or SI signal, and then close based on the specified delay and ramp times.

- CVs 459 through 462 (e.g., the MFW flow rate) are listed as constant values of 1118.9 lbm/sec. This is done as a placeholder for RAVEN to substitute in the actual end of SS values of CVs 459 through 462 using the RAVEN variable “ssmfw.”
- CV 472 is listed as a constant value of 0.0. This is used to turn off the SS charging flow.
- CV 473 is listed as a constant value of 0.0. This is used to turn off the SS letdown flow.
- CV 482 is listed as a constant value of 0.0. This is used to turn off the SS PRZ heater.
- CV 483 is listed as a constant value of 0.0. This is used to turn off the SS PRZ spray.
- CV 641 is listed as a constant value of 0.0. This is used to disable the PRZ PORV.
- CV 60 is copied from the SS input, and two additional cells are added to the calculation. This was done because previously, the SG level calculation maxed out at a value insufficient to trigger the SG high level trip.
- Trip 501 is listed to trip when CV 60 (e.g., the SG level) is greater than or equal to 48.217 ft. Note that this is an arbitrary setpoint used to get timing relatively consistent with the FSAR analysis.
- Trip 640 is listed to trip when Trip 501 and Trip 402 are true. Since Trip 402 is always true, this changes Trip 640 to trip when Trip 501 is true.
- General Table 640 is listed with values identical to the SS input. This input does not necessarily need to be here, but it is generically listed in the TR input files to allow the analyst to change the trip used for MFW.
- General Table 650 is listed, with values identical to the SS input. This input needs to be here so that the first three valve position entries in the table can be replaced with the end of SS values using the RAVEN variable “ssstmvlv.” This step is necessary to turn off the steam flow controller, but have the SS steam flow persist.

4.12.2 Scenario-Specific RAVEN Inputs

The RAVEN distribution means are set as shown in

Table 4-19. The inputs are consistent with the FSAR, as described below. The remaining inputs are assumptions that are not specifically mentioned in the FSAR:

- The SS conditions are generally set to analysis-specific values from the FSAR.
- The MFW is set to ramp down over 1 second after the high SG level SI trip, and then the AFW never comes on.
- An MDC of 0.5 $\Delta k/g/cm^3$ is used.
- The reactor trip is set to occur on low SG level of 27.1 ft., while all other trips are disabled.
- The MSIV is immediately ramped down over 1 second from the reactor trip time.
- The pump motors are set to never trip.
- The PRZ safety valve opening pressure is set to 2574.0 psia, as this pressure is just below the next point in the table (2575 psia), and it is not expected that the pressure will reach this point.

Table 4-19. Summary of RAVEN inputs for feedwater system malfunctions.

Distribution	Description	Unit	Mean
cltempdist	Cold Leg Temperature	°F	556.9
corepdist	Core Power	W	3.643E+09
fwtempdist	Feedwater Temperature	°F	448.7
hltempdist	Hot Leg Temperature	°F	619.9
przleveldist	PRZ Level	ft.	29.4
przpressdist	PRZ Pressure	psia	2250
rcsflowdist	RCS Volumetric Flow	gpm	9.56E+04
rcsmflodist	RCS Mass Flow	lbm/sec	9684.028
rcsmflorrdist	RCS Mass Flow in Vessel	lbm/sec	-9684.028
sgleveldist	SG Level	ft.	40.1
stmpressdist	SG Steam Pressure	psia	941
sgflowdist	SG Flow Rate	lbm/sec	1132.639
dpvessdist	Vessel Pressure Drop	psi	46.5
dphldist	Hot Leg Pressure Drop	psi	1.2
dpxldist	Crossover Leg Pressure Drop	psi	3.1
dpcldist	Cold Leg Pressure Drop	psi	3.3
dpsgdist	SG Primary Pressure Drop	psi	45.5
corbypdist	Core Bypass Flow	%	5
przphirxtdist	High PRZ Pressure Reactor Trip Setpoint	psia	1.00E+09
przplorxtdist	Low PRZ Pressure Reactor Trip Setpoint	psia	-1.00E+09
przlhirxtdist	High PRZ Level Reactor Trip Setpoint	ft.	1.00E+09
rcsflolorxtdist	Low RCS Flow Rate Reactor Trip Setpoint	lbm/sec	-1.00E+09
sglevlorxtdist	Low SG Level Reactor Trip Setpoint	ft.	27.1
mfwdeltimedist	MFW Delay Time	sec	0.001
mfwramptimedist	MFW Ramp Time	sec	1
afwdeltimedist	AFW Delay Time	sec	1.00E+08
afwramptimedist	AFW Ramp Time	sec	1.00E+08
afwflodist	AFW Flow Rate	lbm/sec	105.65
pmpmotdeldist	Pump Motor Trip Delay Time	sec	1.00E+09
achfluxdist	Average Channel Maximum SS Heat Flux	BTU/sec-ft^2	99.954
hchfluxdist	Hot Channel Maximum SS Heat Flux	BTU/sec-ft^2	164.93
initreactdist	Initial Reactivity	$	0
mdcdist	Moderator Density Coefficient	Δk/g/cm^3	0.5
accbordist	Accumulator Boron Concentration	Mass Frac	1.90E-03
chgbordist	Charging Boron Concentration	Mass Frac	2.60E-03
accvoldist	Accumulator Water Volume	ft^3	900
acctempdist	Accumulator Temperature	°F	120
accpressdist	Accumulator Pressure	psia	600

Distribution	Description	Unit	Mean
sitrplspdist	Low Steam Pressure SI Signal	psia	-1.00E+09
sitrpdeldist	SI Signal Delay Time	sec	0.1
msivdeldist	MSIV Delay Time	sec	0.001
msivrampdist	MSIV Ramp Time	sec	1
rccadeldist	RCCA Delay Time	sec	1
rcpheatdist	RCP Heat Generation	MW	1.00E-05
przsafdist	PRZ Safety Valve Open Pressure	psia	2574
rcsbordist	RCS Initial Boron Concentration	Mass Frac	8.82E-04

4.12.3 Steady State Results

The steady state observations for the feedwater malfunction are explained in detail in FY-2020 [2].

4.12.4 TR Boundary Conditions

The TR boundary conditions for the feedwater malfunction are explained in detail in FY-2020 [2].

4.12.5 TR Results

The RELAP5-3D results are compared to the run from the FSAR in the paragraphs below.

The TR PRZ pressure is shown in Figure 4-140. The RELAP5-3D run pressurizes earlier than the FSAR run due to the earlier reactor trip; the PRZ is higher, but much shorter in duration.

The TR hot rod heat flux as a fraction of nominal is shown in Figure 4-141. The RELAP5-3D run has a much smaller heat flux increase and the reactor trips earlier.

The TR core power as a fraction of nominal is shown in Figure 4-142. The RELAP5-3D run has a much smaller power increase and the reactor trips earlier.

The TR maximum cladding temperature is shown in Figure 4-143. There is no FSAR plot for this. The RELAP5-3D run continues at the SS temperature until the reactor trip.

The TR hot spot oxidation is shown in Figure 4-144. There is no FSAR plot for this. There is no significant oxidation accrual during this TR.

The TR average core moderator temperature is shown in Figure 4-145. The RELAP5-3D run encounters a much smaller increase in temperature, and decreases earlier, due to the earlier reactor trip.

The TR DNBR is shown in Figure 4-146. The DNBR is similar prior to reactor trip, and in both cases, it increases after trip. The RELAP5-3D run immediately goes to 0 after trip. In RELAP5-3D, this indicates that the heat structure is in a HT mode, which does not even calculate CHF (i.e., single-phase liquid). As such, this is consistent with the very high DNBR observed in the FSAR run.

The TR reactor vessel change in temperature is shown in Figure 4-147. The TRs are very similar, except that the RELAP5-3D run decreases much earlier due to the earlier reactor trip.

The TR fuel centerline temperature is shown in Figure 4-148. There is no FSAR plot for this. The fuel centerline temperature continues at approximately the SS temperature until reactor trip, when it drops very quickly.

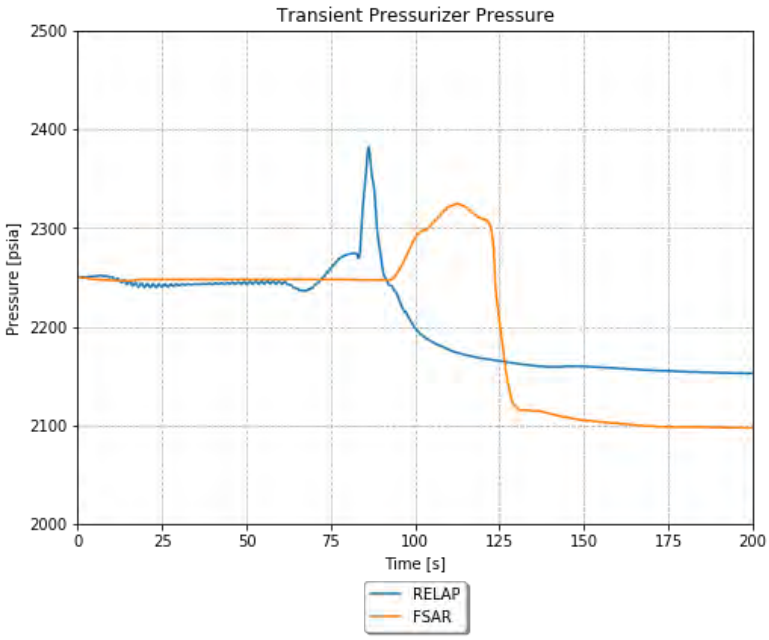

Figure 4-140. TR PRZ pressure for the feedwater malfunction scenario.

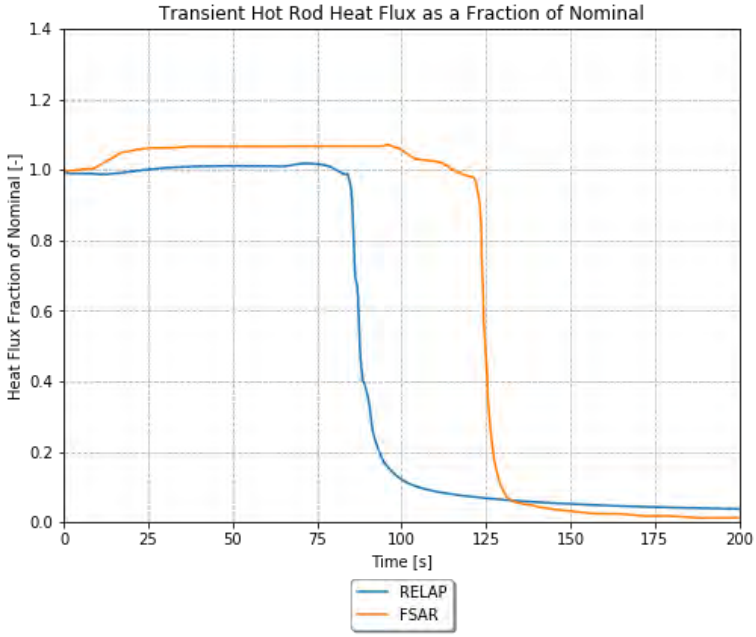

Figure 4-141. TR hot rod heat flux as a fraction of nominal for the feedwater malfunction scenario.

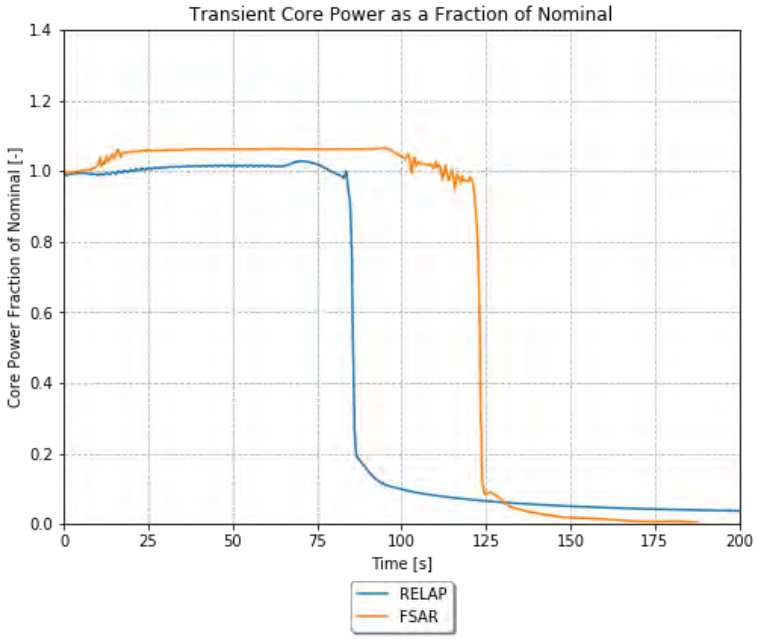

Figure 4-142. TR core power as a fraction of nominal for the feedwater malfunction scenario.

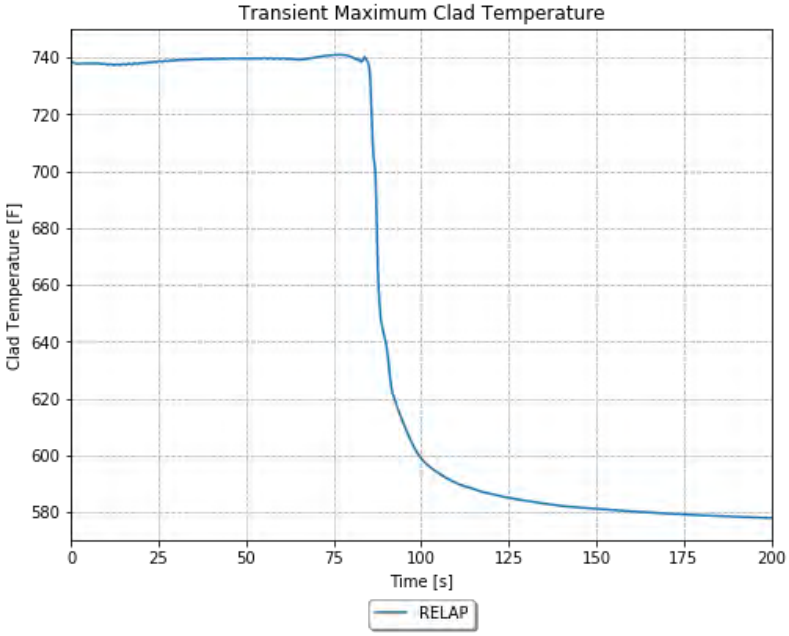

Figure 4-143. TR maximum clad temperature for the feedwater malfunction scenario.

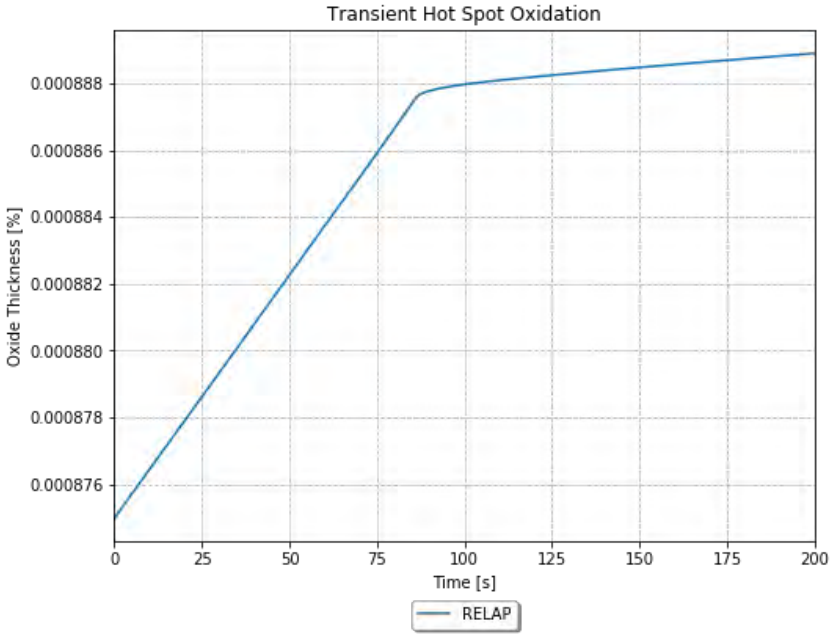

Figure 4-144. TR hot spot oxidation for the feedwater malfunction scenario.

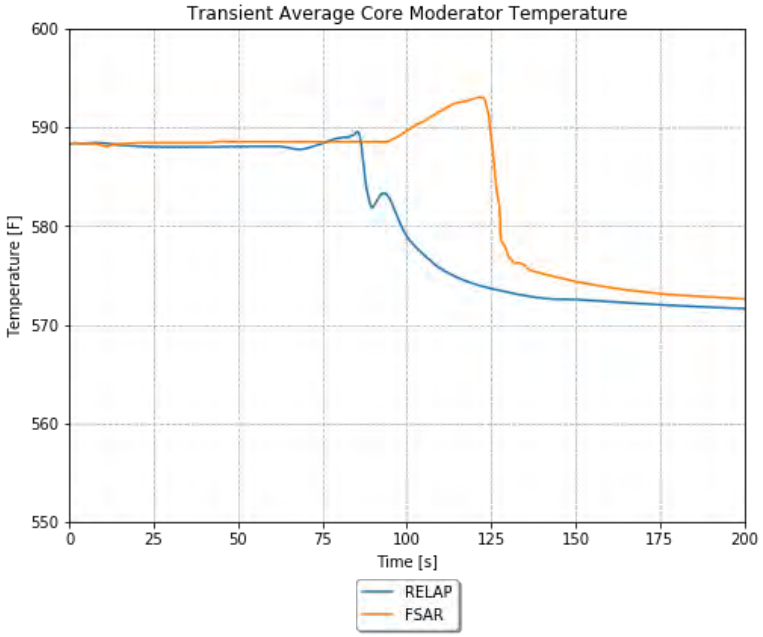

Figure 4-145. TR average core moderator temperature for the feedwater malfunction scenario.

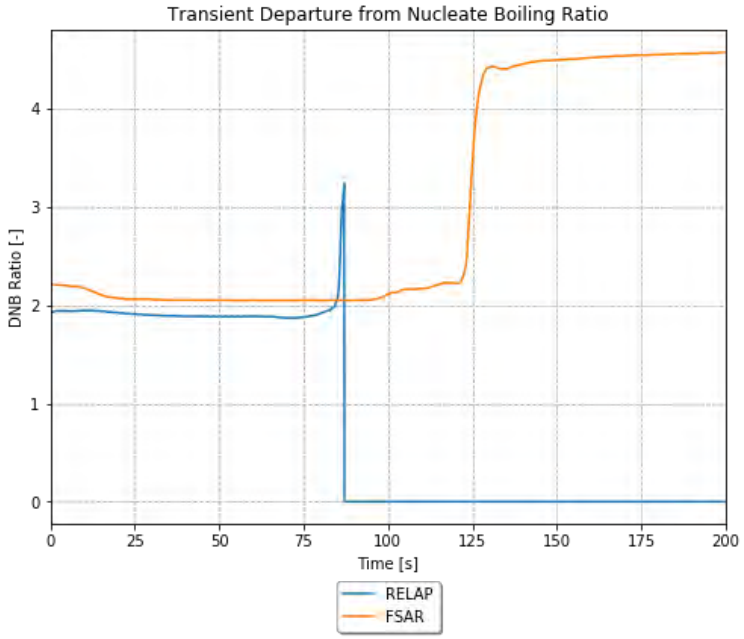

Figure 4-146. TR DNBR for the feedwater malfunction scenario.

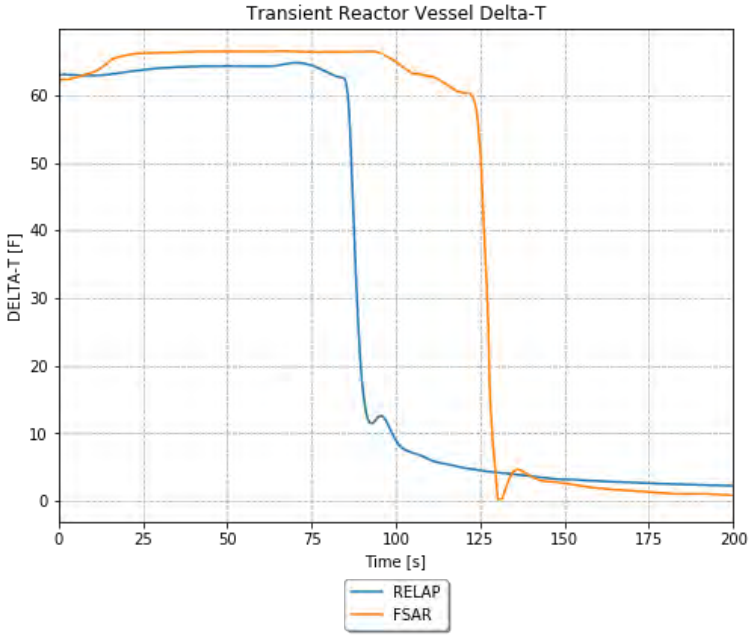

Figure 4-147. TR reactor vessel change in temperature for the feedwater malfunction scenario.

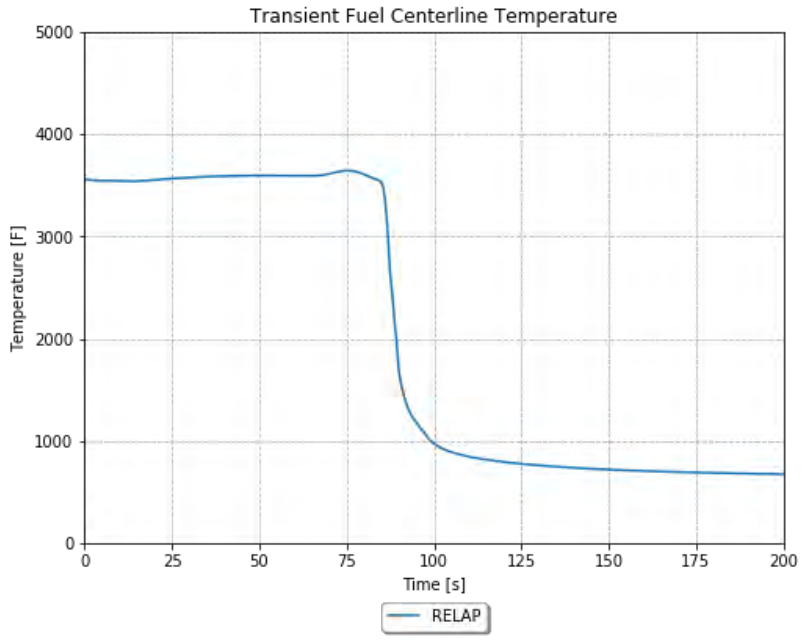

Figure 4-148. TR fuel centerline temperature for the feedwater malfunction scenario.

4.12.6 Adherence to Acceptance Criteria

The final results for the feedwater malfunction are compared to the results from the FSAR and the acceptance criteria in Table 4-20. The acceptance criteria are based on examination of the FSAR sections, and the applicable sections of the standard review plan.

Table 4-20. LOCA final results.

Result	FSAR	RELAP5-3D	Acceptance Criteria
RCS Maximum Pressure [psia]	~2325	2380	2750
DNBR [-]	~2	~1.8	1.24
Fuel Centerline Temperature [°F]	N/A	~3700	4700

The RELAP5-3D simulations meet all acceptance criteria for the feedwater malfunction scenario. Some of the potential input differences between the FSAR simulations and the RELAP5-3D simulations are discussed in following section. These may drive some of the differences in results between the FSAR analysis and the RELAP5-3D simulations, in addition to code differences.

4.12.7 Scenario-Specific Limitations and Conditions for Usage

The following limitations apply specifically to the feedwater malfunction case:

- The SG level setpoints (high-high and low-low) are unknown, but reasonable values are assumed. Note that the timing differences from the FSAR run observed in this case are primarily due to the uncertainty on this setpoint, as it determines the timing.
- No information is given on the rate of turning off the MFW or main steam, but short ramps are assumed.
- The FTC may not be consistent with the FSAR analysis.
- As it is not explicitly mentioned in the FSAR section, all SI is assumed inoperable.

- As they are not explicitly mentioned in the FSAR section, all PRZ pressure controlling systems are assumed inoperable.

4.13 Steam Generator Tube Failure

This event is referred to as a steam generator tube rupture (SGTR).

The accident that is examined is the complete severance of a single SG tube. This event is considered an ANS Condition IV event, a limiting fault. The accident is assumed to take place at full power with the reactor coolant contaminated with fission products corresponding to continuous operation with a limited number of defective fuel rods. The accident leads to an increase in contamination of the secondary system due to leakage of radioactive coolant from the RCS. In the event of a coincident LOOP or failure of the condenser steam dump system, discharge of activity to the atmosphere takes place via the SG power-operated relief valves, as well as safety valves if their setpoint is also reached.

The operator is expected to determine that an SGTR has occurred, to identify and isolate the faulted SG, and to complete the required recovery actions to stabilize the plant and terminate the primary to secondary break flow. These actions should be performed on a restricted time-scale in order to minimize contamination of the secondary system and ensure termination of radioactive release to the atmosphere from the faulted unit.

Consideration of the indications provided at the control board, together with the magnitude of the break flow, leads to the conclusion that the recovery procedure can be carried out on a time-scale that ensures break flow to the secondary system is terminated before water level in the affected SG rises into the main steam pipe. Sufficient indications and controls are provided to enable the operator to carry out these functions satisfactorily.

If normal operation of the various plant control system is assumed, the following sequence of events is initiated by a tube rupture:

1. PRZ low pressure and low-level alarms are actuated and charging pump flow increases to maintain PRZ level. On the secondary side, steam flow/feedwater flow mismatch occurs since feedwater flow to the affected SG is reduced because of primary coolant break flow to that unit.
2. The main steamline radiation monitors, condenser air ejector radiation monitor, and/or SG blowdown liquid monitor will alarm, indicating a sharp increase in radioactivity in the secondary system. The high radiation level alarm from the SG blowdown process monitor automatically isolates the system and terminates discharge. The high radiation level alarm from the air ejector monitor automatically diverts the air ejector and steam seal exhauster blower discharges through a filtration unit.
3. The decrease in RCS pressure due to continued loss of reactor coolant inventory leads to a reactor trip signal on low PRZ pressure or OTΔT. Resultant plant cooldown following reactor trip leads to a rapid decrease in RCS pressure and PRZ level, and a SI signal initiated by low PRZ pressure follows soon after reactor trip. The SI signal automatically terminates normal feedwater supply and initiates auxiliary feedwater addition.
4. The reactor trip automatically trips the turbine, and if OPA, the steam dump valves open, permitting steam dump to the condenser. In the event of a coincident LOOP, the steam dump valves automatically close to protect the condenser. The SG pressure rapidly increases, resulting in steam discharge to the atmosphere through the SG power-operated relief valves, as well as the safety valves if their setpoint is reached.
5. Following reactor trip and SI actuation, the continued action of the auxiliary feedwater supply and borated SI flow—supplied from the refueling water storage tank—provides a heat sink that absorbs some of the decay heat. This reduces the amount of steam bypass to the condenser, or in the case of LOOP, steam relief to the atmosphere.

SI flow results in increasing RCS pressure and PRZ water level. The RCS pressure trends toward the equilibrium value where the SI flow rate equals the break flow rate.

4.13.1 Scenario-Specific Inputs in the TR Input File

The TR input file is defined as follows:

- Upfront cards are included that specify this is a restart TR run, which uses the last available printout in the restart file.
- The end time is set to 6000 seconds, consistent with the analysis in the reference plant FSAR. The max time step is set to 0.05 seconds, as this is a value that is reasonable for a relatively stable simulation such as this.
- The minor edits are used to specify the variables used in the plots.
- CV 405 (e.g., the reactivity controller) is listed as a constant value of 0.0 $. This is done as a placeholder for RAVEN to substitute in the actual end of SS value of CV 405 using the RAVEN variable “ssreact.” This step is necessary to turn off the reactivity controller, but make the SS reactivity adder persist.
- CVs 435 through 438 (e.g., the steam valve position) are changed to be functions of General Table 650. This allows them to be set to the SS valve position prior to the reactor trip or SI signal, and then close based on the specified delay and ramp times.
- CVs 459 through 462 (e.g., the MFW flow rate) are listed as constant values of 1118.9 lbm/sec. This is done as a placeholder for RAVEN to substitute in the actual end of SS values of CVs 459 through 462 using the RAVEN variable “ssmfw.”
- CV 472 is listed as a constant value of 0.0. This is used to turn off the SS charging flow.
- CV 473 is listed as a constant value of 0.0. This is used to turn off the SS letdown flow.
- CV 482 is listed as a constant value of 0.0. This is used to turn off the SS PRZ heater.
- CV 483 is listed as a constant value of 0.0. This is used to turn off the SS PRZ spray.
- The pump inputs are specified using Variable Trips 450 through 453, which are set to be false immediately, so the motor trip takes precedence. This is done by setting them to trip at a time greater than or equal to 1E9 seconds in the TR input file.
- Trip 410 is listed as a time greater than or equal to 43.8 seconds. This is done to represent the time of reactor trip from the FSAR analysis.
- The following inputs are related to modeling the SI:
    - In order to trigger the initial SI, Trip 470 is specified to be CV 180 less than 1920 psia. This number is based on the approximate RCS pressure from the FSAR analysis at the time of SI actuation. Note that due to the re-specification of Trip 631, the SI delay value is unused, and no delay is implemented.
    - When Trip 507 is true, RCS depressurization has been completed. Thus, CV 652 is added as the time of Trip 507 plus 180 seconds.
    - Trip 508 is set as time greater than or equal to CV 652.
    - Trip 666 is set to be true when Trip 507 and Trip 508 are true.
    - Trip 631 is specified to be true when Trip 470 is true, and Trip 666 is false.

- The following inputs are related to modeling the feedwater:
  - Components 181, 281, 381, and 481 are copied into the TR input file. Dummy values are inserted into the locations of the numerics. The operators from the SS for 'afwdeltime,' 'afwramptime,' and 'afwflo' are all added to the TR as well in the 'models.xml' file. The only changes are for the trip to be set to 660 for Components 181, 281, and 381; and 661 for Component 481.
  - Trip 500 is added, which is set to be true when time is less than or equal to 1200 seconds.
  - Trip 501 is added, which is set to be true when time is less than or equal to 420 seconds.
  - Trip 660 is added, which is set to be true when Trip 500 and Trip 640 are true.
  - Trip 661 is added, which is set to be true when Trip 501 and Trip 640 are true.
- The following inputs are related to modeling the SG PORVs:
  - Three new time-dependent volumes are added: Components 464, 465, and 466. The inputs are set identical to those for Component 462.
  - Three new trip valves are added: Components 188, 288, and 488 (i.e., Loop 3 is arbitrarily chosen to be the loop without a PORV). They all supply a connection from the outlet of Cell 1 of Components 174, 274, or 474 and to the inlets of Cell 1 of Components 464, 465, and 466. The trip is set to be 662 for Components 188 and 288; and 663 for Component 488.
  - Trip 502 is set to be true when time is greater than or equal to 2702 seconds.
  - CV 650 is set to be CV 175 (e.g., the saturation temperature in the Loop 1 hot leg) minus CV 160 (e.g., temperature in the Loop 1 hot leg). Thus, it is representative of the RCS subcooling.
  - Trip 503 is set to be a time greater than or equal to 3498 seconds.
  - Trip 662 is set to be true when Trip 502 is true, and Trip 503 is false.
  - Trip 504 is set to be true when time is greater than or equal to 1202 seconds.
  - Trip 505 is set to be true when time is less than or equal to 2162 seconds.
  - Trip 663 is set to be true when Trips 504 and 505 are true.
- The following inputs are related to modeling the PRZ PORV:
  - When Trip 503 is true, RCS cooldown has been completed. Thus, CV 651 is added as the time of Trip 503 plus 300 seconds.
  - Trip 506 is set as time is greater than or equal to CV 651.
  - Trip 664 is set to be true when Trip 503 and Trip 506 are both true.
  - Trip 507 is set as pressure in Cell 1 of Component 153 is less than the pressure in Cell 1 of Component 474. This trip is set to latch.
  - Trip 665 is set to be true when Trip 664 is true, and Trip 507 is false.
  - General Table 690 is copied into the TR input file. It is changed so that it is governed by Trip 665, and the table is set to be 0 at all negative values, and 1.0 at all positive values.
  - CV 641 is copied into the TR input file and is changed to be a function of time with Table 690.
- General Table 640 is listed with values identical to the SS input. This input does not necessarily need to be here, but it is generically listed in the TR input files to allow the analyst to change the trip used for MFW.

- General Table 650 is listed with values identical to the SS input. This input needs to be here so that the first three valve position entries in the table can be replaced with the end of SS values using RAVEN variable “ssstmvlv.” This step is necessary to turn off the steam flow controller, but have the SS steam flow persist.
- CV 849 is defined to be the mass flow rate to the atmosphere from the ruptured SG.
- CV 850 is defined to be the mass flow rate to the atmosphere from the intact SGs.
- Component 463 (e.g., the valve modeling the break between the SG tubes and the secondary side) is included in the TR input file so that it can be changed to be open.

4.13.2 Scenario-Specific RAVEN Inputs

The RAVEN distribution means are set as shown in Table 4-21. Inputs are consistent with the FSAR, as described below. Remaining inputs are assumptions that are not specifically mentioned in the FSAR:

- The SS conditions are generally set to analysis-specific values from the FSAR.
- The MFW is set to ramp down over 5 seconds after the reactor trip, and then the AFW ramps up between 30 and 35 seconds after the reactor trip. The AFW flow rate is set consistent with the FSAR analysis.
- The reactor trip is set to occur on low PRZ pressure of 1935 psia, and all other trips are disabled.
- The MSIV is immediately ramped down over 1 second from the reactor trip time.
- The pump motors are set to trip 2 seconds after reactor trip.
- The PRZ safety valve opening pressure is set to 2500.0 psia.

Table 4-21. Summary of RAVEN inputs for SGTR.

Distribution	Description	Unit	Mean
cltempdist	Cold Leg Temperature	°F	556.2
corepdist	Core Power	W	3.651E+09
fwtempdist	Feedwater Temperature	°F	448.7
hltempdist	Hot Leg Temperature	°F	620.6
przleveldist	PRZ Level	ft.	30.356
przpressdist	PRZ Pressure	psia	2200
rcsflowdist	RCS Volumetric Flow	gpm	9.36E+04
rcsmflodist	RCS Mass Flow	lbm/sec	9684.028
rcsmflorrdist	RCS Mass Flow in Vessel	lbm/sec	-9684.028
sgleveldist	SG Level	ft.	40.1
stmpressdist	SG Steam Pressure	psia	941
sgflowdist	SG Flow Rate	lbm/sec	1132.639
dpvessdist	Vessel Pressure Drop	psi	46.5
dphldist	Hot Leg Pressure Drop	psi	1.2
dpxldist	Crossover Leg Pressure Drop	psi	3.1
dpcldist	Cold Leg Pressure Drop	psi	3.3
dpsgdist	SG Primary Pressure Drop	psi	45.5
corbypdist	Core Bypass Flow	%	5
przphirxtdist	High PRZ Pressure Reactor Trip Setpoint	psia	1.00E+09

Distribution	Description	Unit	Mean
przplorxtdist	Low PRZ Pressure Reactor Trip Setpoint	psia	1935
przlhirxtdist	High PRZ Level Reactor Trip Setpoint	ft.	1.00E+09
rcsflolorxtdist	Low RCS Flow Rate Reactor Trip Setpoint	lbm/sec	-1.00E+09
sglevlorxtdist	Low SG Level Reactor Trip Setpoint	ft.	-1.00E+09
mfwdeltimedist	MFW Delay Time	sec	0.001
mfwramptimedist	MFW Ramp Time	sec	5
afwdeltimedist	AFW Delay Time	sec	3.00E+01
afwramptimedist	AFW Ramp Time	sec	3.50E+01
afwflodist	AFW Flow Rate	lbm/sec	72.863
pmpmotdeldist	Pump Motor Trip Delay Time	sec	2
achfluxdist	Average Channel Maximum SS Heat Flux	BTU/sec-ft^2	99.954
hchfluxdist	Hot Channel Maximum SS Heat Flux	BTU/sec-ft^2	164.93
initreactdist	Initial Reactivity	$	0
mdcdist	Moderator Density Coefficient	Δk/g/cm^3	-0.042
accbordist	Accumulator Boron Concentration	Mass Frac	1.90E-03
chgbordist	Charging Boron Concentration	Mass Frac	2.60E-03
accvoldist	Accumulator Water Volume	ft^3	900
acctempdist	Accumulator Temperature	°F	120
accpressdist	Accumulator Pressure	psia	600
sitrplspdist	Low Steam Pressure SI Signal	psia	800
sitrpdeldist	SI Signal Delay Time	sec	42
msivdeldist	MSIV Delay Time	sec	0.001
msivrampdist	MSIV Ramp Time	sec	1
rccadeldist	RCCA Delay Time	sec	1
rcpheatdist	RCP Heat Generation	MW	1.00E-05
przsafdist	PRZ Safety Valve Open Pressure	psia	2500
rcsbordist	RCS Initial Boron Concentration	Mass Frac	0.00E+00

4.13.3 Steady State Results

The steady state observations for the SGTR are explained in detail in FY-2020 [2].

4.13.4 TR Boundary Conditions

The TR boundary conditions for the SGTR are explained in detail in FY-2020 [2].

4.13.5 TR Results

The RELAP5-3D results are compared to the runs from the FSAR in the paragraphs below.

The TR PRZ pressure is shown in Figure 4-149. The RELAP5-3D run follows the FSAR run pretty well. Between about 1000 and 4000 seconds, the RELAP5-3D run is consistently lower than the FSAR run, but follows similar behavior. After the large depressurization at ~3800 seconds, the RELAP5-3D run continues to repressurize, while the FSAR run goes back down. This is likely because the RELAP5-3D

run never hits a point where the secondary side and primary side pressures are equal, so the SI keeps going in the RELAP5-3D run.

The TR core power as a fraction of nominal is shown in Figure 4-150. There is no FSAR plot for this. The RELAP5-3D run has a small power increase, and then a reactor trip and a reasonable decay heat curve.

The TR maximum cladding temperature is shown in Figure 4-151. There is no FSAR plot for this. The RELAP5-3D run has a short, but large temperature excursion during the initial power excursion.

The TR hot spot oxidation is shown in Figure 4-152. There is no FSAR plot for this. A non-negligible amount of oxidation is accrued during the clad temperature spike, but no appreciable oxidation is accrued after that.

The TR DNBR is shown in Figure 4-153. There is no FSAR plot for this. The DNBR is nearly always at 0 for this TR. During the power/clad temperature spike, there appears to be some movement, but it is hard to see what. It is safe to say that during the clad temperature spike, it undergoes CHF, and based on the low clad temperature for the rest of the TR, it is likely in single-phase liquid.

The TR PRZ level is shown in Figure 4-154. The RELAP5-3D run follows the FSAR run pretty well. Between about 1000 and 3500 seconds, the RELAP5-3D run is consistently lower than the FSAR run, but follows similar behavior. After the large depressurization at ~3800 seconds, the RELAP5-3D run continues to increase the level, while the FSAR run goes back down. This is likely because the RELAP5-3D run never hits a point where the secondary side and primary side pressures are equal, so the SI keeps going in the RELAP5-3D run.

The TR secondary side pressures are shown in Figure 4-155. For the intact SGs, the RELAP5-3D run follows the FSAR run very well. For the ruptured SG, the patterns that are followed are similar, but the RELAP5-3D run has significantly lower pressure. This explains why the RELAP5-3D run never actually hits the requirement that the RCS pressure get below the secondary side pressure.

The TR intact loop primary temperatures are shown in Figure 4-156. The temperatures in the RELAP5-3D run drop significantly more than those in the FSAR run, but otherwise follows the FSAR run behavior pretty well.

The TR broken loop primary temperatures are shown in Figure 4-157. The temperatures in the RELAP5-3D run drop significantly more than those in the FSAR run, but otherwise follows the FSAR run behavior pretty well.

The TR differential pressure between the RCS and the ruptured SG is shown in Figure 4-158. The RELAP5-3D run follows the FSAR run well, until the end of the TR, when the continued SI operation causes the RELAP5-3D to run to be significantly higher.

The TR mass flow between the RCS and the ruptured SG is shown in Figure 4-159. The RELAP5-3D run follows the FSAR run well, until the end of the TR, when the continued SI operation causes the RELAP5-3D to run to be significantly higher.

The TR ruptured SG water volume is shown in Figure 4-160. The general behavior is consistent between the RELAP5-3D run and the FSAR run, but the RELAP5-3D run has generally more exaggerated reactions.

The TR ruptured SG water volume is shown in Figure 4-161. The general behavior is consistent between the RELAP5-3D run and the FSAR run, but the RELAP5-3D run has generally more exaggerated reactions.

The TR mass flow to the atmosphere from the ruptured SG is shown in Figure 4-162. The general behavior is consistent between the RELAP5-3D run and the FSAR run.

The TR mass flow to the atmosphere from the intact SGs is shown in Figure 4-163. The general behavior is consistent between the RELAP5-3D run and the FSAR run.

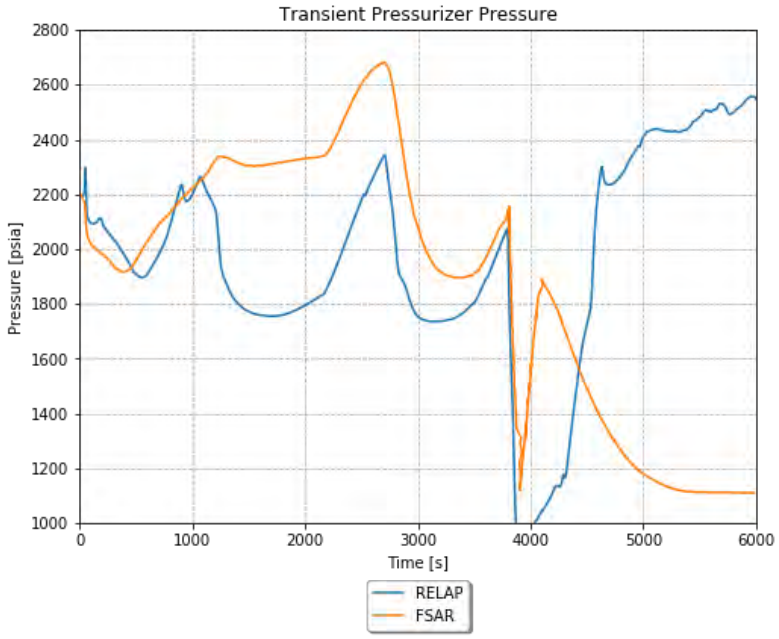

Figure 4-149. TR PZR pressure for the SGTR scenario.

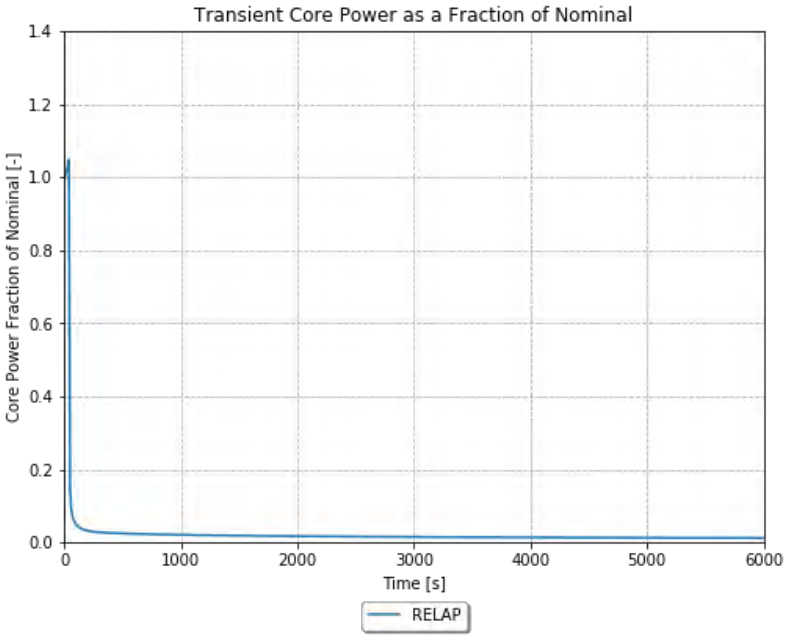

Figure 4-150. TR core power as a fraction of nominal for the SGTR scenario.

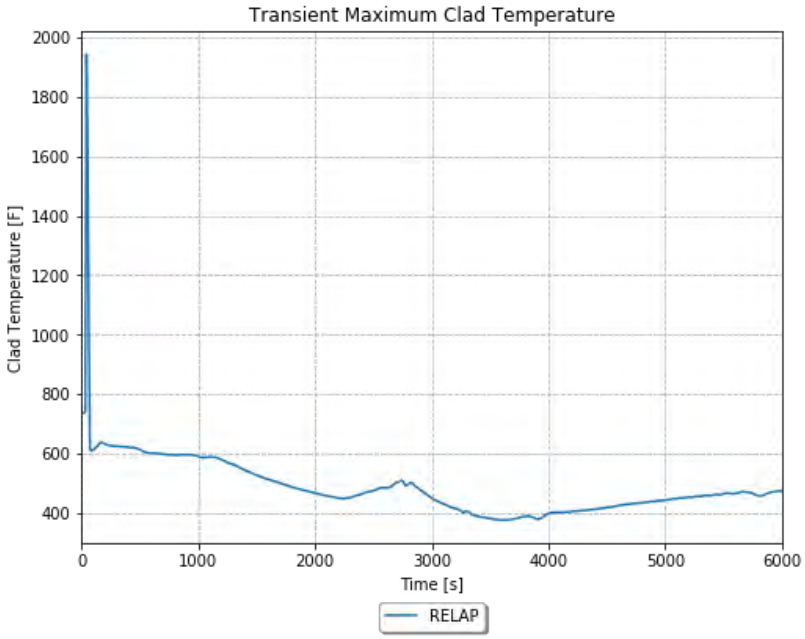

Figure 4-151. TR maximum clad temperature for the SGTR scenario.

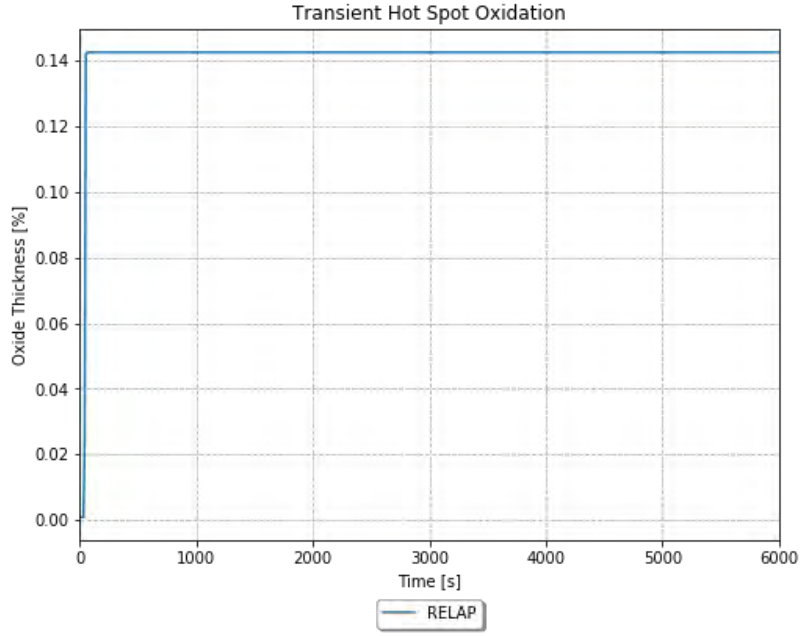

Figure 4-152. TR hot spot oxidation for the SGTR scenario.

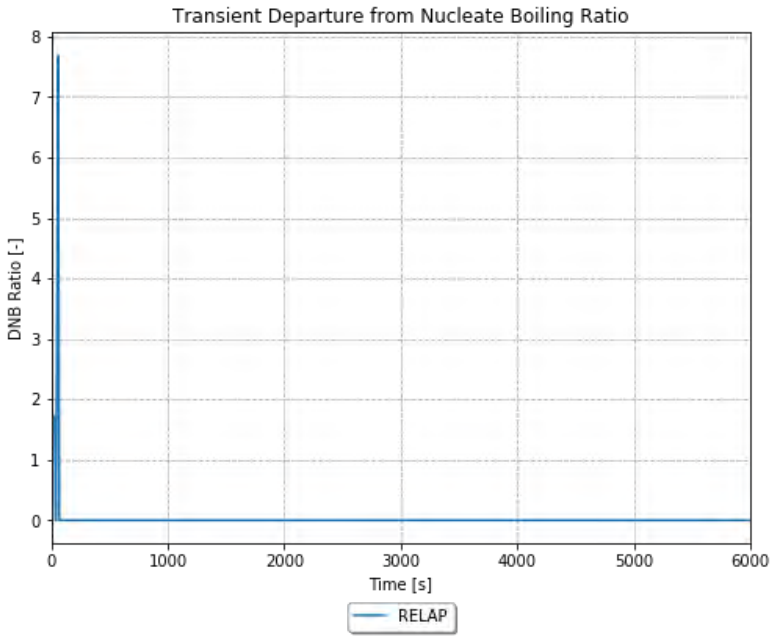

Figure 4-153. TR DNBR for the SGTR scenario.

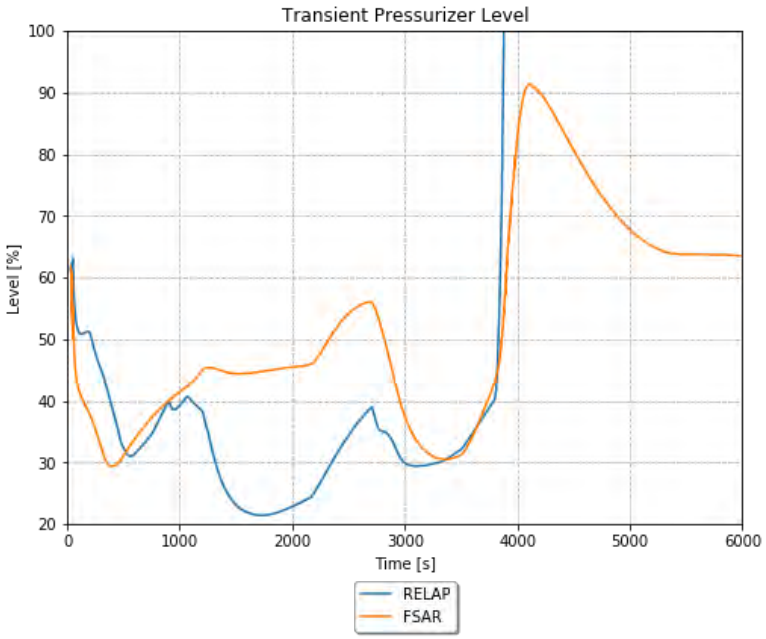

Figure 4-154. TR PRZ level for the SGTR scenario.

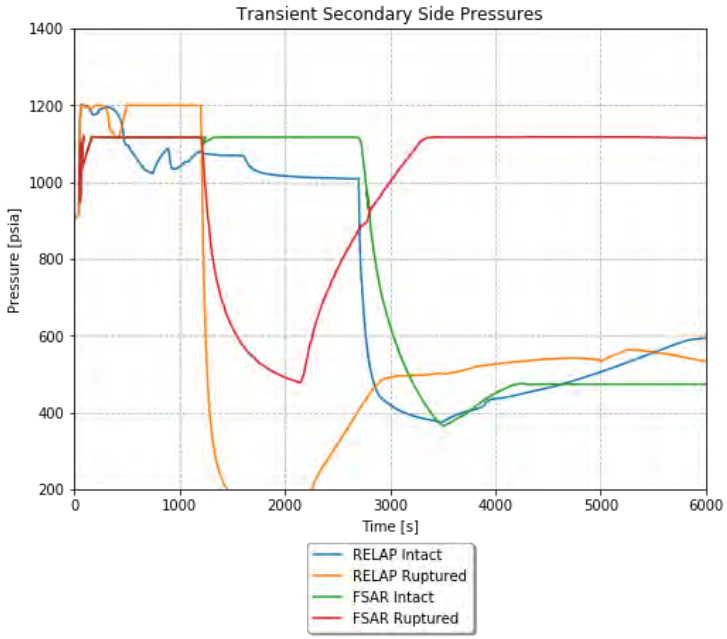

Figure 4-155. TR secondary side pressures for the SGTR scenario.

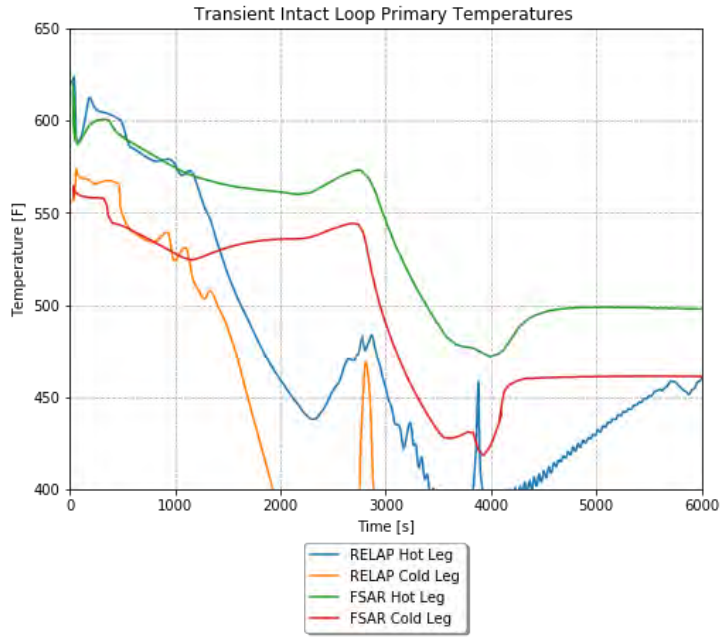

Figure 4-156. TR intact loop primary temperatures for the SGTR scenario.

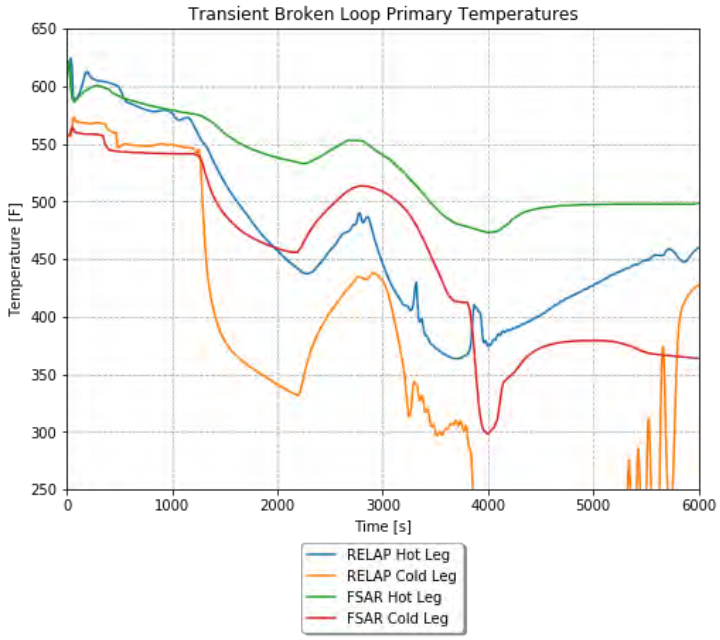

Figure 4-157. TR broken loop primary temperatures for the SGTR scenario.

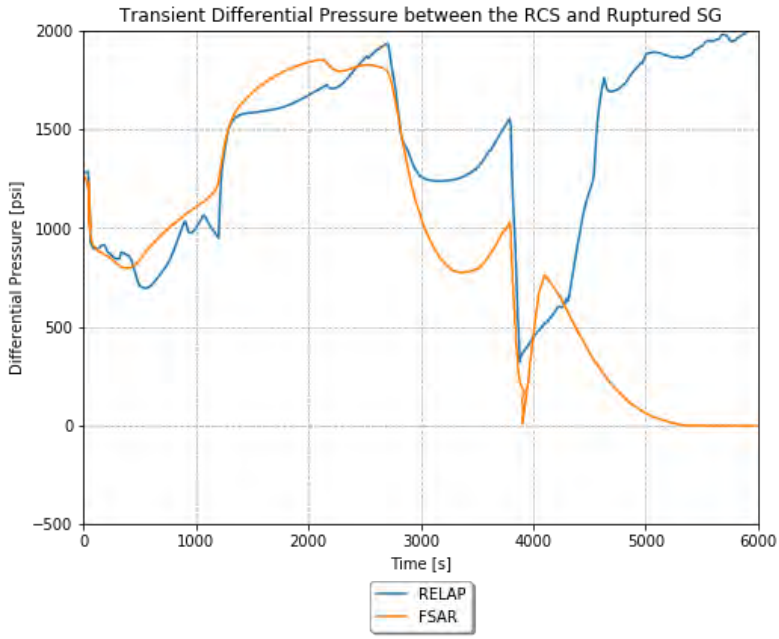

Figure 4-158. TR differential pressure between the RCS and ruptured SG for the SGTR scenario.

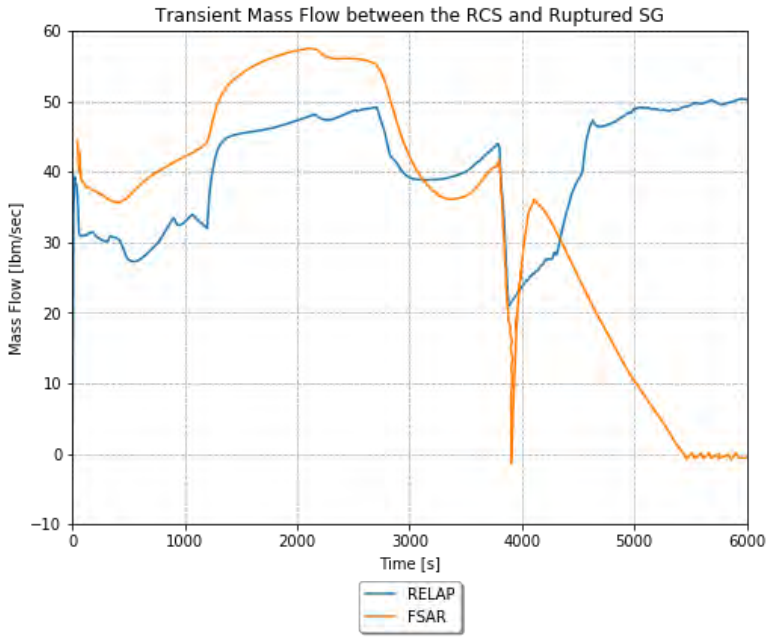

Figure 4-159. TR mass flow between the RCS and ruptured SG for the SGTR scenario.

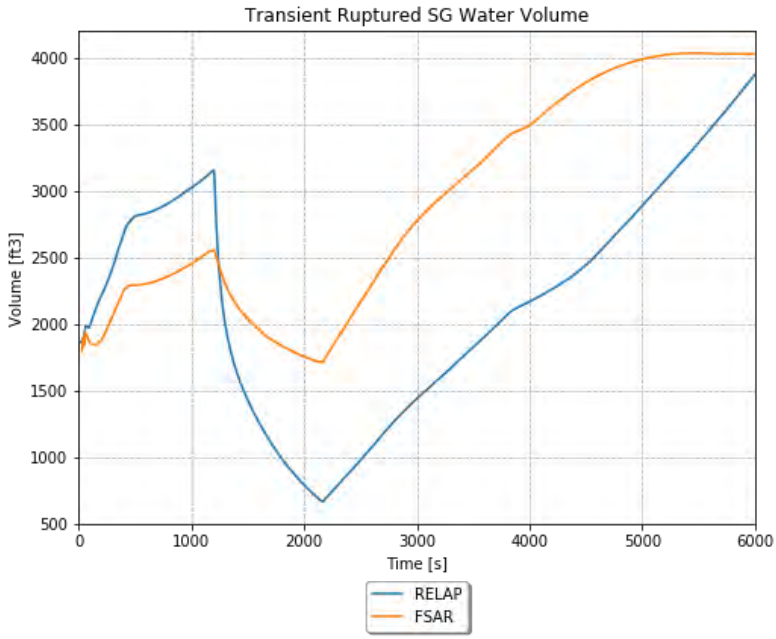

Figure 4-160. TR ruptured SG water volume for the SGTR scenario.

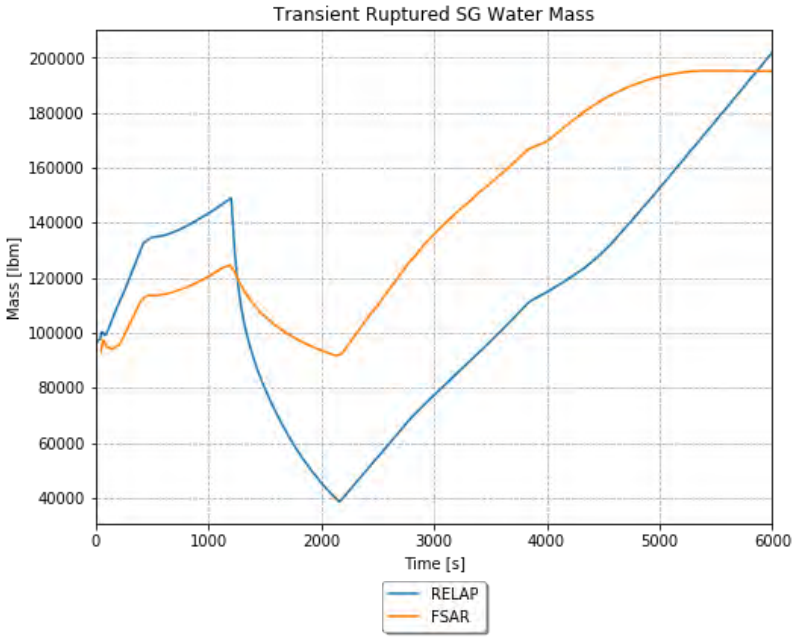

Figure 4-161. TR ruptured SG water mass for the SGTR scenario.

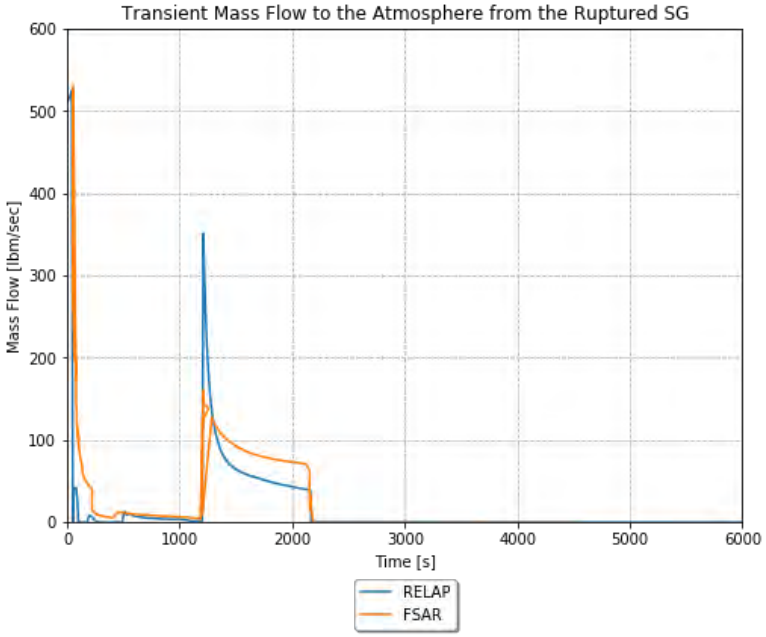

Figure 4-162. TR mass flow to the atmosphere from the ruptured SG for the SGTR scenario.

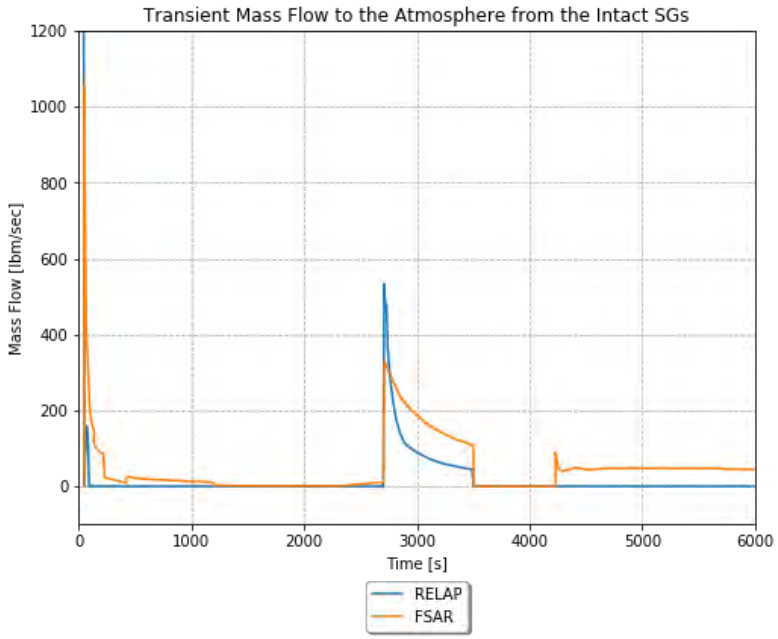

Figure 4-163. TR mass flow to the atmosphere from the intact SGs for the SGTR scenario.

4.13.6 Adherence to Acceptance Criteria

The final results for the SGTR are compared to the results from the FSAR and the acceptance criteria in Table 4-22. The acceptance criteria are based on the examination of the FSAR sections, and the applicable sections of the standard review plan.

The RELAP5-3D simulation does not meet all acceptance criteria for the SGTR scenario. The run undergoes CHF briefly and violates the max PCT criterion. Some of the potential input differences between the FSAR simulations and the RELAP5-3D simulations are discussed in the following section. These may drive some of the differences in the results between the FSAR analysis and the RELAP5-3D simulations, in addition to code differences.

Table 4-22. SGTR final results.

Result	FSAR	RELAP5-3D	Acceptance Criteria
RCS Maximum Pressure [psia]	~2700	2575	2750
DNBR [-]	N/A	< 1	1.24
Fuel Centerline Temperature [°F]	N/A	1920	2200

4.13.7 Scenario-Specific Limitations and Conditions for Usage

The following limitations apply specifically to the SGTR case:

- The break modeling is a valve component positioned in the appropriate place. However, because the tubes are lumped into a single channel, it is believed that this may cause an overprediction of break flow (e.g., a huge volume with an SB is different than a small volume with the same break and a more circuitous path to the break from a larger volume). The model should be updated to determine a better modeling scheme for the tube rupture.
- Approximations of the MDC and FTC are used.

- Minimal geometric information on the SG PORVs was found, so the flow through these valves may be unreliable.
- In general, the operator actions for this TR had to be forced at times consistent with the FSAR analysis. When trying to use logic that duplicated the parameters driving the operator actions, the sequence of events was messed up and the TR looked very dissimilar to the FSAR analysis.
- The OTΔT trip setpoint is not modeled, but it was the source of reactor trip in the FSAR analysis.
- The SI flows used have no basis located in the FSAR.

4.14 Spectrum of Rod Cluster Control Assembly Ejection Accidents

This event is referred to as a rod ejection accident (REA).

This accident is defined as the mechanical failure of a control rod mechanism pressure housing, resulting in the ejection of a RCCA and drive shaft. The consequence of this mechanical failure is a rapid positive reactivity insertion together with an adverse core power distribution, possibly leading to localized fuel rod damage. This event is classified as an ANS Condition IV incident.

There is a significant amount of information in the FSAR for this event, but much of it is background for explaining the modeling assumptions made. The analysis herein will be a simplified combination of the average core and hot spot analyses from the FSAR.

Based on the available plots, there are two limiting runs, which should be simulated: beginning of life (BOL) HFP and end of life (EOL) HZP.

4.14.1 Scenario-Specific Inputs in the TR Input File

The TR input file is defined as follows:

- Upfront cards are included that specify this is a restart TR run, which uses the last available printout in the restart file.
- The end time is set to 10 seconds for both cases, consistent with the analysis in the reference plant FSAR. The max time step is set to 0.001 seconds, as this is a value that is reasonable for a very erratic simulation such as this.
- The minor edits are used to specify the variables used in the plots.
- The control logic for reactivity is described as follows for the BOL HFP case:
  - The ejected rod worth is modeled using CV 405, which is updated to be a function of time using new General Table 614.
  - General Table 614 is specified as a table with the rod worth in dollars specified at all points in time. The rod worth of 0.0024 Δk/k is divided by the beta value of 0.0057 to obtain a worth of 0.421052632 $.
  - It was originally set up so that the SS value for CV 405 was added to the value present in the TR input file using an operator in the ‘models.xml’ file (e.g., expression is ‘%card%+ssreact’). This was to ensure that the constant from the SS to maintain 0 reactivity is preserved. However, it was discovered that re-specifying the kinetics cards with “initial reactivity” set to 0.0 appeared to reset the reactivity. As such, this operator is not necessary.
  - The delayed neutron fraction affects the beta over lambda value in the RELAP5-3D kinetics input. The base value of 297/sec for beta over lambda is used with the known assumption of 0.0075 for beta to determine a lambda value of 2.5252…e-5. The beta value for this case is 0.0057, so a new beta over lambda value of 226.0/sec is used. In order to enter this value, the entirety of the kinetics input must be copied over into the TR input file.

- The trip reactivity of 4.0% Δk requires an update. Although the original inputs are also based on 4.0% Δk, the delayed neutron fraction has changed. Thus, the trip worth is recalculated as 0.04 Δk/k divided by 0.0057 to obtain 7.01754 $. General Table 613 is copied from the SS file, and the y factor is changed to -7.01754.

- The control logic for reactivity is described as follows for the EOL HZP case:
  - The same CV 405 and General Table 614 inputs from the BOL HFP case are used, except that the rod worth in General Table 614 is updated. The rod worth of 0.0084 Δk/k is divided by the beta value of 0.0046, to obtain a worth of 1.8261 $. Note that initial runs using this value resulted in run failure due to excessive power (e.g., on the order of 10^12 W). As such, the value was altered to obtain a reasonable power spike without failure. A value of 1.15 $ was settled upon.
  - The delayed neutron fraction affects the beta over lambda value in the RELAP5-3D kinetics input. The beta value for this case is 0.0046, so a new beta over lambda value of 182.2/sec is used. In order to enter this value, the entirety of the kinetics input must be copied over into the TR input file.
  - The trip reactivity of 2.0% Δk requires an update. Thus, the trip worth is recalculated as 0.02 Δk/k divided by 0.0046 to obtain 4.347826 $. General Table 613 is copied from the SS file, and the y factor was initially changed to -4.347826. However, this value was insufficient to prevent a runaway power increase. A value of -20 was used to produce reasonable results.
- Trip 410 is listed to achieve reactor trip at an identical time to the FSAR analysis:
  - For the BOL HFP case, Trip 410 is set as a time greater than or equal to 0.05 seconds.
  - For the EOL HZP case, Trip 410 is set as a time greater than or equal to 0.22 seconds.
- CVs 419, 420, 421, and 422 (e.g., the pump inputs) are set as constant values consistent with the end of SS Pump Speed, and these values will be replaced by RAVEN using variable “sspmpvel.” This causes the pumps to simply continue operating like normal SS.
- CVs 435 through 438 (e.g., the steam valve position) are changed to be functions of General Table 650. This allows them to be set to the SS valve position prior to the reactor trip or SI signal, and then close based on the specified delay and ramp times.
- CVs 459 through 462 (e.g., the MFW flow rate) are listed as constant values of 1118.9 lbm/sec. This is done as a placeholder for RAVEN to substitute in the actual end of SS values of CVs 459 through 462 using RAVEN variable “ssmfw.”
- CV 472 is listed as a constant value of 0.0. This is used to turn off the SS charging flow.
- CV 473 is listed as a constant value of 0.0. This is used to turn off the SS letdown flow.
- CV 482 is listed as a constant value of 0.0. This is used to turn off the SS PRZ heater.
- General Table 650 is listed with values identical to the SS input. This input needs to be here so that the first three valve position entries in the table can be replaced with the end of SS values using the RAVEN variable “ssstmvlv.” This step is necessary to turn off the steam flow controller, but have the SS steam flow persist.

4.14.2 Scenario-Specific RAVEN Inputs

The RAVEN distribution means are set as shown in Table 4-23. The inputs are consistent with the FSAR, as described below. The remaining inputs are assumptions that are not specifically mentioned in the FSAR:

- The SS conditions are generally set as follows:
  - The BOL HFP case is set to use standard thermal design procedure values.
  - The EOL HZP conditions are generally set to nominal values, with the following exceptions:
    - Core power, which is set to 1 W, since RELAP5-3D does not allow a lower number.
    - RCS temperatures, which are set to a constant 560 °F, as there is insufficient power to reach a higher temperature or a significant gradient between hot and cold.
    - The SG and PRZ levels are set lower than the other nominal cases, as the convergence logic was having difficulty with higher values.
- The FW is set so that the SS MFW continues throughout the TR and the AFW never comes on. This is done by setting all the related timing distributions to be progressively higher values far greater than the TR end time.
- The main steam is set so that the SS value continues throughout the TR. This is done by setting all of the related timing distributions to be progressively higher values far greater than the TR end time.
- Because the rod drop behavior in General Table 613 has a built-in delay of 0.5 seconds before the rods begin to move, and the FSAR analysis reflects a 0.5 second delay from the reactor trip signal to the beginning of rod entry into the core, the RCCA delay time distribution is set to 0.0 seconds.
- The pump motors are set to never trip.
- The SI delay is set to an arbitrarily high value to prevent SI actuation.

Table 4-23. Summary of RAVEN input for REA.

Distribution	Description	Unit	Mean (BOL HFP)	Mean (EOL HFP)
cltempdist	Cold Leg Temperature	°F	556.2	560
corepdist	Core Power	W	3.636E+09	1.000E+00
fwtempdist	Feedwater Temperature	°F	448.7	448.7
hltempdist	Hot Leg Temperature	°F	620.6	560
przleveldist	PRZ Level	ft.	29.4	19
przpressdist	PRZ Pressure	psia	2250	2250.1
rcsflowdist	RCS Volumetric Flow	gpm	9.36E+04	9.36E+04
rcsmflodist	RCS Mass Flow	lbm/sec	9684.028	9684.028
rcsmflorrdist	RCS Mass Flow in Vessel	lbm/sec	9684.028	-9684.028
sgleveldist	SG Level	ft.	40.1	32
stmpressdist	SG Steam Pressure	psia	941	941
sgflowdist	SG Flow Rate	lbm/sec	1132.639	1132.639
dpvessdist	Vessel Pressure Drop	psi	46.5	46.5
dphldist	Hot Leg Pressure Drop	psi	1.2	1.2
dpxldist	Crossover Leg Pressure Drop	psi	3.1	3.1
dpcldist	Cold Leg Pressure Drop	psi	3.3	3.3
dpsgdist	SG Primary Pressure Drop	psi	45.5	45.5
corbypdist	Core Bypass Flow	%	5	5
przphirxtdist	High PRZ Pressure Reactor Trip Setpoint	psia	2.51E+03	2.51E+03

Distribution	Description	Unit	Mean (BOL HFP)	Mean (EOL HFP)
przplorxtdist	Low PRZ Pressure Reactor Trip Setpoint	psia	1.71E+03	1714.7
przlhirxtdist	High PRZ Level Reactor Trip Setpoint	ft.	4.89E+01	4.89E+01
rcsflolorxtdist	Low RCS Flow Rate Reactor Trip Setpoint	lbm/sec	8.43E+03	8.43E+03
sglevlorxtdist	Low SG Level Reactor Trip Setpoint	ft.	27.1	2.71E+01
mfwdeltimedist	MFW Delay Time	sec	1.00E+06	1.00E+06
mfwramptimedist	MFW Ramp Time	sec	1.00E+07	1.00E+07
afwdeltimedist	AFW Delay Time	sec	1.00E+08	1.00E+08
afwramptimedist	AFW Ramp Time	sec	1.00E+09	1.00E+09
afwflodist	AFW Flow Rate	lbm/sec	105.65	105.65
pmpmotdeldist	Pump Motor Trip Delay Time	sec	1.00E+09	1.00E+09
achfluxdist	Average Channel Maximum SS Heat Flux	BTU/sec-ft^2	99.954	99.954
hchfluxdist	Hot Channel Maximum SS Heat Flux	BTU/sec-ft^2	164.93	164.93
initreactdist	Initial Reactivity	$	0	0
mdcdist	Moderator Density Coefficient	Δk/g/cm^3	-0.042	-0.042
accbordist	Accumulator Boron Concentration	Mass Frac	1.90E-03	1.90E-03
chgbordist	Charging Boron Concentration	Mass Frac	2.40E-03	2.40E-03
accvoldist	Accumulator Water Volume	ft^3	900	900
acctempdist	Accumulator Temperature	°F	120	120
accpressdist	Accumulator Pressure	psia	600	600
sitrplspdist	Low Steam Pressure SI Signal	psia	8.00E+02	800
sitrpdeldist	SI Signal Delay Time	sec	1.00E+09	1.00E+09
msivdeldist	MSIV Delay Time	sec	1.00E+08	1.00E+08
msivrampdist	MSIV Ramp Time	sec	1.00E+09	1.00E+09
rccadeldist	RCCA Delay Time	sec	0	0
rcpheatdist	RCP Heat Generation	MW	1.00E-05	4.25E+00
przsafdist	PRZ Safety Valve Open Pressure	psia	2500	2500
rcsbordist	RCS Initial Boron Concentration	Mass Frac	0.00E+00	0.00E+00

4.14.3 Steady State Results

The steady state observations for the rod ejection cases are explained in detail in FY-2020 [2].

4.14.4 TR Boundary Conditions

The TR boundary conditions for the rod ejection cases are explained in detail in FY-2020 [2].

4.14.5 TR Results

The RELAP5-3D results are compared to the runs from the FSAR in the paragraphs below.

4.14.5.1 BOL HFP

The TR PZR pressure is shown in Figure 4-164. There is no FSAR plot for this. The RELAP5-3D run experiences a significant pressurization as the core power increases. This pressurization triggers all PRZ depressurization devices.

The TR core power as a fraction of nominal is shown in Figure 4-165. The RELAP5-3D run has a very large power increase, over 2 times the nominal power. This is significantly more than the FSAR curve.

The TR maximum cladding temperature is shown in Figure 4-166. There is no FSAR plot for this. The RELAP5-3D run has a large temperature excursion during the initial power excursion, and gradually cools after the power reduces.

The TR hot spot oxidation is shown in Figure 4-167. There is no FSAR plot for this. A significant amount of oxidation is accrued during the power excursion, but the duration is short enough that it ends up being a small amount.

The TR DNBR is shown in Figure 4-168. There is no FSAR plot for this. The DNBR appears to drop to 0 around the time of the clad temperature excursion. This drop to 0 is interpreted to be due to CHF.

The TR fuel center, fuel average, and clad outer temperatures are shown in Figure 4-169. The RELAP5-3D fuel center temperature is less than the FSAR value, while the RELAP5-3D fuel average temperature is higher than the FSAR value. This may indicate a higher thermal conductivity for the RELAP5-3D pellet material. In either case, the RELAP5-3D prediction is fairly close to the FSAR. The clad outer temperature is very close throughout the TR, though a bit lower.

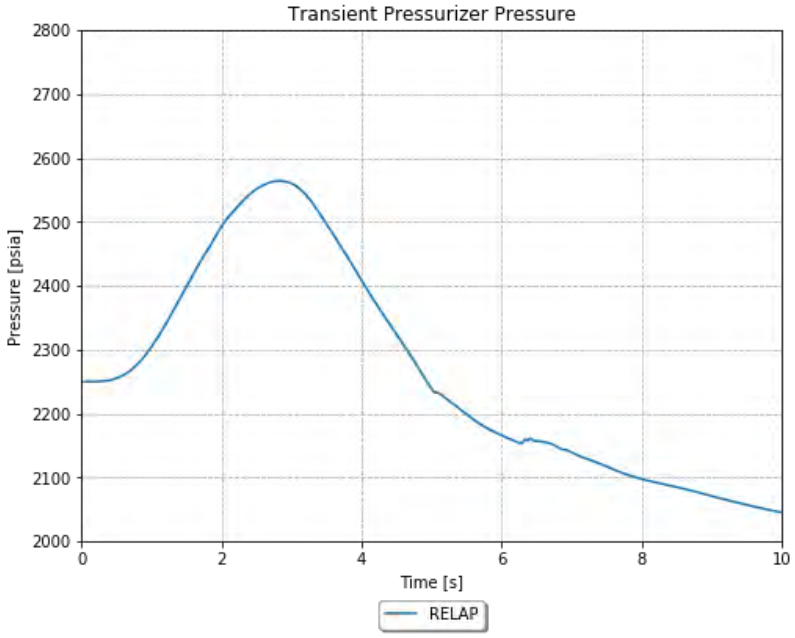

Figure 4-164. TR PZR pressure for the REA scenario (e.g., BOL HFP).

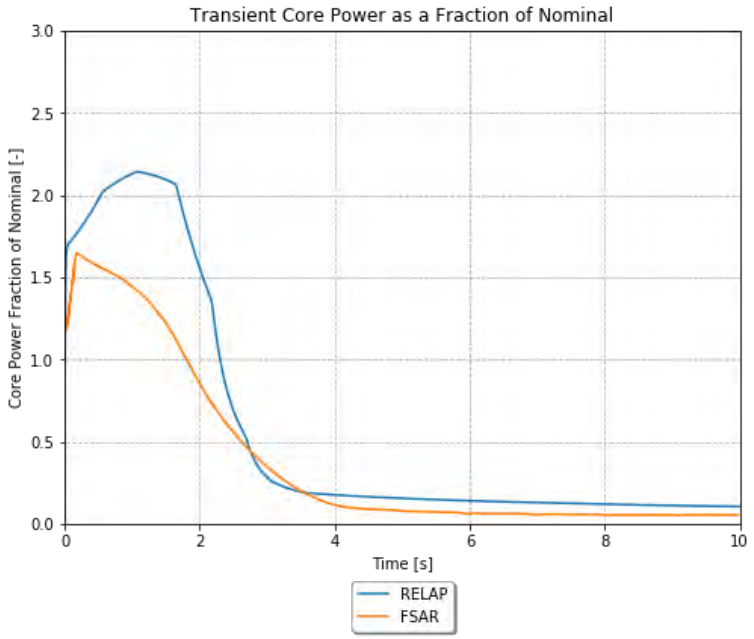

Figure 4-165. TR core power as a fraction of nominal for the REA scenario (e.g., BOL HFP).

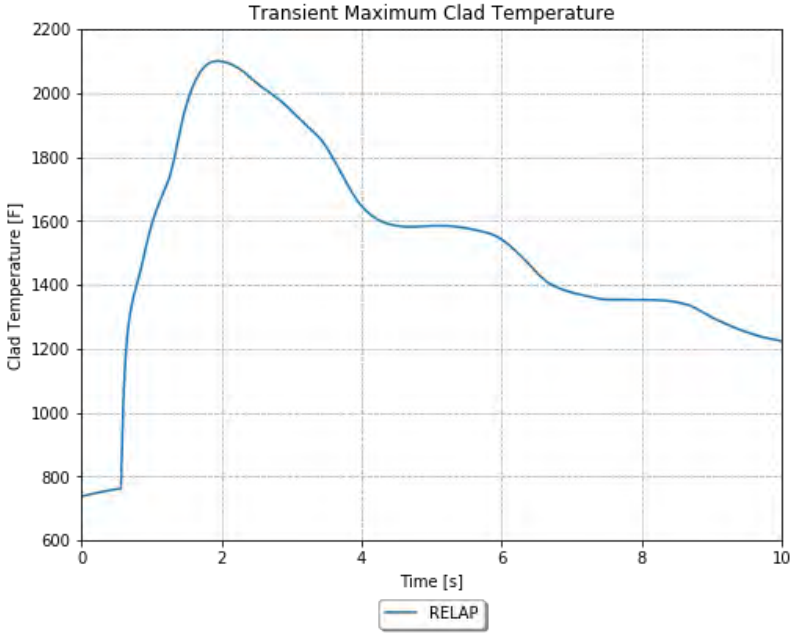

Figure 4-166. TR maximum clad temperature for the REA scenario (e.g., BOL HFP).

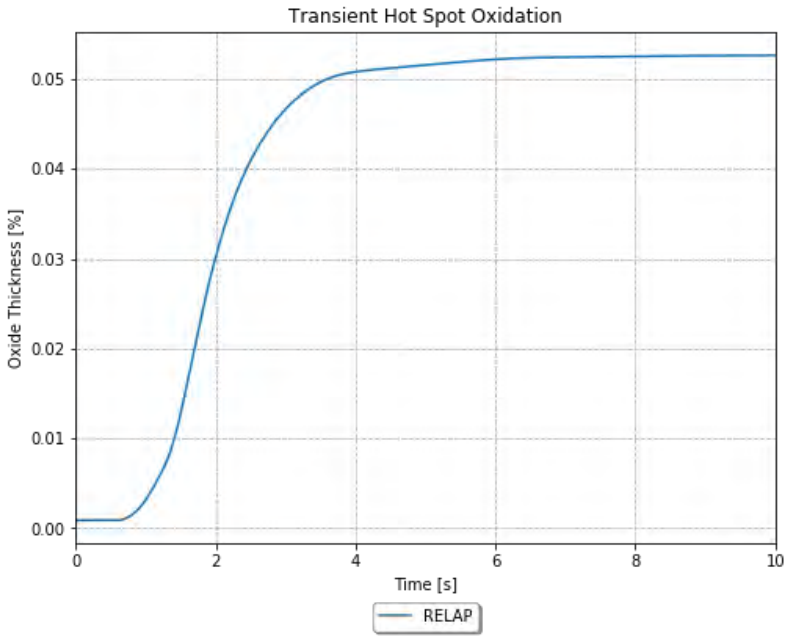

Figure 4-167. TR hot spot oxidation for the REA scenario (e.g., BOL HFP).

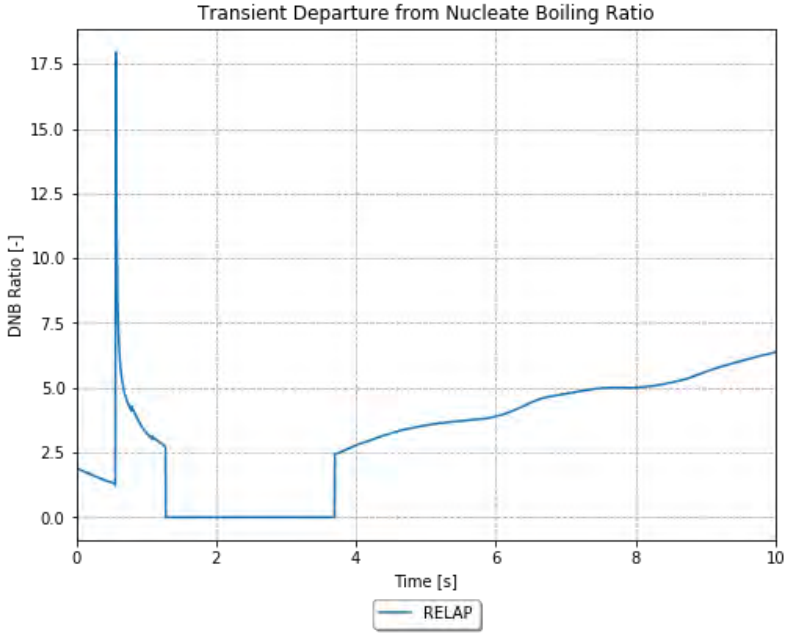

Figure 4-168. TR DNBR for the REA scenario (e.g., BOL HFP).

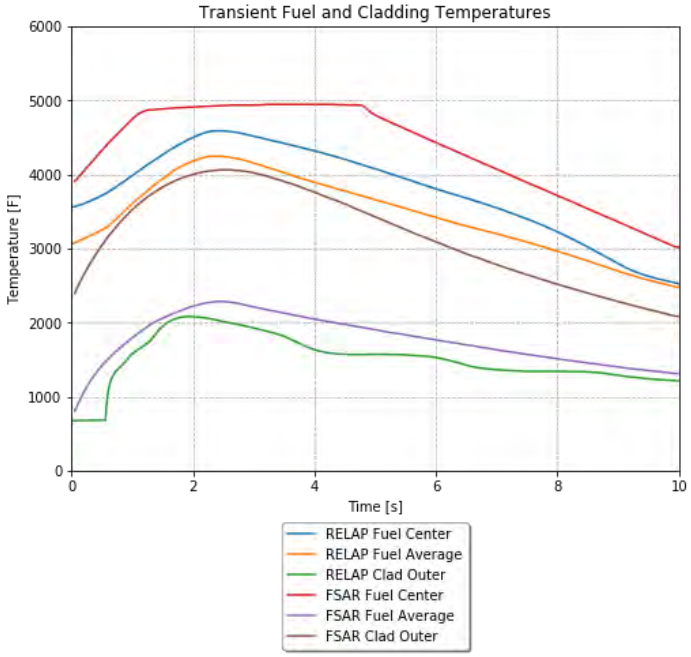

Figure 4-169. TR fuel and cladding temperatures for the REA scenario (e.g., BOL HFP).

4.14.5.2 EOL HZP

The TR PRZ pressure is shown in Figure 4-170. There is no FSAR plot for this. The RELAP5-3D run experiences a significant pressurization as the core power increases. This pressurization triggers all PRZ depressurization devices.

The TR core power as a fraction of nominal is shown in Figure 4-171. The RELAP5-3D run has a very large power increase, almost 10 times the nominal power. This is significantly less than the FSAR curve and is later. In addition, the excursion more gradually goes back down.

The TR maximum cladding temperature is shown in Figure 4-172. There is no FSAR plot for this. The RELAP5-3D run has a small temperature excursion during the initial power excursion and cools after the power reduces.

The TR hot spot oxidation is shown in Figure 4-173. There is no FSAR plot for this. A negligible amount of oxidation is accrued during the power excursion.

The TR DNBR is shown in Figure 4-174. There is no FSAR plot for this. The DNBR appears to be 0 early on and then 0 again after the clad temperature excursion. This drop to 0 is interpreted to be due to being in a single-phase liquid.

The TR fuel center, fuel average, and clad outer temperatures are shown in Figure 4-175. All three temperature curves are far lower for RELAP5-3D than for the FSAR analysis.

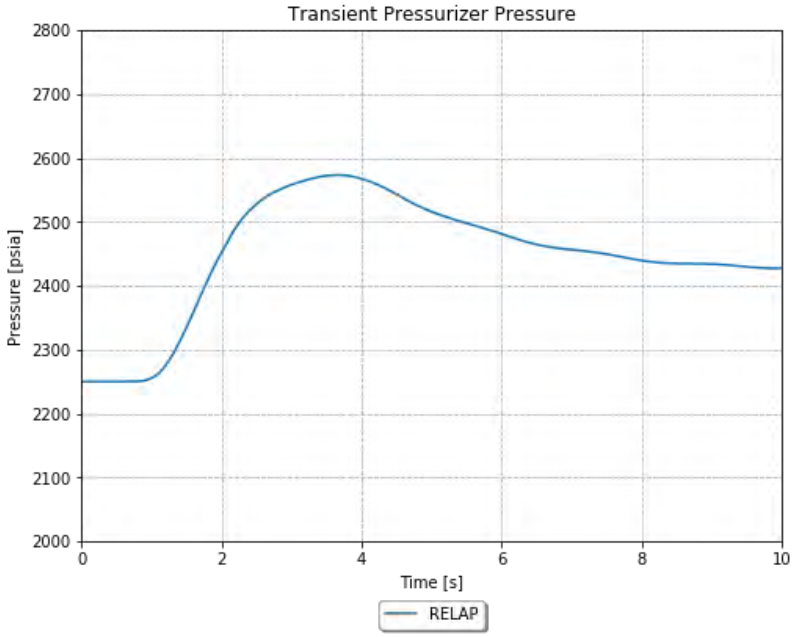

Figure 4-170. TR PRZ Pressure for the REA scenario (e.g., EOL HZP).

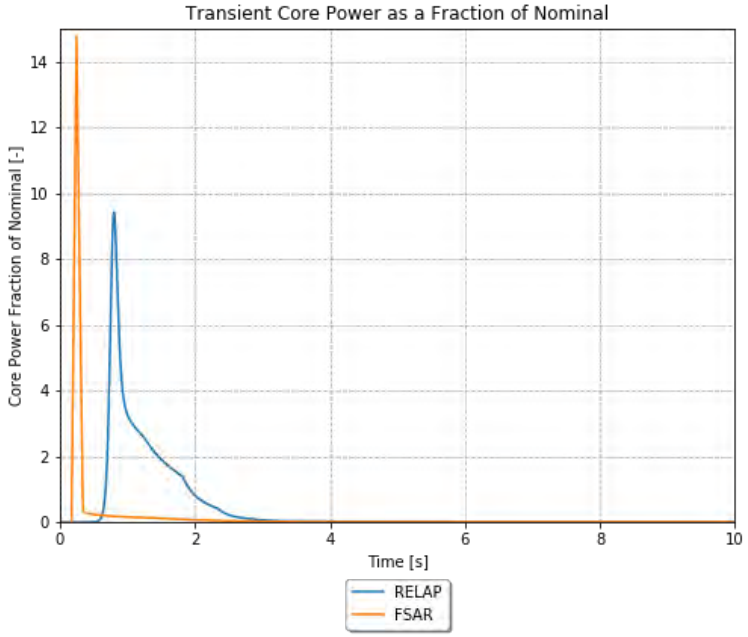

Figure 4-171. TR core power as a fraction of nominal for the REA scenario (e.g., EOL HZP).

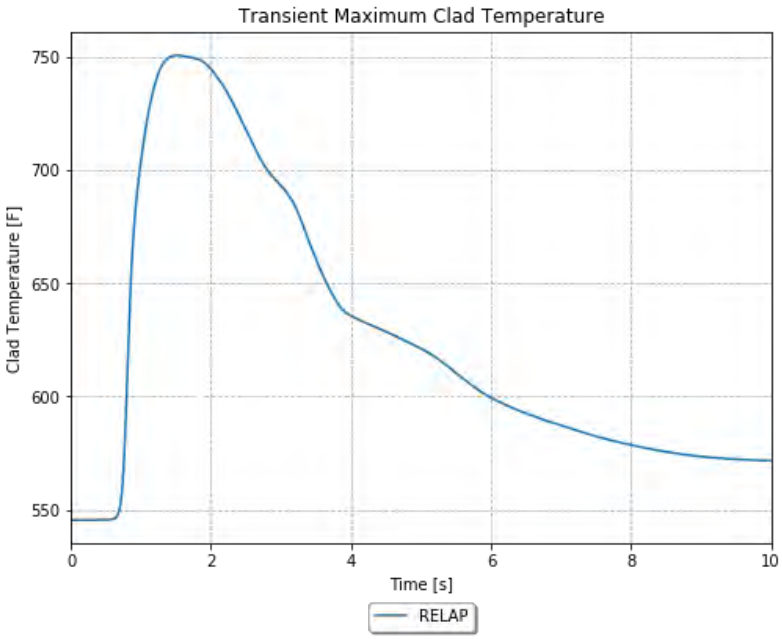

Figure 4-172. TR maximum clad temperature for the REA scenario (e.g., EOL HZP).

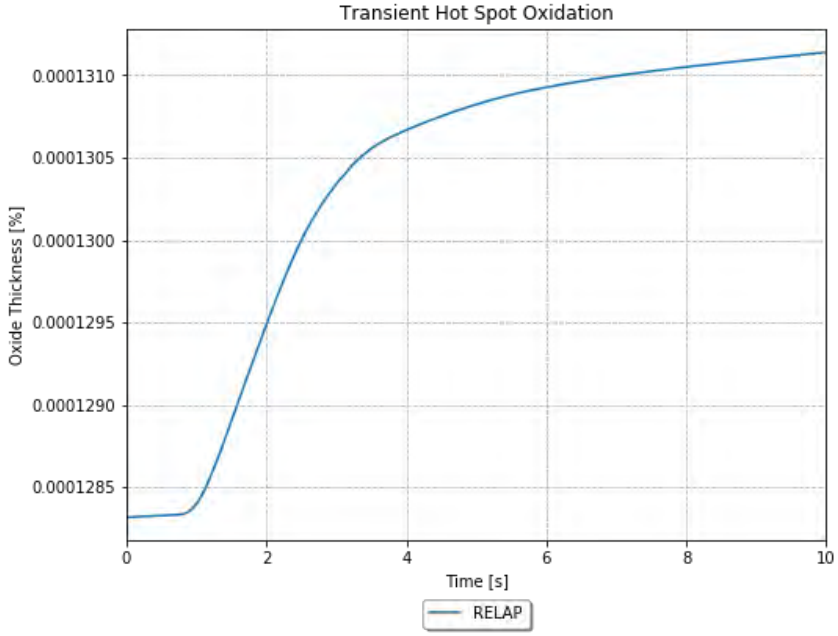

Figure 4-173. TR hot spot oxidation for the REA scenario (e.g., EOL HZP).

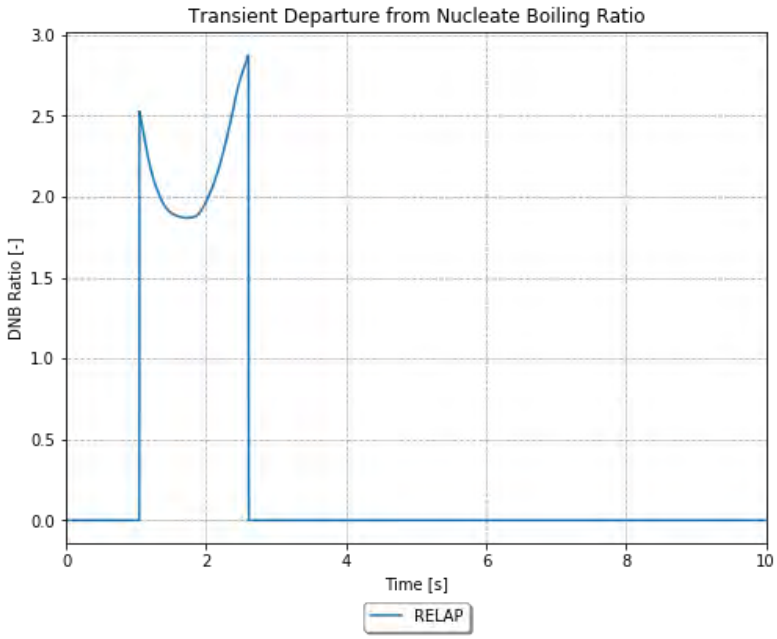

Figure 4-174. TR DNBR for the REA scenario (e.g., EOL HZP).

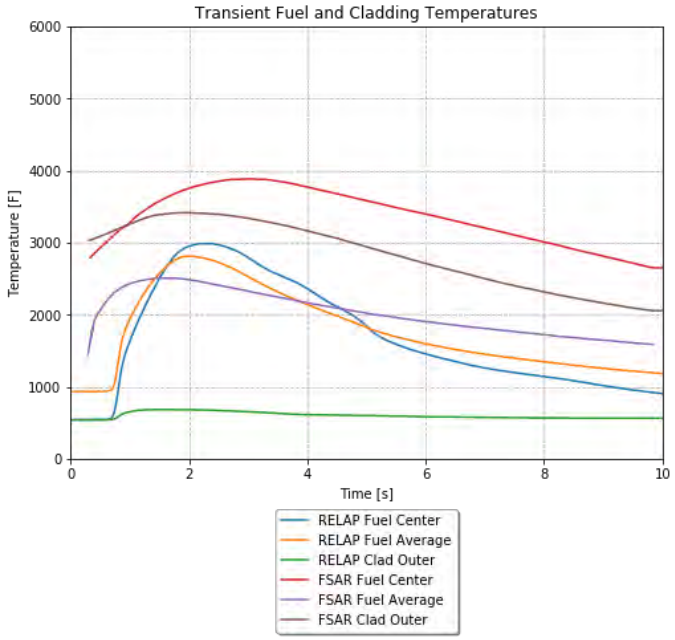

Figure 4-175. TR fuel and cladding temperatures for the REA scenario (e.g., EOL HZP).

4.14.6 Adherence to Acceptance Criteria

The final results for the REA are compared to the results from the FSAR and the acceptance criteria in Table 4-24. The acceptance criteria are based on examination of the FSAR sections, and the applicable sections of the standard review plan.

Table 4-24. REA final results.

Result	FSAR (BOL HFP)	RELAP5-3D (BOL HFP)	RELAP5-3D (EOL HZP)	FSAR (EOL HZP)	Acceptance Criteria
RCS Maximum Pressure [psia]	N/A	2500	N/A	2580	2750
DNBR [-]	N/A	< 1	N/A	~1.8	1.24
Maximum Fuel Temperature [°F]	> 4900	~4600	> 4800	~3000	4700

The RELAP5-3D simulations meet all acceptance criteria for the REA scenario, except the BOL HFP case experiences brief CHF. Some of the potential input differences between the FSAR simulations and the RELAP5-3D simulations are discussed in following section. These may drive some of the differences in results between the FSAR analysis and RELAP5-3D, in addition to code differences.

4.14.7 Scenario-Specific Limitations and Conditions for Usage

The following limitations apply specifically to the rod ejection cases:

- For the EOL HZP case, the ejected rod worth had to be decreased, and the trip rod worth had to be increased relative to their FSAR values. Without these changes, the run failed on a massive power excursion.
- The doppler feedback reactivity weighting is not used, because this weighting is based on a more complex core model than is present in this model. In addition, approximations of the MDC and FTC are used.
- No assumptions are given for the MFW, so it is assumed that the MFW continues at the SS value.
- No assumptions are given for the main steam flow, so it is assumed that the MSIV remains open at the SS value.
- Given the sensitivity to rod drop time for this analysis, the reactor trip is forced at a time consistent with the FSAR analysis, and the time between the trip and when the rods begin to drop is 0.5 seconds.
- No assumptions are given for the pump speed, so it is assumed that the pumps continue at the SS velocity.
- No assumptions are given for the PRZ controls, so it is assumed that the controls all function consistently with the SS, other than the heaters, which are turned off.

4.15 Uncertainty Analysis of LBLOCA

The LBLOCA TR is considered the most limiting event of the events in Chapter 15 of the FSAR. Using the information presented in the LBLOCA section of this report, six parameters were chosen as important values. Lower and upper bounds were created based on the given values. The parameters and their ranges are presented in Table 4-25. All values are varied using a uniform distribution. Five of the six parameters are input into the steady state portion of the event. The discharge coefficient is input in the TR since the break connections are applied using the TR input deck. A small sampling of 100 runs was executed. Of those 100 runs, 25 cases failed during the simulation. The failed cases are a combination of the cladding temperature reaching non-physical temperatures and nonconvergence related to non-condensables. A failure rate of 25% is extremely high and must be reduced with future revisions. One possible issue resides in the RELAP5-3D BEPU version used due to the interfacial friction multiplier being global. If this multiplier can be isolated to specific components—specifically the MULTID component—the failure rate is expected to decrease.

Table 4-25. Monte Carlo parameter ranges for LBLOCA uncertainty analysis.

Parameter	Default	Lower Bound	Upper Bound
Core Power [w]	3.66E+09	3.58E+09	3.73E+09
Discharge Coefficient [-]	0.6	0.42	0.78
System Pressure [psi]	2250	2200	2300
Accumulator Temperature [°F]	120	80	120
Accumulator Volume [ft^3]	900	765	1035
Accumulator Pressure [psi]	611.3	611.3	811.3

Figure 4-176 shows the mean value for the vessel mass at each time-step. The shaded region is the 5th and 95th percentile of all the runs results. The initial rapid decrease in liquid inventory varied greatly between the runs. Around 50 seconds, most cases start to see the liquid inventory increase, decrease, and increase slowly to leveling off. It is important to note most failures were found to occur in the range of 45–65 seconds, which is where the rapid inventory changes are occurring. Figure 4-177 shows a similar style plot for the downcomer level. Also, the FSAR data is added as it was available. The FSAR shows that the data has a higher liquid level throughout the TR. The total vessel mass in Figure 4-176 is likely lower than the actual data as well, since in general, the plots show similar trends. Figure 4-178 shows the same plot setup for the maximum clad temperature. Cases where the temperature reaches values above 2200°F should be considered failed as well, due to these temperatures going beyond what is considered acceptable. Cases that failed likely show similar trends to the HT cases that were successful. The simulation mean for the clad temperature shows values much lower than the FSAR data, but the variation between cases is very large.

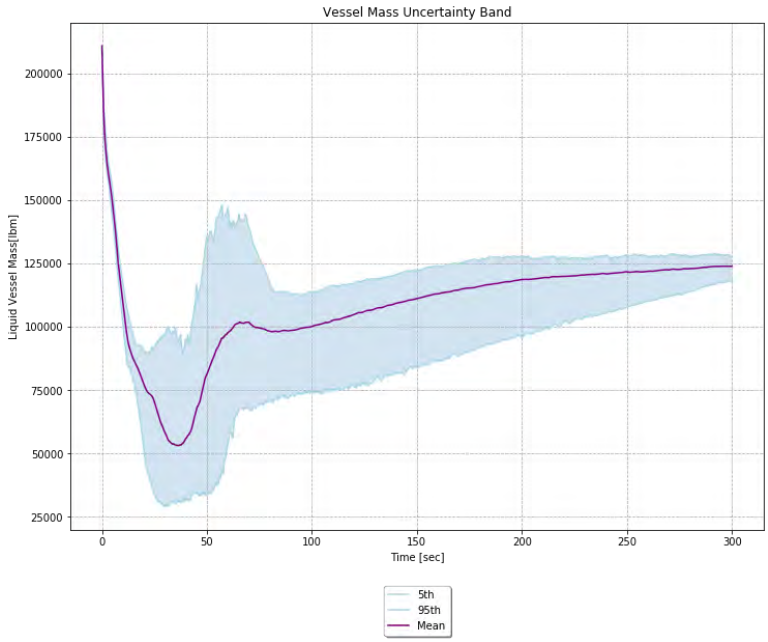

Figure 4-176. LBLOCA Monte Carlo sampling. TR vessel liquid mass uncertainty results.

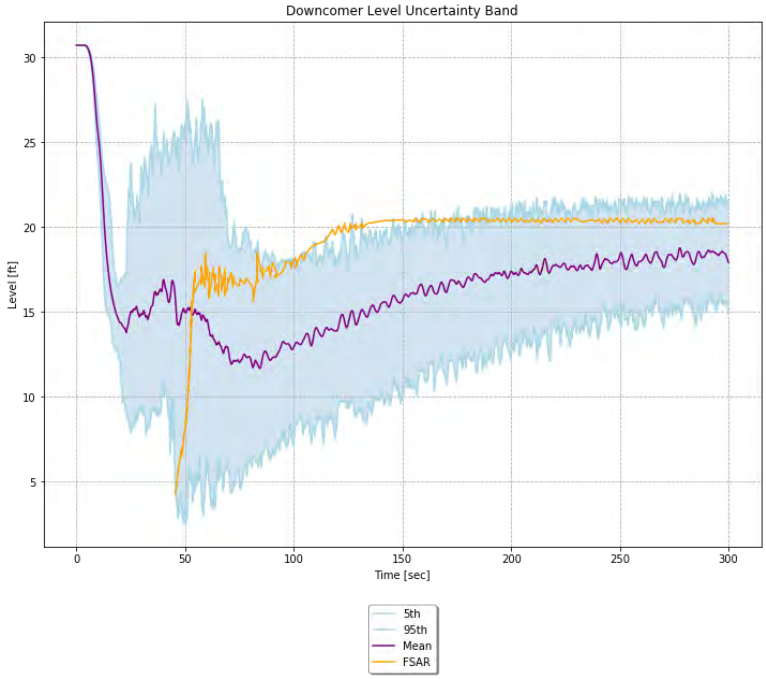

Figure 4-177. LBLOCA Monte Carlo sampling. TR downcomer level uncertainty results.

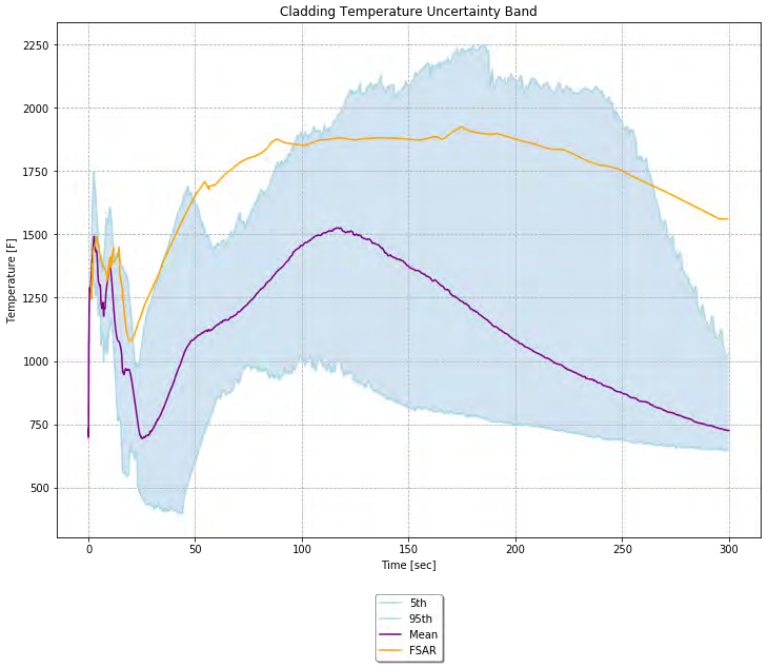

Figure 4-178. LBLOCA Monte Carlo sampling. TR maximum clad temperature results.

4.16 Summary of DBA Analysis

In general, the RELAP5-3D simulations are in acceptable range to the values in FSAR. Using MULTID option in reactor modeling improved RELAP5-3D simulation of limiting DBA scenarios. However, modeling constraints are also identified in RELAP5-3D. Following updates of RELAP5-3D should be performed as they considered to be highly important for future full deployment of plant reload optimization framework:

- With the MULTID component update, the results were found to improve for cases that required a refined vessel model, specifically the LBLOCA. However, the core modeling is too coarse, both axially and radially. The following issues are still outstanding and should be taken into consideration with future updates.
    - The lower plenum nodalization should be studied for effects on fluid retention during LBLOCA blowdown.
    - The downcomer nodalization should be studied for effects on ECCS bypass.
    - The core and upper plenum modeling should be redesigned considering both the upper plenum structures above each fuel assembly and for handling power variation in assemblies.
    - Components should be added or modified to properly model core bypass flow and tune the model to obtain an appropriate value.
- A new method for automatic calculation of power distribution inputs for the core based on peaking factor inputs and power shape definition should be created.
- The kinetics model should be updated consistent with the increased detail in the vessel model. In addition, control logic should be assembled that allows the analyst to enter coefficients of reactivity exactly consistently with the FSAR inputs. As of now, approximations are made which fit into the existing RELAP5-3D input structure.
- The material properties for the fuel rods and pellets should be examined for suitability. The existing inputs have extremely erratic and non-physical dependence on temperature.
- Additional work should be done to determine the actual conditions experienced during HZP operation at the plant, and the model should be updated to appropriately model HZP. Most of the HZP TRs herein never actually reach a fully converged SS.
- Studies of the choked flow models should be performed, as the break flow in the RELAP5-3D runs herein generally differs significantly from the FSAR analyses they are emulating.
- The broken loop SG nodalization should be re-visited with SGTR events in mind. Currently, all tubes being part of one pipe component likely overestimates break flow.
- The following model updates are considered of lower importance but should be considered, nonetheless.
- Either the optimizer which obtains acceptable RCS loop DPs should be finished or run-specific loss coefficient multiplier inputs should be added. As it is, some RCS loop pressure drops are very close, while others are far off from the desired value.
- A containment model should be constructed to obtain a better run-specific backpressure curve for LBLOCA and possibly to be able to assess containment response criteria.
- Model changes due to SG tube plugging level should be implemented to automatically calculate based on an assumed percentage of tube plugging.

- Additional reactor trip and SI signal setpoints may be implemented, if sufficient information to perform the modeling is found.
- The following model updates are considered to be of low importance.
- Sensitivity studies to obtain SS acceptance bands with justification.
- Additional SS convergence criteria, potentially including, but not limited to, upper head temperature, SG recirculation ratio, and more granular pressure drops across the vessel.
- The PRZ spray line geometry may be updated.

Finally, run-specific boundary condition assumptions which are not based on explicit descriptions from the FSAR may be investigated for significance to results.

5. CONCLUSION AND FUTURE PLAN

This report summarizes research conducted in FY-2021. During this time, the project progressed from the planning and methodology development phase to the early demonstration phase. The highlights of the activities are:

- Development and deployment of a multi-objective optimization process using GA.
- Development and test of an approach for an optimization process acceleration using artificial intelligence, which significantly reduces computational burden.
- Demonstration of plant reload optimization framework with a generic PWR based on performance of neutronics and thermo-hydraulic analyses.
- Assessment of ten limiting DBA scenarios in TR cases for the fuel reload optimization framework demonstration.
- Identification of selective DBA scenarios, as shown in Table 4-1, for evaluation of the transition from deterministic to risk-informed approach for fuel analyses.

5.1 Industry Perspectives on Plant Reload Optimization

During FY-2021, the project has been actively communicated with the industry stakeholders and the following perspectives were identified:

1. There is a synergetic opportunity to consider new methods to optimize fuel reloads considering the near-term deployment of ATF products. The synergy is in the ability to 'ease' the licensing burden of a new methodology (i.e., reload optimization platform) since it will undergo licensing process at the same time as ATF licensing.
2. Utilities typically do not 'push' on margin recovery like the one that could be offered by a robust optimization of the reload analysis. This project will help industry to at least 'characterize' the unquantified analytical margins and demonstrate possibilities of greatly increased operational flexibility.
3. Some utilities expressed interest in the ability to consider more advanced core design optimization techniques for BWRs. Therefore, the ability to extend platform capabilities to BWRs in the near future is of great interest to some utilities.
4. Automation of the process to the point where the analysis can be done on at each reload opens up margins already. While automation is one of best practice, it has to be considered carefully such as to minimize additional cost for licensing and/or development efforts. The automated platform should be designed to minimize learning effort of the platform.
5. The methodology must fit within customer business lines. This means minimum interferences with established processes by utilization and integration of already-approved codes and methods. This requires a plug-and-play architecture of the framework, which is the goal of this project.

Given these premises, the original roadmap for the development of the methodology remains applicable. However, the recommended next step is to consolidate the following two end-to-end demos to illustrate the mechanics and the benefits of the analysis.

5.1.1 Baseload Equilibrium Core Design

This is a rather simplistic and somewhat idealistic scenario. The core is assumed to operate all the time during each cycle at 100% nominal power. The objective is to optimize the core design by minimizing the number of feed assemblies—the objective function—while subject to the following constraints:

- Max FΔH
- Max FQ
- Max Burnup (62,000 MWD/MT)
- 24-months cycle

The FDH and FQ peaking factors are determined by the system response analysis, which may include the thermo-mechanical issues on the fuel rods. For real applications, there could be more constraints, but this simplistic view address some of the most important constraints and can provide an initial end-to-end demonstration of the methodology.

5.1.2 Representative Industry Core Design

For industry applications, a variety of operational TRs (Condition I and II events) must be considered. On top, actual axial offset control methods, or peaking factor surveillance technical specifications must be accounted for. The best-known procedures considered by plant operators are the Constant Axial Offset Control or Relaxed Axial Offset Control.

This adds a layer of complexity in the core design, which also needs to consider power maneuvers and/or load-follow operation modes. This TR injects the effect of poisons and xenon TRs, which push peaking factors to higher values.

As a surrogate to emulate these complexities, a typical load-follow maneuver is considered in addition to the baseload operation, as shown in Figure 5-1 below.

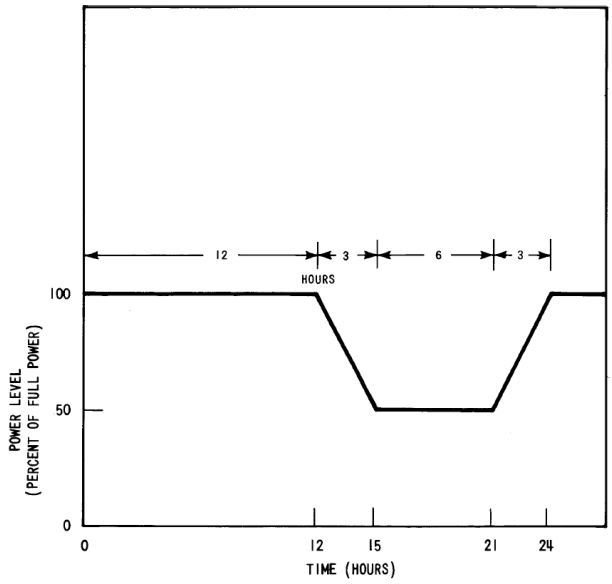

Figure 5-1. Example of load-follow maneuver.

These TRs are analyzed with the core physics tool with the same constraints expressed in Section 5.1.1. Additional implicit constraints must be considered in the analysis. These include technology specifications and regulatory limits. The complete analysis described in this section, including fuel performance features, can represent an end-to-end demonstration, which can be offered to industry stakeholders as the starting point for further customization toward a final practical solution.

5.2 Future Plan

The plant reload optimization framework needs robust computational tools, which industry can use with confidence. Tools for the system analysis (i.e., RELAP5-3D) and optimization and surrogate modeling (i.e., RAVEN) have been showing high maturity in development with full verification and validation. However, tools for core design and fuel performance need comprehensive assessment for plant reload optimization framework applicability.

The following activities will be performed in FY-2022:

- A comparison study of reactor core design and fuel performance computer codes to determine tool capability and applicability for the fuel reload optimization framework. This task will provide a summary of available tools that could be used by utilities within the framework offering flexibility to employ already-approved fuel performance evaluation tools, which reduces efforts for regulatory approvals.
- Development and demonstration of a risk-informed approach for the regulatory-required fuel reload safety analyses. The risk-informed approach will allow further optimization of core configuration offering additional economic benefits in terms of reduced new fuel volume.

Based on the project technology roadmap is shown in Figure 1-1, following out year activities are planned:

- By 2023, perform enhancements of RELAP5-3D computer code to better support uncertainty quantification for DBA analyses, especially LOCA. The proper uncertainty quantification is important to reduce conservatisms and, as the result, increase safety margins.
- By 2023, further enhance genetic algorithm with multi-objective optimization which will allow more advanced optimization.
- By 2023, complete an economic benefit assessment for the new fuel management plan.
- By 2023, extend the framework capabilities for other core configurations (i.e., PWR with ATFs and a 24-month refueling cycle, generic BWR).
- By 2024, complete demonstration of industry use case for equilibrium scenarios (i.e., normal plant operation).
- By 2024, complete demonstration of ready-for-deployment framework to the industry.
- By 2025, prepare a Topical Report that demonstrates the framework and its capabilities, including all regulatory-required steps for a typical License Amendment Request. Support the Topical Report review and approval process by the U.S. Nuclear Regulatory Commission.

6. REFERENCES

1. Nuclear Energy Institute, Nuclear Costs in Context, 2020.
2. A. Alfonsi, et al., RISA Plant Reload Process Optimization: Development of design basis accident methods for plant reload license optimization, INL/EXT-20-59614, Idaho National Laboratory, 2020.
3. J. Holland, Genetic algorithms, Scientific American, Vol. 267.1, pp. 66-73, 1992.
4. K. Deb, et al., A fast and elitist multiobjective genetic algorithm: NSGA-II, IEEE Transactions on Evolutionary Computation, Vol. 6, No. 2, pp. 182-197, 2002.
5. Z. Michalewicz, Genetic Algorithms. + Data Structures. = Evolution Programs, Third, Revised and Extended Edition, Springer, 1996.
6. J. McCall, Genetic Algorithms for Modelling and Optimization, Journal of computational and Applied Mathematics, Vol. 184, pp. 205-222, 2005.
7. M. Marseguerra, E. Zio, Basics of Genetic Algorithms Optimization for RAMS Applications, Reliability Engineering and System Safety, Vol. 91, pp. 997-991, 2006.
8. Towards Data Science, Evolution of a salesman: A complete genetic algorithm tutorial for Python, https://towardsdatascience.com/evolution-of-a-salesman-a-complete-genetic-algorithm-tutorial-for-python-6fe5d2b3ca35.
9. Towards Data Science, Introduction to Optimization with Genetic Algorithm, https://towardsdatascience.com/introduction-to-optimization-with-genetic-algorithm-2f5001d9964b.
10. T. Points, Tutorial Points, https://www.tutorialspoint.com/genetic_algorithms/index.htm.
11. P. Daniel, et al., Comparing Images Using the Hausdroff Distance, IEEE Transactions on Pattern Analysis and Machine Intelligence, Vol. 15, No. 9, pp. 850-863, 1993.
12. A. Epiney, et al., RISMC industry application #1 (ECCS/LOCA): Core characterization automation: Lattice codes interface for PHISICS/RELAP5-3D, Nuclear Engineering and Design, Vol. 345, pp. 15–27, 2019.
13. A. Alfonsi, et al., Combining RAVEN, RELAP5-3D, and PHISICS for Fuel Cycle and Core Design Analysis for New Cladding Criteria." ASME. ASME J of Nuclear Rad Sci., Vol. 3(2), 2017.
14. A. Zoino, et al., Performance-based ECCS cladding acceptance criteria: A new simulation approach, Annals of Nuclear Energy, Vol. 100, Part 2, pp. 204-216, 2017.
15. NRC, Standard Review Plan for the Review of Safety Analysis Reports for Nuclear Power Plants: LWR Edition, U.S. Nuclear Regulatory Commission, NUREG-0800, 2017.